



Swansea University
Prifysgol Abertawe



Swansea University E-Theses

The stabilisation of PVC plastisol using hydrotalcite (HT).

Martin, Glyn

How to cite:

Martin, Glyn (2007) *The stabilisation of PVC plastisol using hydrotalcite (HT)*. thesis, Swansea University.
<http://cronfa.swan.ac.uk/Record/cronfa42522>

Use policy:

This item is brought to you by Swansea University. Any person downloading material is agreeing to abide by the terms of the repository licence: copies of full text items may be used or reproduced in any format or medium, without prior permission for personal research or study, educational or non-commercial purposes only. The copyright for any work remains with the original author unless otherwise specified. The full-text must not be sold in any format or medium without the formal permission of the copyright holder. Permission for multiple reproductions should be obtained from the original author.

Authors are personally responsible for adhering to copyright and publisher restrictions when uploading content to the repository.

Please link to the metadata record in the Swansea University repository, Cronfa (link given in the citation reference above.)

<http://www.swansea.ac.uk/library/researchsupport/ris-support/>



Swansea University
Prifysgol Abertawe

The Stabilisation of PVC Plastisol Using Hydrotalcite (HT)

Glyn Martin

Doctorate of Engineering Thesis

EPSRC Engineering Doctorate Centre for Steel Technology
Swansea University, Materials Research Centre

ProQuest Number: 10805271

All rights reserved

INFORMATION TO ALL USERS

The quality of this reproduction is dependent upon the quality of the copy submitted.

In the unlikely event that the author did not send a complete manuscript and there are missing pages, these will be noted. Also, if material had to be removed, a note will indicate the deletion.



ProQuest 10805271

Published by ProQuest LLC (2018). Copyright of the Dissertation is held by the Author.

All rights reserved.

This work is protected against unauthorized copying under Title 17, United States Code
Microform Edition © ProQuest LLC.

ProQuest LLC.
789 East Eisenhower Parkway
P.O. Box 1346
Ann Arbor, MI 48106 – 1346



DECLARATION

This work has not previously been accepted in substance for any degree and is not being concurrently submitted in candidature for any degree.

Signed(candidate)

Date .. 22/02/08

STATEMENT 1

This thesis is the result of my own investigations, except where otherwise stated. Other sources are acknowledged by footnotes giving explicit references. A bibliography is appended.

Signed(candidate)

Date .. 22/02/08

STATEMENT 2

I hereby give consent for my thesis, if accepted, to be available for photocopying and for inter-library loan after expiry of a bar on access approved by Swansea University.

Signed(candidate)

Date .. 22/2/08

Acknowledgments

I would like to thank my industrial sponsors Corus Colors and Akzo Nobel for their support, exceptional interest and the encouragement they have given me over the last 4 years of research. A special thanks should go to Michael Leonard and Anis Zakaria for their help, support and use of Akzo Nobel equipment to create the commercial coatings used in this work. I would also like to give special thanks to Paul Jones who took on industrial supervision midway through my research to give my work a more industrial focus and relevance. I would also like to thank Vernon John for his input to the project during the initial stages.

I would like to give a big thanks to everyone in the Corrosion Group for their support, kindness and pleasurable experience during the last 4 years of research. I would in particular like to thank Andrew Robinson for his endless support, thoughts and expertise throughout my project to make it as is it today. I would also like to thank Arwel John, Jia Chai and Dave Thomson for their help with the experimental side of things and it was greatly appreciated.

Great thanks must be given to Dave Worsley for his encouragement, technical knowledge, ideas and input. The supervision has been excellent throughout and has enabled the research to thrive and prosper.

I would like to finally thank my parents and family for their unconditional love, support and guidance throughout my years of study.

Summary

The main focus of this EngD Thesis is an investigation into the use of Hydrotalcite (HT) as a photodegradation stabiliser for polyvinyl chloride (PVC) used as a coating for pre-finished steel. The work builds on the use of model systems, both unplasticised and plasticised, in comparing HT with other commercial stabilisers and culminates with the full formulation and testing of paint systems containing all the relevant commercial pigments and stabilisers.

In the first section of work, a flat panel reactor was used to accurately measure the rates of photogenerated carbon dioxide (CO₂) as an *in-situ* measurement of degradation. In unplasticised PVC pigmented with 30% photoactive titanium dioxide, there was a transition to a higher rate of CO₂ evolution after a set amount of degradation which is attributed to the formation of hydrochloric acid. In this instance, the addition of up to 10% HT in model system removes this catalytic effect as the HT exchanges chloride ions for carbonate. This initial result suggested that HT could be a useful stabiliser and the results on model systems showed it to be far more consistent in its performance over a wide range of concentrations compared to commercial barium/zinc and tin based stabilisers.

In model films containing plasticiser molecules based on phthalates the effect of HCl catalysis was not found to occur. An increase in initial rate of CO₂ evolution and an absence of HCl production indicates preferential attack on the plasticiser rather than the PVC matrix. When more sulphonic acid ester (phthalate free) systems are used, acidic fragments and HCl are produced and these lead to a similar acceleration in degradation with UV exposure time observed with PVC alone. This indicated that in such systems the addition of a stabiliser that could remove hydrochloric acid would be beneficial.

In near commercial PVC plastisol systems prepared on steel substrates, HT has been compared to historic (tin), existing (barium zinc) and future (calcium zinc) stabilisers. In all cases, regardless of titanium dioxide grade, the HT performed very well in terms of colour retention and gloss following QUVA weathering cycles with

the HT preventing dehydrochlorination within the coating which leads to darkening on exposure.

In the final section of work completely stabilised and fully formulated paint systems were prepared using the HT and commercial stabilisation systems and exposed to extended QUVA and QUVB cycles. Even in these systems the HT is demonstrated to perform consistently and is in almost all respects superior to existing stabilisation chemistries. The positive effects are shown for both white and coloured systems.

In a summary, it seems that HT is able to stabilise PVC coatings applied to steel substrates and exposed to arduous weathering cycles. This stabilisation reflects the ability of HT to remove hydrochloric acid within the film which reduces dehydrochlorination, coating darkening and degradation. HT is a cheap mineral material and is extremely easy to blend into paint and as such is a potentially promising pigment addition to make to painted product to reduce acid catalysed degradation.

Contents Page

Chapter 1: Literature Review

1.0	Introduction	1
1.1.1	Organically Coated Steels (OCS)	1
1.1.2	Components of PVC Plastisol	5
1.1.3	Failure and Degradation of Paints	6
1.2	Photochemistry	7
1.2.1	Mechanism of Photodegradation	7
1.2.1.1	The Quenching of Excited States	10
1.2.1.2	Physical Aspects of Electronic Energy Transfer	10
1.2.1.3	Radiative Energy Transfer	10
1.2.1.4	Non-Radiative Energy Transfer	11
1.2.1.5	Energy Transfer in Rigid Polymer Matrices	12
1.3	Photodegradation of Polymer	14
1.3.1	Degradation Mechanisms	17
1.3.1.1	Initiation	17
1.3.1.2	Propagation	19
1.3.1.3	Termination	21
1.3.2	Dehydrochlorination of PVC	23
1.4	Ultra Violet (UV) Stabilisation of Polymers	24
1.4.1	Ultra Violet Absorbers	24
1.4.2	Hindered Amine Light Stabilisers (HALS)	26
1.5	Thermal Degradation	28
1.5.1	Mechanism of Thermal Degradation	29
1.5.1.1	General Degradation	30
1.5.2	Oxidation Reactions	31
1.6	Thermal stabilisation of PVC	33
1.6.1	The Binding of Hydrogen Chloride	33
1.6.2	The Exchange of Labile Chloride Atoms	33
1.6.3	Addition of Stabilisers or Their Reaction Products to Polyene Sequences	35
1.6.4	Hydrotalcite	37
1.7	Plasticisers	39

1.7.1	The Mechanisms of Plasticisation	39
1.7.2	Production Process	42
1.8	Titanium Dioxide	43
1.8.1	Manufacturing Process of TiO₂	44
1.8.1.1	The Sulphate Process [43]	44
1.8.1.2	The Chloride Process [43]	45
1.8.1.3	Surface Treatments	46
1.8.1.4	Grinding and Finishing	47
1.8.2	Characteristics of TiO₂	50
1.8.3	The Photoactivity of TiO₂	52
1.8.4	Photocatalysis by TiO₂ [50]	54
1.8.4.1	Effects and Influences of TiO₂	56
1.9	Weathering and Accelerated Tests	58
1.9.1	Natural Exposure	59
1.9.1.1	Natural Exposure Rigs	60
1.9.1.1.1	Adjusted Angle Open Back Rack	60
1.9.1.1.2	Adjusted Angle and Standard Black Boxes	60
1.9.1.1.3	Heated Black Box	61
1.9.1.1.4	Fresnal Reflector Test (EMMA/EMMAQUA)	61
1.9.2	Artificial Exposure Methods	62
1.9.2.1	Carbon Arc	63
1.9.2.2	Xenon arc sources	63
1.9.2.3	Fluorescent Tube lamps (UVA)	63
1.9.3	Physical Measurement Techniques for Evaluating Weathering	64
1.9.3.1	Gloss Loss and Chalking	64
1.9.3.2	Colour Retention	65
1.9.3.3	Crazing and Cracking	65
1.9.3.4	Contact Angle	66
1.9.3.5	Weight Loss and Film Thickness	66
1.9.4.1	Chemical Test Methods Used to Follow Degradation	66
1.9.4.2	Infra-red Spectroscopy	67
1.9.4.3	Fourier Transform Infra-red (FTIR)	70
1.9.4.4	Chromatography	70

1.10	Recent Developments in the Rapid Evaluation of Photodegradation.	72
1.11	Conclusions and Aims	74
1.12	References	75
<u>Chapter 2: Experimental Procedures</u>		
2.1	Paint Formulation Techniques	78
2.1.1	Standard Pigmented Model PVC Systems	78
2.1.2	Plasticised Model PVC Systems	79
2.1.3	Acid Scavenger / Anion Exchange Pigmented Model PVC Systems	79
2.1.4	Model PVC Systems Containing Commercially Used Organic Stabilisers.	80
2.1.5	Near Commercial TiO ₂ Pigmented Plastisol PVC Systems	81
2.1.6	Fully Commercial TiO ₂ Pigmented Plastisol PVC Systems	81
2.2	Sample Preparation	82
2.2.1	Flat Panel Samples (CO ₂ Reactor) [2]	82
2.2.2	Flat Panel Samples (Weight Loss)	83
2.2.3	Hydrochloric Acid Evolution Samples	83
2.2.4	Commercial Plastisol Coated Steel Samples	84
2.3	Carbon Dioxide Reactor	85
2.3.1	Irradiation Apparatus	85
2.3.1.1	Flat Panel Reactor	86
2.3.2	Calibration of the FTIR Flat panel Reactor	89
2.4	Fourier Transform Infrared Spectrophotometer	92
2.4.1	Automatic Data Collection	92
2.4.2	The Time Interval Set-up	92
2.4.3	The Scan Settings Tab	93
2.4.4	Process Tab	94
2.4.5	The Log File	95
2.5	Hydrochloric Acid Evolution Apparatus	96
2.6	Weight Loss Apparatus	101
2.7	Conventional Accelerated Weathering	102
2.7.1	UV-A and UV-B Accelerated Weathering	103

2.7.2	Gloss Measurement	104
2.7.3	Colour Measurement	105
2.8	References	106

Chapter 3: Stabilisers in Model System

3.1	Introduction	107
3.1.1	Aims and Objectives	107
3.2	Experimental	108
3.2.1	Stabilisers	108
3.2.2	Preparation of the Test Coatings	108
3.2.3	Photodegradation of Stabiliser Systems	109
3.2.4	Weight Loss	109
3.2.4	Identification and Quantification of HCl	110
3.3	Results and Discussion	111
3.3.1	Effect of Stabiliser System of CO ₂ Evolution	111
3.3.2	HCl Evolution	119
3.3.3	Weight Loss	123
3.4	Conclusions	128
3.4.1	CO ₂ evolution	128
3.4.2	HCl Evolution	129
3.4.3	Weight Loss	130
3.5	References	132

Chapter 4: Plasticisers in Model System

4.1	Introduction	133
4.1.1	Aims and Objectives	134
4.2	Experimental	135
4.2.1	Plasticisers	135
4.2.2	Preparation of the Test Coatings	135
4.2.3	The Photodegradation of Plasticised Systems	136
4.2.4	Weight Loss	136
4.2.5	Identification and quantification of HCl	137
4.3	Results and Discussion	138
4.3.1	Effect of Plasticiser Type on Model PVC Systems	138
4.3.2	HCl Evolution	142

4.3.3	Effect of Plasticiser Loading on Initial and Secondary Rates of CO ₂ Production.	143
4.3.4	Weight loss	147
4.4	Conclusions	151
4.5	References	152

Chapter 5: Near Commercial Systems

5.1	Introduction and Aims	153
5.2	Experimental	153
5.2.1	Sample Preparation	153
5.2.2	Accelerated Weathering (QUVA)	157
5.2.3	Gloss Loss Measurements	158
5.2.4	Colour Change Measurements	158
5.3	Results and Discussion	159
5.3.1	HPS200, Mk II and HP200 base with No Pigment	159
5.3.2	HPS200, Mk II and HP200 base with K2220 TiO ₂	160
5.3.3	The Effect of Different Pigments Using HPS200 Base	161
5.3.4	Gloss Retention of Whites.	162
5.3.5	Gloss Retentions of HPS200 and HP200 Coloured Pigments	163
5.3.6	Colour Reflectance of HPS200 and HP200 Coloured Pigments	165
5.4	Conclusions	167
5.5	References	168

Chapter 6: Fully Commercial Systems

6.1	Introduction and Aims	169
6.2	Experimental	169
6.2.1	Sample Preparation	169
6.2.2	Accelerated Weathering in QUVA	170
6.2.3	Accelerating Weathering in QUVB	171
6.2.4	Gloss Loss Measurements	171
6.2.5	Colour Change Measurements	171
6.3	Results and Discussion	172
6.3.1	White Formulations (QUVA)	172
6.3.2	White Formulations (QUVB)	173
6.3.3	Goosewing Grey Formulations (UVA)	175

6.3.4	Van Dyke Brown Formulations (UVA)	177
6.4	Conclusion	179
6.5	References	181

Chapter 7: Conclusions and Future Work

7.1	Conclusions and Future Work	182
------------	------------------------------------	------------

Appendix 1

Appendix 2

Chapter 1

Literature Review

1.0 Introduction

1.1.1 Organically Coated Steels (OCS)

More than half of the worldwide production of organically coated steel (OCS) is used in the construction sector, anything from a warehouse to prestige stadiums. Around 24% is used for the appliance industry e.g. white goods, while around 26% is shared equally by the automotive industry and general engineering [1]. Examples of organically coated strip steels used in construction are shown in Figure 1.1.



Figure 1.1: Example of OCS applications.

In all cases, it is essential for the coating to protect the steel product from the environment it will be used in. In the case of buildings, a long term durability and warranty is required with a market driven requirement for new colours and shades. Unprotected steel showing major corrosion is not aesthetically pleasing or desirable. OCS is becoming an increasingly popular option due to its wide range of colours and finishes. The coating also provides a protective barrier against corrosion for the underlying substrate with guarantees for over 30 years being offered. Manufacturers' guarantees of

products are based on the geographical location of the building and whether a particular panel is south facing or a roofing section. Corus manufactures the 'Colorcoat' system which is a PVC based plastisol coating.

The 'Colorcoat' systems for building application are based on mild strip steel (typically 0.7mm for roofing and 0.55mm for wall cladding). The mild strip steel is coated with ~20µm thick zinc based coating (hot dip galvanising) to provide sacrificial galvanic protection in the event of a coating breach and at the cut edges of the panels.

The strip is typically treated with a chromate solution, which increases the adhesion of the paint layers to the metal and to act as a corrosion inhibitor. A primer is then applied to the strip by coil coating. The primer used for PVC plastisols is usually an acrylic based system, applied thickness of 5µm. The primer also includes corrosion inhibitors typically SrCrO₄. The reverse side of the strip usually has a polyester based primer.

In OCS used in construction is coated with a different layer depending on the facing side. The internal facing side is generally coated with a 10µm polyester back coat. The external face that is exposed to the weather has been coated with 200µm top coat of a commercial PVC plastisol paint system. The coating is a high performance paint that has been developed by Corus and its' partners since the 1960s.

As environmental legalisation is introduced there is an increased pressure for more environmentally friendly additions containing less heavy metal components, phthalate plasticiser replacements and the replacement of Cr (VI) primers. This EngD project is driven by the need for continual improvement and development of PVC plastisol based paints with more environmentally friendly additives.

There are various modes of failure for coated products including gloss loss, colour change, delamination and corrosion of the base metal. Some examples are shown in Figure 1.2 through to Figure 1.4.



Figure 1.2: An example of Colour change and fading making the building unsightly and any replacement panels obvious.



Figure 1.3: Faded Van Dyke Brown OCS same original dark brown colour different supply origin showing delamination and exposure of galvanized substance on the right (grey colour).



Figure 1.4: The corrosion of the metal substrate at a cut edge.

1.1.2 Components of PVC Plastisol

PVC Plastisol is made up of many different components with the main being the polymer resin (giving the coating its structure), a pigment (giving the coating its hiding power and colour) and a solvent (making the coating fluid during application). Other minor components including filler and additives are shown in Table 1.1 and 1.2 with a brief description of their function.

Table 1.1: Typical additives and their effects [2].

Additive	Effect
Lubricants	Reduce adhesion between polymer and processing equipment.
Fillers	Little physical benefit, cost reduction.
Flame Retardants	Resistance to fire.
Bio-stabilisers	Resistance to microbial attack.
Antistats	Dissipation of static charges.
Viscosity Regulators	Maintain regular viscosity.
Thermal Stabilisers	Provide resistance to thermal degradation.
Plasticisers	Improve workability, flexibility and distensibility.
UV Absorbers	Reduce the degradative effects of UV exposure.

Table 1.2: Typical formulation for a commercial plastisol coating with approximately 40% of the resin being a filler polymer.

Component	Per Hundred Resin (PHR)
Primary Plasticisers	24
Secondary Plasticisers	9
Plasticise/diluent	10
Epoxy stabiliser	3
Heat Stabiliser	3
UV Absorber	0.1-0.2
Fire Retardants	6.5
TiO ₂ Pigment	0-20
Solvent	As required.

1.1.3 Failure and Degradation of Paints

There are many failure modes for coating and these include incorrect preparation, chipping and undercutting, surface roughness and osmotic blistering. All of these failure mechanisms described are as a result of incorrect or defective production methods. This EngD thesis is more focussed on the degradation as a result of long term UV and environment exposure. Ultraviolet light is a problem due to the fact that its wavelength can activate or excite certain materials (e.g. polymer matrix or pigments (TiO_2)). Degradation activated by UV is relatively slow but is a significant problem as these products carry at least a 30 year corrosion failure warranty [3, 4]. This can be exceptionally demanding as degradation of paints by UV light can affect the integrity and severely changes the appearance of the coating. The appearance of the coating will degrade far quicker than the integrity, although on an industrial type of building this may not be a problem. As the construction industry take advantage of the many benefits of OCS it is necessary to produce products that remain aesthetically pleasing throughout their life.

1.2 Photochemistry

The two possible modes of failure from photochemical excitation are:

- Heterogeneous, where semi conducting materials (e.g. TiO₂) can absorb light forming excited states which destroy the surrounding polymer.
- Homogenous, where organic chromophores within the polymer absorb UV light leading to the breakdown in its structure.

This section is just a simple introduction to the basic principles of photochemical degradation of polymers and a more detailed review can be found elsewhere. [5-8].

1.2.1 Mechanism of Photodegradation

For a molecule to undergo a photochemical reaction, it must first absorb light energy. For this to happen the molecule needs to contain a chromophore. This can be present as an intrinsic functional group within the molecule or as an external impurity. For the purpose of this section we consider the impurities to be purely organic and therefore only homogenous photodegradation will be considered to occur.

The initial step of light absorption does not bring about any chemical change but merely promotes the electron from the valence band to the conduction band (a higher unoccupied orbital). This results in the formation of an excited singlet state (S*) and for this to occur the photon of light in question must have an amount of energy greater than or equal to the difference between the ground state and the first excited singlet state as shown in Figure 1.5.

Any excess energy required for the promotion to the next excited step is lost through vibration within the molecule. The energy of the photon is inversely proportional to the wavelength and the energy of a photon is given by Equation 1.1.

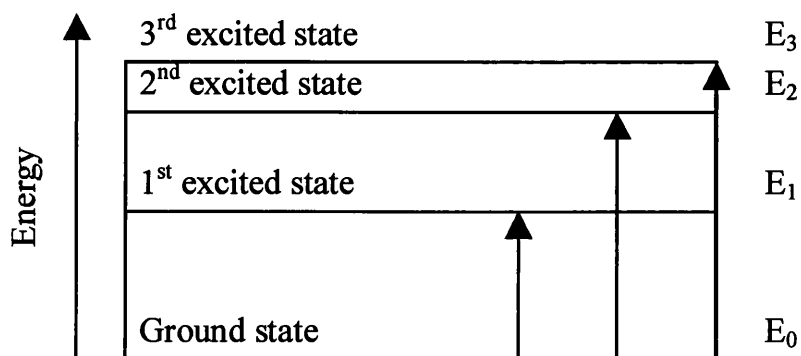


Figure 1.5: Energy levels of excited states.

$$E = \frac{hc}{\lambda}$$

E	=	Energy of the photon (Jmol ⁻¹)
h	=	Planck constant (Js)
c	=	Speed of light (ms ⁻¹)
λ	=	Wavelength of the light (m)

Equation 1.1: Energy of a Photon

Excited singlet molecules (S*) can lose their energy extremely rapidly in a number of ways as shown in Figure 1.6. The most common is internal conversion (IC) back to the ground state which occurs where energy is lost thermally. More importantly energy can be lost through inter-system crossing ISC (catalysis) and this route occurs many orders of magnitude less than internal conversion (recombination). The inter-system crossing creates excited triplet states which are much longer lived and undergo bond cleavage.

The relative importance of the different deactivation pathways depends upon the absorbing chromophore, as aromatics usually undergo fluorescence whilst carbonyls tend to undergo inter-system crossing (ISC) and create a triplet state (T).

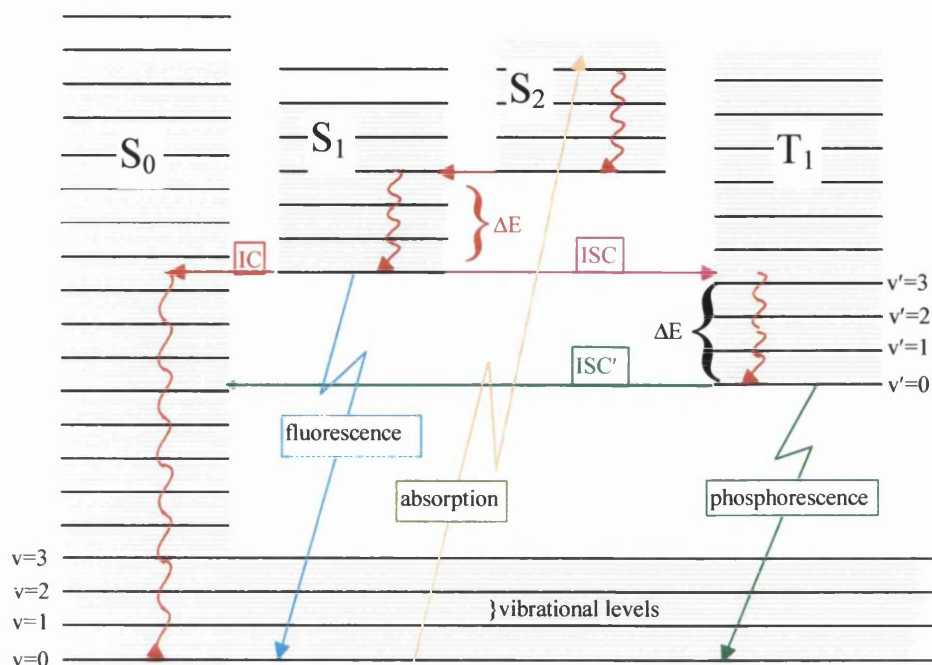


Figure 1.6: Jablonski diagram illustrating the energy deactivation pathways available.

Table 1.3: Required cleavage energies for certain bonds [9].

Wavelength of radiation (nm)	Energy (KJ Einstein ⁻¹)	Bond broken	Bond dissociation (Einstein – kJmol ⁻¹)
250	479	C-H	380 to 420
275	436	O-H	420
300	399	C-OH	380
325	368	C-C	340
350	342	C-O	320
375	319	C-Cl	320
400	299	RO-O	150
500	239	RO-OR	140

It is the bond cleavage reaction that is of interest since it is this process that generates the free radicals. This is desirable for use in UV curing [10, 11] or undesirable and prevented for photo-stabilisation of polymers [9, 12-14]. Table 1.3 lists the photon energies for different wavelengths and the bonds that they are capable of cleaving. The energy of the photon must exceed the bond dissociation energy in order for bond cleavage to occur, although it is still necessary for the photon to be absorbed by the chromophore.

1.2.1.1 The Quenching of Excited States

Even though excited states decay rapidly, it is often still desirable and preferable to accelerate this process. A quencher can be used to accelerate the decay, either to the ground state or to a lower excited state.



This quenching can be achieved through many different routes, which include complex formation, heavy atom quenching, oxygen quenching and energy transfer. These mechanisms are beyond the scope of this study and a more detailed description can be found in the literature [10, 11, 13, 15-18].

1.2.1.2 Physical Aspects of Electronic Energy Transfer

Energy transfer can occur between different parts of the same molecule or between two molecules. These are known as intramolecular and intermolecular energy transfer respectively. There are various factors that contribute to energy transfer these include; the distance between the donor and acceptor, the relative orientations of the donor, spectroscopic properties, optical properties of the matrix and the effect of collisions on the motion of the donor and the acceptor whilst the donor is excited.

As energy transfer is not 100% efficient, energy can be lost as light or heat thus the energy of the excited acceptor will be less than that of the original excited donor.

1.2.1.3 Radiative Energy Transfer

The process of radiative energy transfer occurs when a photon is emitted by the excited donor molecule with subsequent absorption of that photon by the acceptor molecule. The efficiency of this transfer depends on the amount of spectral overlap between two molecules (Figure 1.7).

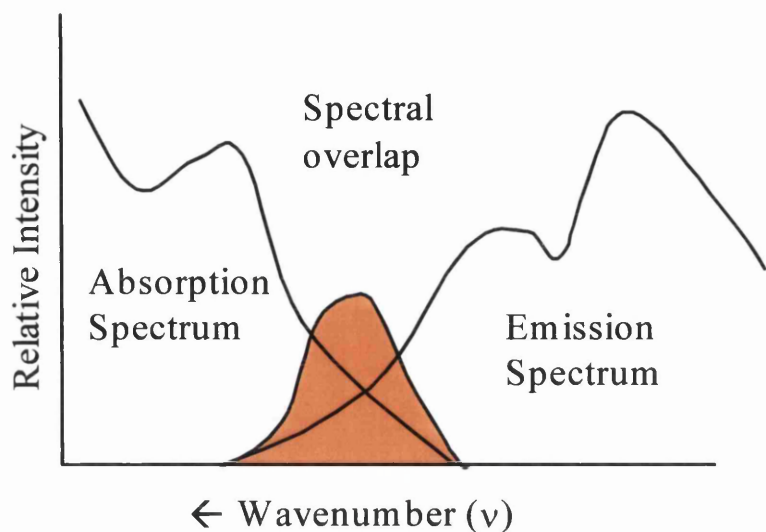


Figure 1.7: Overlap of absorption and emission spectra.

The transfer of energy can only occur at similar wavelengths and the energy transfer is long range in nature (greater than the size of molecules and uses intermediate photons for transfer, thus there is no direct interaction).

1.2.1.4 Non-Radiative Energy Transfer

Non-radiative energy transfer can occur via two mechanisms. The first operates over short range and occurs through the overlap of electron clouds where the molecules have to be within 1 to 1.5 nm gap for it to be considered to be in molecular contact. The transfer of energy is via an electron exchange mechanism. The second mechanism is slightly longer in range with a 5-10 nm gap between molecules and the energy transfer in this case is through dipole-dipole interaction.

1.2.1.5 Energy Transfer in Rigid Polymer Matrices

Intermolecular energy transfer can occur from:

Small molecules → Macromolecular chromophores
Polymeric chromophores → Small molecular chromophores
Polymeric chains → Polymeric chains.

Intra-molecular energy transfer can occur within the same polymeric molecule. There are two types of energy transfer where the first occurs between localised chromophores and the second being long range energy transfer that occurs across loops in the polymer chain as schematically shown in Figure 1.8.

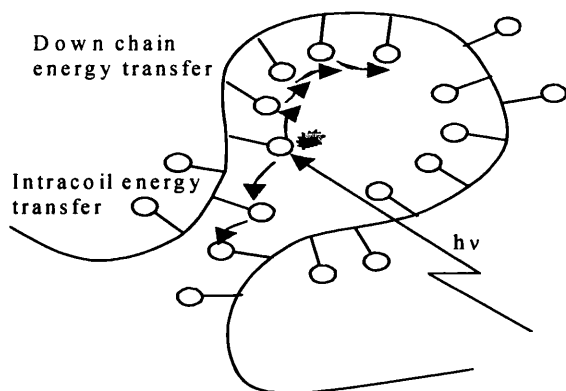


Figure 1.8: Intramolecular energy transfer within a polymer chain.

The local energy transfer can travel down a chain and is able to cover very long distances [13, 18]. The migrating excitation can move along the polymer chain until it comes close enough to another excitation centre and undergoes annihilation. This can occur between two triplet or singlet states if two photons are absorbed on the same polymer chain (Figure 1.9).

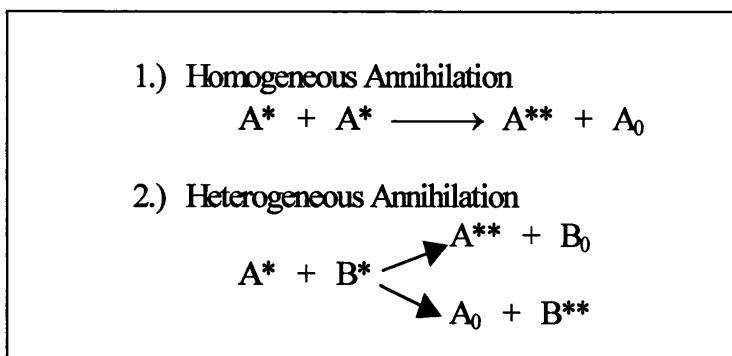


Figure 1.9: Annihilation process of excited states.

The highly excited states can be deactivated by luminescence or dissociate into free radicals (Figure 1.10) as shown earlier.

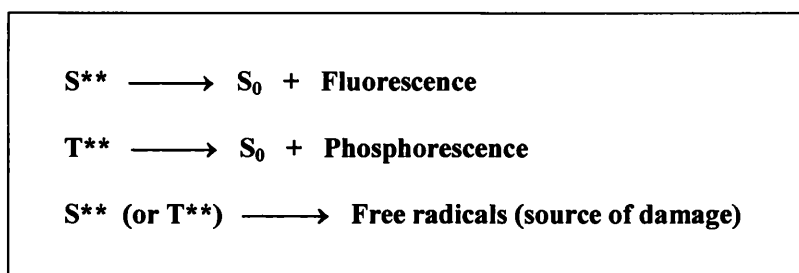


Figure 1.10: Radiative deactivation of highly excited states.

A process known as delay fluorescence can sometimes occur and is caused via triplet-triplet annihilation to form a T^{**} state. This then decays to form a ground state and an excited singlet which then emits fluorescence.

1.3 Photodegradation of Polymer

Polymers in general are fairly stable materials, although when exposed to the physical effects of the environment some chemical and/or physical changes will gradually occur. The occurrence and rate of these changes is primarily dependent on the intensity and wavelength of any UV irradiation [19, 20].

These changes can be induced either homogeneously or heterogeneously and the distinction between these two routes lies in the presence and classification of any chromophore. These chromophores can be either organic or inorganic and part of the structure or act as external impurities.

Table 1.4: The photoactive Chromophoric groups of type A and B polymers.

Type A Polymers	Example Chromophoric groups	Example Polymers
In type A polymers the chromophores are impurities within the structure introduced during polymerisation or processing. They may even have been added as a separate component of the system.	---C=C---C=C--- $\text{---C---} \quad \text{---C=C---C---}$ $\begin{array}{c} \text{O} \\ \parallel \\ \text{---C---} \end{array} \quad \begin{array}{c} \text{---C=C---} \\ \parallel \\ \text{O} \end{array}$	Poly(vinyl halides)
	$\text{POOH} \quad \text{Ti}^{+4}, \text{Al}^{+3}, \text{Fe}^{+3}$ $[\text{P---H}^+ \text{---O}_2] \quad \left[\begin{array}{c} \text{---C=C---} \\ \vdots \\ \text{O}_2 \end{array} \right]$	Polyacrylics Poly(vinyl alcohols) Aliphatic esters Polyurethanes
Type B Polymers		
In type B polymers the chromophores are an integral part of the chemical structure. They can be part of, or as side groups attached to, the polymer backbone.		Poly(ethyleneterephthalate)
		Poly(2,6-dialkyl-1,4-phenylene ether) Poly(ethersulphone)

Table 1.4 shows and defines these different routes although there is a suggestion that some polymers absorb light energy via both routes [13, 17, 18]. The routes involved

are sometimes referred to as type A polymers and type B polymers and a schematic of the chromophore distributions within each type is shown in Figure 1.11.

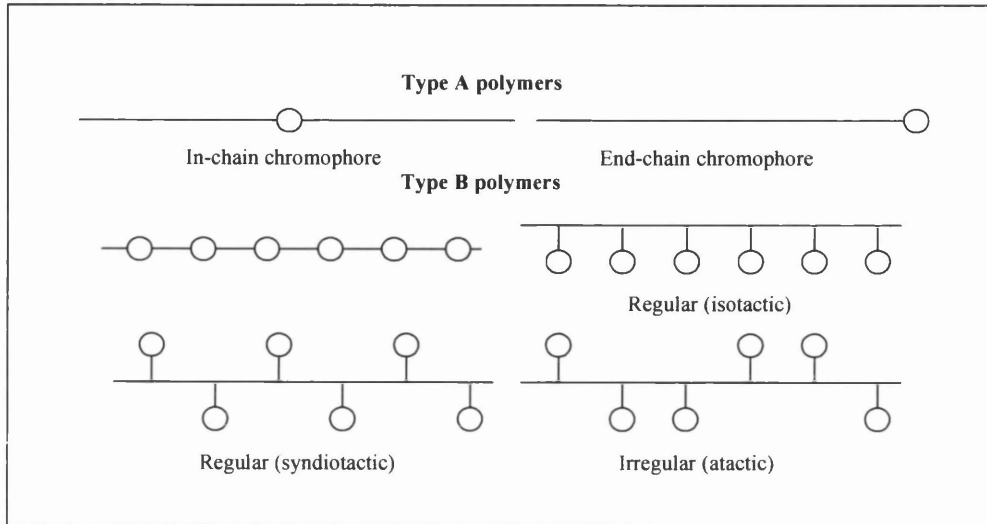


Figure 1.11: The formation of chromophores on type A and B polymers.

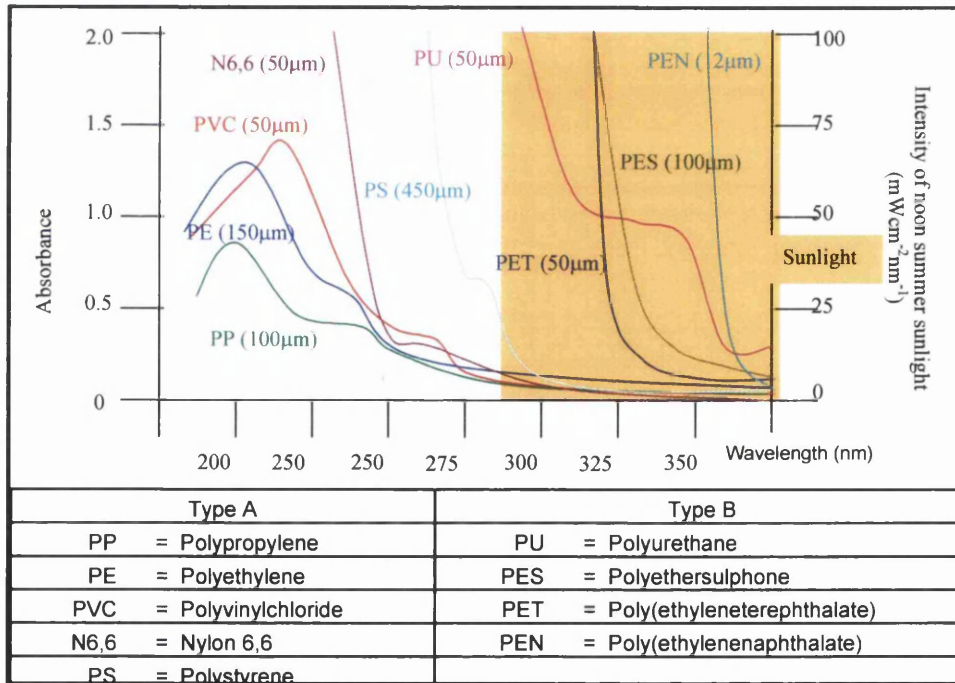


Figure 1.12: The absorption spectra of some common polymers.

Figure 1.12 shows the UV absorption spectra of some typical polymers overlaid with the emission spectra of natural sunlight and how the two differ. The differences

between the two polymer types are quite distinctive as type A have absorption outside the normal spectra of sunlight, whereas type B lie within the spectral range of sunlight.

Table 1.5 shows the activation maxima of certain polymers and these maxima lie primarily at the higher end of the sunlight spectrum in the UV range. Type A polymers are relatively unsusceptible but the absorption spectra of type B polymers overlaps with these typical activation maxima indicating a high susceptibility to degradation of light.

Table 1.5: Activation maxima of selected polymers.

Polymer	Bonds present	Absorption (max.)
Polyolefins	C-C, C-H	140nm ($\sigma=\sigma^*$)
Poly(vinylhalides)	C-Halogen, C-C, C-H	190nm ($n=\sigma^*$)
Poly(vinylalcohol)	C-C, C-H, C-O, O-H	200nm ($n=\sigma^*$)
Polybutadiene	C-C, C-H, C=C	220nm ($\pi=\pi^*$)
Polystyrene	C-C, C-H, C=C	230-280nm ($\pi=\pi^*$)
Aliphatic polyamides	C-C, C-H, N-H, C=O, C-N	220nm ($n=\pi^*$)

1.3.1 Degradation Mechanisms

Degradation mechanisms include photodegradation, photo-thermal degradation (oxidation), photo-oxidation, photolysis and photo-hydrolysis. However regardless of which degradation mechanism takes place it is widely believed that all the mechanisms involve free radical processes [9, 13]. It is also accurate to say that for most cases the degradation processes are similar to those found in thermal degradation with the only significant difference being the initiation step and the nature of the degradation products. Figure 1.13 shows the three major steps of initiation, propagation and termination involved in the free radical process.

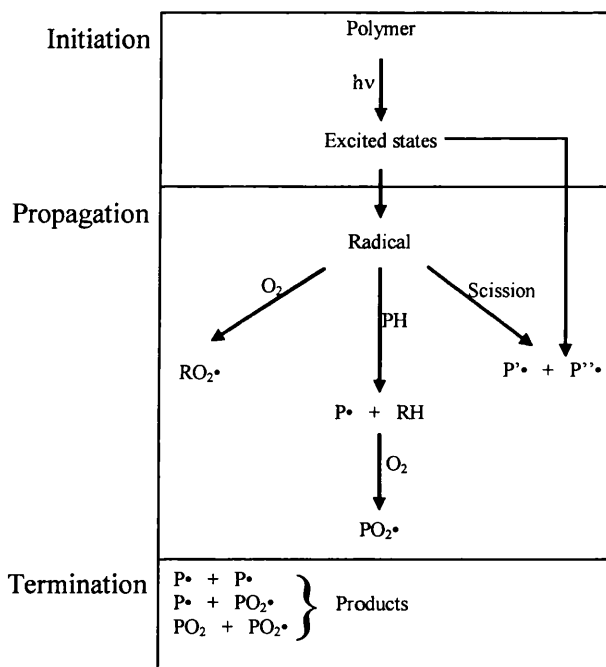


Figure 1.13: The overview of the free radical degradation mechanism.

1.3.1.1 Initiation

The processing of a polymer can have a significant effect upon its stability, its end use and the nature of the initiation process [21]. Table 1.6 shows some of the known chromophores that may be introduced by processing and their relevant process. The chromophores are introduced during de-polymerisation and/or processing stages as laid out by the Bolland-Gee auto oxidation mechanism shown in Figure 1.14.

Table 1.6 also shows some of the chromophores that are present in type B polymers and in this case the chromophore makes up part of the backbone of the polymer which will result in scission of the backbone when photo-cleavage occurs. Due to the high concentration of the aromatic chromophores and their tendency to be highly UV absorptive the reactions tend to develop quickly and therefore lead to the breakdown of the polymer backbone. A dramatic change in mechanical properties of the polymer will occur and thus type B polymers have a very limited use for exterior applications.

Table 1.6: Typical chromophores and their photochemical reactions

Functional Groups	Photochemical reaction	Process
Hydroperoxides	$\text{POOH} \xrightarrow{h\nu} \text{PO}\cdot + \cdot\text{OH}$	Homolytic cleavage
Peroxides	$\text{POOP} \xrightarrow{h\nu} \text{PO}\cdot + \text{PO}\cdot$	
Carbonyl	$\text{---CH}_3\text{---}\overset{\text{O}}{\parallel}{\text{C}}\text{---CH}_2\text{---} \longrightarrow \text{---CH}_2\cdot + \cdot\overset{\text{O}}{\parallel}{\text{C}}\text{---CH}_2\text{---}$	Norrish Type I Photocleavage
	$\text{---CH}_2\text{---CH}_2\text{---CH}_2\text{---}\overset{\text{O}}{\parallel}{\text{C}}\text{---} \xrightarrow{h\nu} \text{CH}_3\text{---}\overset{\text{O}}{\parallel}{\text{C}}\text{---} + \text{---CH=CH}_2$	Norrish Type II Photocleavage
	$\text{---}\text{C}_6\text{H}_4\text{---}\overset{\text{O}}{\parallel}{\text{C}}\text{---CH}_2\text{---} \xrightarrow{h\nu} \text{---}\text{C}_6\text{H}_4\text{---}\overset{\cdot}{\underset{\text{O}}{\parallel}}{\text{C}}\text{---CH}_2\text{---} + \text{P}\cdot$	Hydrogen abstraction
Unsaturation	$\text{---}(\text{CH}=\text{CH})_n\text{---}\underset{\text{Cl}}{\text{CH}}\text{---} \xrightarrow{h\nu} \text{---}(\text{CH}=\text{CH})_n\text{---}\overset{\cdot}{\text{C}}\text{H---} + \text{Cl}\cdot$	Allylic cleavage
Metals	$\text{M}^{n+}\text{X}^- \longrightarrow \text{M}^{(n-1)+} + \text{X}^-$	Electron transfer
Phenoxy	$\text{---}\text{C}_6\text{H}_4\text{---O---CH}_2\text{---} \xrightarrow{h\nu} \text{---}\text{C}_6\text{H}_4\text{---O}\cdot + \cdot\text{CH}_2\text{---}$	Cleavage
Polyester	$\text{---}\text{C}_6\text{H}_4\text{---}\overset{\text{O}}{\parallel}{\text{C}}\text{---O---CH}_2\text{---} \xrightarrow{h\nu} \text{---}\text{C}_6\text{H}_4\text{---}\overset{\cdot}{\underset{\text{O}}{\parallel}}{\text{C}}\text{---O}\cdot + \cdot\text{CH}_2\text{---}$	
Polyamide	$\text{---}\text{C}_6\text{H}_4\text{---}\overset{\text{O}}{\parallel}{\text{C}}\text{---NH---CH}_2\text{---} \longrightarrow \text{---}\text{C}_6\text{H}_4\text{---}\overset{\cdot}{\underset{\text{O}}{\parallel}}{\text{C}}\text{---} + \cdot\text{NH---CH}_2\text{---}$	
Polyurethane	$\text{---}\text{C}_6\text{H}_4\text{---NH---}\overset{\text{O}}{\parallel}{\text{C}}\text{---O---CH}_2\text{---}$	$\text{---}\text{C}_6\text{H}_4\text{---}\overset{\cdot}{\text{N}}\text{H} + \text{CO}_2 + \text{CH}_2\text{---}$
		$\text{---}\text{C}_6\text{H}_4\text{---NH}_2$ $\text{---}\overset{\text{O}}{\parallel}{\text{C}}\text{---O---CH}_2\text{---}$

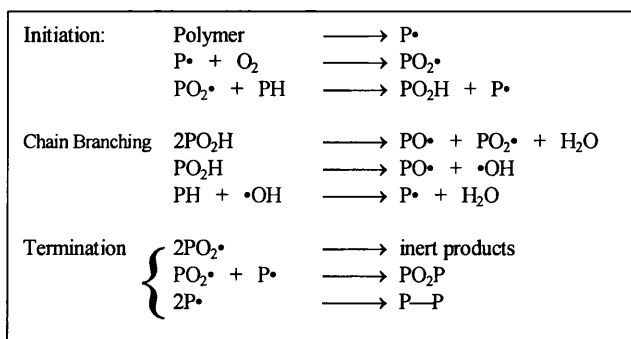


Figure 1.14: Bolland-Gee auto-oxidation mechanism.

When polymers are in their solid state, the mobility of any radical formed is severely restricted and leads to a relatively high recombination rate. This is shown in Figure 1.15 as this phenomenon is known as the Cage effect [18] and leads to a reduction in the efficiency in initiation.

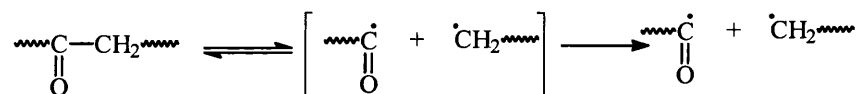
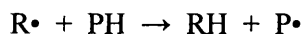


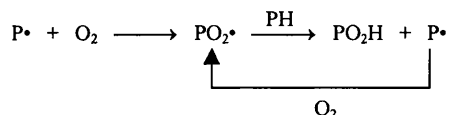
Figure 1.15: Cage recombination effect.

1.3.1.2 Propagation

During the initiation stage highly reactive free radical species (R•) are produced and are easily capable of abstracting a hydrogen from the polymer chain thus forming alkyl radicals (P•) [9, 13, 15].



These alkyl radicals will very quickly react with oxygen to form peroxy-radicals which will in turn also abstract a hydrogen atom and thus reform the polymer radical. This cycle will operate until a collision between two of the free radicals occurs and causes termination.



The uni-molecule pathway described above is not the only route through which degradation can occur. It can also occur via alkoxy or hydroxyl hydrogen abstraction from the polymer. These processes are termed Chain Branching, which is the main reason for auto-accelerated kinetics often observed in the photo-oxidation of the polymers as outlined in Figure 1.16.

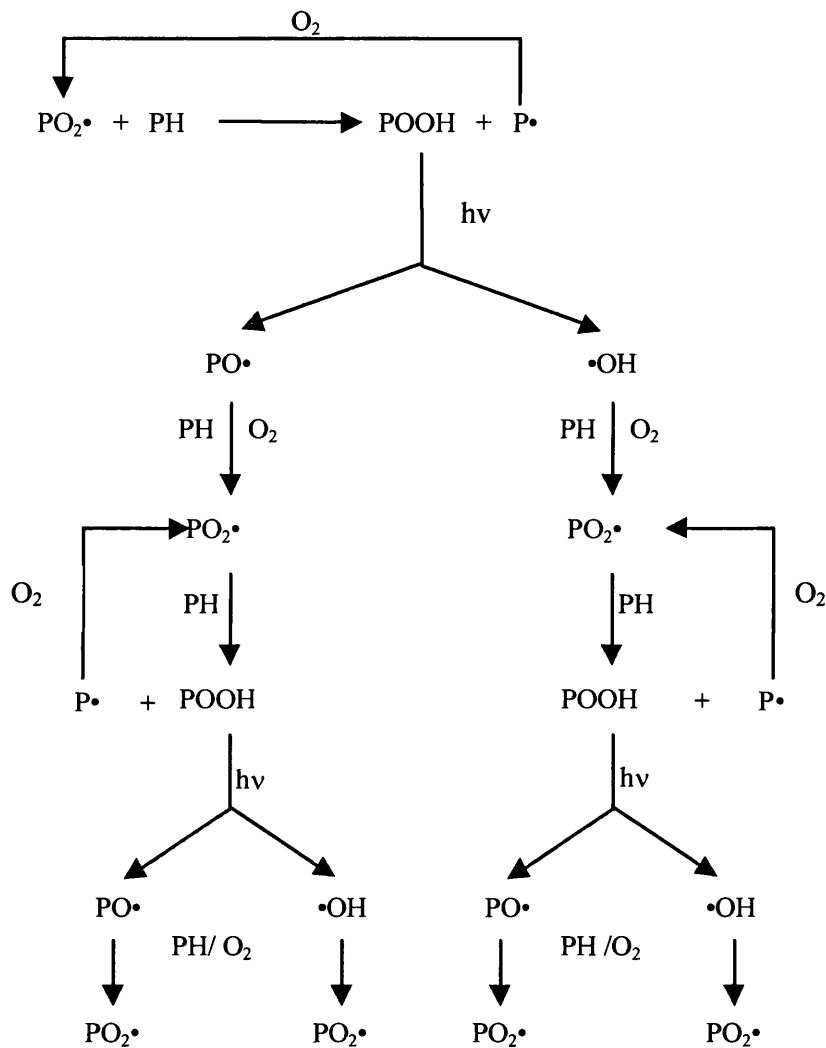


Figure 1.16: Chain branching caused by photo-oxidation.

The polymer matrix will restrict diffusion and as a result reduce the chain branching effect by favouring rearrangement of alkoxy-hydroxy radical pairs formed by the POOH photolysis [13].

This results in a cage reaction (Figure 1.17), which reduces the chain branching effect, but has the effect of producing ketone functions. These ketone functions are very effective chromophores and as a result potential initiators [9, 13, 15, 16].

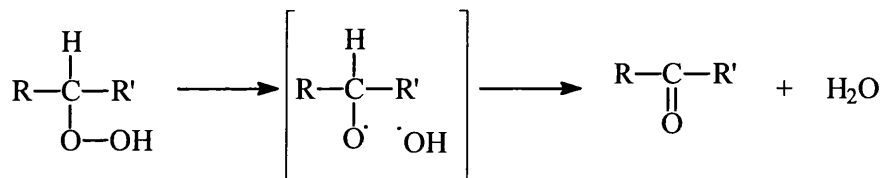
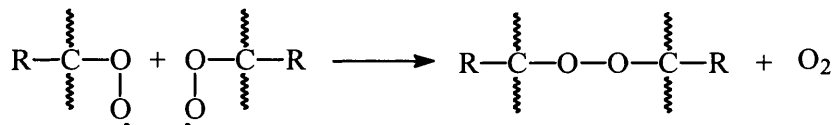


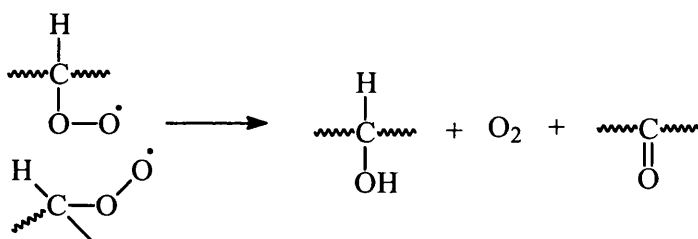
Figure 1.17: Typical cage reaction

1.3.1.3 Termination

Peroxy radicals tend to have relatively long lifetimes of several seconds and they have a high affinity for each other, which leads to the most likely source of termination. Combination of two PO_2^\bullet radicals via a bi-molecular pathway creates an unstable tetra oxide, which will rapidly lose oxygen to form a peroxide bridge between the two polymer molecules. This cross linking reaction will cause an increase in stiffness of the polymer.



Alternative routes through primary and secondary PO_2 radicals can terminate via a disproportionation reaction to produce ketone and alcohol functions [17].



In systems where oxygenation is poor the controlling process will be the diffusion of oxygen into the matrix and as a result alkyl radicals may become involved in the termination process. The termination reaction leads to polymer cross linkages. Overall there are three types of possible bridge group. The chain length after oxidation will be significantly different between different polymer types. It will depend on factors such as chemical structure, light intensity, O₂ permeability and the reactivity of the peroxy and alkoxy radicals. An overall simplified flow diagram of photo-oxidation in polymers is shown in Figure 1.18.

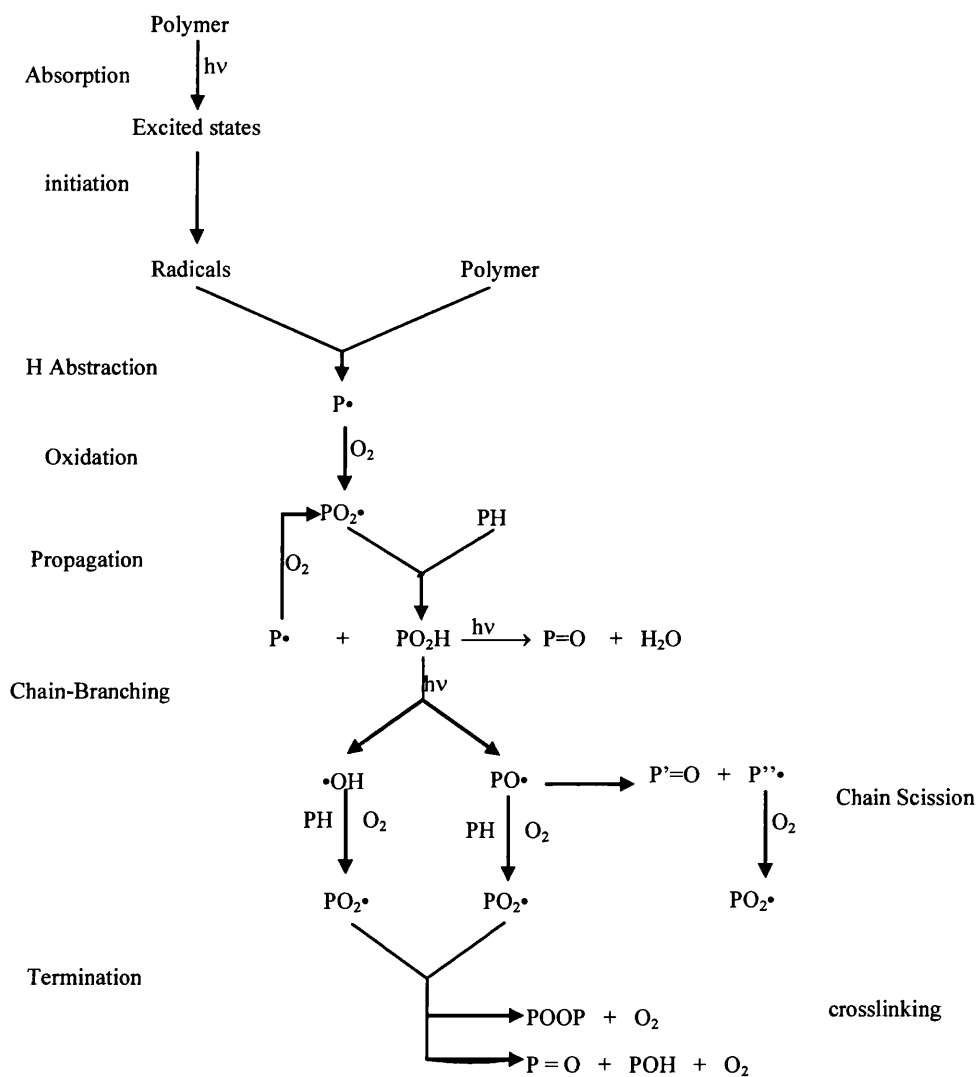


Figure 1.18: Flow diagram of photo-oxidation reactions in polymers

1.3.2 Dehydrochlorination of PVC

Dehydrochlorination of PVC is of particular relevance to this work and the elimination reaction of HCl from PVC is shown in Figure 1.19. This reaction proceeds via cleavage of the C-Cl bond to produce two radicals [13, 17]. The chlorine radical then abstracts a hydrogen atom from a different chain to produce HCl, chain transfer will proceed causing an unzipping action along the chain producing polyconjugation (the conjugated sequence length has been shown to be between 2 and 4 in both air [22, 23] and nitrogen [22]). This leads to conjugated polyenes (poly-ene sequence as shown in Figure 1.20) and causes the yellowing of PVC, as the absorption spectrum of the polymer enters the lower region of the visible spectrum in by the formation of the alternative double bonds.

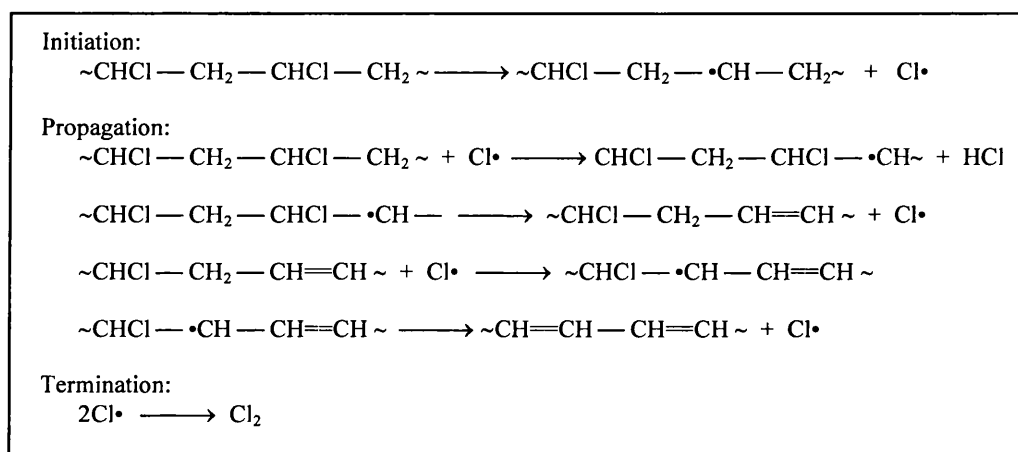


Figure 1.19: The radical dehydrochlorination of PVC



Figure 1.20: The conjugation polyenes and the unzipping of PVC.

1.4 Ultra Violet (UV) Stabilisation of Polymers

Any polymers that are going to be used in a high UV environment must contain UV stabilisation. This can be achieved in one of two ways, either by physically or chemically blocking the photodegradation reaction and four different classes of UV stabilising systems have been developed.

- UV absorber
- UV screening
- Excited state quench
- Free radical scavenging

The two stabilisation methods (Excited state quench and Free radical scavenging) are believed to be the most efficient, although in PVC UV absorbers tend to be the most widely used commercially. When deciding upon the UV stabilisation method it is necessary to consider the compatibility with the polymer type used.

1.4.1 Ultra Violet Absorbers

These are chemicals which preferentially absorb the UV region of light (between 295 nm and 400 nm) over the polymer and are then able to dissipate the energy in a harmless form. Although still allowing the transmission of light above 400 nm in the visible region, Ultra Violet Absorbers (UVA) tend to be most effective when used in thicker coatings and this is due the limitations of the Beer-Lambert law.

A = εcl	A	=	Absorbance
	ε	=	Molar absorbtivity constant
	c	=	Concentration
	l	=	Pathlength (thickness)

Stabilisation by UVAs alone has been discounted commercially as in order to be 100% effective all the absorption would need to occur at the surface of the coating where most of the photodegradation occurs [24-26].

The two main types of UVA are hydroxy-benzophenones and hydroxy-phenyl-benzotriazoles. Hydroxy-benzophenones absorb UV light and convert it into harmless heat energy by forming a reversible six-member hydrogen ring [12, 26, 27]. This reversible reaction of UV absorption and heat dissipation leaves the absorber unchanged and therefore it can undergo many cycles of UV absorbance so long as no other process interferes with the reaction as shown in Figure 1.21. The benzotriazoles work in a slightly different way, as they dissipate the heat by a proton transfer reaction (heat) shown in Figure 1.22.

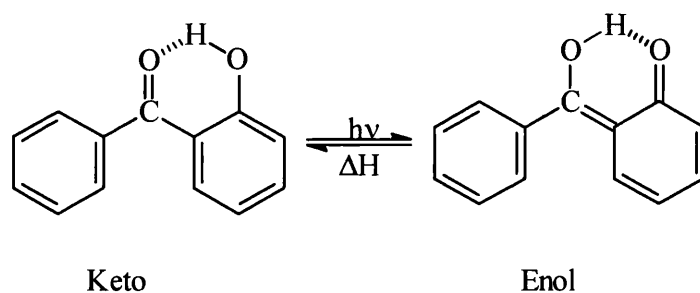


Figure 1.21: Keto/enol tautomorphism energy dissipation mechanism in hydroxy-benzophenone.

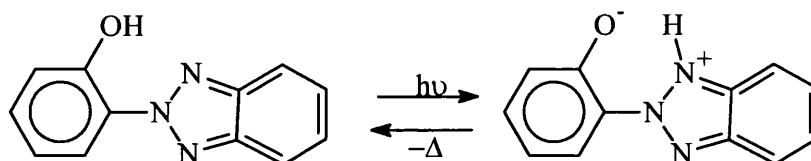


Figure 1.22: Benzotriazole stabilization mechanism in hydroxy-phenyl-benzotriazole.

1.4.2 Hindered Amine Light Stabilisers (HALS)

These are relatively new components in the UV stabiliser market and are particularly effective in polymer applications. The exact mechanism by which they function is not completely understood but it is believed to be a mixture of the following mechanisms listed below and shown in Figure 1.23.

- Chain breaking donor/acceptor redox mechanism through the formation of nitroxyl radicals that terminate and deactivate alkyl and peroxy radicals.
- Decomposition of hydroperoxides by the amine during processing.
- Inhibition of the photoreaction of α , β – unsaturated carbonyl groups in polyolefins.
- Reduction in the quantum yield of hydroperoxide photolysis.
- Singlet oxygen quenching – only polydienes.
- Complexation with hydroperoxides/oxygen.
- Complexation with metal ions.
- Excited state quenching via the nitroxyl radical.

HAL's work by interrupting and disturbing the degradative free radical reactions and they don't rely solely on the physical absorption of UV light, therefore their efficiency is not dependant upon them being at a high concentration on the surface of the coating.

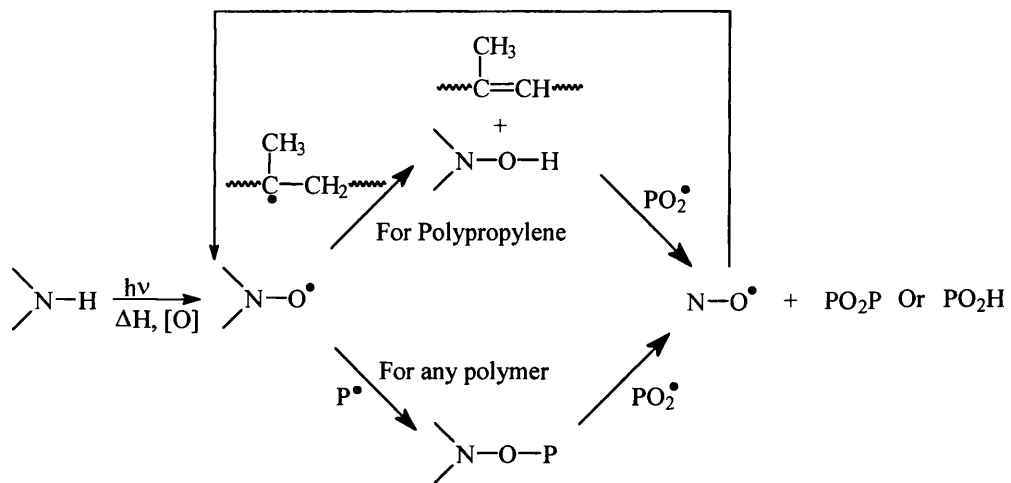


Figure 1.23: Cyclic mechanism of HAL stabilisation [13, 28].

1.5 Thermal Degradation

It is crucial to know and understand this degradation mechanism to distinguish it from other degradation mechanisms that may be of interest. Thermal degradation is probably the only mechanism to which all polymers are susceptible. All polymers are susceptible to heat eventually, although the larger polymer molecules are more susceptible to thermal degradation than their smaller monomer components. This is due to larger molecules being able to be broken down into smaller components whereas monomer components cannot. Also polymers will be more susceptible to thermal degradation as during the commercial processing stage, structural changes can be induced within the polymer leading to a more complex molecule [9, 13, 15, 16]. For example in PVC these structural changes can cause formation of head to head links [16], branches [16, 21], un-saturation [21, 22], and various impurities [21, 22, 29, 30], which are all shown in Figure 1.24.

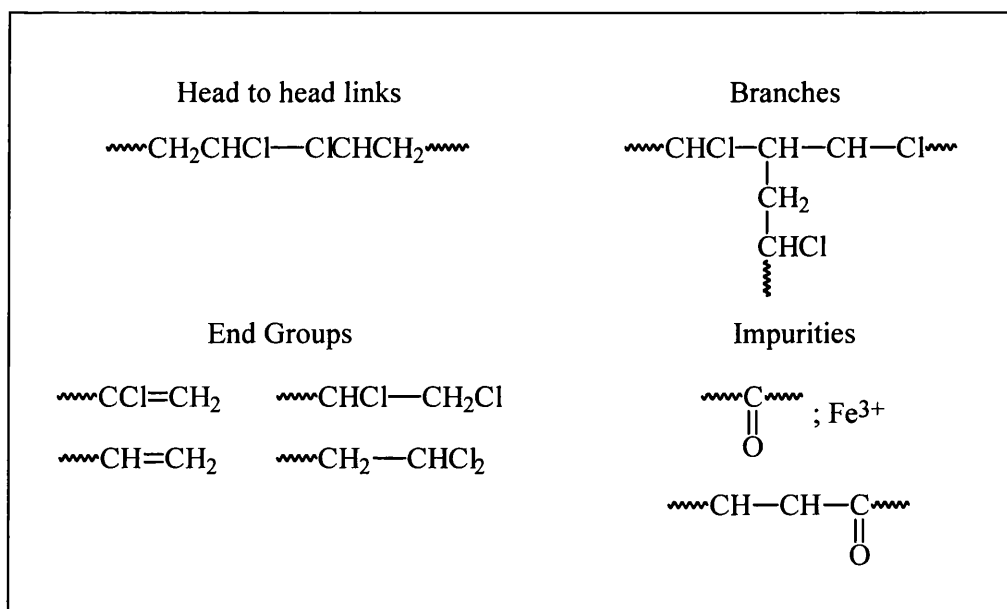


Figure 1.24: Common groups introduced during polymerisation and processing

1.5.1 Mechanism of Thermal Degradation

Different polymers will have their own specific mechanisms of thermal degradation, although these mechanisms tend to fall into one of three general categories (Elimination Reaction, Depolymerisation or Substitution),

Elimination Reaction

In this case degradation products tend to be of low molecular weight and are unrelated to the structure of the polymer. A typical example of this would be the degradation of PVC to produce HCl (dehydrochlorination).

Depolymerisation

This mechanism forms degradation products, which are similar to that of the main polymer but with lower molecular weight via a chain scission process (Radical Depolymerisation).

Functional Group Change

This mechanism is when the functional group of the polymer is changed e.g. in the case of PVC the C-Cl bond can be substituted for a C=C leading to conjugation.

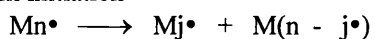
These degradation reactions all lead to changes in the molecular weight distributions of the polymer [22, 31, 32]. This can have a significant effect upon the physical and chemical properties of the polymer.

The overall stability of a polymer is thought to be affected by the strength of the primary valence bonds [13]. This is due to the degradation of the polymer involving the scission of the polymer backbone, therefore the stronger this polymer backbone becomes the more stable the polymer becomes. For example, the introduction of C-F bonds in PTFE makes the polymer much more stable than polyethylene. The introduction of aromatic rings with their bond strength and displacement of C-H bonds also increases stability.

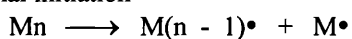
1.5.1.1 General Degradation

Figure 1.25 shows the different processes which are in operation during the degradation process and random initiation will cause the original polymer chain to split into two unequal length fragment radicals.

Random initiation



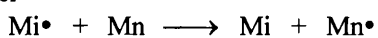
Terminal initiation



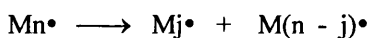
Depropagation



Transfer



Scission



Termination



Figure 1.25: General mechanism of free radical degradation

Terminal initiation represents the loss of a single monomer unit from the end of the original polymer chain to produce a single monomer radical and a macro radical. Depropagation is the splitting of a single monomer unit to form a macro radical. Transfer displays the ability of a radical to transfer its activity to another polymer chain. Scission is the removal of a macro radical from the polymer chain resulting in the formation of two or more macro radicals. Termination is the combination of two macro radicals to produce two unequal length polymer chains.

1.5.2 Oxidation Reactions

In the presence of oxygen most polymers tend to undergo rapid chain scission [29] below their melting points [9, 13, 15]. These species rapidly breakdown to produce more free radicals [33]. This process is autocatalytic and the initiation step is thought to involve either hydroperoxide [34, 35] and/or carbonyl groups [13] as described by the Bolland Gee auto-oxidation mechanism shown in Figure 1.15.

In Figure 1.26 the reaction profile for the formation of carbonyl and hydroperoxide groups are shown. The hydroperoxide initially builds up and this is caused by the oxygen scavenging the alkyl radicals. This reduces rapidly as the number of chain branching steps increases.

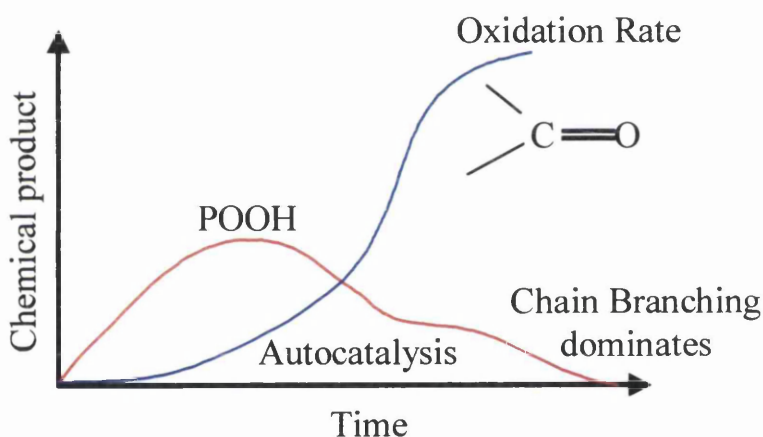


Figure 1.26: Reaction profile for the oxidation of polyethylene [34].

The significant factor affecting the rate of oxidation of the polymer will be the physical state of the polymer. If the polymer is amorphous or crystalline this will affect the rate at which oxygen can diffuse into the polymer as shown in Figure 1.27. Also with the introduction of additions such as plasticisers, this will change the structure of the polymer and therefore the porosity and diffusion characteristics will have changed.

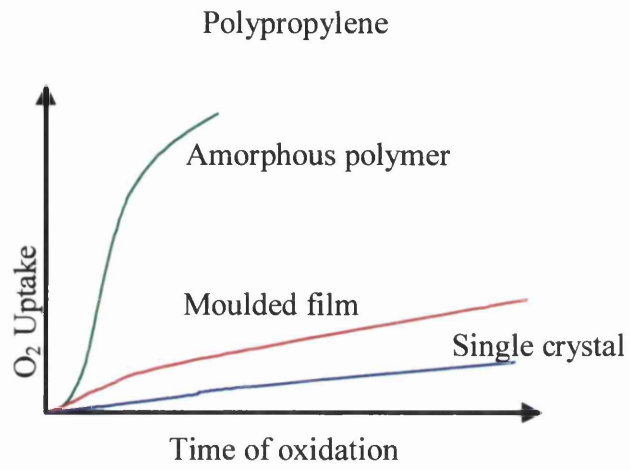


Figure 1.27: Degradation rate of Polypropylene at 130°C for different states [36].

1.6 Thermal stabilisation of PVC

The dehydrochlorination of PVC outlined above and the stabilisation of these polymers is more complex. The HCl in PVC degradation forms a redox complex with the hydroperoxides and accentuates the degradation process. There are a number of methods that stabiliser systems for such polymers act [37].

- Absorb or otherwise neutralise the HCl.
- Displace labile chlorine atoms thus eliminating initiation sites.
- Neutralise or deactivate the stabiliser degradation products, this can be considered as stabilising the stabiliser.
- Classic antioxidant disruption.
- Neutralisation or replacement of polymer impurities such as end groups or metallic impurities.

To complete these functions there are three stabilising reactions.

1.6.1 The Binding of Hydrogen Chloride

An example of this is the addition of sodium carbonate or the use of alkaline inorganic substances in the emulsion polymerisation of vinyl chloride. The modes of operation for some commonly used stabilisers are shown in Figure 1.28.

1.6.2 The Exchange of Labile Chloride Atoms

Barium and Cadmium salt stabilisers operate via this mechanism and the resulting metal chlorides formed during these reactions are strong Lewis acids and can catalyse further ionic dehydrochlorination. The displacement reaction is shown in Figure 1.29.

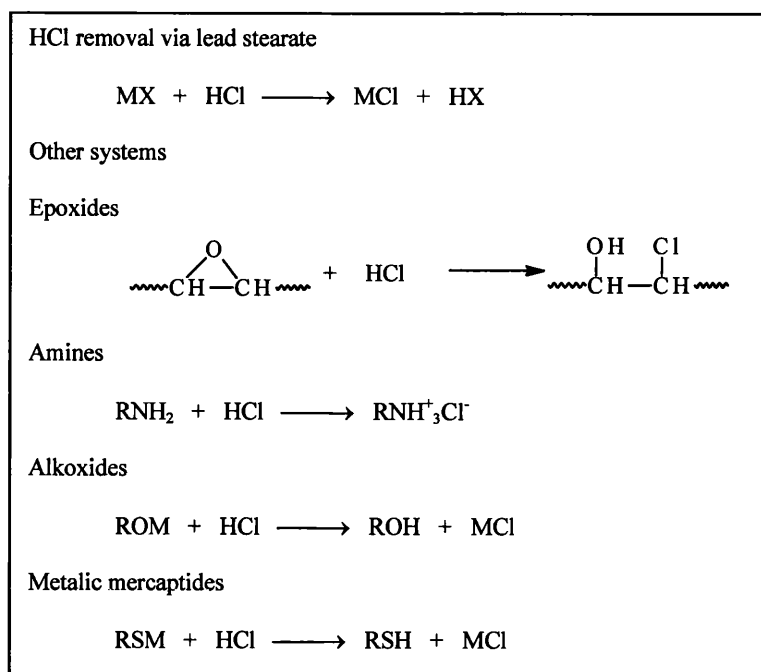


Figure 1.28: Mechanisms of HCl removal.

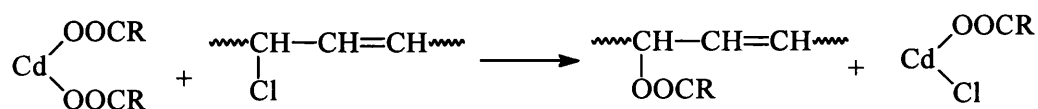


Figure 1.29: Displacement of the labile chlorine atoms by cadmium carboxylates.

The Lewis acids can be removed using less electrophilic alkaline earth metal carboxylates such as barium or cadmium. These reactions are shown in Figure 1.30.

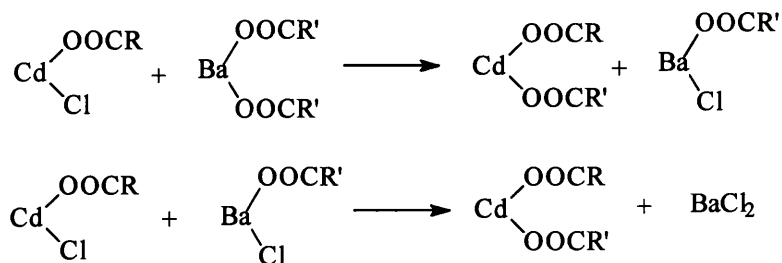


Figure 1.30: Removal of the heavy metal chlorides

It has also been shown that the addition of a chelating agent, such as organic phosphites, in the correct ratio can decidedly improve the overall heat stability of PVC [38]. Figure 1.31 shows effect for a range of chelator to Ba/Cd ratios.

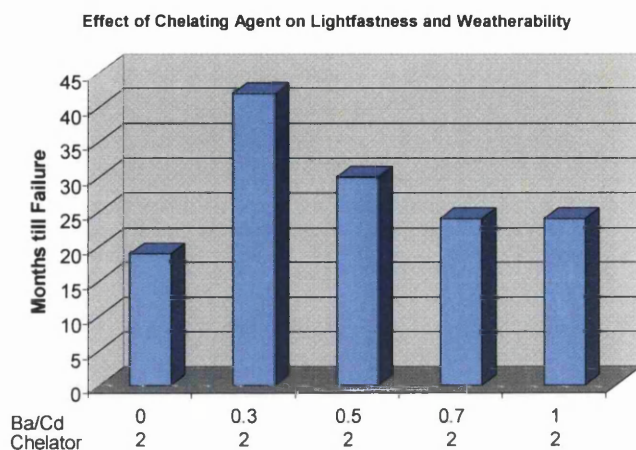


Figure 1.31: The effect of chelating agent ratios on the light fastness and weathering resistance of PVC.

It has also been shown that treatment with organoboron reagents selectively replaces allylic chloride atoms on the PVC chain with hydrogen. This results in an improved dynamic and static thermal stability [39].

1.6.3 Addition of Stabilisers or Their Reaction Products to Polyene Sequences

Tin Maleates undergo a Diels Alder reaction across a double bond as well as a reaction with HCl, as shown in Figure 1.32.

The organo tin mercaptides react with HCl to form the mercaptan and this is capable of an additional reaction across the double bond of a polyene sequence.

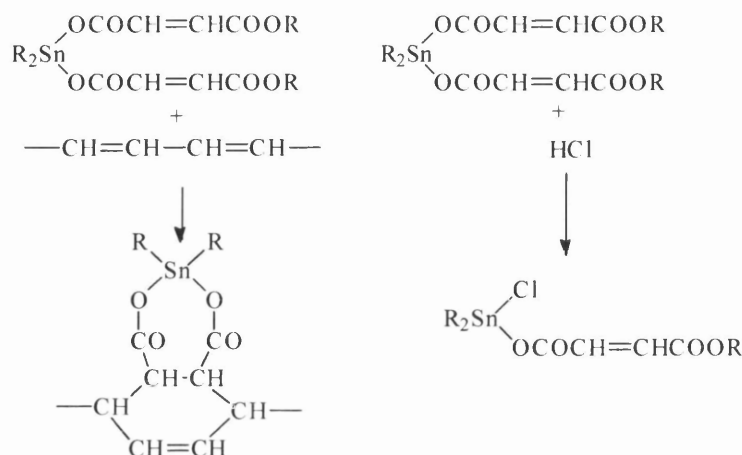


Figure 1.32: Dual action stabilisation mechanism of Tin Maleates.

These stabilisers or stabiliser mechanisms will rarely be used alone in a polymer system and usually complex mixtures of additives will be used to gain the most efficient stabilisation. Quite often the result of multiple stabilisers are not additive, but undergo synergism, where the effect of one complements the other such that the combined effect is greater than the individual components. This is quite often the case where a radical chain inhibitor is used in combination with a metal ion deactivator and a hydroperoxide decomposer. The opposite effect can also occur which is not desirable and here the components are said to interact antagonistically. Figure 1.33 shows both these effects schematically.

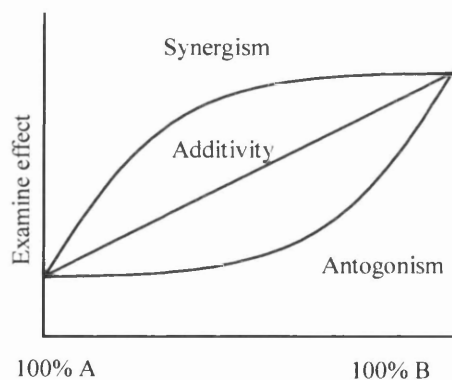


Figure 1.33: The effects of synergism and antagonism.

The synergistic effect is highly desirable and is thought to operate by a mechanism where each component stabilises and protects the other therefore enhancing the performance.

1.6.4 Hydrotalcite

Hydrotalcite (HT) ($\text{Mg}_6\text{Al}_2(\text{OH})_{16}\text{CO}_3 \cdot 4\text{H}_2\text{O}$) is a commercially available white anionic clay. Anionic clays are natural or synthetic lamellar mixed hydroxides containing exchangeable anions [40]. A number of anionic clays exist with differing chemical composition or crystallographic parameters and all fall under the general term Hydrotalcites or layered double hydroxides (LDH) [41]. Hydrotalcite in this thesis refers to a specific Mg/Al hydroxycarbonate known for its ease and low cost of synthesis. Figure 1.34 shows the structure of Hydrotalcite and it exists as a layer type lattice due to the small twofold positively charged cations proximity to the highly polarisable OH^- ions [42].

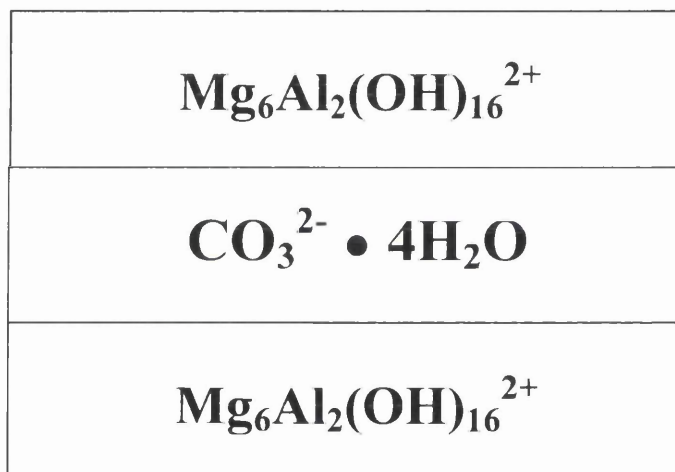


Figure 1.34: The structure of Hydrotalcite [43].

Hydrotalcite has the isomorphous substitution of metal atoms such as Al^{3+} with Mg^{2+} in octahedral positions resulting in the brucite layers becoming charged. Alternative cations can be used provided they have a higher charge than Al^{3+} and similar radius [44]. Electroneutrality is maintained by anions (e.g. CO_3^{2-}) located in the disordered and hydrated interlayer space.

It is possible for clays to accommodate a wide range of anions into the interlayer space although carbonate is the preferred anion with only a few other variations [41, 45, 46]. A wide range of ions have been reported for synthetic clays from organic anions [47, 48] to highly unstable V^{3+} ions [49] allowing the creation of tailor made materials able to fulfil specific requirements. Thus the ability of hydrotalcites (HT) to behave as ion exchangers and the use of HT in plastisol coatings is a way of stopping the evolution of HCl as the Cl ion will exchange with the carbonate to produce a weak carbonic acid which is unable to catalyse photodegradation.

The hydrotalcite (HT) used in this thesis was supplied from Aldrich and in previous work [43] showed hydrophobic tendencies when added to water. After gas chromatography and mass spectrometry the waxy substance coated on the HT showed to be stearic acid (octadecanoic acid) [43]. It has been added to the hydrotalcite by the supplier to improve its dispersal qualities in organic species.

1.7 Plasticisers

Plasticisers are generally high boiling point organic liquids and most are ester based. Plasticisers are added to a polymer to improve specific properties of the film, increasing the workability and flexibility. The plasticisers are known as external plasticisers as they are not part of the molecular structure of the polymer as internal plasticisation refers to modification of the polymer structure to lower its T_g. As plasticisers are not actually part of the structure there is a potential for volatile loss and leaching of the plasticiser. This problem is generally reduced with higher molecular weight plasticisers.

A plasticiser must have the following important characteristics. When mixed with the polymer it should appear effectively homogenous and not show any indication of the plasticisers or chemically interact with the polymer.

1.7.1 The Mechanisms of Plasticisation

Many theories are debatable as an explanation for the physical changes induced by the introduction of plasticisers. The more common theories are shown below of which detailed explanation can be found in literature [6].

- Lubricity Theory
- Gel Theory
- Free Volume Theory
- Solvation Desolvation Equilibrium
- Generalised Structure Theory
- Interaction Parameters
- Spectroscopic Studies of General Interactions

The above theories apply to different parts of the plasticisation process but the plasticisation process can be simplified to:

- Initial mixing which induces wetting of the particles of the resin surfaces.
- Temperature is increased leading to penetration by the plasticiser into the resin particles.
- When the temperature reaches the processing temperature of the resin, the polymer chains separate due to the breakdown of the dipole-dipole interactions. This allows the plasticiser to form solvent like interactions with the resin, leading to the resin now being in a much more formable state.
- When the temperature drops after the formation process, the polymer chain dipole-dipole interactions reform and lead to a new structure incorporating the plasticiser molecules. This creates a plasticised resin with its own unique properties.

A plasticiser can be thought of as a partly strong attractive group which attaches to the resin molecules and partly flexible groups which lie in between these attractive groups. This allows for much greater relative movement between the resin molecules and is shown in Figure 1.35 proposed by the Leuchs model [50]. This model is particularly relevant to the type of plasticisation induced by phthalates.

The use of phthalates varies widely depending on the chain lengths of the R group. Table 1.7 shows the use of phthalates and main side chain lengths. The popularity of phthalates is as would be expected due to the combination of cost effectiveness and high performance characteristics.

Table 1.7: Typical applications of different phthalate species.

Carbon Chain Number	Main Area of Use
1	Solvent for resin cure Initiators
2	Plasticiser for cellulose acetate
3	Unknown in a commercial context
4	Plasticisers for polyvinyl acetate
5	Small amount of use in PVC
6	Relatively unknown commercially
7	Plasticiser for fast processing application
8 to 10	Main group of PVC plasticisers
11 to 13	Low volatility PVC plasticisers
14 to 16	Unknow commercially
17	Processing lubricant for PVC

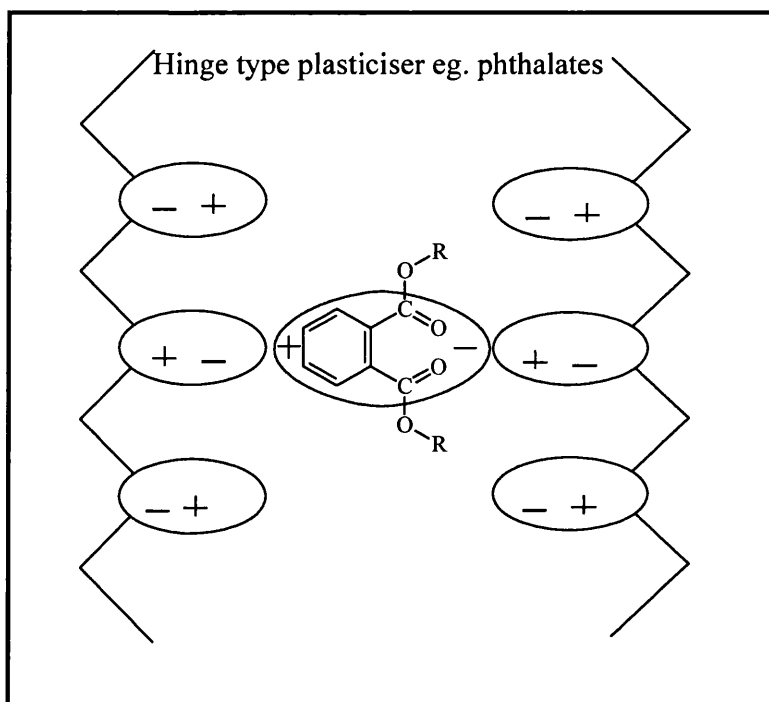


Figure 1.35: Model of a hinge type plasticiser (Leuchs') [50]

1.7.2 Production Process

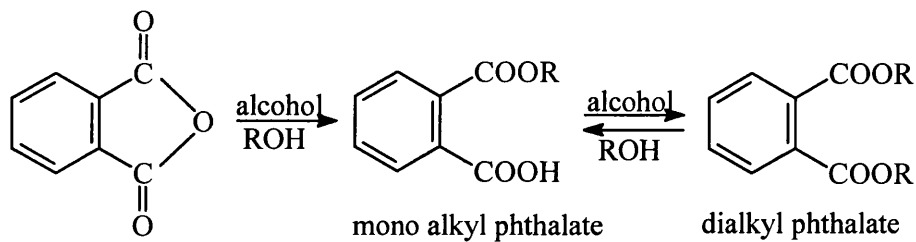


Figure 1.36: Production process of dialkyl phthalate.

The phthalates are manufactured from phthalic anhydride and alcohols via an esterification reaction (Figure 1.36) with the phthalic anhydride produced by catalytic or oxidation of either naphthalene or primarily orthoxylene. More details of the production process and application can be found in the literature [50, 51].

1.8 Titanium Dioxide

Titanium Dioxide (TiO_2) is a white inorganic pigment and accounts for 66% of inorganic pigment trade [52]. The pigment generally makes up 14-20% volume of white paint and is one of the most expensive components.

Titanium dioxide pigment is a fine white powder and is used in paints, plastics and paper. It provides for maximum whiteness and opacity and gives paint high hiding power, meaning the ability to mask or hide a substrate and does this more effectively than any other white pigment. Titanium dioxide is by far the most important material used by the paints industry for whiteness and opacity. These unique properties are derived from the refractive index of titanium dioxide. Titanium dioxide has the highest refractive index of any material including diamond. In Europe, 50% of TiO_2 is used in coatings, 25% in paper and 20% in plastics. The remaining 5% is used in both pigmentary applications (inks, floor covering, sealants, food etc.) and non pigmentary applications (ceramics, welding rods, catalysts, etc) [53].

Two major pigments, titanium dioxide and carbon black have a monopoly within the pigment industry as there is no effective competition. The dominance of TiO_2 in the pigment market is enhanced by the fact that a white pigment is required to make all colours apart from black, while any single coloured pigment is only used in a range of shades.

Titanium occurs in many abundant minerals, five of which serve as ores; Ilmenite (FeTiO_3), Rutile (TiO_2), Anatase (TiO_2), Brookite (TiO_2) and Leucosene ($\text{TiO}_2 \cdot \text{XFeO} \cdot \text{YH}_2\text{O}$).

The first commercial titanium dioxide was Anatase, while today it has been displaced by Rutile in coatings and plastics due to the 20% increase in scattering ability when held in a polymer matrix and enhanced photostability of Rutile. Anatase is still a popular choice in the manufacture of paper and other synthetic fibres where

photostability is less important. These two crystal phases differ in lattice structure, refractive index and photoactivity.

1.8.1 Manufacturing Process of TiO₂

There are two main processes by which TiO₂ is manufactured, the older of which is known as the Sulphate Process which is based on aqueous chemistry while the newer is known as the Chloride Process and uses flame technology. The Sulphate Process is largely a batch process, low tech and labour intensive whereas the newer process is more continuous and generally produces a much higher quality product but requires much higher grade ore.

1.8.1.1 The Sulphate Process [54]

The titanium rich ore (FeTiO₃) is firstly dissolved in hot concentrated sulphuric acid, with the addition of scrap steel to keep the iron and other impurities in their more soluble oxidation states. Lower iron content ores like Rutile or Anatase are advantageous in terms of waste disposal but dissolve too slowly in the acid. The resulting titanyl sulphate solution is hydrolysed thermally to precipitate titanium oxyhydroxide, calcination of this will then yield Anatase. The introduction of Rutile seed crystals can be used during the hydrolysis stage to produce TiO₂ in the Rutile phase. The presence of a small amount of niobium in the ore can create semi-conduction properties within the crystal and absorption of visible light thus causing discolouration.

The size of TiO₂ crystal can be regulated by the addition of phosphorous as it cannot penetrate the crystal lattice and thus remains on the crystal surface. As the crystal grows the actual total surface area of the crystal will decrease and the phosphorous concentration at the surface increase. A critical concentration of phosphorous is reached and it blocks further crystal growth, thus ensuring a homogenous crystal size optimized for light scattering. Phosphorous can be added if the ore doesn't contain enough to get the required crystal size.

1.8.1.2 The Chloride Process [54]

The second manufacturing process is called the chloride process and was developed by DuPont in the 1950's for commercial use. The process is superior to the sulphate process as quality is higher there is less waste disposal and the process requires less energy input. The ore is first prepared by beneficiation to remove unwanted components and prepare the ore for chlorination with the addition of dry pulverized coke. The mixture is then added to the chlorinator and fluidised at 900-1700°C. The chlorination reaction proceeds exothermically and the chamber needs to be cooled. Titanium tetrachloride and various other metal chlorides exit the chamber as a gas mixture with some other blow over particles. The gas mixture is cleaned to leave only titanium tetrachloride (TiCl_4), this is then condensed and purified by distillation. Any remaining contaminants will only be present in levels of parts per million (ppm).

To gain the desired particle size the TiCl_4 is firstly vapourised and then flamed using a specifically designed reactor, which is optimised to prevent plugging and yields the desired crystal size. Due to the reaction being only slightly exothermic the TiCl_4 is preheated to maintain the flame. The flame reactor can be used to introduce co-oxidants such as AlCl_3 , which help to promote the formation of Rutile and minimize aggregation.

The chloride released during the oxidation process is collected and recycled back to the chlorinator with the TiO_2 pigment left behind. Any further chlorine that remains within the solid TiO_2 can be removed using aqueous hydrolysis. A schematic comparison of the two processes is shown in Figure 1.37.

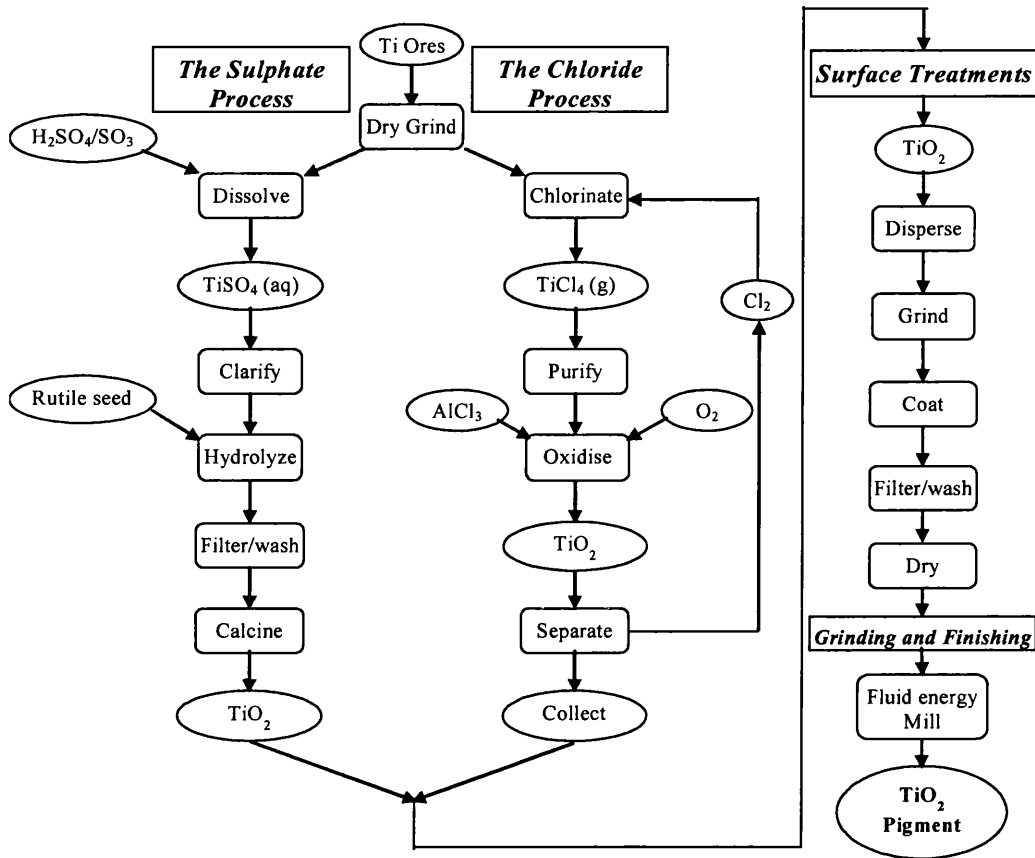


Figure 1.37: outline of the basic processes involved in the chloride and sulphate process.

1.8.1.3 Surface Treatments

Refining and improving the specific properties of titanium dioxide can be performed by the particles being coated with a variety of oxides or oxy-hydrates. These coatings can be used to improve/moderate the durability, gloss and dispersability of the pigment. The processes used for coating the pigment are colloidal in nature meaning that minor alterations in the processing conditions can greatly affect the final product performance. For these reasons the exact conditions used during the processing of pigments tend to be a closely guarded secret within the TiO₂ industry.

Developments in processing methods mean that large agitated vats have been replaced by more continuous types of processing. The most popular precipitates used for surface treatment are aluminium and silicon oxy-hydrates and are added to levels of

about 1%. Although both oxides and oxy-hydrates of zirconium, tin, zinc, cerium and barium are also used with many more suggested in the patent literature [55-57].

The coatings covering the TiO_2 pigments are only a few atoms thick, covering primary particles that are typically of the order of 30nm. Understanding the lattice and chemical nature within these coatings is limited as most structure analysis techniques are not sufficiently sensitive. There are potential problems as to whether the partly silica coating is deposited in amorphous or crystalline form as shown in Figure 1.38. If the coating is microcrystalline in nature this allows penetration of oxygen and water vapour to the surface of the TiO_2 particles.

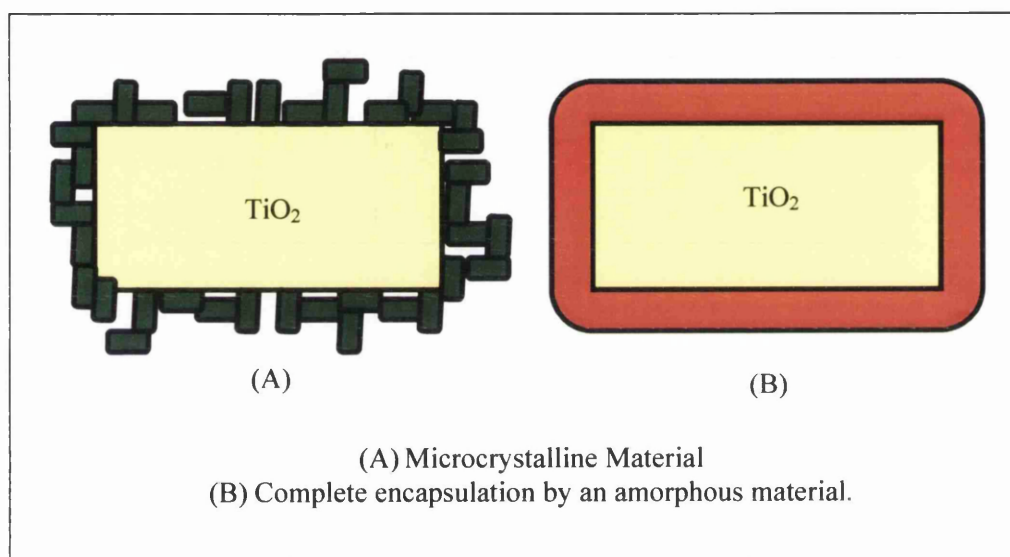
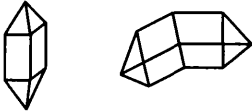
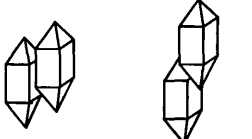
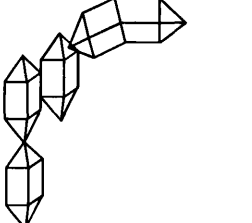


Figure 1.38: Crystalline and amorphous coatings of TiO_2

1.8.1.4 Grinding and Finishing

It is uneconomical and difficult to grind TiO_2 crystals to a uniform sub-micron size due to the high bond strengths and densities. This is overcome by the crystals being actually grown to the required size via chemical reactions or by the ripening of sub-crystalline assemblies.

Table 1.8: TiO₂ particle assemblies.

	<p>Primary Particles: These are single TiO₂ crystals or their crystallographic twins. (twins are two or more lattices inter-grown to some deducible law of symmetry) They range in diameter from 0.1 to 0.3 μm.</p>
	<p>Aggregates: These are primary particles that are connected via grain boundaries, they share crystal faces.</p>
	<p>Agglomerates: These are assemblies of crystallites and aggregates that are bonded together via weak forces, they adhere together at edges and faces.</p>
<p style="text-align: center;">Not Pictured</p>	<p>Flocs: these are associations of smaller particle assemblies that are bonded extremely weakly. They form spontaneously and disperse under modest shear. They are composed of crystallites, aggregates and agglomerates joined across corners or held together by short range attractive forces.</p>

To achieve the maximum hiding power within a coating, it is important to find the optimum particle size for light scattering. The optimum light scattering of TiO₂ pigment used to be found by trial and error of particle size until the introduction of the Mie theory [58]. The theory is used to calculate the best size for the scattering of white and green light. The scattering of green light is important because the human eye is more sensitive to the green light wavelengths and therefore these measurements can be used to calculate the brightness of a pigment as perceived by the human eye.

The slight drawback of the Mie theory is that it assumes particles are all spherical in shape and are of constant particle size. In paint this is a very unlikely scenario although when considering the shapes of the particles and all the different combinations possible

along with the difficulty in describing the distribution of the particles the differences are accepted.

Grinding of the TiO_2 pigment is still required to breakdown agglomerates and aggregates (Table 1.8) which can be formed during the manufacturing stage using a fluid energy mill.

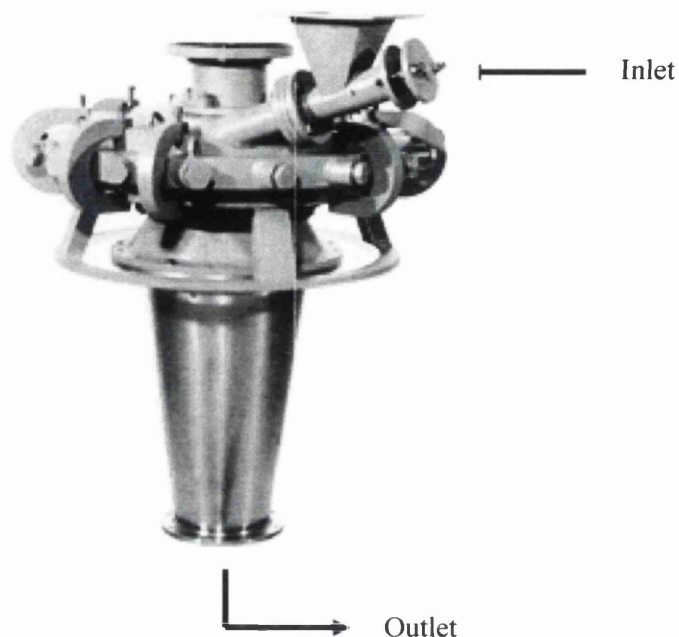


Figure 1.39: A typical fluid energy mill.

A fluid energy mill (Figure 1.39) uses steam (usually) to accelerate the pigment particles to very high speeds and due to the high particle density within the mill collisions occur and are therefore separated. With the enormous number of particles that are present inside the grinding chamber collisions between the wall and particles contribute very little to the grinding effect. The fragments tend to lose speed and are then hit by other particles therefore leading to further breakdown. A fluid energy mill also has the capability to roughly grade the particles by the effect of fluid flowing towards the centre of the chamber where it is discharged. This flow drags particles with it and centrifugal forces oppose this. Larger particles oppose this drag far more and they are thrown

outwards where they are ground further. The exhaust from the fluid mill is then channeled to a cyclone (gas-solid separator) to recover the pigment.

The fluid energy mills are very effective at grinding small particles while a pre-grinding stage is required for large particles especially from the sulphate process. The sulphate process kiln discharge is often pre-milled in a ball mill, which uses a drum half filled with balls where the particles fall under gravity. Once a certain ground size has been obtained, the ball mills become ineffective at grinding and the particles are transferred to fluid mill. Once the required size ($\sim 0.1\mu\text{m}$ to $0.5\mu\text{m}$) has been reached the hot pigment is transferred to transport containers or bags and due to its excellent thermal insulating properties it therefore takes a while to cool.

1.8.2 Characteristics of TiO_2

The main advantage of TiO_2 over other white pigments is its excellent optical properties which out perform the others. TiO_2 is non toxic, unlike some lead based pigments, so combined with its relatively high natural abundance makes it a very economical, high purity and inexpensive particle size control inorganic chemical.

TiO_2 is available commercially in two crystal phases (Figure 1.40). Anatase is used in paper production, foods and less demanding products and Rutile which is predominantly used for paints and in particular exterior paints eg HPS200 etc. Both pigments have extremely high refractive indices, are chemically inert, safe to produce, process and dispose of and similarly priced around £1.40 per kilo.

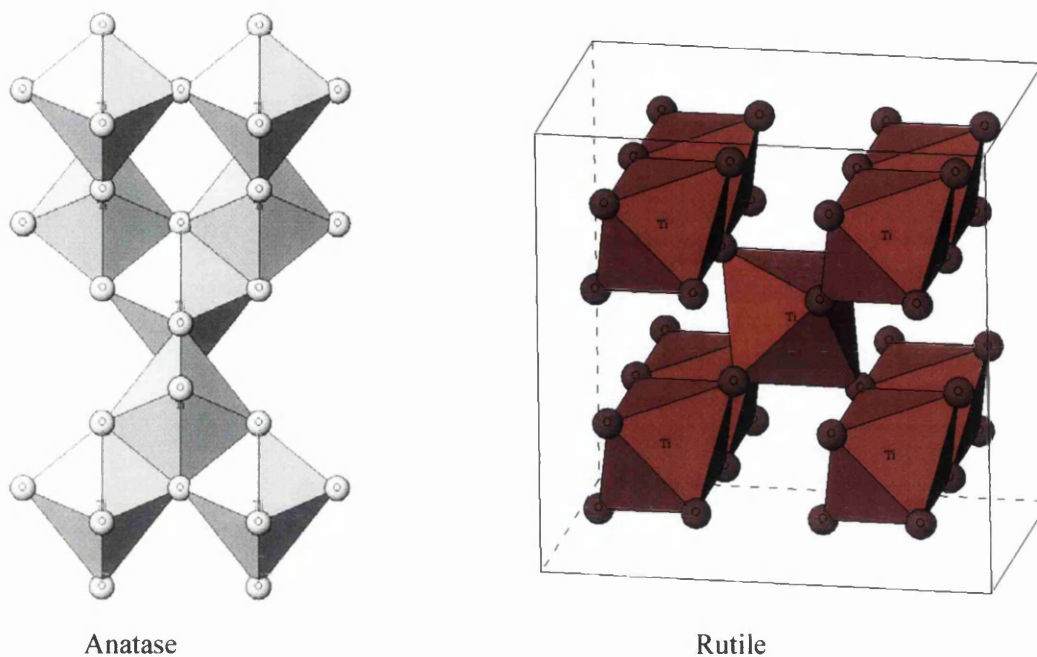


Figure 1.40: Structure of Anatase and Rutile TiO₂ crystals.

As TiO₂ is so inert in nature it means it can even be used to whiten a variety of different food products. Titanium dioxide also has exceptionally good hiding power when incorporated into a coating and the ability of the paint to hide the substrate. Hiding power is related back to how much pigment is actually required to achieve complete opacity. For a paint to hide a substrate it has to be able to prevent light from passing through the paint film, hitting the substrate and then reflecting through the paint film. Hiding power of paint can be quantified by its contrast ratio (CR):

$$CR = R_b/R_w$$

Where R_w and R_b are the reflectance obtained over standard white and black backgrounds respectively. The hiding power is defined as the spreading rate of paint to give a contrast ratio of 0.98 [59].

This is achieved by black pigments absorbing all the incident light while white pigments achieve opacity by scattering and reflecting all the incident light. As white

pigments do not absorb significant amounts of incident light, they appear white. Due to this difference in hiding methods it is pointless to actually compare the hiding power of different colours.

An equal amount of Rutile actually contains fewer particles but has more effective light scattering properties than Anatase, although Anatase is about ten times more photoreactive at its surface than Rutile [52, 53, 60]. In high UV environment applications the purity of the phase used is of utmost importance and a typical impurity of no more than 1% Anatase is adequate.

1.8.3 The Photoactivity of TiO_2

Titanium dioxide is a network solid which is characterised by the fact that a network of bonds extends throughout the entire solid. Each particle of TiO_2 ($\sim 0.2 \mu\text{m}$) contains $\frac{3}{4}$ of a billion network bonded atoms. This can be contrasted to molecular solids, which consist of individual molecules held together by weak intermolecular forces i.e. no bonds. Network solids can be categorised into three different types, depending upon the energy gap between the conduction and valence bands and is known as the band gap (Figure 1.41).

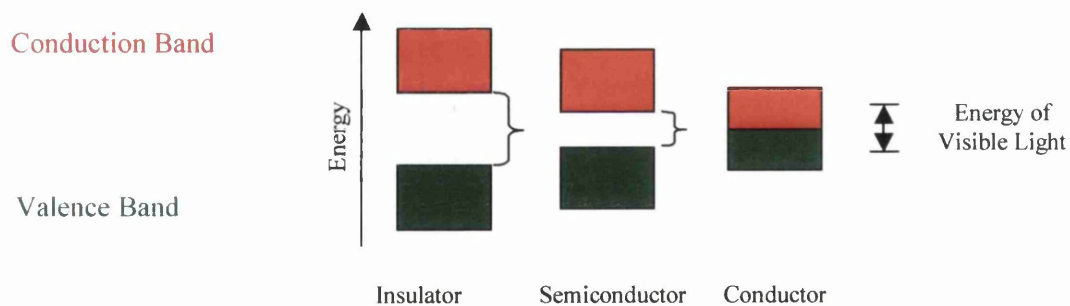


Figure 1.41: Typical energy band gaps.

Titanium dioxide is a semi conductor in nature lying between the two extremities of insulator and conductor. A semi conductor has intermediate band gap energies and with a combination of low temperature and low levels of light will act as insulators.

However when supplied with a small degree of energy (either light or heat) electrons can be promoted from the valance band to the conduction band which leads to the conductive properties.

Titanium dioxide has an energy gap of 3.2eV for the phase rutile. As this band gap is slightly higher than that of visible light and corresponds to UV light (~380nm) TiO₂ appears white. As UV light is incident upon a TiO₂ crystal an electron becomes excited and is promoted from the valence band to the conduction band. This creates a highly mobile electron (e⁻) in the conduction band and an equally mobile hole (h⁺) in the valence band, which will have an effective positive charge on the promotion of the electron. Both of these species are highly reactive. The e⁻ also has a high excess of energy and seeks to lose this energy by migrating to the surface of TiO₂ particle and transferring to another molecule i.e. causing reduction of that molecule. The h⁺ does not have this excess energy so when it migrates to the surface of the TiO₂ particle it can accept another electron in its excited oxidative state. The electron can also lose energy through recombination where light energy is converted to chemical energy.

Within the TiO₂ crystal (Figure 1.42) the valance is made up of oxygen orbitals and the conduction band is made from the titanium orbitals so when an electron is promoted to the conduction band the titanium ion now has a charge of 3⁺ (originally 4⁺) and the oxygen becomes 1⁻ (previously 2⁻).

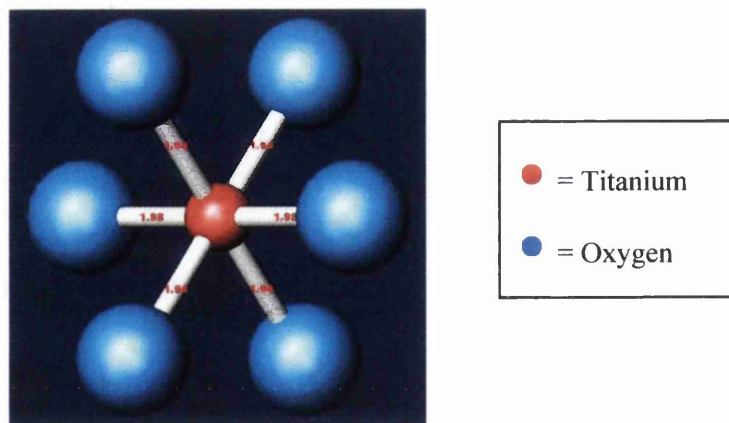


Figure 1.42: Unit cell of TiO₂ (rutile).

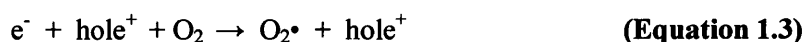
Titanium dioxide is basically an octahedral network of titanium ions which are each surrounded by six oxygen ions. At the surface of the crystal the hydroxyl (OH) groups become attached. This means that hydrogen is now interfering with the idealistic structure of TiO₂ at the surface of the crystal. The overall effect at the surface is that titanium atoms are replaced with hydrogen atoms. Hydrogen atoms can only have a charge of 1⁺ when compared to titanium's charge of 4⁺. This results in a less positive surface potential than that throughout the bulk crystal. This means that electrons prefer to remain within the bulk crystal while the holes tend to migrate away from the higher positive charge towards the surface of the crystal.

1.8.4 Photocatalysis by TiO₂ [61]

If there are no impurities within the structure the band gap lies just outside the wavelength that corresponds to the visible light spectrum. Radiation of <390nm (UV light) is required to promote electrons from the valence band to the conduction band as shown in Equation 1.2.



The greater part of the time the electron will recombine with the hole immediately. However, it is also possible for the excited electron to join a nearby oxygen molecule reducing it and forming a highly reactive oxygen radical (Equation 1.3). As this occurs the positive hole left by the electron is free to oxidize any hydroxyl radicals that maybe present and thus TiO₂ returns to its ground state (Equation 1.4).



This O₂• can undergo further reaction in the presence of water to form perhydroxyl radicals (Equation 1.5).



When all these reactions are brought together the following overall reaction is seen (Equation 1.6).



The TiO_2 is not present as it is completely regenerated to its original state at the end of the reactions and acts purely as a catalyst. However, the radicals (HO_2^\bullet and OH^\bullet) are highly reactive species and it is these species that cause the degradation (mineralisation) of the organic/polymeric components of the coating. The overall process for TiO_2 catalysed photodegradation of a PVC coating is shown in Figure 1.43, although there are likely to be many intermediate reactions also possible [59, 61-63] enroute to CO_2 .

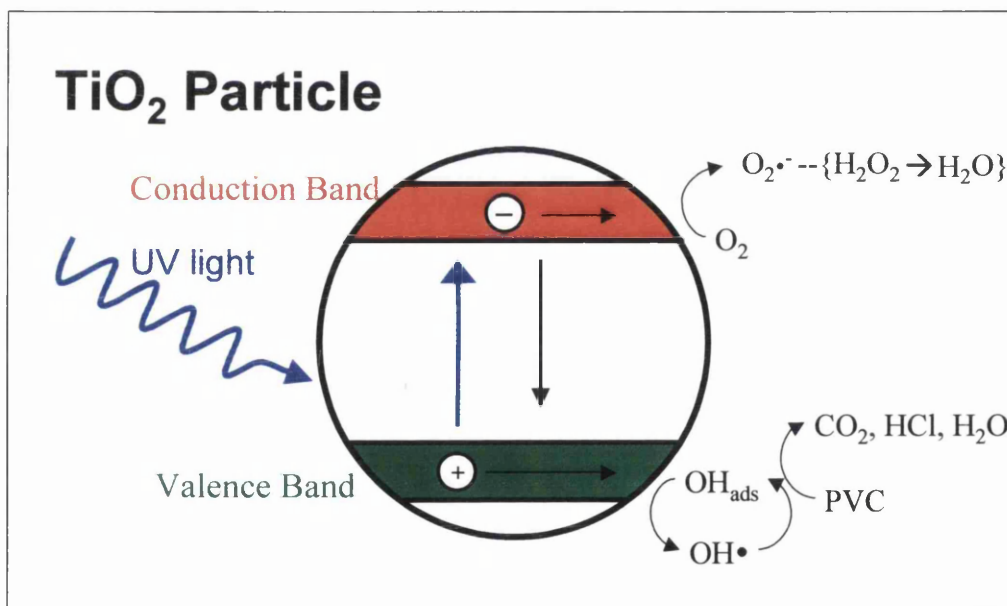


Figure 1.43: Overall process of the photodegradation mechanism of PVC by TiO_2 pigment.

The primary signs of photodegradation on a coating are visible colour loss. After more severe degradation chalking of the coating surface will occur and at this stage the

organic component surrounding the titanium dioxide has been consumed by the oxidation reaction caused by the free radicals producing CO_2 and H_2O . The chalking is where the TiO_2 is left on the surface of the coating after the consumption of the organic components as shown in Figure 1.44. The breakdown in polymer chains surrounding the TiO_2 particles can also lead to change in physical properties of the paint making the coating stiff and brittle leading to cracking and increased porosity of the coating.

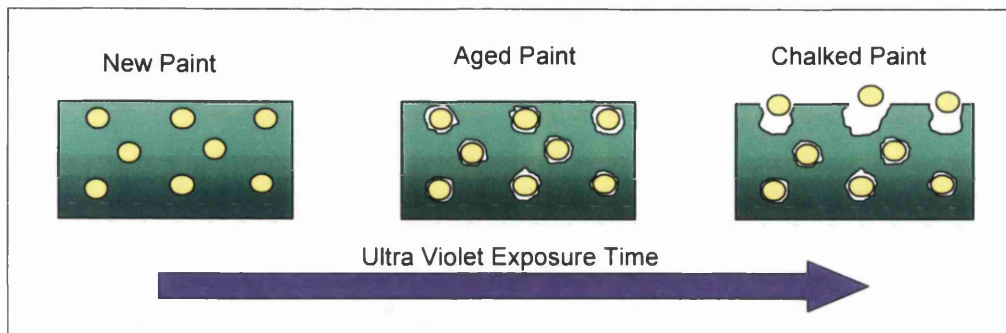


Figure 1.44: Chalking of TiO_2 pigmented paint.

1.8.4.1 Effects and Influences of TiO_2

The TiO_2 grade, photoactivity and dispersion can have an important effect on the performance of a polymer coating. A highly photoactive grade of TiO_2 exhibits high UV absorbance protecting the polymer but will attack the polymer around the particles of titanium dioxide. One obvious solution to this is to use a less photoactive pigment, although with the lower UV absorbency rate this may lead to a more direct attack on the polymer by the UV light. The favored method is to use a surface treatment of TiO_2 as previously discussed e.g. silicon and aluminum oxides. This then protects the polymer from the TiO_2 , whilst not actually degrading the TiO_2 's ability to absorb and scatter UV light. There are other factors that may affect the effectiveness of titanium dioxide and these include the thickness of the coating film and poor dispersion or flocculation of the pigment particles.

In thin coatings it is common for UV to penetrate the coating and reflect back off the substrate, thus not all the UV radiation is absorbed. Therefore less degradation will occur although the coating may not exhibit complete opacity.

The dispersion of the pigment within the PVC is important but not quite what might be first assumed. A well dispersed pigment will lead to good UV absorption/scattering and protection of the binder, although if the binder is reasonably photostable in comparison with the pigment, some flocculation or agglomeration maybe desirable. This due to the fact that particles will shadow each other from the UV radiation and therefore absorb less UV and lead to less catalysed photodegradation in the binder.

1.9 Weathering and Accelerated Tests

In order to improve on any given paint system it is necessary to evaluate the current performance and compare it to a benchmark against other systems thus giving a definitive answer as to whether it has improved or not. The most ideal method would be to test the paint system in the expected service environment in real time. Given these materials are expected to last 30+ years this is impractical. Therefore it becomes necessary to produce a method of accelerating the degradation so that reliable comparisons can be made in a much shorter time period.

The durability of a coating can be described as “its resistance to undesirable changes caused by the natural environment to which it is exposed during its lifetime” [13]. The major influences of the environment on degradation include sunlight (UV), temperature, oxygen, water and pollutants. These influences can act either alone or in combination with each other or other environmental factors such as wind and seasonal periodicity.

The way degradation manifests itself can vary greatly depending upon the coating and the environmental conditions exposed to. Some common indicators of degradation include loss of gloss, discolouration, chalking and physical indications such as cracking of the paint. The primary function for using a polymer coating is to act as a barrier and protect the underlying substrate from corrosion therefore its resistance to weathering is extremely important.

The rate at which coatings degrade is governed by the site of exposure, temperature, rainfall and the intensity of UV exposure. The cyclic nature of these factors can influence the rate at which the coating degrades [64, 65]. All these factors combine to make it exceptionally difficult to create an artificial environment which mimics the varying real life environments faced by a new coating. The accelerated tests tend to be one of the following forms.

- 1) The use of more extreme conditions than those expected during its normal service life i.e. the use of lower wavelength radiation from either xenon arc or carbon arc lamps, or through higher intensity incident radiation. However this method provides an unnatural environment and can lead to different chemical processes occurring within the coating and therefore different degradation processes being promoted than would otherwise be expected.

- 2) Evaluation of chemical changes that are occurring within the coating prior to physical manifestations of degradation. Certain techniques are available now that are actually capable of picking up on minute changes that are occurring within the polymer that can be extrapolated out to give an idea of long term performance.

1.9.1 Natural Exposure

When the service environment in which the product is going to be used has been established it is possible to use one of the many testing sites around the world which give a similar environmental effect. The location of the more widely used weathering sites are situated in areas where there are climatic extremes. In this way the natural exposure is achieved even though some environmental variables may be more extreme than would normally be experienced during service. This combined with some of the novel test rigs described later leads to an accelerated or slightly more extreme test than would be necessary for service conditions but at the same time still using purely natural acceleration. Below is a list of some of the more popular climatic weathering stations around the world and many more are quoted in the literature [66-69].

Florida: This provides a sub tropical climate that has been the standard for environmental testing for a number of years. It provides high UV exposure, high temperature, and high humidity providing a good reproducible acceleration of European climates.

Arizona: With a low rainfall of only 200mm and an average high temperature of 26°C, providing a hot dry climate. After Florida it's the most quoted testing area for outdoor weathering.

Hook of Holland: Provides an environment that is both industrial and marine in nature and is so an aggressive corrosive environment in which to determine corrosion stability.

During the nature exposure experiments it is important to track the experimental conditions experienced including rainfall, pH of the rain, radiation exposure and the initial time of exposure due to the seasonal variations experienced at the weathering site.

1.9.1.1 Natural Exposure Rigs

Depending on the type of weathering required there are a large number of testing rigs available to help accelerate the degradation process at these weathering sites.

1.9.1.1.1 Adjusted Angle Open Back Rack

The panels tested in this system are supported on two thin rails at the top and bottom of the panel which leaves the back of the panel free to radiate heat. The rack is usually angled at 45 degrees from horizontal, south facing during the winter and as the seasonal angle of the sun varies, it is decreased in 10 degree stages to 5 degrees south in the summer.

1.9.1.1.2 Adjusted Angle and Standard Black Boxes

This system was designed by General Motors to simulate the temperatures experienced by a horizontal surface under direct sunlight and the box itself is described in ASTM (American Society for Testing and Materials) recommended practice G 7-77a. The air space within the box is such that it simulates the conditions created inside closed cars.

1.9.1.1.3 Heated Black Box

The design is very similar to the conventional black box and the heater element is designed to provide sunny day temperatures on cloudy or overcast days. There are moisture sensors on the panel to deactivate the heater if the surface is hot and as long as no moisture is detected. The heater is thermostatically controlled between 8am and 4pm

1.9.1.1.4 Fresnel Reflector Test (EMMA/EMMAQUA)

This consists of a rotatable rack upon which mirrors are mounted and the mirrors are used to focus the sunlight from a large surface area onto the test panel. The rack automatically tracks the angle of the sun therefore increasing the efficiency of the irradiation. Fans are used to circulate the air across the back of the panels to prevent overheating while programmable jet-nozzles can deliver water at designated times. Measurements by the DSET laboratories show that this focused irradiation is approximately 10 times greater than that on a stationary rack.

1.9.2 Artificial Exposure Methods

The main advantage of using a completely artificial exposure technique is that it is fully controllable, defined and reproducible. However it is only useful if all the degradation processes that occur accelerate to the same extent. The use of radiation of a higher energy than that of natural exposure has the added complication of introducing new higher energy photochemistry that does not occur under normal conditions. Table 1.9 and Figure 1.45 show some artificial exposure methods compared with sunlight as spectrum distribution of irradiance. The commercially accelerated methods available usually use one of a relatively small number of light sources which include carbon arc, xenon arc and fluorescent tubes (UV-A, UV-B).

Table 1.9: Comparative distribution of irradiance.

Wavelength (nm)	Sunlight %	6500 W Xenon arc %	Carbon arc %	Fluorescent source %
300	0.01	0.01	0.5	14
300-340	1.6	1.5	2.5	70
340-400	4.5	5	11	13
Total to 400	6.1	6.5	14	97
400-750	48	51.5	34	3
750	46	42	52	0
Total to 750	94	93.5	86	3

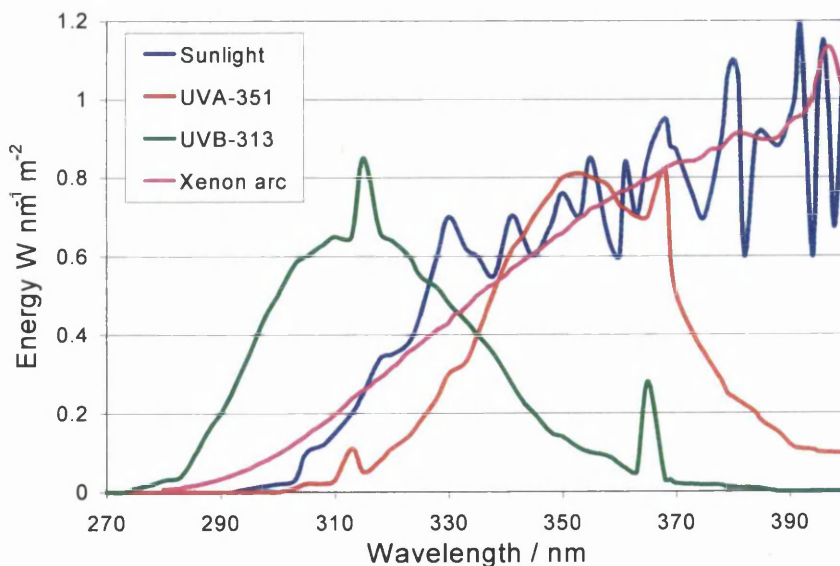


Figure 1.45: UV spectrum of sunlight and UV-A, UV-B and Xenon arc lamps.

1.9.2.1 Carbon Arc

The spectral output of the carbon arc lamp has little in common with that of natural sunlight, mainly consisting of three intense peaks between 250 and 450 nm. It is currently being phased out of the test standards for metals and plastics although it is still commonly used for textile evaluation.

1.9.2.2 Xenon arc sources

It provides a much better simulation of sunlight than the carbon arc, although filters are required to remove UV radiation shorter wavelength than that experienced from natural exposure. It also contains a high intensity of infrared radiation and so some kind of IR filter must be employed to prevent overheating of the samples. The close simulation of natural sunlight and the ability to control the source automatically combine to make Xenon arc sources a useful artificial exposure method.

1.9.2.3 Fluorescent Tube lamps (UVA)

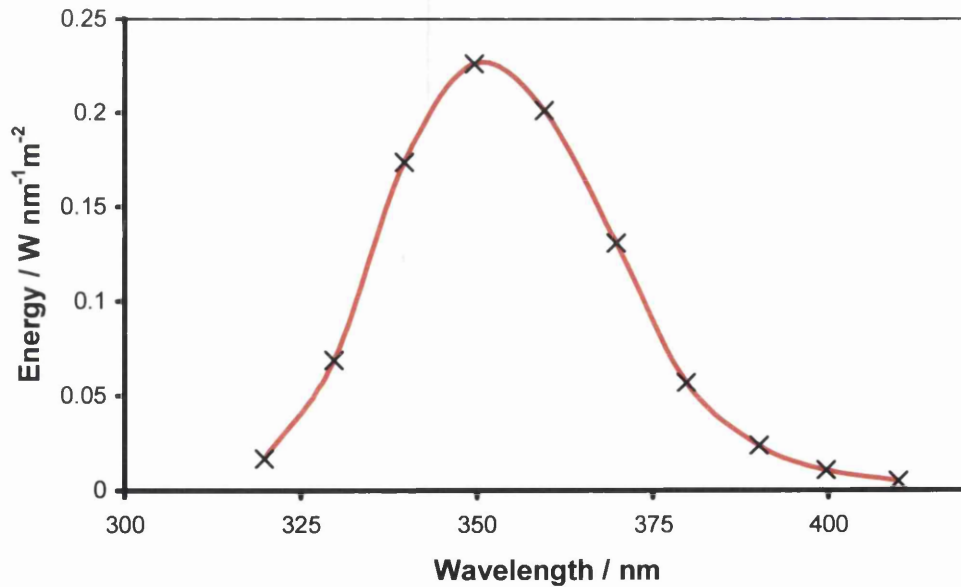


Figure 1.46: Typical black light UV lamp emission spectra [70].

These are most commonly available as UV-A and UV-B spectral output. They produce very little heat and are much cheaper to maintain and run than xenon arc lamps. The UV-B lamps contain radiation of high intensity below that of the solar cut off and as such provide a high degree of acceleration, though it has been shown that chemical reactions can occur that would not be expected under natural conditions. Figure 1.46 illustrates the spectral output of the UV-A lamps which will be used for most of this thesis.

1.9.3 Physical Measurement Techniques for Evaluating Weathering

The standard method of assessing the performance of coatings exposed at natural weathering sites is the measurement of gloss loss, colour retention, crazing and cracking. Although other methods such as contact angle (polarity) weight loss/film thickness can also be used.

1.9.3.1 Gloss Loss and Chalking

The gloss of a coating reflects the overall surface roughness. When the binder is photo-oxidised it becomes more pitted and the gloss level is reduced. In extreme conditions the exposure of the insoluble pigment particles can be seen as a chalky deposit upon the surface of the coating. In general gloss loss is a lead up to chalking and can be measured by monitoring the reflection of the light from the surface. The extent of chalking is usually carried out visually or using a tape pull. Both these techniques are very fast and easy ways to monitor the extent of degradation. In addition, gloss loss is capable of measuring degradation caused by mechanical stressing as well as photo-oxidation. The disadvantages of these measurements are that they are physical measurements and so are not as sensitive as some of the chemical tests available.

The standard statement in terms of durability is usually quoted as the minimum time the coating will maintain a gloss value of greater than 50% its original value (gloss half life). Gloss loss is one of the major measurements for following degradation of polymer films and is used throughout the literature [71].

For practical reasons, the gloss of a sample is measured relative to that of a primary standard whose gloss is in turn determined relative to that of the theoretical standard [72]. This theoretical standard is specified to be a highly polished plain black glass with an index of refraction at the wavelength of sodium D line, 589.3 nm, of $n_D = 1.567$. The specular reflectance of un-polarised light for this index is calculated using the Fresnel equations and assigned a gloss value of 100 for each of the three standard geometries incident angles of 20° , 60° and 85° [73].

1.9.3.2 Colour Retention

This is an aesthetic effect that is not picked up by the usual gloss/chalking tests but is quite obvious to the naked eye. A pigmented film is able to undergo colour changes in three ways; colour fading, colour darkening or yellowing of the polymer due to polyene formation, from the scission of the polymer backbone and dehydrochlorination (in PVC). The overall colour change can be measured using electronic colour sensors, a three-colour procedure where any colour can be described in relation to the primary colours red, green and blue [74].

Another method is using a spectrophotometer, which records the reflectance spectrum (proportion of light reflected at any given wavelength) and is used throughout this thesis. A more detailed discussion can be found in recently published work [74] and a full description of the instrumentation and technique is covered in 2.7.3.

1.9.3.3 Crazeing and Cracking

Exposure of polymer coatings to the effects of weathering will result in chain scission of the longer more flexible polymer chains to form shorter more brittle ones. This results in areas of stress on the coating becoming less flexible with possible cracking and flaking of the coating. It is possible for unexpected failure due to cracking to occur prior to any gloss loss or chalking.

1.9.3.4 Contact Angle

As the surface of the polymer becomes oxidised, it becomes more polar, this results in higher surface tension as degradation proceeds. The extent of the polarity can be estimated by measuring the contact angle made by a drop of de-ionised water. The lower the contact angle is, the higher the polarity and hence the greater the degradation that has occurred. Although it can be used to monitor degradation, it is not significantly faster and is more likely to be used as a corroborative source of evidence. Although it does highlight any difference in wetting, which will inevitably affect the corrosion rate.

1.9.3.5 Weight Loss and Film Thickness

As the polymer weathers, there is a gradual loss of surface material (Figure 1.44). This enables the monitoring of degradation via the dry film thickness (DFT) or the actual weight loss. The loss of DFT has been used to help demonstrate the effect of molecular weight upon durability.

1.9.4.1 Chemical Test Methods Used to Follow Degradation

Attempts to correlate accelerated weathering performance with that of Florida and other weathering sites has been documented with some success. However there is an increasing amount of work being carried out using various chemical techniques that have been and are continuing to be developed. As our understanding of degradation and oxidation processes occurring during weathering increases so too do the range of chemical techniques available. Outlined below are some of the techniques used in the literature.

1.9.4.1 Infra-red Spectroscopy

An infra-red spectrophotometer can be used to record the infrared spectrum of a compound as the intensity of the beam of infrared radiation passed through the sample is compared with the intensity of a reference beam. The source of infra-red radiation is usually a ceramic rod heated to around 1500°C, which emits infrared radiation covering a range of wave numbers ($200\text{cm}^{-1} - 4000\text{ cm}^{-1}$).

A liquid sample is usually held as a thin film between two sodium chloride discs while a solid sample is power mixed with potassium bromide and crushed under heavy pressure to form a disc. New accessories and techniques have allowed testing of a mobile or stationary gaseous phase by using a suitable alkali halide windowed analysis cell. The use of alkali halides such as sodium chloride and potassium bromide is essential as they are transparent to infrared radiation whereas glass windows would absorb most of the radiation. This means that all samples have to be completely dry before their spectra can be recorded. In a conventional spectrometer the level of intensity of the sample beam is compared with that of the reference beam for a range of wave numbers. A computer is used to record and plot a graph or spectrum of the percentage transmission against wave number. The sample beam is typically 90% of the intensity of the reference beam when no absorption is occurring, but this can drop to 50% or less at wave numbers where absorption is occurring.

A chemical bond has a natural frequency of vibration as well as particular patterns of vibration. The significance of molecular vibration is that a molecule will absorb electromagnetic radiation whose frequency is the same as any of the vibrations in the molecule. The vibrations in the molecule will increase in amplitude as a result of the energy absorbed from the radiation. Although there is an important restriction to this behaviour which is that the absorption of radiation can only occur if the vibration is accompanied by a change of dipole in the molecule. Thus molecules of hydrogen (H_2) or chlorine (Cl_2) will not absorb radiation whereas polar molecules such as hydrogen chloride (HCl) will.

Table 1.10: Typical infrared absorptions.

Functional Group	Structural Representation	Bond	Wavenumber (cm ⁻¹)
Alkanes	H ₃ C-CH ₃	C-H stretch	2850-3000
		CH ₂ /CH ₃ bend	1450-1470
Alkenes	RCH=CH ₂	=C-H stretch	3080-3140
		C=C stretch	1645
	R ₂ C=CH ₂	=C-H stretch	3080-3140
		C=C stretch	1650
	cis-RCH=CHR	=C-H stretch	3020
		C=C stretch	1660
	trans-RCH=CHR	=C-H stretch	3020
		C=C stretch	1675
	R ₂ C=CHR	=C-H stretch	3020
		C=C stretch	1670
R ₂ C=CR ₂	C=C stretch	1670	
Alkynes	RC≡CH	≡C-H stretch	3300
		≡C-H bend	600-700
		C≡C stretch	2100-2140
	RC≡CR	C≡C stretch	2190-2260
Alcohols	ROH	O-H stretch	3200-3650
Carboxylic Acids	RCOOH	O-H stretch	2500-3300
		C=O stretch	1710-1760
Esters	RCOOR'	C=O stretch	1735-1750
Aldehydes, ketones	RCOH, RCOR'	C=O stretch	1690-1750
Ethers, alcohols	R ₃ COR'	C-O stretch	100-1260
Amines	R ₂ NH	N-H stretch	3250-3500
Nitriles	RCN	C≡N stretch	2220-2260

The radiation that is absorbed as a result of molecular vibrations lies in the infrared region of the electromagnetic spectrum. Particular vibrations in particular bonds give rise to absorption in a particular part of this infrared region. Table 1.10 shows some typical organic bonds along with their relevant infrared excitation wave numbers.

The peaks are where the absorbance occurs for example the 1700 one for CO groups. The recordings of the infrared spectra show transmittance as deep troughs and each peak in the spectrum is characteristic of a vibration of a particular molecule structure. Figure 1.47 shows an example of typical polyurethane coating absorption with a TiO₂ pigment.

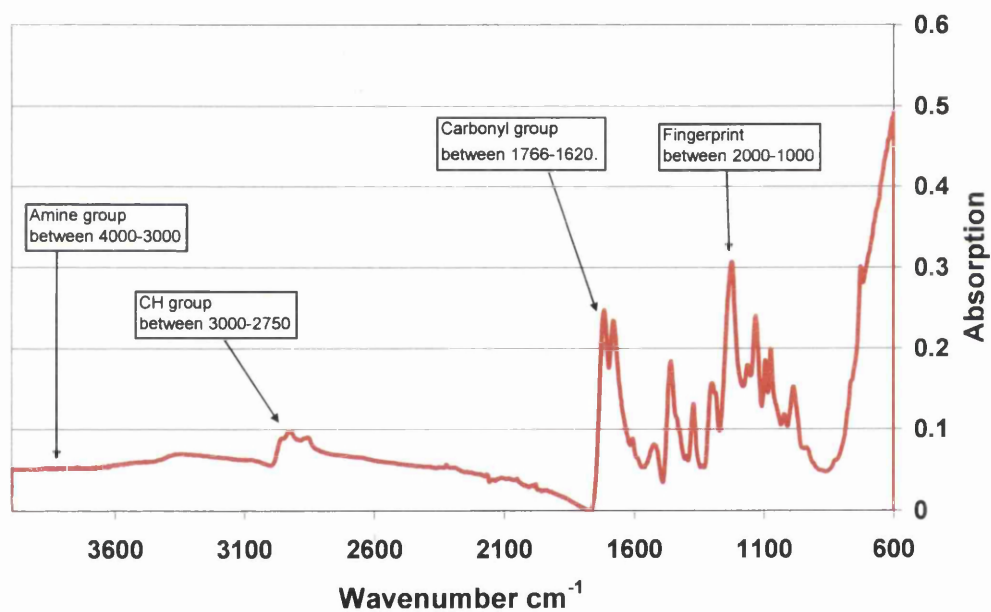


Figure 1.47: The Infra-red spectra of a polyurethane.

1.9.4.2 Fourier Transform Infra-red (FTIR)

As detailed above traditional Infra-red (IR) spectrophotometers use a signal split into discrete wavelengths which are examined in sequence and compared to a reference sample beam. The Fourier Transform Infra-red (FTIR) spectrophotometer works in a slightly different way as it is capable of scanning all the wavelengths of interest in a single scan. This makes the scanning of samples much quicker and with a greater accuracy. The apparatus and optics used are relatively simple but complicated manipulation of the data by a computer is required to achieve the usual absorbance vs wave number plot. The data can also be further manipulated by using other techniques to improve the clarity of the final spectrum. These techniques include: baseline correction, scale expansion, plot modification and plot smoothing. Although one of the most useful features of the modern software is the ability to digitally add or subtract other spectrum and also the ability to compare spectrums with those previously stored in a database.

A more detailed description of the equipment, mechanisms used and latest advances can be found in the literature [75].

1.9.4.3 Chromatography

In the chemical analysis forum, truly specific identification of samples is very difficult to achieve due to the many interference signals which can be present. Improving the purity of the test sample is one of the easiest ways to alleviate this problem. Chromatography can be used to separate and purify a test sample.

It was first used by Tswelt in 1906 to separate plant pigments by passing them through various glass columns packed with finely ground calcium carbonate. The separate species appeared as coloured bands on the column.

The same basic idea is still used today but in a variety of different methods. The chromatographic technique can be used for the separation, identification and determination of the chemical components within a complex mixture. Chromatography is unique in its general applicability and its powerful nature can be used to separate gaseous and volatile substances by gas chromatography and non-volatile and polymeric materials by liquid chromatography.

The basis of chromatography revolves around a mobile phase in which an “analyte” test substance is dissolved. This mixture is then flowed over an immiscible stationary phase usually in a column. The separation of the analyte test substance is dependant on the partition coefficient for each component of the analyte between the mobile and stationary phase. Any component that has a strong affinity for the mobile phase will stay in solution longer than components that have a stronger affinity for the stationary phase and therefore the mixture becomes separated.

Table 1.11: different types of chromatography and their methods.

General classification	Specific method	Stationary Phase	Type of equilibrium
Liquid chromatography Mobile Phase : Liquid (LC)	Liquid-Liquid, partition chromatography	Liquid adsorbed on a solid	Partition between immiscible liquids
	Liquid-bonded phase	Organic species bonded to a solid surface	Partition between liquid and bonded surface
	Liquid solid, or adsorption	Solid	Adsorption
	Ion exchange	Ion-exchange resin	Ion exchange
	Size exclusion	Liquid in interstices of a polymeric solid	Partition/seiving
Gas Chromatography Mobile Phase: Gas (GC)	Gas-Liquid	Liquid adsorbed on a solid	Partition between gas and liquid
	Gas-bonded phase	Organic species bonded to a solid surface	Partition between liquid and bonded surface
	Gas-solid	Solid	Adsorption
Supercritical Fluid Chromatography Mobile phase: Supercritical fluid (SFC)		Organic species bonded to a solid surface	Partition between supercritical fluid and bonded surface

The specific type of chromatography depends entirely upon the nature of the analyte, i.e. whether it be gas, liquid or in some cases super critical fluid lays out the nature of each route as shown in Table 1.11. Chromatography can be carried out either vertically in a column where the stationary phase is packed into a tube, or horizontally in a planar medium where the stationary phase takes the form of a flat plate.

Once the sample under analysis has been separated out a variety of different detectors, up to mass spectrometers can be used to identify the different species present.

1.10 Recent Developments in the Rapid Evaluation of Photodegradation.

As shown in Figure 1.43 one of the key degradation products of TiO₂ catalysed degradation of organic materials is CO₂ and this is used as an indicator for photodegradation. In recent work [26, 76] this has been used to measure TiO₂ photoactives. The CO₂ evolved through photodegradation can be measured with FTIR spectroscopy when incorporated into a closed loop system. The rate of CO₂ evolution relates directly to activity on reported data shown in Figure 1.48. Green represents a A graded pigment, yellow is a B grade and red is a C graded pigment. It is key to note that the grades assigned by the TiO₂ manufacturer and the rates of CO₂ evolution are in good agreement with the use of this new test method of rapid evaluation of photodegradation of films and additives. It is also key to note that the A grade RTC60 doesn't perform as well as other A graded pigment and is no longer produced commercially. Its rate of CO₂ evolution is more comparable to poor B grade pigment K2300.

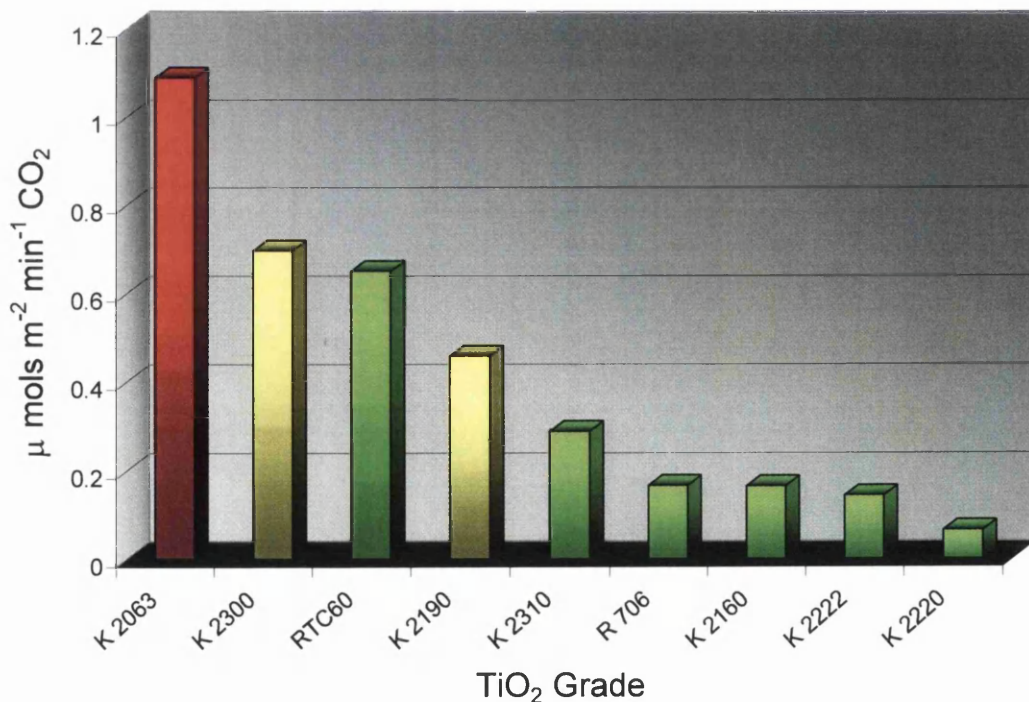


Figure 1.48: The rate of CO₂ rate after 200 minutes of irradiation with UVA light as a function of pigment grade.

The test system has been used to access the effects of other coating additives such as plasticiser [37], Ultra-violet absorbers, HALS [26] and pigment colours. The correlation of flat panel work [26] and the previously used irradiation of tubes are comparable with the benefit of better coating thickness and larger surface areas. The flat panel reactor has helped to evaluate pigment performance and has been shown to be fast, accurate and effective. The performance of the pigment is most likely to be down to the different surface coatings and the effectiveness in which they shield the pigment from the surrounding polymer matrix [26].

Other recent work [77] also uses this technique but in a smaller volume in a non circulated headspace for evaluating polyethylene, polyvinylchloride and polypropylene degradation. The material coupons are activated by light shone perpendicularly onto the sample with simultaneous IR evaluation of the CO₂ in the headspace.

In this thesis the re-circulating flow system will be used to measure degradation kinetics as it offers a very rapid means of screening coating additives and changes in concentrations.

1.11 Conclusions and Aims

Photodegradation continues to provide the coating industry with various challenges to give a coating with durability of over 30 years with increasing pressure to change additives to less toxic alternatives. The focus of this thesis will be to use the rapid test method for evaluating coating stability in an attempt to improve coating stability using less toxic ingredients.

The first stage of the programme is to investigate the effect of the type and concentration of thermal/photodegradation stabilisers in model PVC paints pigmented with a photoactive grade of titanium dioxide. The aim of this initial work is to establish quickly the potential efficiency of conventional stabiliser systems and the naturally occurring clay Hydrotalcite (HT) in preventing degradation initiated [78] by combination of UVA light and an active type of TiO_2 . This system was chosen since rapid screening was possible using only a few hours of UV exposure by measurement of photogenerated carbon dioxide using FTIR spectroscopy.

In the next section of the programme, the aim was to add an additional compound to the model paint in the form of a range of traditional phthalate and less toxic phthalate free (sulphonic acid ester) plasticisers compounds. This work again was designed to use the rapid screening method by using the FTIR based measurement of photogenerated carbon dioxide.

Having used the model system to demonstrate stabiliser effectiveness in systems that could degrade in hours, the next phase of the programme was to evaluate how the stabiliser systems (based on HT and also conventional chemical stabilisers) would perform in both near commercial (with failure in QUVA in 1000-2000 hours) and full stabilised paints (typically with 6000 hours QUVA exposure). In these latter panels the effects of coating colour and titanium dioxide type were also evaluated such that the ultimate phthalate free plasticised coating could be specified.

1.12 References

1. Trehewy, K.R., Chamberlain, J.,, *Corrosion for Science Engineerin*, ed. 2nd Edn. 1995: Longman (UK).
2. Lambourne, R.a.S., T.A., *Paint and Surface Coatings*: Woodhead Publishing Ltd.
3. Products, B.S.S., *The Colorcoat Buildings*. 1995.
4. Products, B.S.S., *Commercial Information Database*. 1999.
5. Conan, D.O., and Drisko, R.L.,, *Elements of Organic Photochemistry*. 1976, New York: Plenum Press.
6. Sears, J.K., Darby, J.R.,, *The Technology of Plasticisers*. 1982, New York: Wiley and Sons.
7. Calvert, J., Pitts, J., , *Photochemistry*. 1970, New York: Wiley.
8. Birks, J.B., *Photophysics of Aromatic Molecules*. 1970, New York: Wiley.
9. Cheremisinoff, P.E., *Handbook of Polymer Science and Technology Vol. 3: Applications and Processing Operation*. 1989, New York: Marcel dekker inc.
10. Decker, C., *Advances in Chemistry Series*. 1996. **249**: p. P319.
11. Decker, C., *Polymer Internaional*. 1998. **45**: p. P133.
12. Cortolano, F.P., *J. Vinyl Technology*. 1993. **15**(No. 2): p. P69.
13. Allen, N.S., and Edge, M.,, *Fundamentals of Polymer Degradation and Stabilisation*. 1992, London: Elsevier Applied Science Publishers Ltd.
14. Rene de la Rie, E., *Studies in Convervaion*. 1988. **33**: p. P9.
15. Allen, N.S., *Engineering Plastics*. 1995. **8**(No. 4): p. P247.
16. Braun, D., *Pure & Appl. Chem*. 1981. **53**: p. 549.
17. George, G.A., *Materials Forum*. 1995. **19**: p. P145.
18. Rabek, J.F., *Photodegradation of Polymers: Physical Characterisations and Applications*. 1996, Berlin: Springer-Verlag.
19. Andrady, A.L., Searle, N.D.,, *J. Applied Polymer Science*, 1989. **37**: p. P2789.
20. Kamp, G., Sommer, K., Zirngiebl, E.,, *Progress in Organic Coatings*, 1991. **19**(No. 1): p. P69.
21. Scott, G., *Advances in Chemistry Series*, 1978. **169**: p. P30.
22. Jian, L., Dafei, Z., , *Polymer Degradation and Stability*, 1991. **31**: p. P1.
23. Braun, D.S., D., , *Polym. Bull.*, 1985. **14**: p. P39.
24. Cuncliffe, A.V., Davis, A.,, *Polymer Degradation and Stability*, 1982. **4**(No. 1): p. 17.
25. Gardette, J.L., Gaumet, S., Phillippart, J.L., , *J. Applied Polymer Science*, 1993. **48**(No. 11): p. 1185.
26. Robinson, A.J., *The Development of Organic Coatings for Strip Steels with Improved Resistance to Photodegradation*. EngD Thesis, University Of Wales Swansea, 2005.
27. Scott, G.E. *Developments in Polymer Stabilisation 1*, ed. E.A.S. Publications. 1979, London.
28. Scott, G.E. *Developments in Polymer Stabilisation 5*, ed. E.A.S. Publications. 1982, London.
29. Scott, G., *Polymer Degradation and Stability*, 1995. **48**(No. 3): p. P315.
30. Braun, D., Wolfe, M., , *Angew. Makromol. Chem.*, 1978. **70**: p. P71.
31. Hamid, S.H., Amin, M.B., , *J. Applied Polymer Science*, 1995. **55**(No. 10): p. 1315.

32. Berlanga-Duarte, M.L., Angulo-Sanchez, J.L., Gonzalez M.C., , J. Applied Polymer Science, 1996. **60**: p. 413.
33. Rabek, J.F., Canback, G., Ranby, B., , J. Applied Polymer Science, 1979. **35**: p. 209.
34. Mielewski, D.F., Bauer, D.R., Gerlock, J.L.,, Polymer Degradation and Stability, 1991. **33**(No. 1): p. 33.
35. Zweifel, H., Chimia,, 1993. **43**(No. 10): p. 390.
36. Hahnfield, J.L., Devore, D.D.,, Polymer Degradation and Stability, 1993. **39**(No. 2): p. 241.
37. Searle, J.R., *Titanium Dioxide Pigment Photocatalysed Degradation of PVC and Plasticised PVC Coatings*. EngD University of Wales Swansea, 2002.
38. Bredereck, P., J. of Vinyl Technology, 1986. **8**(No. 2): p. 46.
39. Pourrahmady, N., Bak, P.I.,, J. of Macromolecular Science - Pure and Applied Chemistry, 1994. **A31**(No. 2): p. 185.
40. Vaccari, A., *Clays and catalysis: a promising future*. Applied Clay Science, 1999. **14**: p. P 161.
41. Drits V., A., et al., , *Clays and Clays Minerals*. 1987. **35**: p. P 401.
42. Oswald, H.R., and Asper R., *Physics and Chemistry of Materials with Layered Structures*, ed. E. R.M.A Lieth. 1977. P 73.
43. Watson, T.M., *Corrosion Mechanisms and Inhibition on Organic Coated Packaging Steels*. 2006, University of Wales Swansea: Swansea.
44. Shannon R.D, *Acta Crystallographica A*. 1976. **32**::: p. P 751.
45. Miyata S, *Anion-Exchange Properties of Hydrotalcite like compounds*. Clays and Clay Minerals, 1983. **31**(4): p. P 305-311.
46. Reichle W.T., *Anionic clay minerals*. Chem Tech, 1986. **16**(58): p. p58-63.
47. Kendig M and Hon M, *A hydrotalcite like pigment containing an organic anion corrosion inhibitor*. Electrochemical and solid state letters, 2005. **8**(3): p. P B10-B11.
48. McMurray H.N., a.W.G., . *Inhibition of filiform corrosion on organic coated aluminium alloy by hydrotalcite like anion exchange pigments*. Corrosion, 2004. **60**(3): p. P 219-228.
49. Rives V., e.a., *Inorganic Chemistry*. 1993. **32**: p. p 5000.
50. Wilson, A.S., *Plasticisers: Principles and Practice*, ed. T.I.o. Materials. 1995, London.
51. Vymazal, Z., Vymazalona, Z., , European Polymer Journal, 1991. **27**(No. 11): p. P1265.
52. Material, P.R.A.C., *Introduction to Paint Technology*. 1999.
53. Braun, J.H., J. of Coating Technology, 1997. **69**(No. 868): p. P56.
54. Barksdale, J., *Titanium its occurrence, chemistry, and technology*. 1966: The Ronald Press Company.
55. Gruzdev, Y.A., *Surface Treatment of Pigment Titanium Dioxide*.
56. Braun, J.H., *White Pigments*. 1995: Federation Series on Coatings Technology.
57. Pochekovskii, R.A., *Modification of Titanium Dioxide Pigment*.
58. Bohren, C.F., and Huffman, D.R., *Absorption and scattering of light by small particles*. 1983: John Wiley & Sons.
59. Von Fraunhofer, J.A., Boxall, J., , *Concise Paint Technology*. 1977: Paul Elek (Scientific Books) Ltd.
60. Adams, R., European Coating Journal, 1996. **June**: p. P395.

61. Marganski, R.E., Diebold, M.P., , *Photocatalytic Properties of Titanium Dioxide*. Modern Paint and Coatings, 1999. **May**: p. P30.
62. Mills, A., Morris, S., Davies, R., , J. Photochem. Photobiol. A:Chem., 1993. **70**: p. P183.
63. Mills, A., Holland, C., Davies, R.H., Worsley, D.A.,, J. Photochem. Photobiol. A:Chem., 1994. **83**: p. P257-263.
64. Worsley D.A., M., A., Smith, K., and Hutchings, M.G.,, J. Chem. Soc.,, 1995: p. 1119.
65. Sayyed, G.A., d'Oliveira, J.C., Pichat, P., , J. Photochem. Photobiol. A:Chem., 1991. **58**: p. P99.
66. Hamid, S.H., Amin, M.B., Maadhah, A.G., Al-Jarallah, A.M., , *Polymeric Materials: Science and Engineering*, 1992. **67**: p. P399.
67. Bell, B., Beyer, D.E., Maeker, N.L., Papenfus, R.R., Priddy, D.B., , J. Applied Polymer Science, 1994. **54**(No.11): p. P1605.
68. Qayyum, M.M., White, J.R., , *Polymer Degradation and Stability*, 1993. **41**(No. 2): p. P163.
69. Hu, X.J., *Abstracts of Papers of the American Chemical Society* 1993. **206**(No. Pt2): p. P333.
70. Mills, A., Davies, R.H., Worsley, D.A.,, *Purification of water by semiconductor photocatalysis*. Chemical Society Reviews, 1994: p. P417-425.
71. Morse, M.P., *Preformance of Organic Coatings*. American Society for Testing Materials 1982. **ASTM STP 781**.
72. Cremer, N., *Product finishing*. 1997. **June**: p. P23.
73. Jarrold, J., *Polymer, Paint and Coatings Journal*, 1997. **932**(No. 3): p. P21.
74. Wijdekop, M., *The weathering of organic coated steel and application of mathematical modeling*. EngD Thesis, University Of Wales Swansea, 2004.
75. Hannah, R.W., Swinehart, J.S.,, *Experiments in Techniques of Infrared Spectroscopy*. 1974: Perkin-Elmer.
76. Worsley D.A., S., J.R.,, *Photoactivity test for TiO₂ pigment photocatalysed polymer degradation*. Materials Science and Technology, 2002. **18**: p. P681.
77. Jin, C., *FTIR Studies of TiO₂ Pigmented Polymer Photodegradation*, . PhD, University of Newcastle upon Tyne 2004.
78. Martin, G.P., Robinson, A.J., and Worsley, D.A., , *Hydrotalcite mineral stabilisation of titanium dioxide photocatalysed degradation of unplasticised polyvinylchloride*. Materials Science and Technology, 2006. **22**(No. 3): p. 375-378.

Chapter 2

Experimental Procedures

2.1 Paint Formulation Techniques

The work carried out during this project centred predominantly upon the testing of different coating components within the simple Titanium Dioxide (TiO_2) pigmented model paint system. The model paint system uses three basic paint components, a resin (Poly Vinyl Chloride (PVC)), a solvent (Tetrahydrofuran (THF)) and a pigment (TiO_2). Various additions and changes to the model paint system were made whilst investigating the possible effects on the rates of photodegradation. The techniques used for formulating these model paints are outlined within this section, and throughout the entire thesis coating additions are referred to as percentage additions. These percentages relate to the amount of the resin (PVC) component compared to the amount of pigment (TiO_2) within the paint, and is measured on a weight for weight basis. This is commonly referred to as P.H.R (parts Per Hundred Resin) for example an addition of 1g of TiO_2 to a paint containing 10g of PVC resin would give a loading of 10 P.H.R = 10%.

2.1.1 Standard Pigmented Model PVC Systems

Numerous model coatings were produced to test a variety of different coating components and stabilisers. All of the model systems used Degussa P25, which is the un-stabilised, highly photoactive grade of TiO_2 . Degussa P25 was used to give a fast reproducible semiconductor catalysed photodegradation rate whilst assessing the effects of different coating components and stabilisers.

In-order to formulate the model paint system TiO_2 was dispersed in a small amount of THF, approximately 25ml. This ensures the TiO_2 particles have a homogenous dispersion. The dispersion was mixed using the high shear mixer (Heidolph Type RZR1 Variable Speed Mixer) for 2-3 minutes before the remainder of the THF was added (100ml total). The TiO_2 and THF mixture is stirred at the constant rate of approximately 1000 rpm by the high shear mixer while 10g PVC (Aldrich MW ca 95000) was added continuously over a relatively short period. This allowed for an even dissolution of the PVC thus ensuring agglomeration of the PVC did not occur. Once all the PVC had been dissolved the solution was transferred to a solvent bottle (100ml Graduated Pyrex Media Bottle (Fisher)) and then stored in the dark to avoid any possible

photodegradation. A magnetic stirrer bar is added to the bottle and stirred for a further 48 hours using a stirrer plate to ensure complete homogenisation as well as complete pigment deagglomeration and PVC dissolution.

2.1.2 Plasticised Model PVC Systems

A common addition to commercial PVC coating systems are plasticisers, they can change and improve the physical properties of PVC to make them suitable for a much wider range of applications e.g. Colorcoat for exterior panels of buildings.

A number of plasticised model paints were prepared. Throughout the experimental work all plasticised model paints consisted of the same basic components. A model paint consisting of 100ml THF, 10g PVC and 3g (30%/30 P.H.R) of Degussa P25 TiO₂ which was prepared using the method described in 2.1.1. An analytical balance was then used to add the required amount of plasticiser to the paint. Before the paint was transferred to a solvent bottle with a magnetic stirrer, a final mix using the high shear mixer was applied. The paint was stirred in the dark for a further 48 hours using a stirrer plate to ensure complete homogenisation as well as complete pigment and plasticiser deagglomeration and PVC dissolution.

2.1.3 Acid Scavenger / Anion Exchange Pigmented Model PVC Systems

Accelerative autocatalytic effects of hydrochloric acid during the degradation process of TiO₂ pigmented PVC systems are known [1]. The addition of an acid scavenger has been used to investigate this phenomenon further. The acid scavenger used was an anion exchange mineral called Hydrotalcite (magnesium aluminium hydroxycarbonate supplied by Aldrich). A range of model paints were prepared using various concentrations of Hydrotalcite (HT). HT was used as a stabiliser addition on its own and in various concentrations mixtures with K2220. Initially two paints were prepared:

- 1) 30% Degussa P25 TiO₂ and 10% Hydrotalcite
- 2) 30% Degussa P25 TiO₂ and 10% K2220

Both paints were made in the same way as described in Section 2.1.1 with all the pigment being initially dispersed in a small quantity of THF. K2220 is a stabilised form of TiO₂ that would not interfere with photodegradation in the time frame of the irradiations used and was added to keep the total pigment concentration constant. This was to negate any possible shielding effects of the Hydrotalcite. The hydrotalcite was used on its own in another series of films to show the effect without the addition of K2220.

Appropriate proportions of paints 1 and 2 were then blended together with a range of secondary pigment concentrations ranging from 0.5% to 10% so as to give a range of Hydrotalcite concentrations whilst keeping total pigment concentration constant and the level of active Degussa P25 constant. The resultant mixtures were transferred to solvent bottles and a magnetic stirrer bar added. The paints were stirred for a further 48hrs using a stirrer plate to ensure complete homogenisation of the two paints.

2.1.4 Model PVC Systems Containing Commercially Used Organic Stabilisers.

Commercial PVC paint systems contain stabilisers to improve physical properties and temperature resistance in both the processing and final applications of the products.

Stabiliser additions (10%) were performed during the weighing out the pigment and the adding of the solvent and resin using the method in section 2.1.1. Again all model systems containing stabilisers were made using the same basic paint consisting of 100ml THF, 10g PVC and 3g of Degussa P25 TiO₂ and the required stabiliser additions. The same method as described in 2.1.3 was used to blend together a range of organic stabiliser concentrations ranging from 0.5% to 10% so as to give a range of stabiliser concentrations whilst keeping total pigment concentration constant and level of active Degussa P25 constant. Paint 1 was a 10% loading of BaZn, CaZn or Sn1/Sn2 with a 30% Degussa P25 and paint 2 was just a standard model system with 30% Degussa P25 only.

2.1.5 Near Commercial TiO₂ Pigmented Plastisol PVC Systems

The near commercial coatings were made at Akzo Nobel Industrial Coatings (Darwen). A range of plastisol formulations used including the current formulation and 2 historical fully formulated samples. A base formulation excluding the all stabilisers and pigment was supplied in a ready made batch by Akzo Nobel. Using an industrial high shear mixer the required amounts of base, TiO₂ pigment, colour pigments and stabilisers were mixed in a standard paint can. The resultant plastisol was mixed until the particle size reduced to <10µm. The plastisol was placed in a vacuum chamber and all the trapped air introduced during mixing was removed. Finally the plastisol was chilled to room temperature and viscosity checked, any adjustments were made by the addition of the appropriate solvent. The paint can lid was affixed and paint stored until required for use.

2.1.6 Fully Commercial TiO₂ Pigmented Plastisol PVC Systems

The fully commercial coatings were made at Akzo Nobel Industrial Coatings (Darwen). A range of plastisol formulations were mixed up using the currently used formation. A base formulation excluding the all stabilisers and pigments was supplied in a ready made batch by Akzo Nobel. Using an industrial high shear mixer the required amounts of base, TiO₂ pigment, colour pigments and stabilisers were mixed in a standard paint can. The resultant plastisol was mixed until the particle size reduced to <10µm. The plastisol was placed in a vacuum chamber and all the trapped air introduced during mixing was removed. Finally the plastisol was chilled to room temperature and viscosity checked, any adjustments were made by the addition of the appropriate solvent. The paint can lid was affixed and paint stored until required for use.

2.2 Sample Preparation

2.2.1 Flat Panel Samples (CO₂ Reactor) [2]

The development of the CO₂ reactor is a new method of modelling coating performance by the use of flat panels as a substrate and to allow the irradiation of the topside of the coating in much the same way as it would happen in real applications.

The irradiation apparatus can accommodate glass panels of approximately 9.5cm x 22cm used to maximise the irradiated surface area and provides a very flat surface therefore not creating any dead space under the panel in the irradiation cell.

The procedure for coating the panels consisted of adding two layers of electrical insulation tape (140µm) down each side of the glass panel to give a consistent height profile to the dried coating of approximately 20µm (reproducibility within a film was $\pm 2.5\%$ and film to film $\pm 5\%$). Paint was poured onto a secondary panel then drawn down the panel to be coated using a glass bar as shown by Figure 2.1. In this way any excess paint was drawn off at the bottom of the panel. Drawing down was performed in a single smooth movement so as to avoid skinning. The pouring plate was employed to remove the effect of skinning which occurred during the time between pouring and drawing down and also to produce a uniform finish to the sample panel.

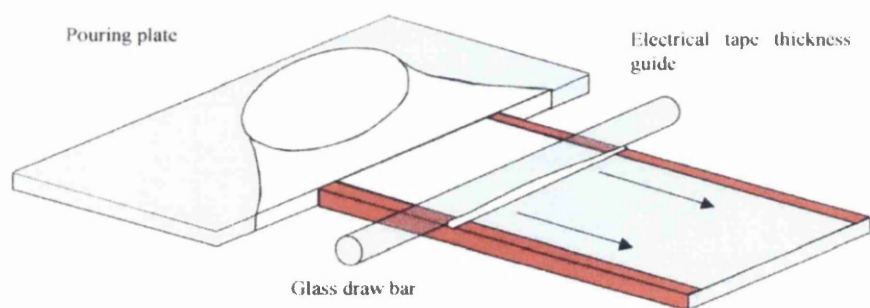


Figure 2.1: Casting process used to draw the paint over the glass panels.

The panels were allowed to dry in a draught free environment so as to slow the rate of solvent evaporation. An evaporation rate that is too fast can lead to pinholes occurring in the coating. The removal of the tape used in the casting process was achieved by placing a glass template over the film and slicing down both sides with a scalpel. This separated the paint film from the tape and allowed for its removal without disturbing the final sample film. To achieve a uniform size between samples the glass template used had a width of 7cm meaning that the sample film size was always 7cm x 22cm (154cm²). Finally all panels were stored in the dark for a minimum of seven days to insure that all THF had evaporated and thus negate any effect it may have on CO₂ evolution in the reactor.

2.2.2 Flat Panel Samples (Weight Loss)

The procedure for coating the panels consisted of adding two layers of electrical insulation tape down each side of the glass panel and produced as above in section 2.2.1. The panels are 9cm x 8cm with the tape placed on the shortest side and to achieve a uniform size between samples the glass template used had a width of 6.5cm meaning that the sample film was always 6.5cm x 8cm (52cm²). This size was used so that 3 panels could be placed under each set of lamps. Finally all panels were stored in the dark for a minimum of seven days to insure that all THF had evaporated and thus negate any effect it may have on CO₂ evolution and weight loss to the sample.

2.2.3 Hydrochloric Acid Evolution Samples

The samples used in the test developed to quantify the levels of hydrochloric acid production were created in borosilicate glass tubes (Fisons o.d. 20mm, i.d. 16mm, length 0.25m). A standard disposable pipette was used to insert 10ml of paint at one end of a borosilicate tube. The paint was allowed to flow down the tube in such a way that a continuous coating was formed on the inside of the tube. Rotation of the tubes was then employed for 10-15 minutes ensuring an even coating was maintained until the paint had become immobilised on the inside of the tube. The film thickness was ~60µm and found to be reproducible to within ±15%. Storage for seven days was sufficient to ensure all THF had evaporated from the film. Finally a small length of

Tygon Masterflex tubing (06429-15) was affixed to the end of the tube to act as a connector using a 2 pack epoxy adhesive (Dunlop SAS 520). The epoxy was allowed to harden for 48hrs before use.

2.2.4 Commercial Plastisol Coated Steel Samples

The preparation of near commercial plastisol samples involved curing the panels to a peak metal temperature (PMT) of 220°C and instantaneous quenching in water. Using glass as a substrate was not feasible so a commercially supplied steel substrate was used. The steel was supplied in the form of pre-primed (compatible chromate pre-treatment) Galvalloy (4.2% Aluminium 95.8% Zinc coated steel) samples measuring 16cm x 18cm. A standard 200µm drawdown bar was placed at the edge of the panel and ample plastisol formulation was dispensed at the front of the bar. The bar was drawn across the surface in one smooth movement with all excess plastisol being drawn off at the bottom of the sample. Each sample was cured to a PMT of 220°C in a standard sample furnace (typically for 50 seconds) then water quenched to room temperature. Finally each panel was guillotined to the required sample size.

2.3 Carbon Dioxide Reactor

In section (1.8.4) it is shown that carbon dioxide (CO₂) is one of the main volatile gases evolved during the photocatalytic degradation of organic species. The Carbon Dioxide Reactor uses this occurrence to quantify the kinetics of photodegradation occurring within any given system. The FTIR spectrum for CO₂ comprises a double peak that occurs between 2300 and 2400 cm⁻¹. This is quantifiable by integration of the peak area and an automated programme has been written which takes the full FTIR spectrum and integrates the CO₂ peak area between 2250 and 2450 cm⁻¹. This then allows for the quantification of CO₂ circulating in the headspace following suitable calibration as will be described below. In all cases the initial headspace within the system was taken from the ambient environment (ca 78% Nitrogen, 21% Oxygen) and an initial scan taken as a baseline to CO₂ evolved during irradiation.

Through repeated experimentation it has been found that results from this method exhibit a scatter of significantly less than 5%. However throughout this work the results shown are repeated with a 5% error in respect of a representative set of results typically taken from a minimum of three repeat tests.

2.3.1 Irradiation Apparatus

The irradiation apparatus is fundamentally made up of three main components connected together with lengths of tubing. The components are an irradiation chamber (Flat Panel Reactor Cell) where the samples are irradiated, a pump to circulate the atmosphere within the system, and an FTIR gas detection cell to allow for the monitoring of any volatile degradation products. The basic layout of the system is shown in Figure 2.2. The three sections make up a sealed unit which enables the concentration of CO₂ and any other degradation intermediates to build up over time thus aiding in the detection and identification.

The pump is a KNF Neuberger LABOPORT pump (Model number N86KN.18) 6l/min neoprene diaphragm pump. Since the volume of the complete apparatus for the system used is less than a litre, the flow rate of the pump ensures that constant mixing is occurring within the

system which reduces the detection time for gas evolution. The CO₂ concentration was measured in an IR gas cell (10cm pathlength, 140ml volume standard IR gas cell with calcium fluoride windows). Calcium fluoride is IR transparent at the wavelengths which are being used and is less hygroscopic than potassium bromide or sodium chloride thus less prone to ‘fogging’ which causes the IR base absorbance to increase.

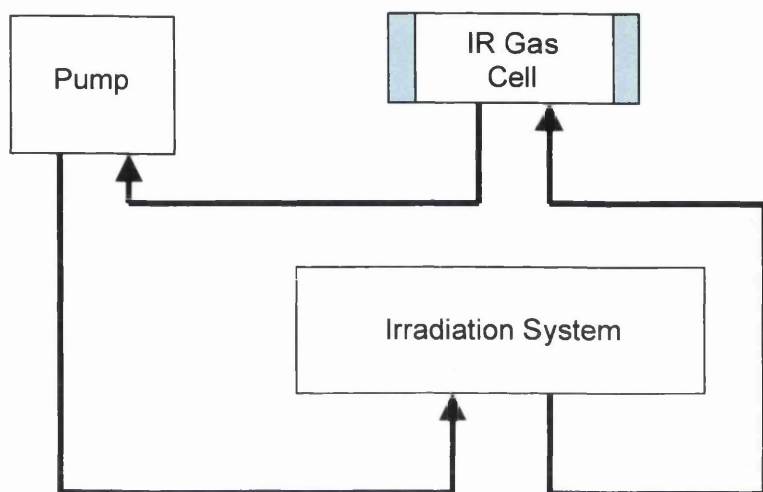


Figure 2.2: General flow diagram for the CO₂ flow system.

2.3.1.1 Flat Panel Reactor

The principle of this system is to create a large area, small volume cell with the benefit of being able to irradiate a variety of flat samples. Two banks of 6 x 8w Coast Wave Blacklight UVA lamps (Coast Air: irradiation λ_{max} 355-365 nm, length 30cm intensity = 4×10^{17} photons s⁻¹ measured by potassium ferrioxalate actinometry [3]) are used to irradiate the flat panel sample. The reactor itself was made from aluminium and the flow system from Swagelock ¼” OD PFA tubing and Swagelock ¼” OD Gas fittings. The barest minimum of Tygon tubing (which displays very low CO₂ permeability) was used to connect the flow system to the various other parts of the apparatus.

Illustrated in Figure 2.3 is the construction of the cell. The Cell was constructed from a single block of aluminium milled to produce a flat sample stage. The sample is introduced

through the narrow sample introduction port in the end of the cell, providing a much smaller area that has to be sealed than would be otherwise possible. The glass panel is sealed to the cell using a two pack epoxy adhesive (Dunlop SAS 520), which is subsequently protected from direct irradiation via reflective aluminised tape. In order to ensure rapid gas mixing and minimum dead volume of gas, inlets and outlets are arranged down either side of the sample stage. The 24, ½ mm inlets provide a 50% smaller surface area than the ¼" OD tubing, to ensure a pressurised supply of the headspace gas. The outlet arrangement had a 25% larger surface area than ¼" OD tubing, this is again to provide a rapid pressurised mixing and efficient exhausting of gases from the cell assembly itself.

To test the response of the cell increasing levels of CO₂ concentration, 1ml (1000µl) volumes of CO₂ were introduced at regular intervals and the signal from IR recorded as shown in Figure 2.4. The time taken for the CO₂ levels to reach a steady state in the IR gas cell and flat panel reactor after the injection is really quick indicating that the gas mixing is effective. The irradiation of flat panel samples (glass) allows the precise surface area and thickness of the coated sample to be defined. By the calibration of the apparatus a calculation of CO₂ evolution versus coating surface area can be obtained from the response of FTIR, therefore allowing quantification of the rate of CO₂ evolution as a result of degradation to be achieved.

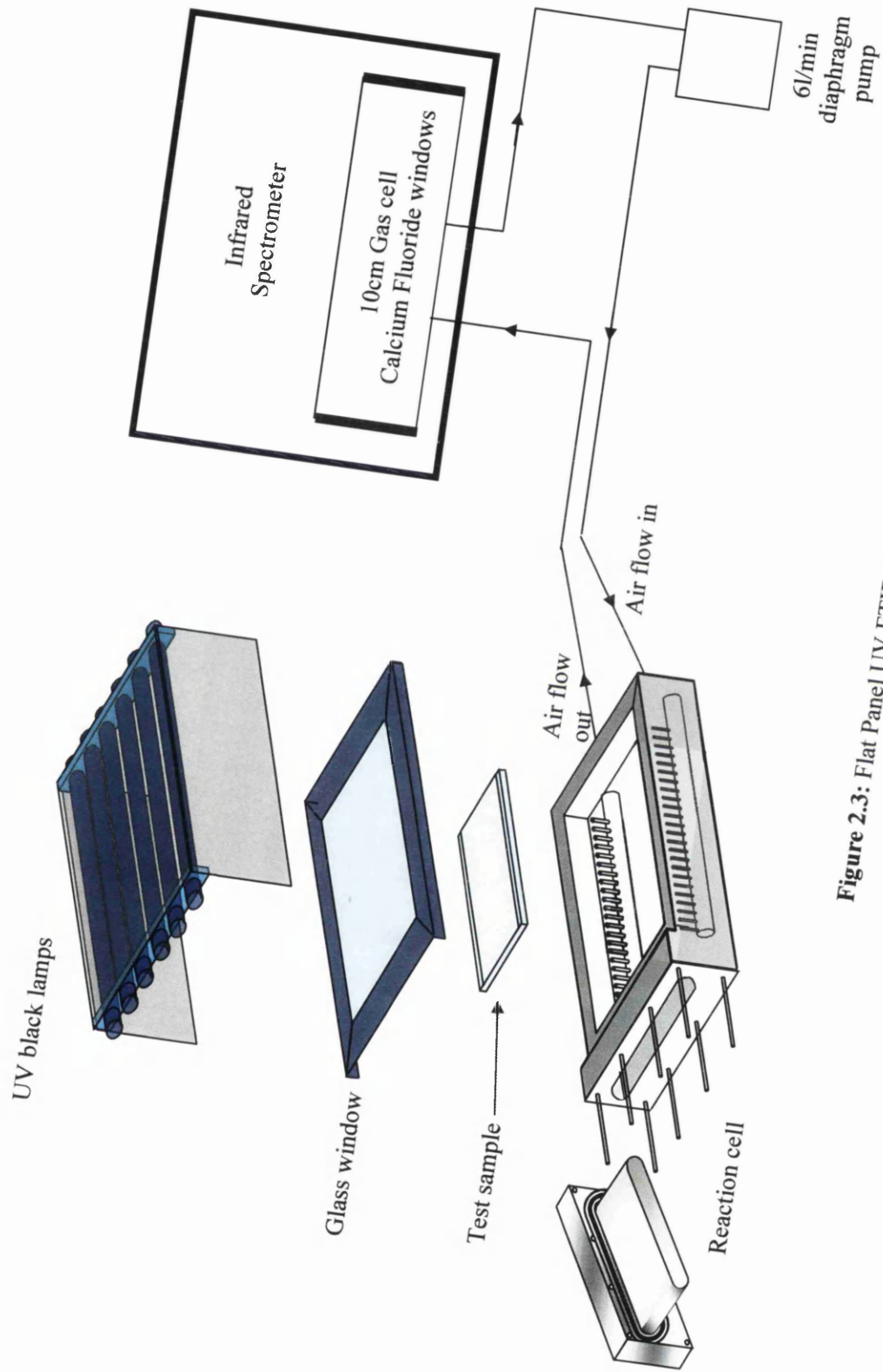


Figure 2.3: Flat Panel UV FTIR Reactor

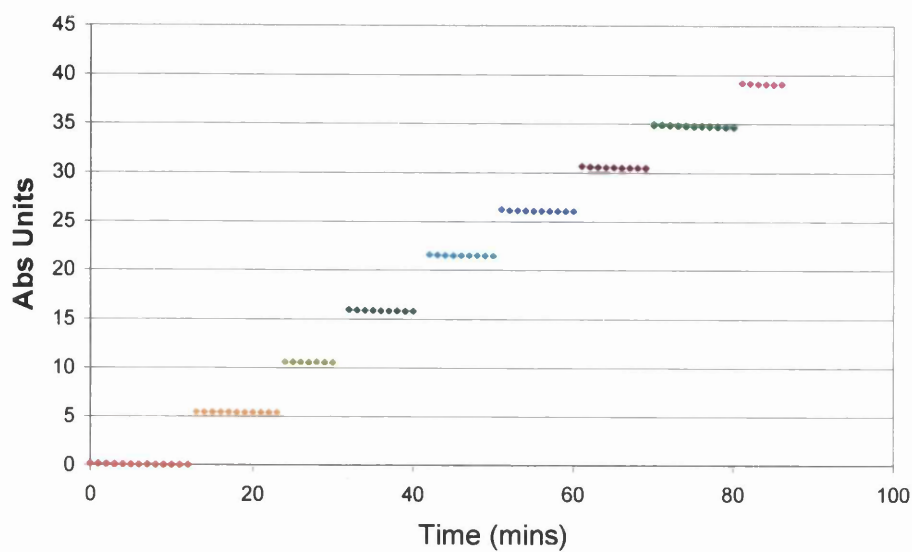


Figure 2.4: The response of the Flat Panel Reactor during multiple injections of 1ml (1000µl) CO₂.

2.3.2 Calibration of the FTIR Flat panel Reactor

In order to report results in the format of CO₂ concentrations, the apparatus had to be calibrated. The CO₂ evolved in the system as a result of irradiating the flat panel samples is measured by the automated software using the FTIR. The conversion factor is used to convert the FTIR response (absorption units) to volume of CO₂ as a function of irradiated surface area. This is calculated through calibration of the apparatus with the introduction of known concentrations of CO₂ gas into the system and it is possible to measure the response versus the concentration of CO₂ in the headspace allowing the measurements to be reported as a volume (µmolm²). This then gives an accurate view of the degradation kinetics as a function of irradiated surface area. The response to successive injections of 1000µl CO₂ was measured and plotted as shown in Figure 2.4. The instantaneous response to each introduction of CO₂ in absorption units is calculated and plotted against a precise volume of CO₂ as shown in Figure 2.5.

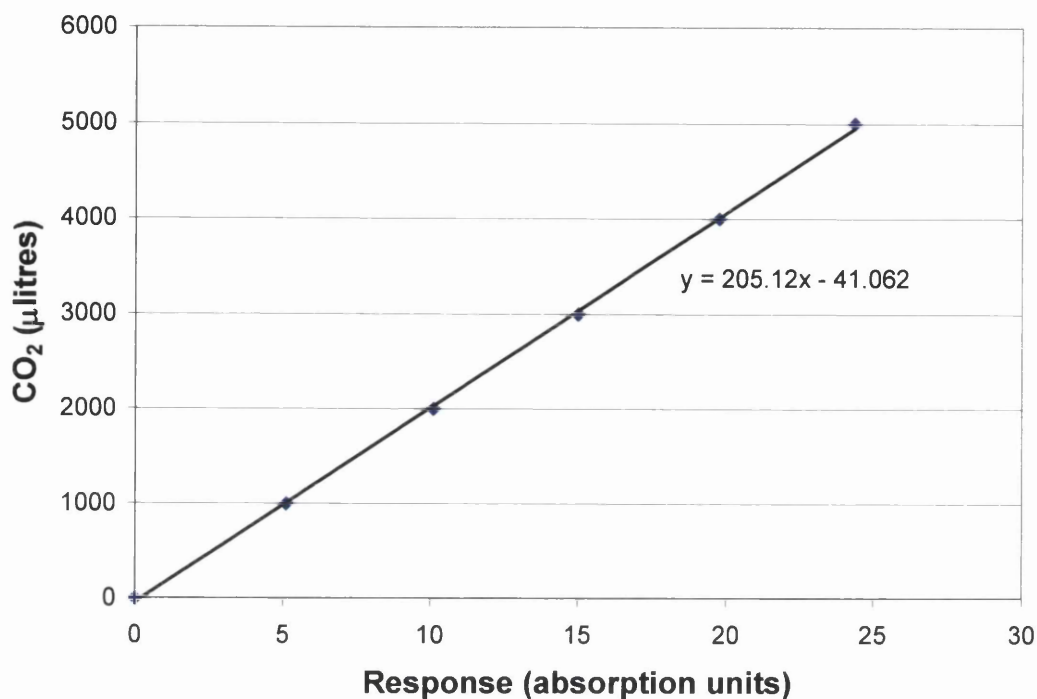


Figure 2.5: Typical Response of the Apparatus to Injections of 1000µl CO₂.

The gradient of the plot shown in Figure 2.5, gives the volume of CO₂ gas required to provide a system response of 1 absorption unit on the FTIR. This volume can be converted to moles by dividing the volume by that of 1 mole of gas at room temperature and pressure (r.p.t). This value can then be divided through by the surface area of the panels used to give the required conversion factor from absorption units to mole of CO₂ per unit area (m²), accounting for variation in sample size as shown in Figure 2.6.

Calculation of CO₂ required producing 1 abs unit response

$$205.12 \mu\text{l} = 1 \text{ abs unit}$$

$$\therefore 1 \text{ abs unit} = 205.12 \times 10^{-4} \text{ dm}^{-3}$$

$$1 \text{ mol gas at r.t.p.} = 24 \text{ dm}^3$$

$$205.12 \times 10^{-4} / 24$$

$$\therefore 1 \text{ abs unit} = 8.546667 \mu\text{mol CO}_2$$

Calculation of CO₂ evolution per area unit

(for sample size of 154cm² or 0.0154m²)

$$1/0.0154$$

$$\therefore 64.94 \text{ panels in } 1\text{m}^2$$

Calibration factor to convert abs units to $\mu\text{mol.m}^{-2} \text{CO}_2$

$$8.546667 \times 64.94$$

$$= 554.9787$$

Figure 2.6: An Example of a Calibration Calculation

2.4 Fourier Transform Infrared Spectrophotometer

The kinetic experiments outlined in the previous two sections all look at the rate of CO₂ production from the photodegradation of PVC films, using a Perkin Elmer Spectrum 2000 Fourier Transform Infrared Spectrometer (FTIR). The time span required for these experiments are generally within 24 hours due to the use of the highly photo active pigment of Degussa P25. Without the use of automation software the work would become impractical, potentially inaccurate and provide less control over the time interval between scans. In order to automate the scanning process, a Visual Basic program has been written [4] and was used to control the instrument and automate the scans at a desired time interval.

2.4.1 Automatic Data Collection

Using the Spectrum Obey API for Visual Basic 4, it is possible to take control of many of the functions of the IR instrument. These include both practical aspects such as scanning and aligning, and data processing functions such as those used to calculate areas or normalise the data. The primary application enables automated data capture to be defined by the user prior to running the experiment. The set-up and running of the experiment is outlined below.

2.4.2 The Time Interval Set-up

The timer control tab (Figure 2.7) allows for variable interval timed scans throughout the experiment. This enables more scans to be done during the initial period of exposure without producing too many data files that could not be easily processed. Also available is a text box capable of taking an unlimited amount of text concerning the set-up and aims of the experiment. This enables a complete record to be taken along with the data files. The log file is used as a complete record of the program's activities during the time of the experiment. Any alteration, such as "lamps on" or "injection of CO₂", during that time can also be logged within this file via the use of the experiment window and the ability to add comments to the log file.

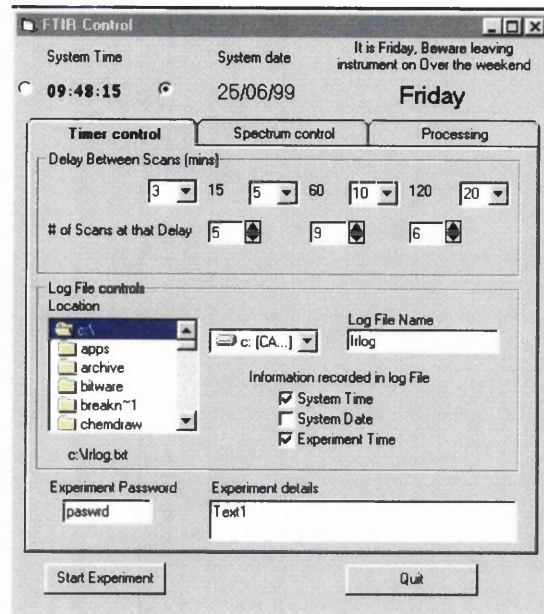


Figure 2.7: The Software setup tab concerning the log file and time intervals

2.4.3 The Scan Settings Tab

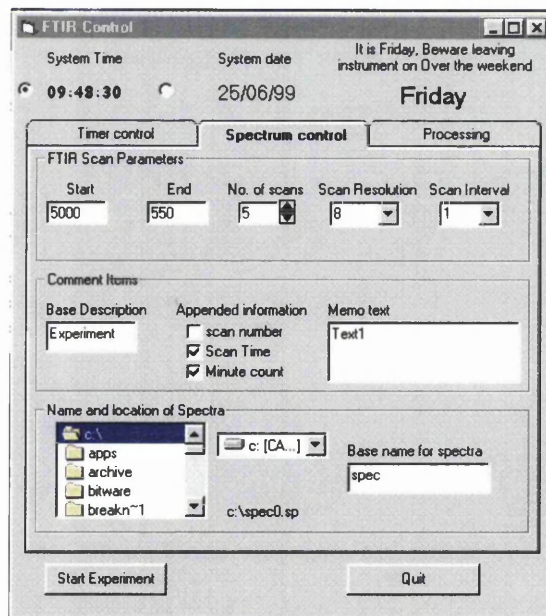


Figure 2.8: Software options controlling the location and scan options available

This tab (Figure 2.8) allows control of the type of scan that is performed, both the scan resolution and wavenumber can be altered and recorded via this tab. The file name and location for each spectra file saved is also defined within this tab, spectra files are numbered sequentially and the time they were recorded is noted within the log file.

2.4.4 Process Tab

The process options tab (Figure 2.9) allows for automatic processing of the spectra as they are recorded. It is important to note that the original data is not changed in any way, just the integrated area under a predefined set of peaks is recorded with the log file. Also, for uses such as calibration or background monitoring the option not to record spectra files is included here. This allowed for highly detailed analysis of the kinetic information (peak investigations) without recording vast amounts of spectra data.

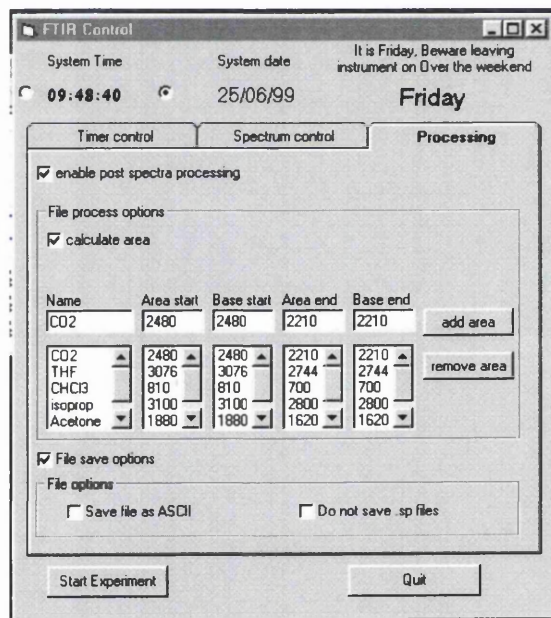


Figure 2.9: Spectra processing control tab

2.4.5 The Log File

The log file generated during the experiment contains a complete list of the programs automated actions during the experiment, and also includes any user initiated scans. The larger part of the results are also included here, as the pre-calculated areas are listed beneath the area title provided during the experiment set-up.

2.5 Hydrochloric Acid Evolution Apparatus

The production of Hydrochloric Acid (HCl) should occur during the photocatalytic degradation of PVC (Section 1.8.4). In previous practical work [4], the presence of HCl hadn't been identified. It was originally thought HCl was undetectable as it was being produced in such small quantities or the HCl molecule was being retained within the PVC.

After further work [5], it was found after several hours of testing using the flat panel reactor with stainless steel tubing small brown particles were collecting in certain parts of the apparatus. EDX analysis showed that there were various elements present that could only have come from the stainless steel pipes used to connect the components of the system together. It also identified the presence of chloride and this suggests that Hydrochloric Acid is being produced. It must have been preferentially attacking the stainless steel tubes before it could be detected by the FTIR. The tubing used in the apparatus is now Telfon tubing of the same size. Once the stainless steel tubing was removed from the system, the aluminium of the reactor itself began to be attacked and corroded.

While it could be possible that other organic acids may have been produced none of them were strong enough to corrode both Stainless Steel and Aluminium. This seemed to confirm that Hydrochloric acid was being produced, however a method of detecting the amount and presence of HCl required the design of a different reactor.

Accurate detection of HCl is somewhat tricky especially in the quantities and environment in which our particular samples were evolving it. A solution was found by the use of a commercial "Dräger Tube System" made by Dräger Limited to detect the presence of HCl. Dräger Tube system is an established method for measuring and detecting contaminants in the soil, water and air. In the case of air sampling the system works by using a pump to pass a known volume of air through a graduated detector tube. The Dräger tubes are species specific and in the case of Hydrochloric acid, Bromophenol

Blue is used as the reactant indicator. When HCl comes in contact with the Bromophenol Blue the resulting product changes to a yellow colour.

Two variants of the Hydrochloric acid specific tubes are available from Dräger at 10ppm and a 500ppm. These detection levels are dependant upon a certain volume of air being passed through the detector tube. The complete system involves one of these tubes being connected to a small hand pump which draws 100ml of air through the tube per stroke. Typically most tubes require 10 strokes to pass the required amount of air (1 litre) through the tube for the indicated scale to be accurate. However, the system in its original setup is unsuitable for detecting the varying amounts of HCl evolved by an irradiated sample in an experiment. A new setup was designed that uses the Dräger tube to measure the total amount of HCl at any point in time rather than air sampling. The new setup is shown in Figure 2.10. Fundamentally it consists of a Fisons o.d. 20mm, i.d. 16mm, length 0.25m tube internally coated with the sample paint as described in section 2.2.3. This is then surrounded by a horse shoe arrangement of 12 x 8w UV-A lamps). The glass tube has a Tygon tube connector bonded into one end while the other end is left open. The Tygon tube connected in series first to a HCl specific Dräger tube then to a variable speed peristaltic pump. During the experiment a shield was placed around the Tygon tube and bonding epoxy to ensure they were not degraded by the UV light. To initiate the experiment the UV lamps and pump are switched on. The pump was set at a relatively slow speed ca ~ 0.1 litre per minute. This is to ensure a constant flow of air into the open end of the sample tube and that no HCl could escape. As HCl is being produced it would be drawn through the sample tube and into the Dräger tube where it reacts with the contents of the tube (Bromophenol Blue). As more HCl is evolved more of the Bromophenol Blue progressively reacts, changing colour from blue to yellow and the reaction frontier moves down the tube to a time lapse camera (Canon PowerShot G3) which was used to take an image every 10 minutes. This gave a series of photos similar to those seen in Figure 2.11, from which it is possible to calculate the time at which the reaction frontier passed each of the tube markers.

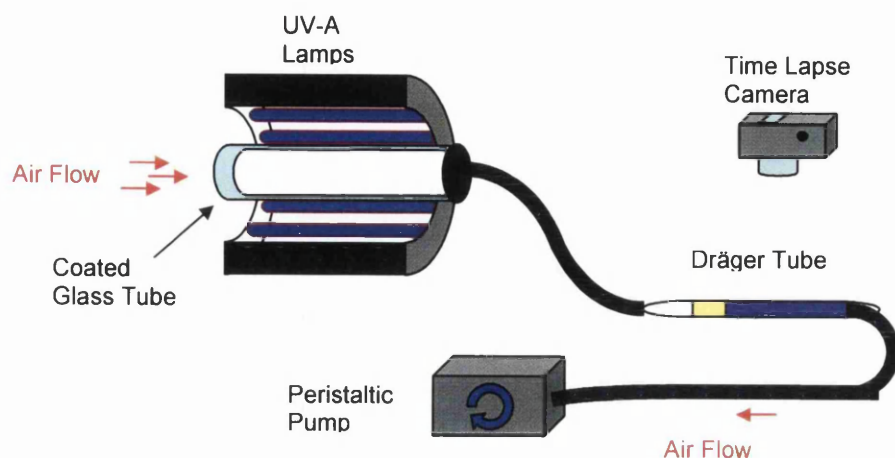


Figure 2.10: Hydrochloric acid detection apparatus.

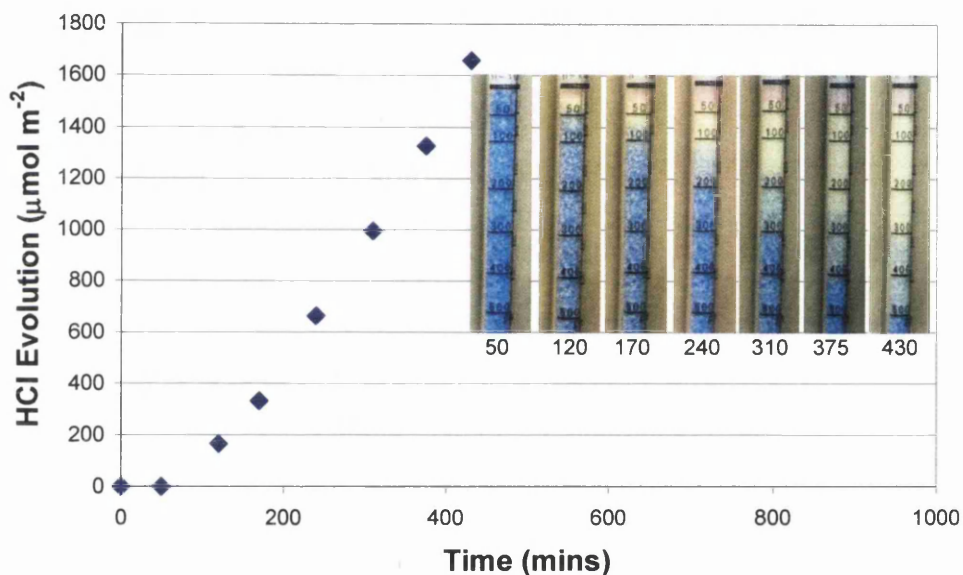


Figure 2.11: Progressive detection and quantification of Hydrochloric acid in Dräger tubes for a typical Degussa P25 TiO_2 pigmented model paint system.

The marks on the side of the Dräger tube were originally calculated for a known amount of air to be passed through them and expressed in terms of ppm. Knowing the amount of gas intended to be passed through the tube and the mass per unit volume used to calculate the ppm values, it is possible to convert each marker into a finite molar amount of HCl that has been evolved and consequently reacted by the Bromophenol Blue. Figure 2.12 shows the calculation that converts the ppm value to a molar value.

Value taken from tube literature \rightarrow 1 ppm HCl = $1.52 \times 10^{-3} \text{ g m}^{-3}$

Volume of air passed through tube = 10 strokes \times 100ml = 1 litre

$$1\text{m}^3 = 1000 \text{ litres}$$

$$1\text{ ppm graduation} = \frac{1.52 \times 10^{-3} \text{ gm}^{-3}}{1000 \text{ litres}} = 1.52 \times 10^{-6} \text{ g HCl}$$

$$1\text{ ppm graduation} = 1.52 \times 10^{-6} \text{ g}$$

$$\text{Atomic weight of Cl} = 35.453\text{g}$$

$$\text{Atomic weight of H} = 1.008\text{g}$$

$$\text{Atomic weight of HCl} = 36.461\text{g}$$

$$\frac{\text{mass ppm}^{-1}}{\text{mass mole}^{-1}} = \text{moles ppm}^{-1} \rightarrow \frac{1.52 \times 10^{-6}}{36.461} = 4.169 \times 10^{-8}$$

Conversion Factor \rightarrow 1 ppm graduation = 4.169×10^{-8} moles

This agrees with the conversion factor obtained from the assumption that

$$1\text{ ppm} = 1 \times 10^{-6} \text{ moles HCl per mole of gas}$$

For any gas 1 mole = 24 litres (298K)

$$1\text{ ppm} = 1 \times 10^{-6} \text{ moles per 24 litres}$$

$$\text{Moles HCl in 1 litre} = \frac{1 \times 10^{-6}}{24} = 4.166 \times 10^{-8} \text{ moles}$$

Figure 2.12: Calculation of Dräger tube conversion factor.

In a similar manner to the results of the CO₂ reactor it was desirable to express the results in the form of moles per unit area. The conversion factor was divided by the surface area of the individual sample (~0.01256m²) calculated from the i.d. of the tubing used.

2.6 Weight Loss Apparatus

Most of the work carried out in this research has centred on the volatile products (CO_2 and HCl) of TiO_2 pigmented PVC. This work, was designed to look at the coating loss of the model films during degradation. The apparatus is shown in Figure 2.13, which consists of the same sample type as use in the CO_2 reactor but on a smaller surface area. The making of the sample panels are described in section 2.2.2 and 3 panels are place under a bank of 6 x 8w UVA lamps. The glass panels are weighed before coating and after before being irradiated for 18 hours everyday for 7 days. The samples were started on a Monday and weighed every working day for 7 days using analytical scale as in Figure 2.14.



Figure 2.13: Weight loss Apparatus.



Figure 2.14: Analytic scales.

2.7 Conventional Accelerated Weathering

To follow work carried out with model coatings using the novel accelerated test methods is a range of commercially used samples, which were mainly investigated using the conventional accelerated weathering technique of Ultra Violet (UVA) exposure. Although there are many different accelerated weathering techniques available UV-A exposure was selected for two reasons. Firstly this is the same type of light source that is used in the CO₂ reactor (section 2.3). Also UVA lamps are the best available simulation of sunlight in the critical short wavelength UV region between 365nm and the solar cut off at 295nm [6]. Figure 2.15 shows similarity in spectral emission between both UVA 340 lamps and sunlight at these lower wavelengths.

Some panels of the fully commercial panels were exposed to UV-B in order to compare results in more extreme conditions. Figure 2.15 shows the spectral emission for UVB lamps. UV-B lamps emit most of their light in the UV-B region where the shortest wavelengths of sunlight are found. Photons with wavelengths in this region are highly energetic and therefore responsible for most of the damage done in coatings during weathering and give fast weathering results. Part of the light that UV-B lights emit has wavelengths shorter than the solar cut-off, which means that the photons have more energy than those of sunlight. This causes trigger reactions in coatings that normally would not take place in sunlight.

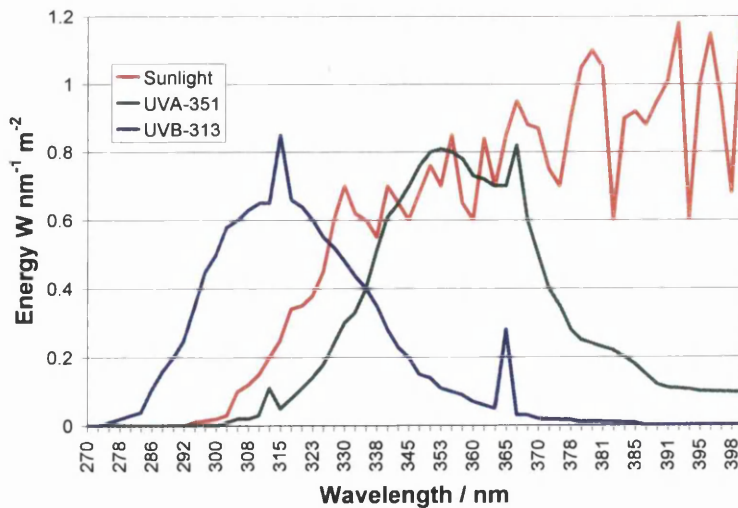


Figure 2.15: Spectral irradiance distribution of UV-A tube⁴

The effects of accelerated weathering in this approach were quantified using a variety of different techniques. The conventional methods of measuring the colour and gloss change were used.

2.7.1 UV-A and UV-B Accelerated Weathering

The sample panels were irradiated using a QUV Accelerated Weathering Cabinet (Q-Panel Company) as shown in Figure 2.16. The machine can subject samples to continuous UV-A or UV-B irradiation, condensation or combination of the two cycles. The condensation cycle simulates the effect of rain followed by sunlight upon the panels. The effects of moisture during weathering are important. Occurrence of gloss and colour change are mostly considered to be UV induced changes, although the presence of moisture during the weathering process can make a big difference to these observations [7]. In general, a synergistic effect between UV irradiation and condensation during weathering is often found. Materials that are resistant to UV irradiation alone and to condensation alone often fail when they are subjected to both [8]. The machine achieves this by having a trough of water beneath the test panels which is heated during the period which the lamps are not operating. The duration and number of cycles can be varied within a standard 24 hour frame. The standard format is 8 hours UV-A exposure followed by 4 hours condensation and this allows two complete cycles in a 24 hour period. The near-commercial panels (Section 5) were weathered for periods of 750 hours at a time which consisted of a total of 500 hours of UV-A irradiation and 250 hours of condensation. The fully commercial (Section 6) were weathered for periods of 1000 hours at a time.



Figure 2.16: Accelerated weathering QUV cabinet.

2.7.2 Gloss Measurement

One technique for measuring coating degradation was the change in gloss level. The gloss of a coating is a measure of the overall surface roughness; a smooth surface will have a high gloss level, making the coating look shiny by reflecting a large portion of the light that falls onto it, especially when the reflection of the light is examined at an angle. During weathering pits and cracks occur on the surface as the binder and the plasticisers get photo oxidised. This phenomenon called micro cracking, will make a surface rough and will therefore decrease the gloss level of the coating.

Gloss can be measured with a simple device, in this case a Minolta Multi Gloss 268 was used. The device is placed on a coating and activated, a tungsten filament lamp (2.5V 60mA) emits a light flash which hits the surface of the coating at an angle. This light flash is reflected by the surface of the coating at the same incident angle, where it is measured by a silicon photo element (Figure 2.17). The angle at which the gloss is measured can be selected manually at 20° , 60° or 85° to the normal of the surface of the coating. In this case a ten point average at 60° for each panel was used.

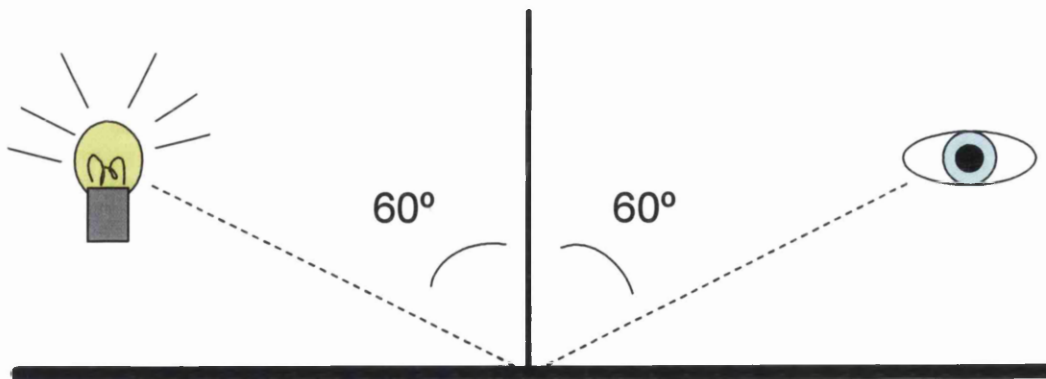


Figure 2.17: Schematic representation of the 60° gloss measurement of a coating.

2.7.3 Colour Measurement

The degradation of plastisol coating is known to cause a darkening effect or more specifically a change in colour. Recent work [9] has shown that the most effective and fundamental way of quantifying colour change is achieved by the measurement of entire reflectance spectrum. Each of the samples undergoing accelerated weathering were measured using a spectrophotometer.

The reflectance spectrophotometer was a Gretag-Macbeth Spectrolino (Figure 2.18) using a $45^{\circ}/0^{\circ}$ geometry. This means that the measured coating is illuminated with a collimated beam of light at a 45° angle with the surface normal, and the reflective response of the coating is measured at 0° angle with the surface normal (at 90° angle to the surface of the coating). This means that the gloss reflectance (the 'mirror' effect which will reflect the incident beam from the coating at a 45° angle in the opposite direction) is excluded from the measurement. Therefore this spectrophotometer was capable of measuring the reflectance spectrum of a coating from 380nm – 730nm excluding gloss effect.



Figure 2.18: Gretag Macbeth reflectance spectrophotometer.

Each panel was measured using the spectrophotometer after each time period (eg 750h or 1000h). Averages of ten different reflectance spectrums for each irradiated panel at each stage of the weathering cycle were used to see the overall change in colour of the panels.

2.8 References

1. Worsley D.A., M., A., Smith, K., and Hutchings, M.G., J. Chem. Soc., 1995: p. 1119.
2. Robinson, A.J., Searle, J.R., and Worsley, D.A., Materials Science and Technology, 2004. **20**: p. 1041.
3. Christensen, P.A., Dilks, A., Egerton, T.A., and Lawson, E.J., Journal of Materials Science, 2002. **37**: p. 1-9.
4. Searle, J.R., *Titanium Dioxide Pigment Photocatalysed Degradation of PVC and Plasticised PVC Coatings*. EngD University of Wales Swansea, 2002.
5. Robinson, A.J., *The Development of Organic Coatings for Strip Steels with Improved Resistance to Photodegradation*. EngD Thesis, University Of Wales Swansea, 2005.
6. *A Choice of Lamps for QU*. 1994, Cleveland: Q-Panel Lab Products.
7. Grossman, D.M., *Correlation questions and answers*, Cleveland: Q-Panel Lab Products.
8. Grossman, D.M., *The weather and how to reproduce it in the laboratory*, Cleveland: Q-Panels Lab Products.
9. Wijdekop, M., *The weathering of organic coated steel and application of mathematical modeling*. EngD Thesis, University Of Wales Swansea, 2004.

Chapter 3

Stabilisers in Model System

3.1 Introduction

Many different additives are used to help stabilise commercial PVC based paint systems against a range of degradative mechanisms. These include thermal stabilisers, acid scavengers and UV stabilisers. Thermal stabilisers and acid scavengers are primarily added to commercial plastisols to help stabilise the product during processing and manufacturing. Most PVC based coating systems require a curing process at elevated temperatures of around 220°C. This temperature can lead to the formulation of acidic species (largely HCl) from the thermal degradation of PVC [1-4]. The thermal and acid scavengers are the most expensive additive after the UV stabilisers and are typically used at a 3% loading. Light stabilisers (~0.1-0.3%) are added to help protect the finished coating from attack by high energy wavelengths of light that the product is exposed to during its life.

3.1.1 Aims and Objectives

As highlighted in the introductory chapter there is an increased pressure for the coating industry to use less heavy metal based stabilisers and make environmentally friendly products. This chapter investigates the effect of the type and concentration of thermal and acid scavengers in model PVC paints. The stabilisers under investigation are BaZn, CaZn, Sn1/Sn2, Hydrotalcite and Hydrotalcite/K2220. The BaZn stabiliser is currently used and replaced the historical use of a combination of two Tin based stabilisers (Sn1/Sn2). The CaZn is the next generation and possible replacement of BaZn. The other two stabilisers are new to use in coatings Hydrotalcite (HT) and a combination of HT and K2220. Hydrotalcite is a non toxic, naturally available material which is a layered magnesium aluminium hydroxycarbonate and K2220 is a very stable TiO₂ pigment from Kronos.

A simple testing procedure has been used to rank the photoactivity of the stabilisers which is based on the evolution of carbon dioxide (CO₂) as described in section 2.3. Other tests based on HCl evolution (section 2.5) and weight loss (section 2.6) have also been used to rank the performance of the stabilisers. The suitability of HT as a stabiliser has been compared with all the commercial stabilisers (BaZn. etc).

3.2 Experimental

3.2.1 Stabilisers

The stabilisers under investigation are shown in Table 3.1. The first three are supplied as a commercial grade and therefore contain several different isomers of the same molecules and minor contaminant compounds. Each stabiliser was incorporated into a model system at levels of 10%, 8%, 6%, 4%, 2%, 1% and 0.5%. The exact formulation of each stabiliser is commercially confidential but they are defined briefly in Table 3.1.

Table 3.1: Stabilisers under investigation

Name	Chemical Name
BaZn	Mixed BaZn containing alkyl-aryl phosphites
CaZn	Mixed CaZn containing alkyl-aryl phosphites
Sn1/Sn2	Maleate Sn stabiliser and a thioester tin stabiliser
Hydrotalcite (HT)	Layered Mg Hydroxycarbonate
HT/K2220	HT/ stable A grade Kronos TiO ₂ pigment

3.2.2 Preparation of the Test Coatings

The model coatings were prepared in a similar manner to that outlined in (section 2.1.4). All model coatings contained 30% loading of the un-stabilised TiO₂ pigment Degussa P25 to ensure rapid degradation. The pigment was initially dispersed into a small amount of THF (Tetrahydrofuran) solvent to ensure good pigment dispersion and de-agglomeration. The remainder of the 100ml THF was then added. 10 grams of powdered, un-plasticised PVC (Aldrich MW ca 95,000) was then quickly and evenly added whilst continuous stirring was maintained, which reduced the level of resin agglomeration to a minimum. The resulting solution was PVC in a solvent solution with TiO₂ pigment suspension. Following this procedure the resulting model system was transferred to a storage bottle and stirred continuously for 24 hours to ensure complete homogenisation. The resulting paint was then stored in darkness to ensure no photodegradation could occur. The stabiliser was incorporated into a standard 30% TiO₂ PVC model system at a level of 10% and diluted down with the addition of more standard model system (without the stabiliser) to the required concentration 0.5% or 1% etc (see section 2.1.4) as shown in Table 3.2.

Table 3.2: The required concentrations of standard model paint and stabilisers.

Required concentration	Standard Model (30% P25)	10% Stabiliser in 30% P25
10%	0g	30g
8%	6g	24g
6%	12g	18g
4%	18g	12g
2%	24g	6g
1%	27g	3g
0.5%	28.5g	1.5g

The procedure for coating the panels with model paints consisted of placing two layers of electrical insulation tape (140 μ m each) down the outside of the glass panel to give a consistent height profile to the dried PVC coating of approximately 20 μ m \pm 2 μ m. Paint was poured onto a secondary panel then drawn down the panel to be coated using a glass bar. All the panels were then allowed to dry for a minimum of seven days to ensure that all the THF had evaporated from the film and thus cancel out any effect it may have on the rate of CO₂ evolution in the reactor or weight loss results. The final surface area of paint films used in the CO₂ flat panel reactor was 220mm x 75mm and 65mm x 80mm for weight loss.

3.2.3 The Photodegradation of Stabiliser Systems

The flat panel reactor used to quantify the photoactivity is outlined in section 2.3.1.1. The paint films were irradiated in the close loop flow system for typically 20 hours. The CO₂ levels contained by the system were constantly measured via a computer controlled FTIR using a 10cm path length gas cell incorporated in the flow system apparatus. The volume of the system was ca 700cm³, and the molar values of CO₂ evolved could be calculated from the calibrated instrument. All 5 stabiliser systems were tested for CO₂ evolution at the concentrations described in Table 3.2.

3.2.4 Weight Loss

The weight loss experiments were carried out as detailed in section 2.6. Three panels (90mm x 80mm) of the same model system were placed under UVA lamps for 18 hours each day and then weighed on an analytical scale for a total duration of 100+ hours. A selection of concentrations of 1%, 2%, 4% and 10% for each of the stabilisers systems were tested for weight loss and HCl evolution.

3.2.4 Identification and Quantification of HCl

Hydrogen chloride (HCl) is a further degradation product from PVC. To detect HCl a modified version of the flow system was developed (see section 2.5). Identical PVC/stabiliser coatings were used on the inside face of borosilicate glass tubes (Fisons o.d. 20mm, i.d. 16mm, length 0.25m). A small length of connecting tube (Tygon) was bonded to the end of the tube which allowed the sample to be connected in series to a detection tube and variable speed peristaltic pump. Laboratory air was drawn through the tubes using a peristaltic pump under similar irradiation conditions to those used in the case of CO₂ evolution experiments. The samples were irradiated using two horse shoe configurations of 6x8w UVA lamps. The HCl was detected using a HCl specific Draeger tube. This essentially contains an indicator immobilised on a resin which changes colour when exposed to HCl. The value recorded on the tube is in ppm and can be converted to an amount of HCl by knowing the volume of gas passed through the tube over the entire duration of the experiment as detailed in section 2.5.

3.3 Results and Discussion

3.3.1 Effect of Stabiliser System on CO₂ Evolution

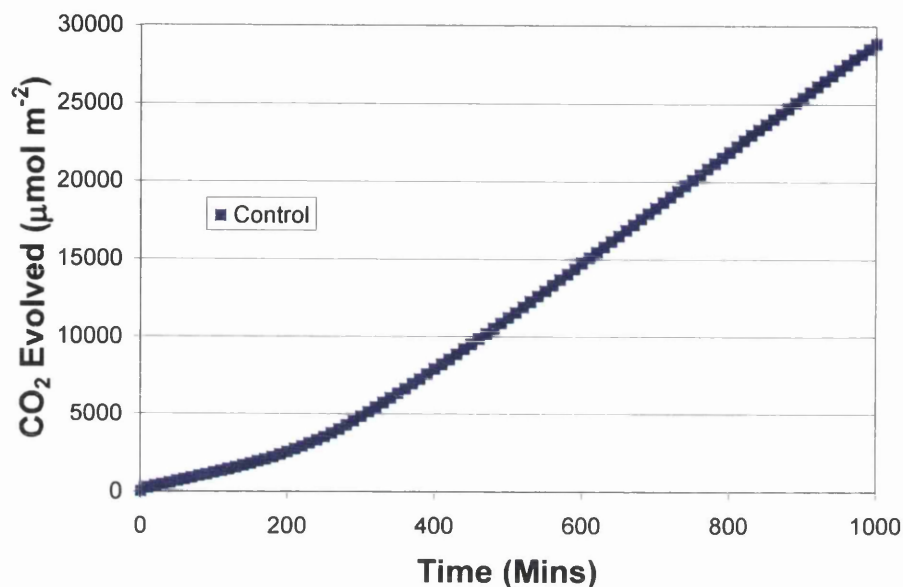


Figure 3.1: CO₂ evolution for control (30% Degussa P25).

It can be seen that for the control (no stabiliser additions) there is an initial rate of CO₂ evolution over the first 200 minutes which then switches to a higher rate. In experiments reported [5] it has been found that strong acids are capable of accelerating TiO₂ photo-catalysed reactions [6] and this is the likely explanation for the rate profile observed for the control.

Figures 3.2 to 3.6 show the CO₂ evolution profiles for model systems (PVC 30% TiO₂) containing 5 different stabilisers at loadings of 0.5%, 1%, 2%, 4%, 6%, 8% and 10%. Figure 3.2 shows the CO₂ plots for the commercial BaZn stabiliser used currently. At high concentrations (6%, 8% and 10%) the BaZn stabiliser shows no acceleration in rate due to it preventing acid catalysis of TiO₂. When the concentration of the BaZn stabiliser is reduced to 4% it does show a secondary rate and increase in photodegradation after 750 minutes. This is probably due to the formation of acid species which the stabiliser can no longer absorb. As the concentration is reduced below the typical commercial levels of 3% this changes and a faster secondary rate begins earlier. At the 0.5% and 1% loadings the initial photodegradation is slightly lower than

the standard model system (30% P25). After 400 minutes photodegradation increases rapidly and after 1000 minutes the total CO₂ evolved is comparable with the standard model system.

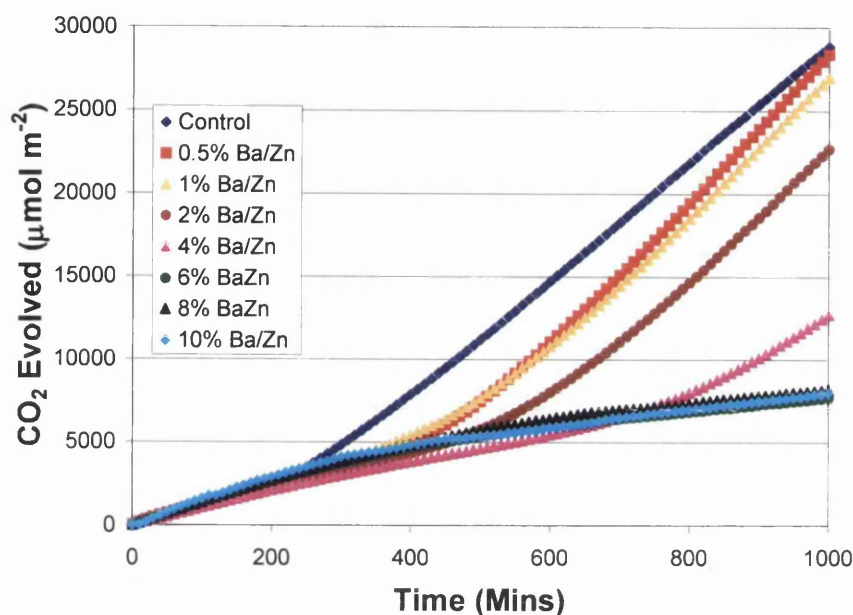


Figure 3.2: CO₂ evolution for various BaZn stabiliser concentrations.

Figure 3.3 shows the CO₂ plots for the new potential commercial CaZn stabiliser and shows a similar profile to the BaZn stabiliser. The main differences are the disappearance of the faster secondary rate for the 4% and for the higher concentrations (10%, 8%, 6% and 4%) photodegradation levels are significantly lower. The transition to a faster secondary rate occurs as the stabiliser concentrations are lowered to 2% and below. The transition to the faster secondary rate occurs after 700 minutes and the CO₂ evolution after 1000 minutes is better than the BaZn stabiliser at 4%. As the concentration of the CaZn stabiliser is reduced to 1% and 0.5% the secondary rate occurs earlier after 400 minutes but still performs slightly better than the same BaZn concentrations and control sample with no stabilisers.

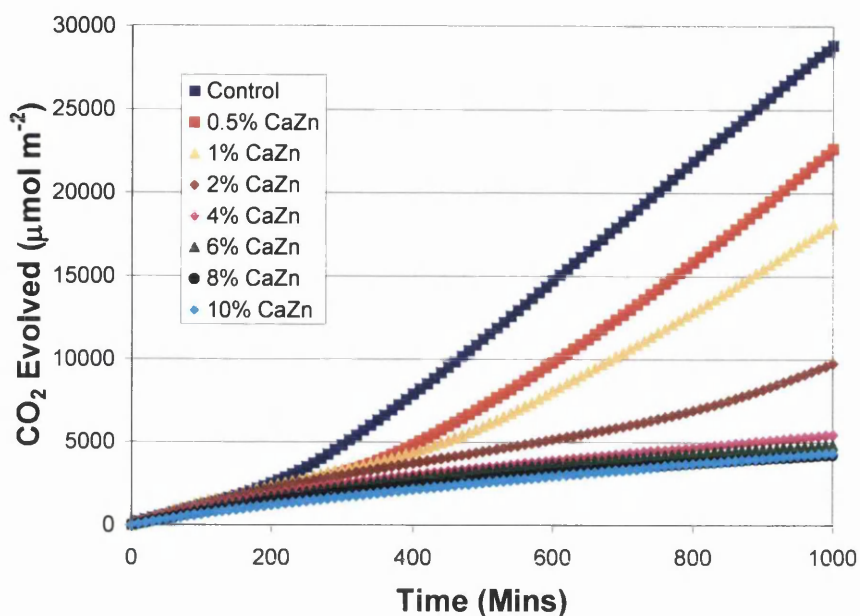


Figure 3.3: CO₂ evolution for various CaZn stabiliser concentrations.

Figure 3.4 shows the CO₂ plots of the historical tin stabiliser (Sn1 and Sn2). This is a 50:50 mixture of a thioester tin stabiliser and a maleate tin stabiliser. The thiotins confer very good heat stability but relatively poor light stability whilst the maleates offer good light stability, but moderate/poor heat stability. At high concentrations (8% and 10%) the Sn1/Sn2 stabiliser shows no catalysis (ie faster secondary rate). When the concentration of Sn1/Sn2 is reduced to 6% it shows an increased secondary rate and increase in photodegradation. This is probably due to the fact that the stabiliser has good light stability and is unable to protect the coating with the use of highly photoactive TiO₂ pigment. As the concentration is reduced to the commercially used levels of 3% and below the initial photodegradation is lower than the control sample with no stabilisers. After 400 minutes photodegradation increases rapidly and after 1000 minutes the photodegradation is comparable to the control sample at 0.5% Sn1/Sn2.

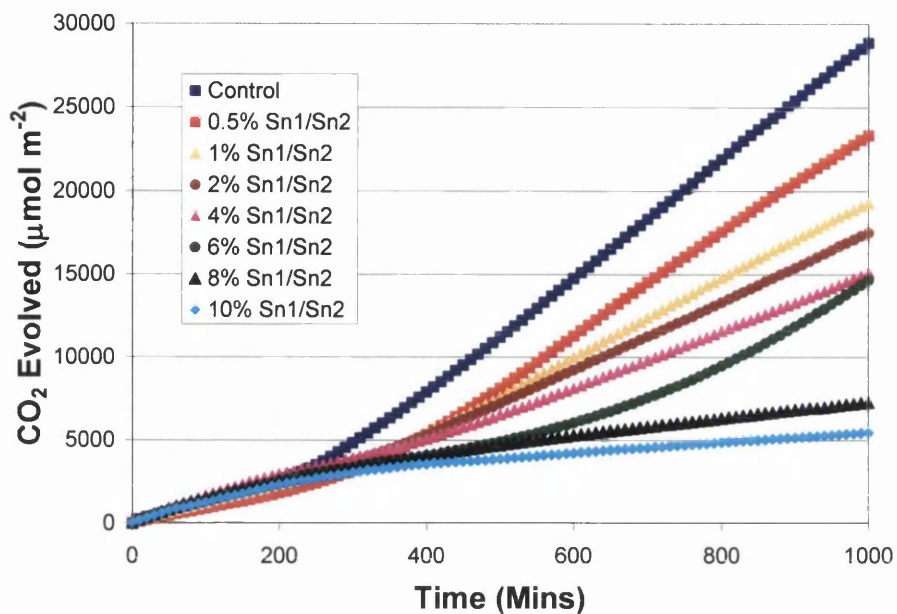


Figure 3.4: CO₂ evolution for various Sn1/Sn2 stabiliser concentrations.

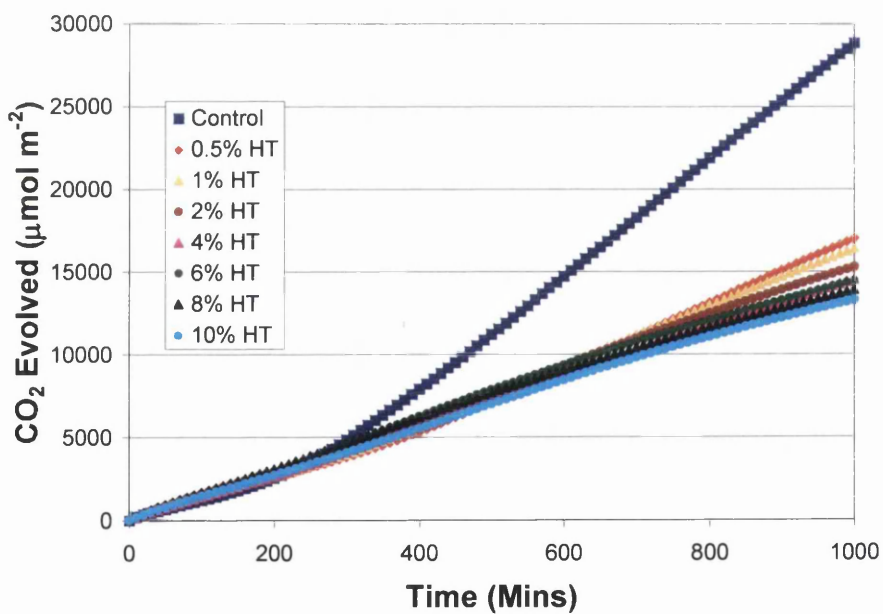


Figure 3.5: CO₂ evolution for various HT stabiliser concentrations.

Figure 3.5 shows the CO₂ plots of the Hydrotalcite (HT) as a stabiliser to un-plasticised PVC. The other plots show the effect of adding HT as a stabiliser, and in the form supplied has a carbonate holding the positively charged layers together. It can be seen by the plots that as the amount of HT is increased above 2% the transition to a faster secondary rate is removed. In the case of acid species being formed (HCl) the matrix will exchange anions with the environment and will exchange one carbonate for two chloride ions. This will therefore reduce the resultant acidity since the acid species would be carbonic acid (H₂CO₃) or bicarbonate (HCO₃⁻). This is therefore insufficient to accelerate TiO₂ photo-catalysed reaction.

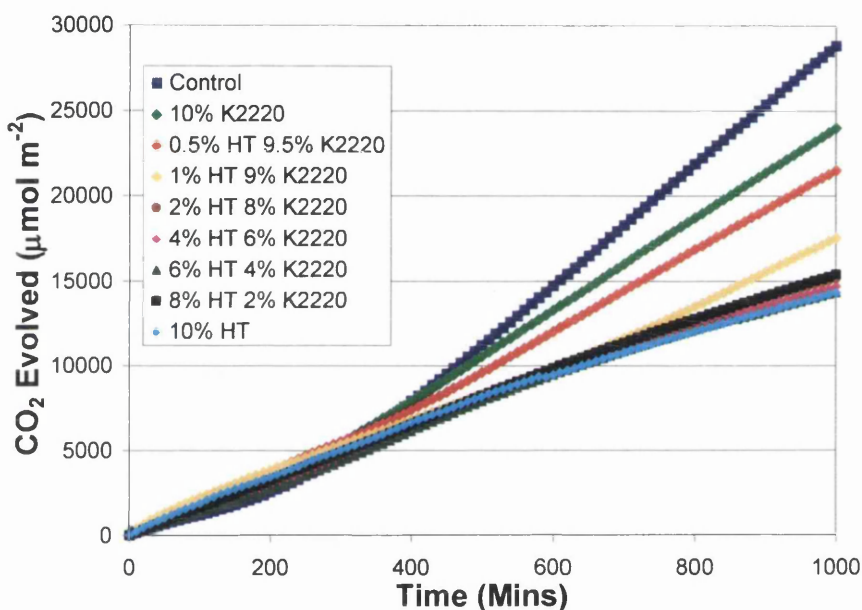


Figure 3.6: CO₂ evolution for various HT/K2220 stabiliser concentrations.

Figure 3.6 shows the CO₂ plots of HT/K2220 as a stabiliser to the un-plasticised PVC. The K2220 is an A grade TiO₂ pigment with a Al/Si oxide coated providing photo stabilisation. The K2220 is added to the HT additions to achieve a total pigment loading of 40%. K2220 is a photostable form of TiO₂ that does not act photo-catalytically in the time frame of the irradiations used. There is a decrease in both the primary and secondary rates when 10% K2220 is added to the paint which is due to the excellent light scattering power of the K2220 pigment. There is no influence on the transition to higher rate upon the addition of this pigment, merely a reduction in the rates of both processes as a result of light scattering by the inert K2220 pigment. All the films have the same pigment loading (40 PHR) and all contain 30 PHR Degussa P25

TiO₂. The difference is that there is (10-x) PHR Kronos K2220 and (x) PHR Hydrotalcite (HT). Figure 3.6 shows that HT addition has very little influence on the initial rates of photodegradation as might be expected from the HT only results. Introduction of the HT pigment again has a profound effect on whether there is a transition to a higher secondary rate. Figure 3.5 and 3.6 indicate that as the HT PHR is increased the initial and secondary rates become more similar to one another.

Figure 3.7 shows the rate ratio between the secondary rates (800-1000 mins) and the initial rates (100-200 mins). The red line indicates the rate ratio for the control sample of 30% P25 TiO₂ which is approximately 2.7 and is an indication there is transition to a faster secondary rate. If the rate ratio is <1 then this indicates that acid catalysis is not taking place. At high concentrations (10% and 8%) all rate ratios are below 1 and the commercial stabilisers (BaZn, CaZn and Sn1/Sn2) performing below a ratio of 0.5 show the secondary rates are lower than the initial rates. At the 6% loading all stabilisers are still showing the secondary rates to be lower than the initial apart from tin stabiliser that is showing a faster secondary rate. As the concentration of the stabiliser is reduced below 4% the rate ratio for the BaZn, CaZn and Sn1/Sn2 becomes closer to the control sample. At 0.5% concentration all of the commercially used stabilisers show a rate ratio higher than the un-stabilised sample. It is important to notice from this graph that the rate ratio for HT and HT/K2220 stabiliser remains below 1 down to 2% loading. Even at the 1% and 0.5% addition HT is stopping the acid catalysis taking place with a significant improvement compared with the un-stabilised and commercial stabiliser systems.

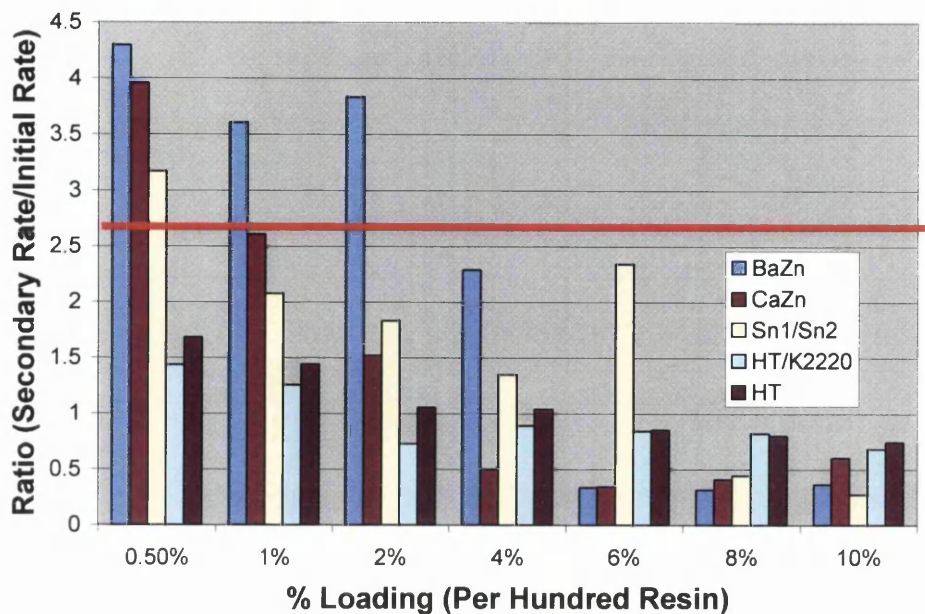


Figure 3.7: The rate ratios of the 5 stabiliser systems at a range of concentrations.

Figure 3.8 shows the final rates of CO₂ evolution between 800-1000 minutes. The red line indicates the standard model system with no stabilisers with a rate ~ 35. It shows a similar trend to Figure 3.7 for concentrations greater than 4% showing a lower rate of CO₂ for the commercial stabilisers (BaZn, CaZn and Sn1/Sn2). As the concentration is reduced to and below 4% the final rate of CO₂ evolution of the commercial stabilisers is higher than HT and HT/K2220 stabiliser. The final rates for BaZn concentrations below 2% are higher than that of the standard model system. At concentrations 0.5% and 1% (Sn1/Sn2 and CaZn) show higher rates of CO₂ than HT. HT shows a similar performance at all concentrations indicating that concentration is not significant and therefore not saturated with Cl⁻. HT shows the lowest rates at concentration 4% and below (apart from 4% CaZn) and is the best performing stabiliser.

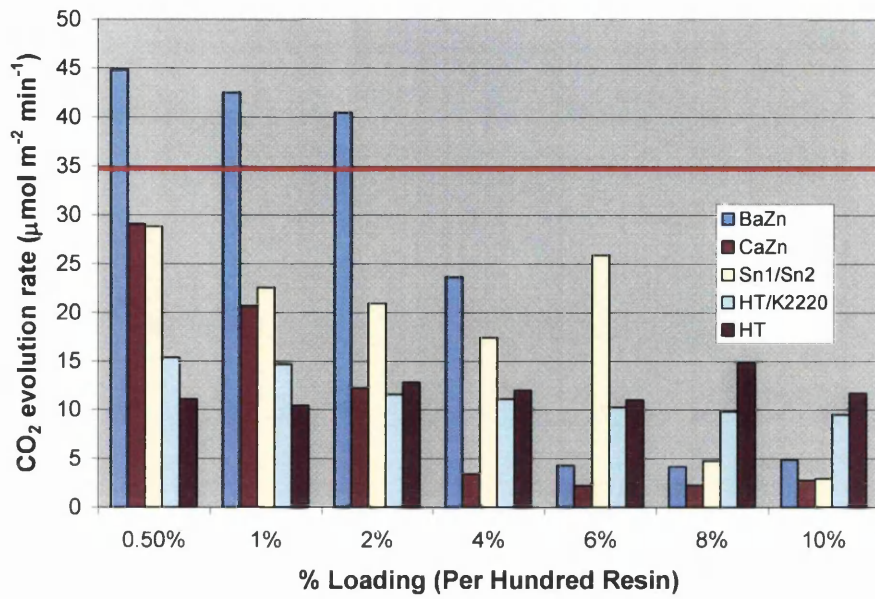


Figure 3.8: The final rate of CO₂ evolution (800-1000 mins) of the 5 stabiliser systems at a range of concentrations.

3.3.2 HCl Evolution

Figures 3.9 to 3.13 show the HCl evolution plots for each stabiliser at 10%, 4%, 2% and 1% concentrations. In Figure 3.9 it can be seen clearly that as the loading of BaZn stabiliser is increased the evolution of HCl is reduced. The un-stabilised PVC film leads to total conversion of the Dräger tube after 580 minutes, with the 1% BaZn taking 880 minutes. As this concentration is increased to 2% BaZn the time taken to finish is 1700 minutes approximately double that of the 1%. When the concentration is increased to 4% and 10% the amount of HCl produced is very small. After 2000 minutes the 4% loading is starting to show an increase in HCl evolution but even after 3000 minutes the 10% BaZn stabiliser is significantly protecting the coating.

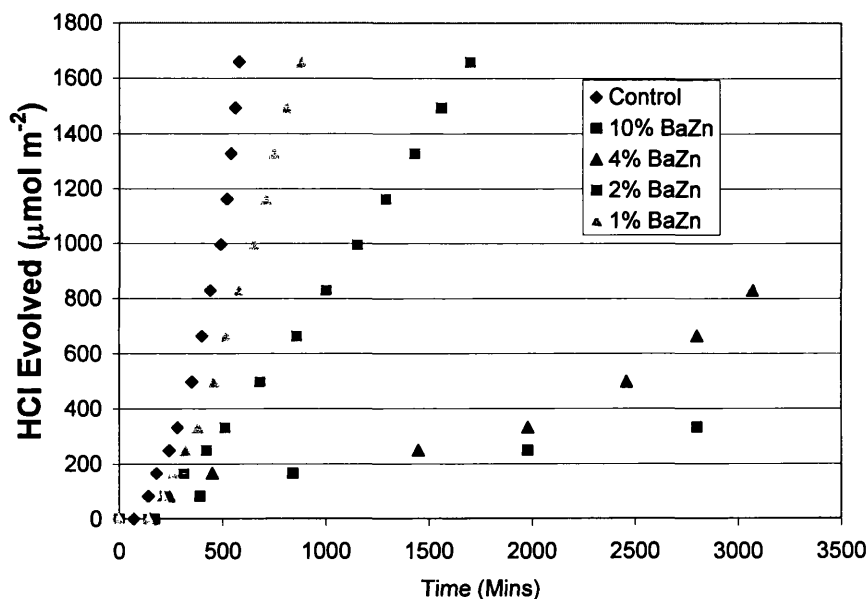


Figure 3.9: HCl evolution profiles of 10%, 4%, 2%, 1% BaZn and un-stabilised PVC.

In Figure 3.10 it can clearly be seen that as the CaZn stabiliser loading is increased the HCl evolution is reduced dramatically. It follows a very similar profile to the BaZn profiles but is showing more stability at the lower concentrations (1% and 2%). This is in line with the CO₂ evolution as the CaZn stabiliser showed less degradation compared with the BaZn. At high concentrations (4% and 10%) the CaZn stabiliser shows very small amounts of HCl evolution and slightly more stability than the BaZn.

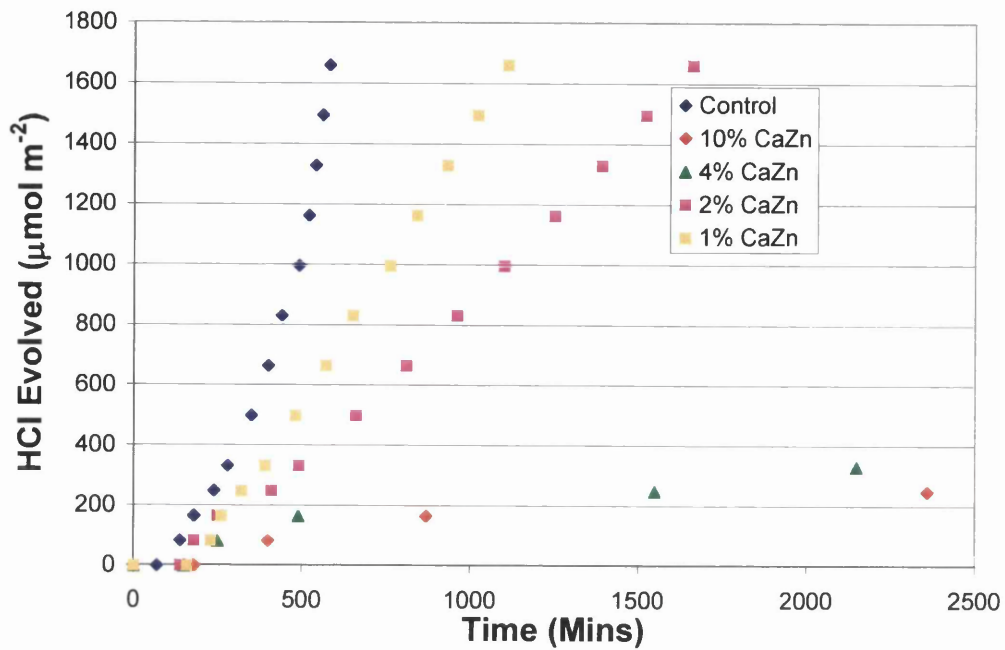


Figure 3.10: HCl evolution profiles of 10%, 4%, 2%, 1% CaZn and un-stabilised PVC.

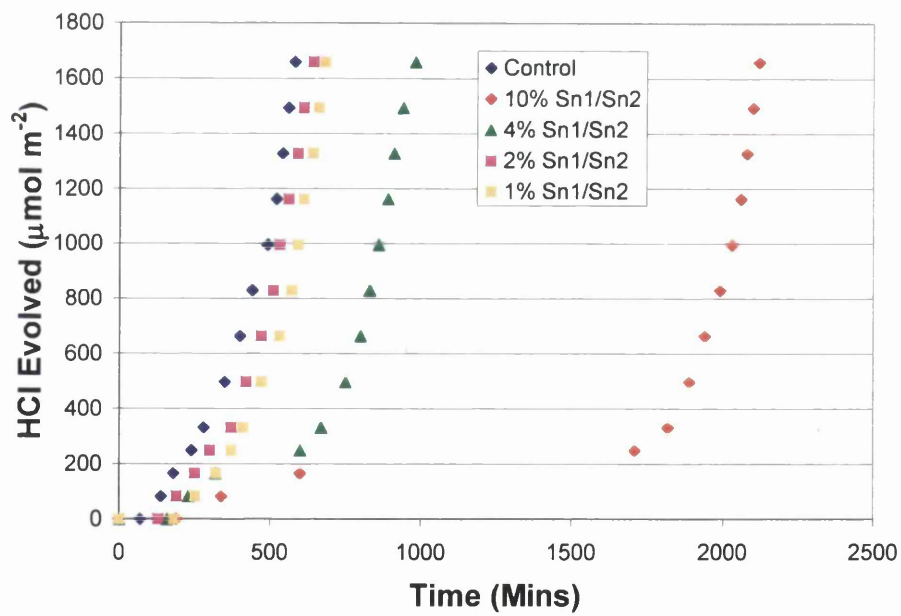


Figure 3.11: HCl evolution profiles of 10%, 4%, 2%, 1% Sn1/Sn2 and un-stabilised PVC.

In Figure 3.11, it can be seen that for low concentrations of Sn1/Sn2 the HCl evolution is very similar to the un-stabilised control system. The 4% loading of Sn1/Sn2 is slow to start although after 500 minutes the HCl profile is the same as the un-stabilised and lower concentrations. The Sn1\Sn2 stabiliser is not as effective as the BaZn and CaZn as even the 10% concentration rapidly forms HCl after 1500 minutes.

Figure 3.12 and Figure 3.13 show as the HT and HT/K2220 loading is increased the HCl evolution decreases. The HCl profiles for HT and HT/K2220 are comparable as the stable TiO₂ is not reacting in the time scale of these experiments. At higher concentrations the HCl evolution is faster than the two organic stabilisers (BaZn and CaZn). The HT addition performs better than the Sn1/Sn2 stabiliser at all the concentrations tested. The HT in the film is able to stop the formation of hydrochloric acid which can catalyse the degradation see Figure 3.7 but is unable to stop HCl completely. In all tests it seems that the commercial BaZn and CaZn stabiliser provides greater resistance to photodegradation leading to HCl gas despite the poor performance in the CO₂ test.

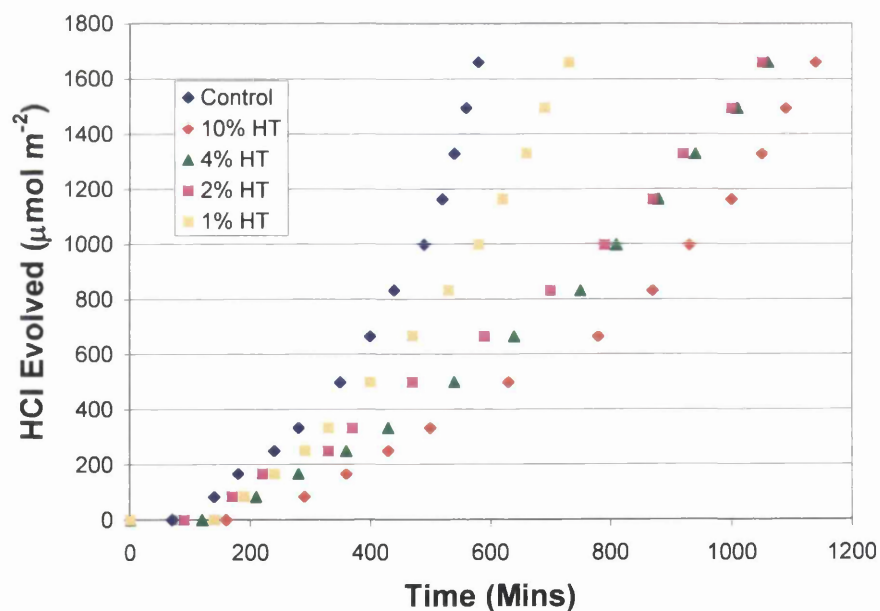


Figure 3.12: HCl evolution profiles of 10%, 4%, 2%, 1% HT and un-stabilised PVC.

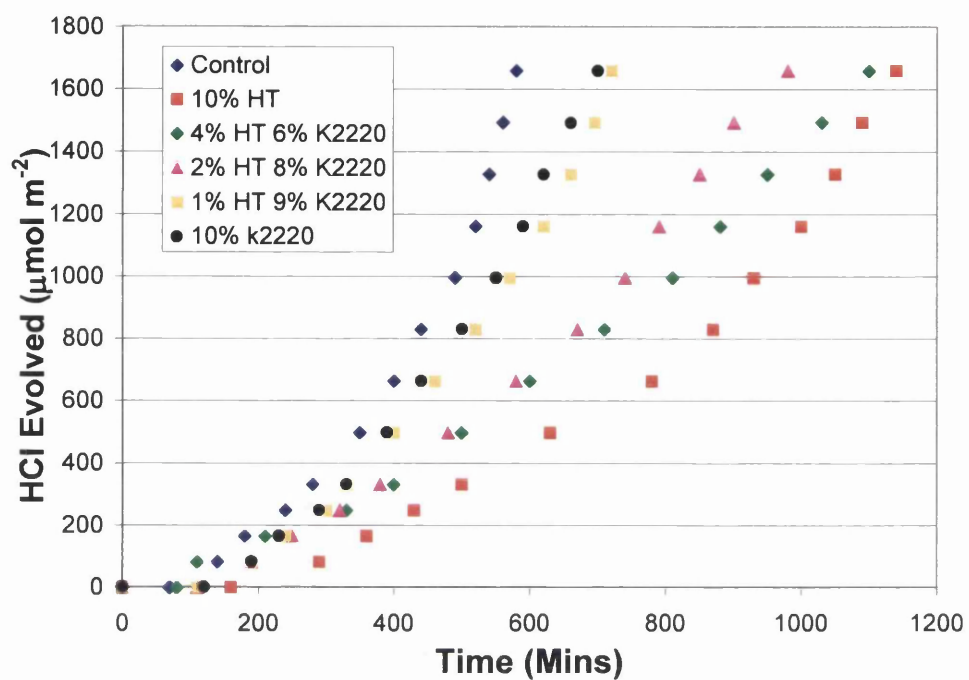


Figure 3.13: HCl evolution profiles of 10%, 4%, 2%, 1% HT/K2220 and un-stabilised PVC.

3.3.3 Weight Loss

Figures 3.14 to 3.18 show the weight loss of the stabilised films after UVA exposure of 6480 minutes. In Figure 3.14 it can be seen that for the first 1000 minutes as the level of stabiliser is increased the coating weight loss is decreased and follows the results for the CO₂. The stabilised systems show less weight loss when compared with the un-stabilised model paint system. Up to 3000 minutes of UVA light the weight loss of the un-stabilised and 1% BaZn are similar and then the un-stabilised rate of weight loss begins to drop off. After 3000 minutes the samples are heavily chalked due to the degradation leaving just the TiO₂ behind. After 3000 minutes the 1% and 2% loadings begin to lose more weight due to the slow degradation of the stabiliser. After 6480 minutes the higher concentrations of 4% and 10% are close to the same total weight loss as the un-stabilised film.

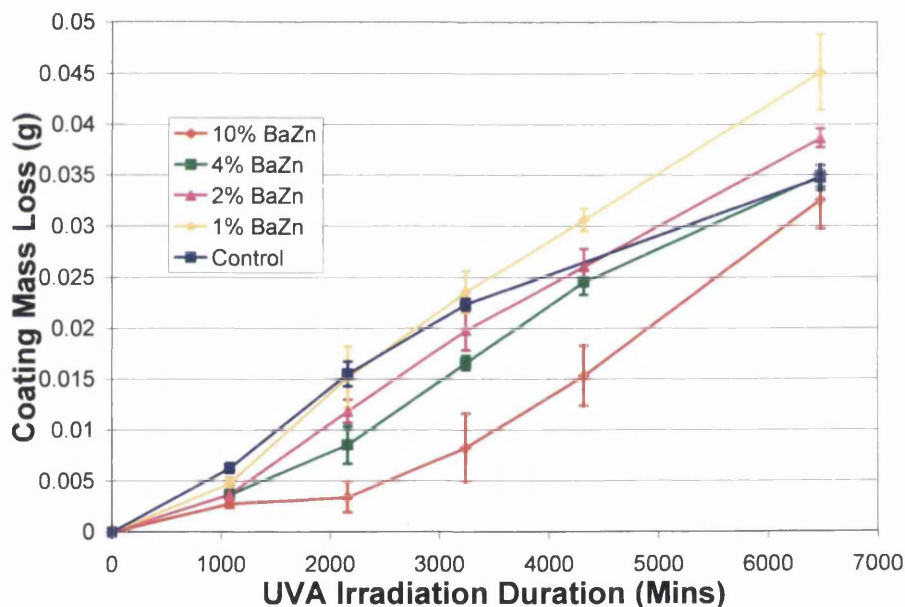


Figure 3.14: Weight loss of coating (g) for 1%, 2%, 4% and 10% loadings of BaZn stabiliser.

In Figure 3.15 it can be seen that for the first 1000 minutes the weight loss for all the CaZn concentrations is very low compared with the un-stabilised system and is less than the BaZn which is comparable to CO₂ results in Figures 3.2 and 3.3. After 1000 minutes the lowest concentration (1%) weight loss starts to increase rapidly and at the end of the experiment is comparable to the un-stabilised system. The 2% concentration shows an increase in weight loss

after 2000 minutes but doesn't lose as much weight as the unstabilised and 1% loaded system. After 3000 minutes the 4% concentration of CaZn starts to lose weight at a rate similar to the lower concentrations. The 10% loses very little weight although does seem start to lose weight as the experiment is about to end. These results seem to indicate that the CaZn stabiliser is preventing weight loss as the concentration is increased. With UVA exposure the CaZn lower concentrations come under attack first as the stabiliser can no longer protect the coating and as time goes on the higher concentrations come under attack as well.

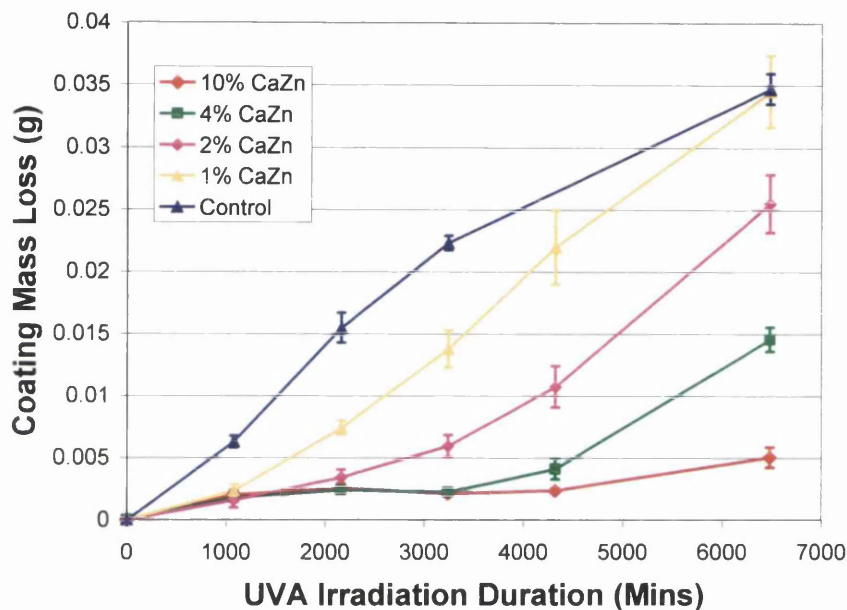


Figure 3.15: Weight loss of coating (g) for 1%, 2%, 4% and 10% loadings of CaZn stabiliser.

In Figure 3.16, the weight loss profiles for the first 1000 minutes follow the same trends as the CO₂ evolution, as concentration is decreased the weight loss increases. After 2000 minutes the un-stabilised control sample shows the most weight loss with less weight loss shown as the concentration of stabiliser is increased. After 3000 minutes, the weight loss for the control sample levels off as the coating is heavily degraded. Although the weight loss for 4%, 2% and 1% continues to increase as the stabiliser is under attack. The 10% concentration starts to show increase in weight loss after 2000 minutes and is approaching the same weight loss as the un-stabilised sample after 6000 minutes.

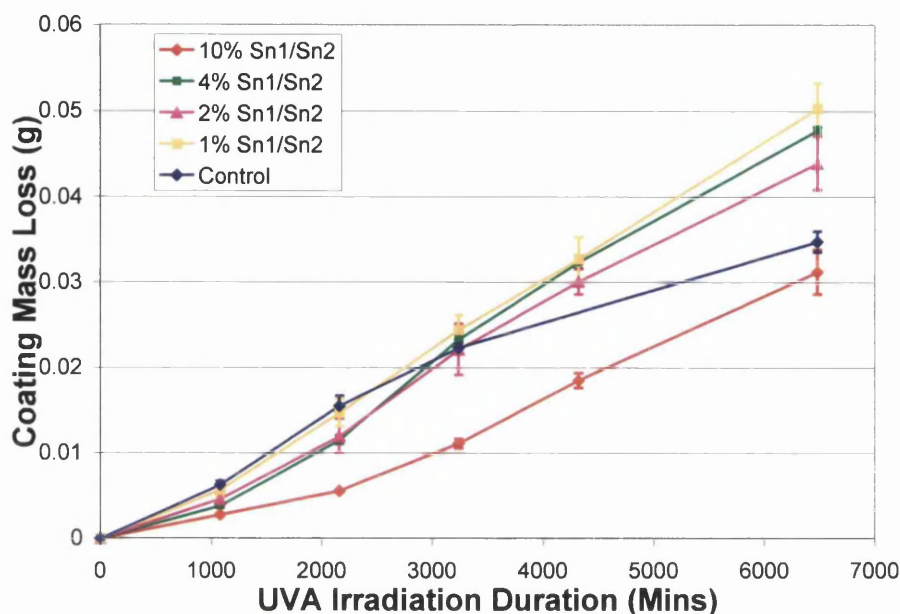


Figure 3.16: Weight loss of coating (g) for 1%, 2%, 4% and 10% loadings of Sn1/Sn2 stabiliser.

In Figure 3.17, the weight profiles after 1000 minutes follow the same trend as the CO₂ evolution, as concentration of stabiliser is decreased the weight loss increases. The weight loss is very similar for all concentrations of HT and the un-stabilised up to 3000 minutes. After 3000 minutes the un-stabilised starts to level off while the HT stabiliser systems show the same weight loss as the initial stages. After 6000 minutes the stabilised system show a slightly higher weight loss compared with the un-stabilised. In this case the HT is removing the acid catalysis but is unable to absorb the intensive light to stop further attack of the PVC matrix from being degraded. The HT is under attack from the UVA light and after long exposure is releasing CO₂ and losing a small amount of weight in this way.

In Figure 3.18, the weight loss profiles follow the same kind of trends as the CO₂ evolution after 1000 minutes, where the concentration is increased. The weight loss for the HT/K2220 stabiliser shows the same levelling off as the un-stabilised control sample after 3000 minutes. The weight loss of the different concentrations show a similar weight loss and after 6000 minutes is lower than the un-stabilised system.

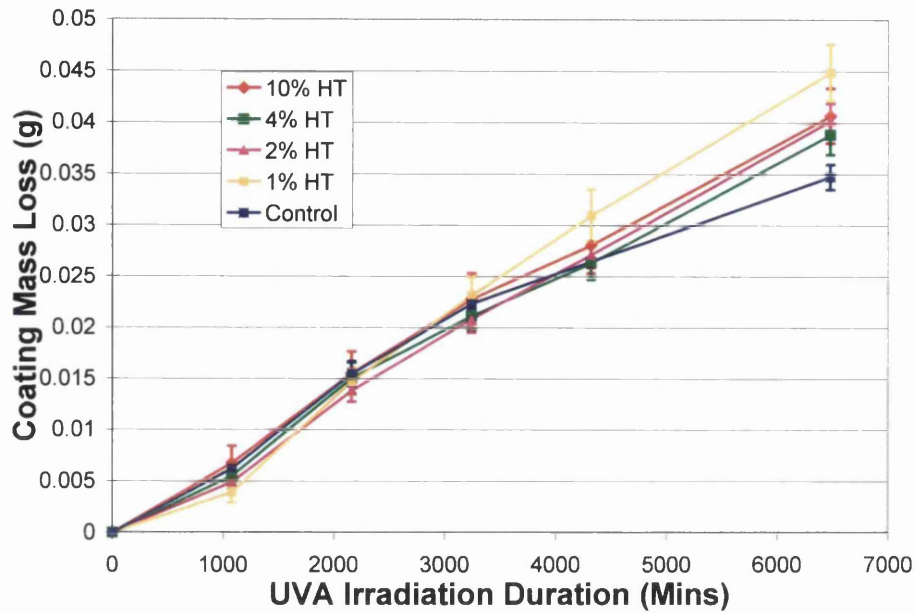


Figure 3.17: Weight loss of coating (g) for 1%, 2%, 4% and 10% loadings of HT stabiliser.

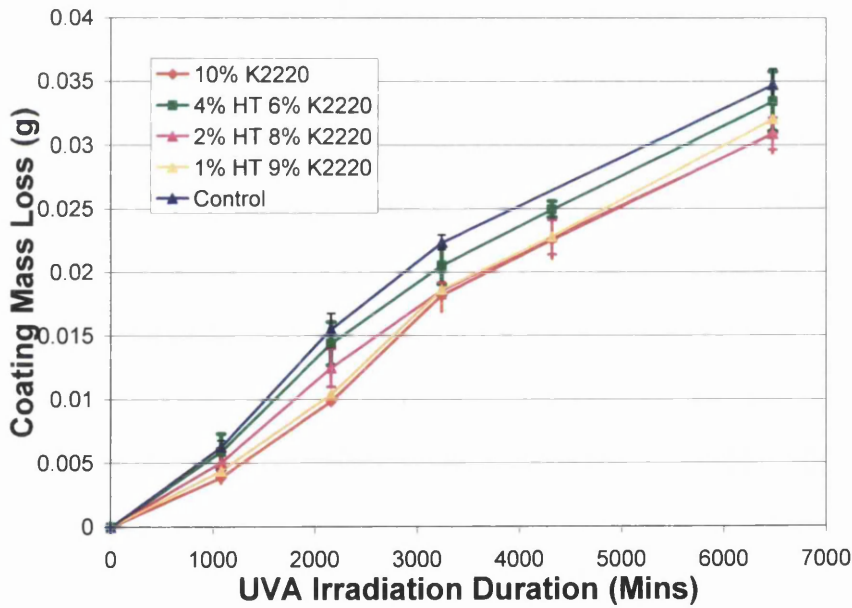


Figure 3.18: Weight loss of coating (g) for 1%, 2%, 4% and 10% loadings of HT/K2220 stabiliser.

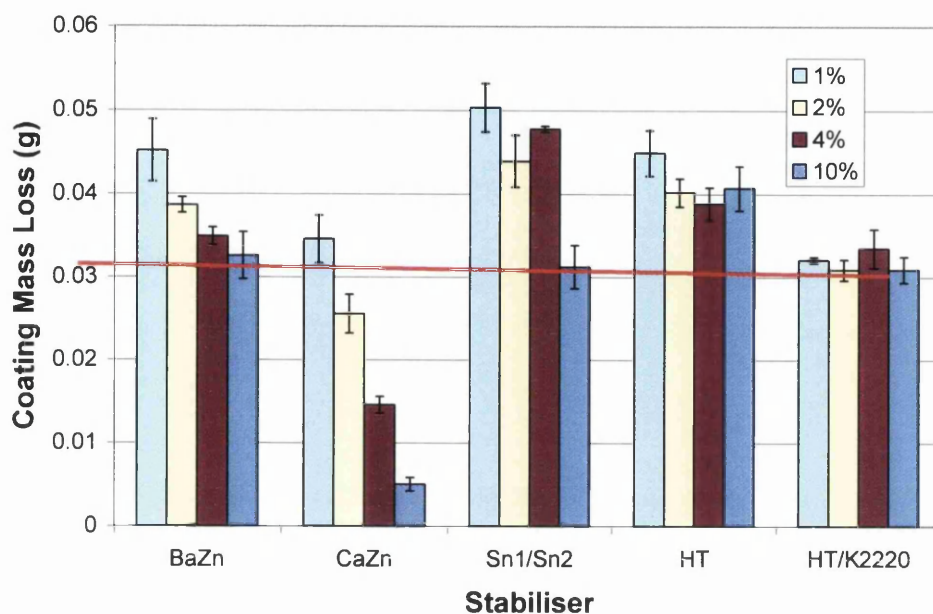


Figure 3.19: Total coating mass loss after 6840 minutes for BaZn, CaZn, Sn1/Sn2, HT and KT/K2220.

Figure 3.19 shows the total coating mass loss for all stabilisers at the end of the weight loss experiment. The red line represents the total mass loss for the un-stabilised. It can be seen that CaZn seems to be the best performing stabiliser with all samples losing less weight than the un-stabilised control. HT/K2220 is the next best followed by BaZn, HT and then Sn1/Sn2. The weight loss is complicated as weight is lost through the known paths of CO₂ and HCl evolution. Unmeasured mechanisms might be occurring where oxidation is being trapped within the coating and increasing the weight. The stabilisers (BaZn and CaZn) bind with Cl⁻ to form metal chlorides and prevent the formation of HCl limiting the weight loss.

3.4 Conclusions

3.4.1 CO₂ evolution

The commercial stabilisers (BaZn, CaZn and Sn1/Sn2) show excellent performance at the high concentrations of 8% and 10%. As the concentrations of the organic stabilisers are decreased below 6% the rate ratio (Secondary rate/Initial Rate) increases over 1 at the point acid catalysis takes place. When the rate ratio is above 1, it shows that there is a transition to a faster secondary rate as seen in the un-stabilised model paint. At low concentration of 0.5% and 1% the rate ratio is significantly higher than the ratio for the un-stabilised system.

HT and HT/K2220 combinations show similar performance indicating that the addition of K2220 to keep the volume fraction the same rules out shielding of the coating by HT. At concentrations between 2% to 10% the rate ratio is below 1 showing that there is change to a faster secondary rate. The carbonate atoms are able to exchange with the Cl⁻ (Figure 3.20) from the HCl evolution and a weaker carbonic acid (H₂CO₃). This acidity is not sufficient to activate the TiO₂ semi-conducting material preventing more rapid photo-degradation over time seen in samples pigmented with TiO₂ alone. Even at the lower concentrations of 0.5% and 1% it is only slightly above 1 and a significant improvement over the organic stabilisers.

Performance ranking of CO₂ evolution (best to worst)

1. HT/K2220 < 2. HT < 3. CaZn < 4. Sn1/Sn2 < 5. BaZn.

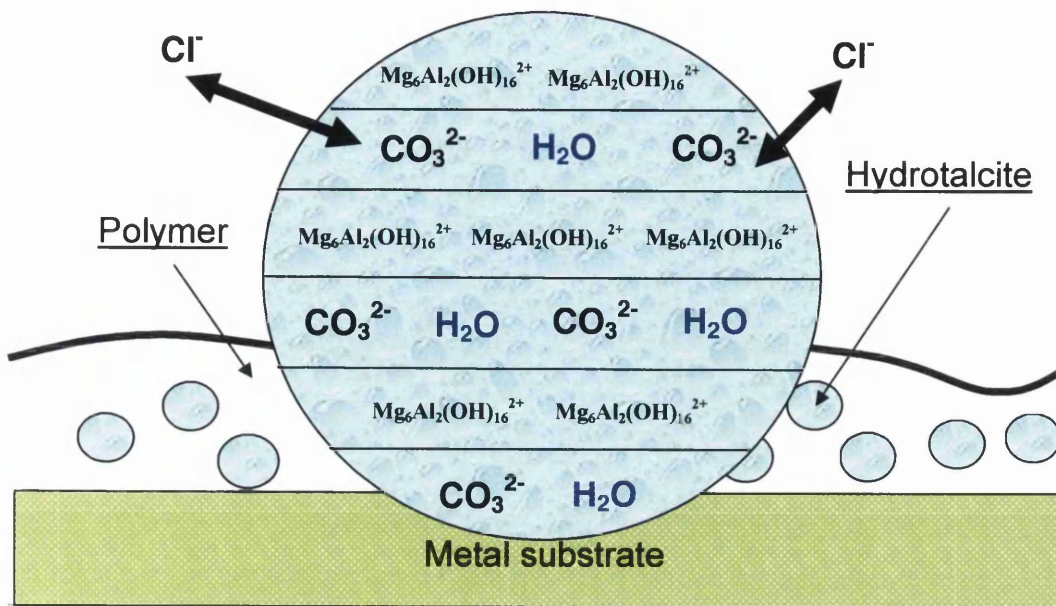


Figure 3.20: How HT works.

3.4.2 HCl Evolution

At high concentrations (CaZn and BaZn) of 4% and 10% the HCl evolution is very small and the rate is very slow as the organic molecules absorb the UVA light and protect the PVC matrix. At low concentrations (1% and 2%) the stabilizer does form HCl although the rate is decreased as more stabiliser is added.

The Sn1/Sn2 stabiliser is the worst of the organic stabilisers at the lower concentrations (1% and 2%) where the rate of HCl evolution is very similar to the un-stabilised system with very little benefit. As the concentration (4% and 10%) is increased the HCl evolution is delayed but still forms in a similar profile as shown in the un-stabilised and low concentrations.

HT and HT/K2220 stops the HCl combining with water (acid catalysis) although is unable to stop the formation of HCl gas. As concentration of HT is increased the rate of HCl evolution is slightly decreased, but not to the same extent as the organic stabilisers. At the low concentrations it performs better than the Sn1/Sn2 and shows similar performance to BaZn and

CaZn. However where commercial plastisol systems are used in concentrations below 3% HT is comparable.

3.4.3 Weight Loss

The Sn1/Sn2 stabiliser at 1%, 2% and 4% show significantly greater weight loss than the un-stabilised system after 6840 minutes. Even the highest concentration of 10% only performs slightly better than the un-stabilised system. The CaZn shows the best performance where 2%, 4% and 10% concentrations show significantly less weight loss than the un-stabilised system. The 1% concentration shows a similar performance to the un-stabilised. The BaZn at low concentration 1% and 2% shows a slight increase to un-stabilised weight loss. The 4% shows a similar performance whereas the 10% has slightly less weight loss.

The HT and HT/K2220 show a similar weight loss at all concentrations to the unstabilised system. The HT concentrations show a slight increase in weight loss whereas the HT/K2220 a slight decrease when compared with the un-stabilised system.

In these experiments a high photo active TiO₂ is being used and with rather long irradiation of nearly 7000 minutes all coatings have been severely attacked. Figure 3.21, shows an example of the Sn1/Sn2 stabiliser at all concentrations (1%, 2%, 4% and 10%). All panels show heavy chalking and large degrees of photodegradation. Whereas Figure 3.22 shows the panels of CaZn where hardly any chalking takes place on the 10% concentration.

Overall HT looks like a promising light stabiliser to help prevent de-hydrochlorination. At lower concentrations it performs similar to organic stabiliser in the model systems using a highly photoactive grade of TiO₂ Degussa P25. Even at a loading of 0.5% it has a benefit of protecting the coating. HT shows a good benefit by cost (half the price BaZn) and is also a more environmentally friendly additive. CaZn also looks promising compared to BaZn from results in this work. Chapters 5 and 6 take the addition of HT further into a commercial plastisol system after these positive results in the model systems where quick results can be achieved.

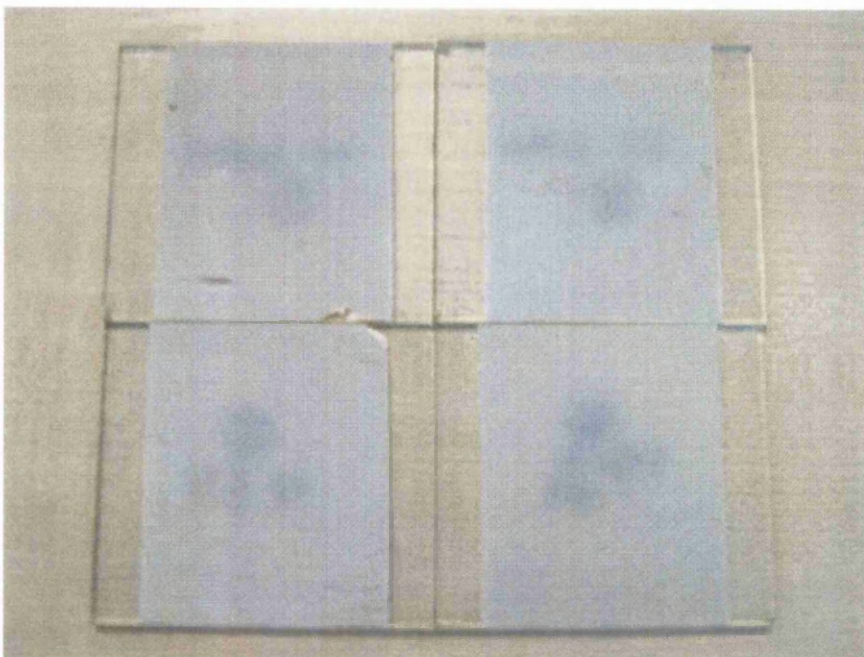


Figure 3.21: Sn1/Sn2 weight loss panels 1% (top left), 2% (top right), 4% (bottom left) and 10% (bottom right).

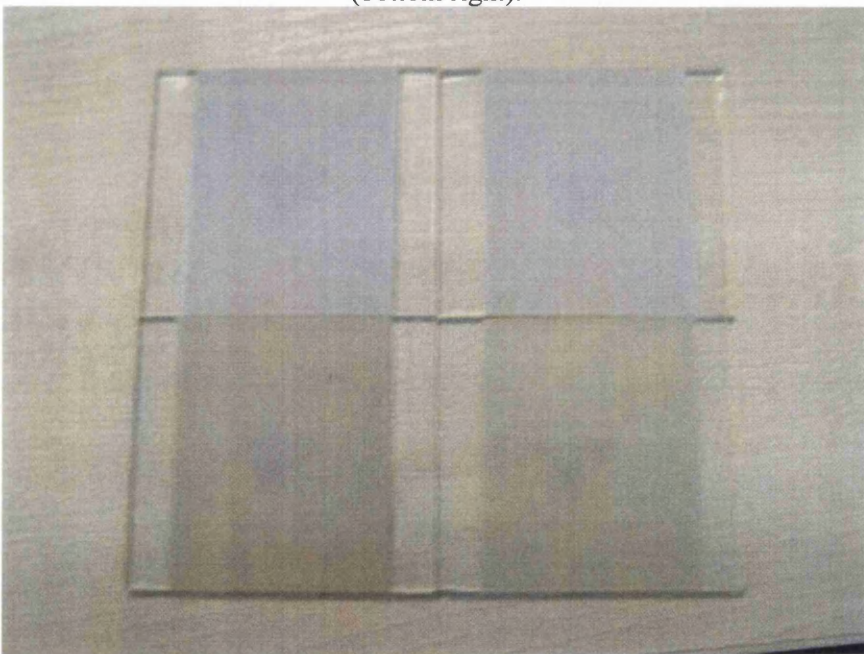


Figure 3.22: CaZn weight loss panels 1% (top left), 2% (top right), 4% (bottom left) and 10% (bottom right).

3.5 References

1. Allen, N.S., and Edge, M., *Fundamentals of Polymer Degradation and Stabilisation*. 1992, London: Elsevier Applied Science Publishers Ltd.
2. Allen, N.S., *Engineering Plastics*. 1995. **8**(No. 4): p. P247.
3. Cheremisinoff, P.E., *Handbook of Polymer Science and Technology Vol. 3: Applications and Processing Operation*. 1989, New York: Marcel dekker inc.
4. Braun, D., *Pure & Appl. Chem*. 1981. **53**: p. 549.
5. Martin, G.P., Robinson, A.J., and Worsley, D.A., , *Hydrotalcite mineral stabilisation of titanium dioxide photocatalysed degradation of unplasticised polyvinylchloride*. *Materials Science and Technology*, 2006. **22**(No. 3): p. 375-378.
6. Worsley, D.A., Mills, A., Smith, K., and Hutchings, M.G.,, *J. Chem. Soc.*, 1995: p. 1119.

Chapter 4

Plasticisers in Model System

4.1 Introduction

Of the substances that make up a PVC plastisol commercial paint, plasticisers are added to the resin in the largest volume fraction with the exception of fillers. They are typically high boiling point, oily organic liquids with the great majority of commercially available plasticisers being esters.

The addition of a plasticiser (~28PHR) to a coating is made for the purpose of modifying the physical properties of the final product [1]. In the case of coated steel products, plasticiser is added to give the organic coating the required flexibility [2, 3] for the manufacturing and forming process as well as resistance to impact damage and stress cracking during external exposure. One failure mechanism in organically coated steels is the loss of flexibility and resilience in the coating, resulting initially in cracking, pin holing and potentially catastrophic delamination. It is therefore of paramount importance that a coating retains flexibility throughout its life.

As plasticisers are not chemically bound to the polymer [4-7], this raises the main technical issues for the industry [8, 9] of the leaching and volatile loss of plasticisers from the coating. The ester groups attached to the benzene ring can attach themselves temporarily to a polymer chain by inter molecular forces, while the flexible alkyl groups provide a separation between different polymer chains [10]. In this way the polymer chains are able to move alongside each other with less friction, which makes the coating more flexible. As these plasticiser molecules are relatively small and mobile it is often the first component to be degraded by UV irradiation and is often the main cause of plasticiser loss. Characteristically high molecular weight plasticisers are used to limit this loss to acceptable quantities during the 20-30 year lifetime of the products.

4.1.1 Aims and Objectives

To be able to offer warranties of up to 30 years, various components of the coating have been changed and improved to give better weathering resistance. The objective was initially to improve the coating performance, but with increasing concern on environment issues it is desirable for plasticisers to be more environmentally friendly and safe. Typically most plasticisers used in the plasticisation of PVC are esters, which are split into several subgroups. Phthalates have been favoured plasticisers for many years, though with concerns about oestrogenic properties and possible environmental effects there has been a move towards the use of non phthalate plasticisers.

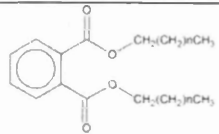
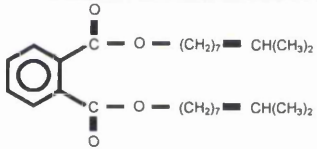
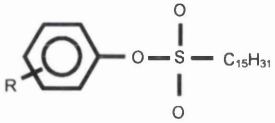
In this section of work the relative performance of three different plasticisers historically used in the PVC plastisol production will be assessed. Two are phthalate based plasticisers whilst the third is a phthalate free sulphonic acid ester. Each plasticiser was included over a range of concentrations in the same model system as used in the previous chapter. The model systems were then evaluated using the CO₂ flat panel reactor [11] which measures the relative kinetics of photodegradation between the different systems. The model systems were irradiated coated within tubes to identify and quantify HCl gas.

4.2 Experimental

4.2.1 Plasticisers

The basic formulae of the three plasticisers under investigation are shown in Table 5.1. Each were supplied as a commercial grade and therefore contained several different isomers of the same molecules and minor contaminant compounds. Each plasticiser was incorporated into a model system at levels of 10%, 30%, 50% and 70%.

Table 4.1: Commercial plasticiser under investigation.

Name	Molecular Structure
Phthalate 1	
Phthalate 2	
Alkylsulphonic phenyl ester (ASPS)	

4.2.2 Preparation of the Test Coatings

The model coatings were prepared in a similar manner to that outlined in (section 2.2.1). All the model coatings contained a 30% loading of the un-stabilised TiO₂ pigment Degussa P25. The pigment was initially dispersed into a small amount of THF (tetrahydrofuran) solvent to ensure good pigment dispersion and de-agglomeration. The remainder of the 100ml of THF was then added. 10 grams of powdered, un-plasticised PVC (Aldrich MW ca 95,000) was then quickly and evenly added whilst continuous

stirring was maintained. This reduced the level of resin agglomeration to a minimum giving a resulting solution of PVC in a solvent solution with TiO₂ pigment suspension. At this stage the required level of plasticiser was added using an analytical balance. Following the addition of the plasticiser the resulting model system was stirred for a further 5 minutes before being transferred with a stirrer bar to a storage bottle and stirred continuously for a further 24 hours to ensure complete homogenisation. The resulting paint was then stored in darkness to ensure no photodegradation could occur.

The procedure for coating the panels with model paints consisted of placing two layers of electrical insulation tape (140µm each) down the outside of the glass panel to give a consistent height profile to the dried PVC coating of approximately 20µm ±2µm. Paint was poured onto a secondary panel then drawn down the panel to be coated using a glass bar. All the panels were then allowed to dry for a minimum of seven days to ensure that all the THF had evaporated from the film and thus cancel out any effect it may have on the rate of CO₂ evolution in the reactor or weight loss results. The final surface area of paint films used in the flat panel reactor was 220mm x 75mm and 65mm x 80mm for weight loss.

4.2.3 The Photodegradation of Plasticised Systems

The flat panel reactor used to quantify the photoactivity in terms of CO₂ evolution is outlined in section 2.3.1.1. The paint films were irradiated in the close loop flow system for 20 hours. The CO₂ levels contained by the system were constantly measured via a computer controlled FTIR using a 10cm path length gas cell incorporated in the flow system apparatus. The volume of the system was ca 700cm³, and the molar values of CO₂ evolved could be calculated from the calibrated instrument as shown previously.

4.2.4 Weight Loss

The weight loss tests were carried out as explained in section 2.6. Three panels (90mm x 80mm) of the same model system were placed under UVA lamps for 18 hours and then weighed every day on an analytical scale for a total duration of 100+ hours.

4.2.5 Identification and quantification of HCl

Hydrogen chloride (HCl) is a further degradation product from PVC. To detect HCl a modified version of the flow system was developed. Identical PVC/Plasticiser coatings were coated on the inside face of borosilicate glass tubes (Fisons o.d. 20mm, i.d. 16mm, length 0.25m). A small length of connecting tube (Tygon) was bonded to the end of the tube which allowed the sample to be connected in series to a detection tube and variable speed peristaltic pump. Laboratory air was drawn through the tubes using a peristaltic pump under identical irradiation conditions to those used in the case of CO₂ evolution experiments. The samples were irradiated using two horse shoe configurations of 6x8w UVA lamps. The HCl was detected using an HCl specific Draeger tube. This essentially contains an indicator immobilised on a resin which changes colour when exposed to HCl. The value recorded on the tube is in ppm and can be converted to an amount of HCl by knowing the volume of gas passed through the tube over the entire duration of the experiment.

4.3 Results and Discussion

4.3.1 Effect of Plasticiser Type on Model PVC Systems

Figures 4.1 to 4.3 show the CO₂ evolution plots for model systems (PVC 30% TiO₂) containing plasticiser loadings of 0%, 10%, 30%, 50% and 70%. In Figure 4.1 there is a clear indication that as plasticiser level is increased so the initial rate of CO₂ evolved increases. This is in line with previous work [10, 12], which showed that increased levels of plasticiser caused increased levels of CO₂ production carried over a short time period of <200 minutes. This assumed the CO₂ evolution rate to be linear, however results in chapter 3 have shown that extended irradiation time can lead to a change in rate within 1000 minutes. In un-plasticised systems (30% Degussa P25), this takes the form of a transition from one linear initial rate to a second much faster rate. This results in HCl and water generation, within the irradiated PVC, resulting in hydrochloric acid, which can catalyse the TiO₂ leading to an acceleration of TiO₂ photocatalysed degradation. This effect has been shown in Chapter 3 to be reduced by addition of an appropriate stabiliser to remove the acid (for example organo-tin, barium/zinc acetate, calcium/zinc acetate or hydrotalcite). This phenomenon is clearly shown here in the control paint that does not contain any plasticiser additions.

With extended irradiation times (Up to 1000 minutes) it is clear that the rate of CO₂ evolution for (610P) phthalate (1) plasticised systems is not linear and after 100 minutes the rate of CO₂ begins to decrease and levels off. Previous work showed that plasticiser was more easily and preferentially degraded than the PVC matrix leading to elevated rates of CO₂ evolution seen in the early stages of irradiation. After 900 minutes, all of the phthalate (Figures 4.1 and 4.2) plasticised samples have produced less CO₂ than the un-plasticised control sample. This would seem to support the fact that the phthalate plasticiser is acting sacrificially to protect the PVC matrix. The addition of the phthalate plasticiser reduces attack on the PVC matrix leading to a reduction of HCl production during exposure and preventing acid catalysis of the TiO₂ as will be demonstrated later (see Figure 4.4).

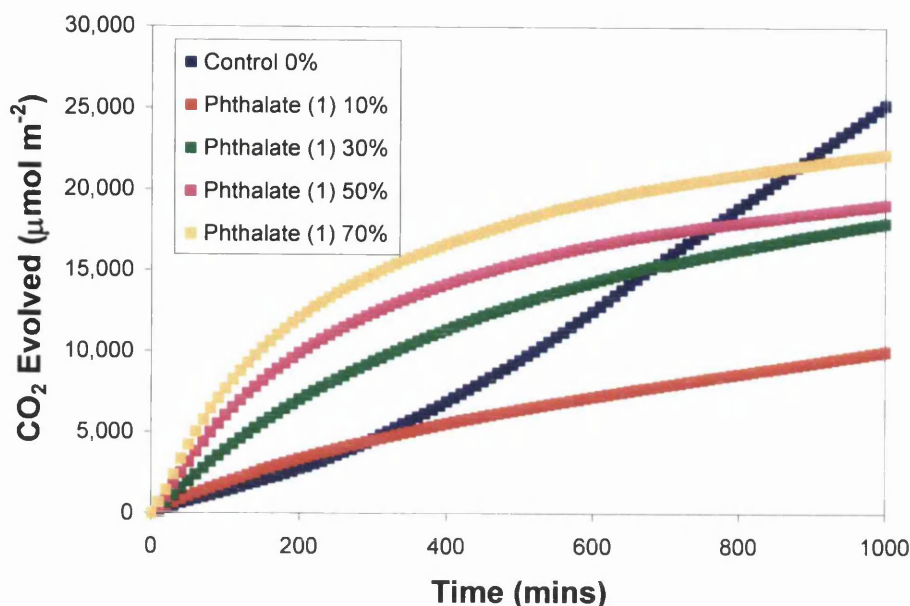


Figure 4.1: CO₂ evolution profiles of 0%-70% phthalate (1) plasticised model PVC systems.

There is a slight difference with the (DIDP) phthalate (2) sample which is a branched version of phthalate 1 plasticiser. In Figure 4.2, although the phthalate (2) samples do follow the same trend as the phthalate 1 samples in that there is a fast initial rate that decreases and levels over time. This levelling off occurs more rapidly in the case of the phthalate (2) plasticiser with all the formulations producing less CO₂ than the unplasticised control sample after 500 minutes. Figure 4.2 also shows that during the early stages of irradiation, plasticiser levels of between 30% and 70% show very similar rates with only the 10% loaded sample being significantly lower whilst the higher loaded samples tail off very quickly with the highest loading of 70% tailing off the quickest. This is the most probable indication of the larger potential for generating intermediate products with higher concentrations of the plasticiser present within the film. At the highest concentrations of plasticiser additions the rate of oxidation will be similar but since there is a higher concentration of phthalate present more will oxidise to precursors of CO₂ than are oxidised all the way to the mineralization product (CO₂). This suggests

that at high loadings the phthalate (2) plasticiser is less likely to be preferentially photo mineralised but is still capable of blocking HCl catalysis and protecting the PVC matrix.

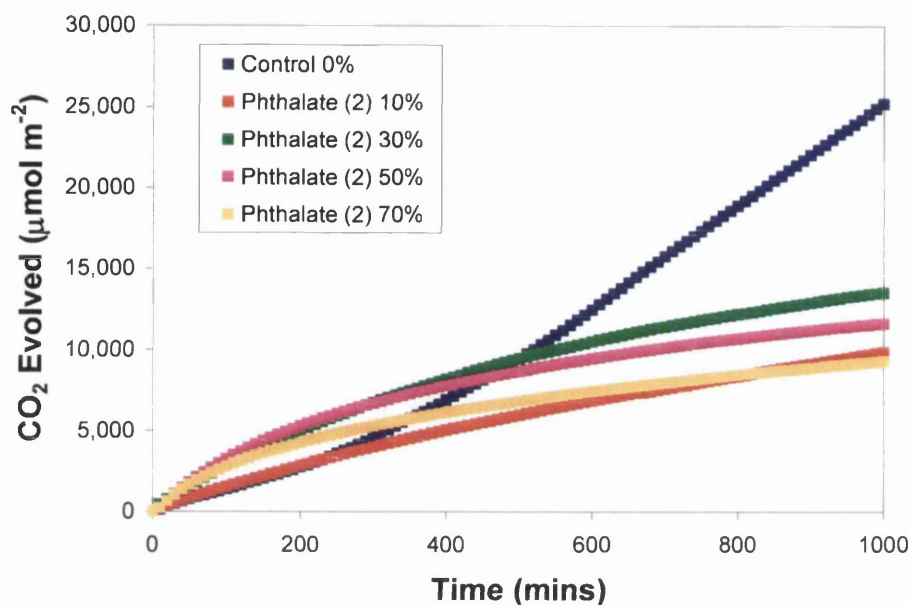


Figure 4.2: CO₂ evolution profiles of 0%-70% phthalate 2 plasticised model PVC systems.

When Alkylsulphonic phenyl ester (ASPS) is used as a plasticiser the profiles of CO₂ evolution shown in Figure 4.3 are very different to either of the phthalate based plasticisers. Although increasing the levels of ASPS plasticiser has the expected effect of increasing the level of initial CO₂ evolution it shows a very different profile than the two phthalate based plasticisers. At the 10% and 30% level it has the same type of profile as the phthalates. The levelling of CO₂ evolution rate does not occur at the highest levels of ASPS additions. For the levels of 50% and 70% the transition to an increased secondary rate is obvious and occurs within 1000 minutes. Throughout the experiment of 1000 minutes the highest levels (50% and 70%) of ASPS evolve more CO₂ than a non plasticised system in contrast to the phthalate. This suggests acid catalysis can occur in the ASPS system at higher plasticiser loadings. Previous work [13], has shown that ASPS degradation produces sulphonic and sulphuric acid fragments. These are the most likely catalysts of degradation.

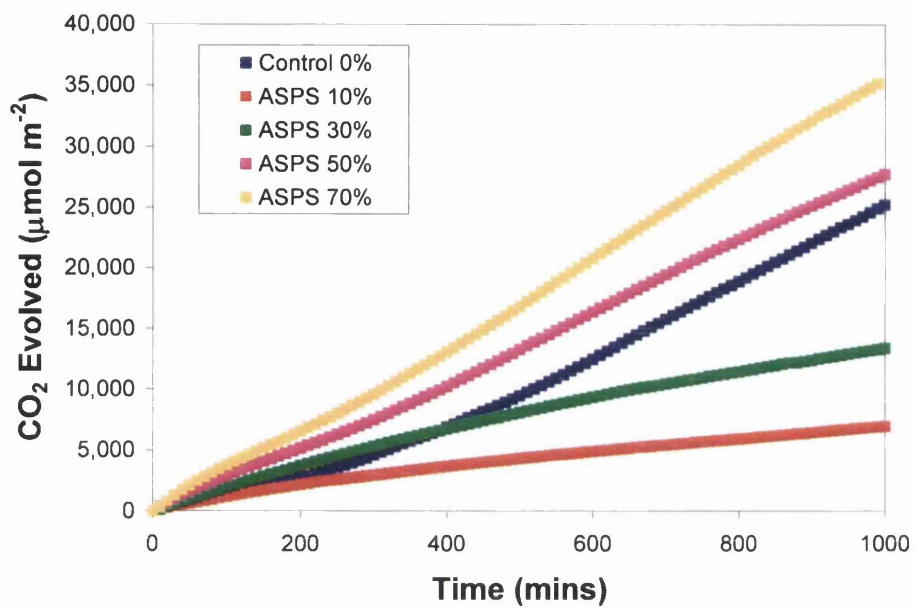


Figure 4.3: CO₂ evolution profiles of 0%-70% ASPS plasticised model PVC systems.

4.3.2 HCl Evolution

Typical HCl evolution profiles are shown in Figure 4.4. In this plot it can be seen that in the absence of plasticiser, HCl is produced very rapidly in the initial stages of the reaction which can subsequently catalyse the photoactive TiO_2 and accelerate photodegradation to CO_2 . It has been shown in the previous chapter that the addition of a stabiliser such as a hydroalcite (which removes the chloride replacing it with carbonate) produces weaker acidic fragments which cannot catalyse the degradation. The phthalate plasticiser produces a very much lower amount of HCl during the time frame of the irradiations shown in Figure 4.5 and evolution plateaus after about 800 minutes. This could reflect either preferential attack on the phthalate over the PVC or that the ester linkage is attacked by any HCl produced leading to weaker carboxylic acid fragments. This is mirrored by the absence of catalysis in Figures 4.1 and 4.2 for CO_2 evolution from the phthalate plasticised PVC films. The ASPS is designed to be more resistant to degradation than the Phthalate and this is reflected in greater observed levels of HCl from ASPS plasticised films through the attack on the PVC matrix. In this instance there is no plateau in HCl produced since there is preferential attack of the plasticiser over the PVC matrix, the amounts of HCl produced are lower than the non plasticised sample. As such although HCl is produced it is not clear that it alone is responsible for the acceleration. It could be that the sulphonic acid fragments are also implicated.

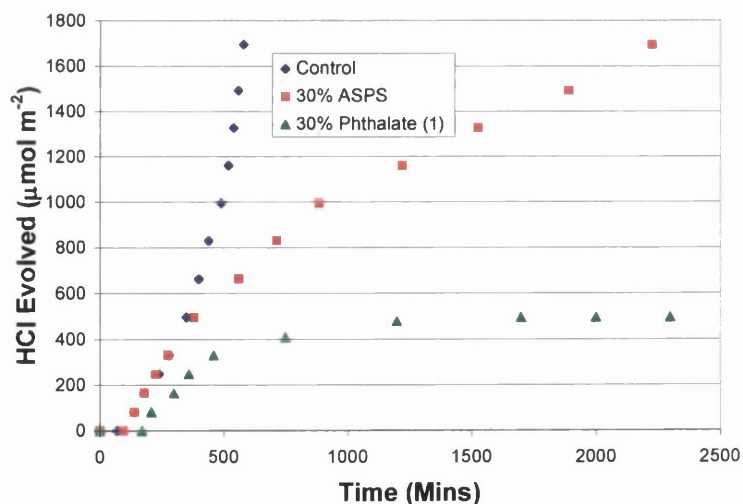


Figure 4.4: HCl evolution profiles for non plasticised, phthalate and sulphonic acid ester plasticised PVC films.

4.3.3 Effect of Plasticiser Loading on Initial and Secondary Rates of CO₂ Production.

The effect of plasticiser loading on the initial and secondary rates of CO₂ evolution taken from repeat experiments shown in Figures 4.1 to 4.3 are illustrated in Figure 4.5. Generally as has been reported previously, there is an increase in the initial rate of CO₂ evolution in the initial stages of degradation as the plasticiser loading is increased. This is consistent with both the increase in oxygen transport from plasticisation and also the rapid oxidation of absorbed plasticiser molecules on the TiO₂ surface. For both the phthalate 2 and ASPS there is some evidence of anti plasticisation (leading to lower degradation rates) in the 10% additions, which leads to a non linear increase in the rate. The secondary rates for both phthalate plasticisers show the effect of reducing the final rate of CO₂ evolution observed in the time frame of the experiment. Not only is the rate reduced but it is reduced to a consistently low level when amounts of plasticiser >10% are used. This indicates that acid catalysis does not occur. This is most likely that the plasticiser is being degraded preferentially to the matrix and hence less HCl is forming. It is also the case that the plasticiser molecule will itself react with any HCl produced breaking the ester bond and producing weaker carboxylic acids. The ASPS plasticiser shows a similar effect at low concentration with the rates reduced over the initial rate. This is not the trend for higher loadings (50% and 70%) indicating the formation of acid fragments from its breakdown which can catalyse the degradation. This is down to the production of sulphonic acid and sulphuric acid from the attack on the plasticiser (a sulphonic acid ester) by the TiO₂ [13].

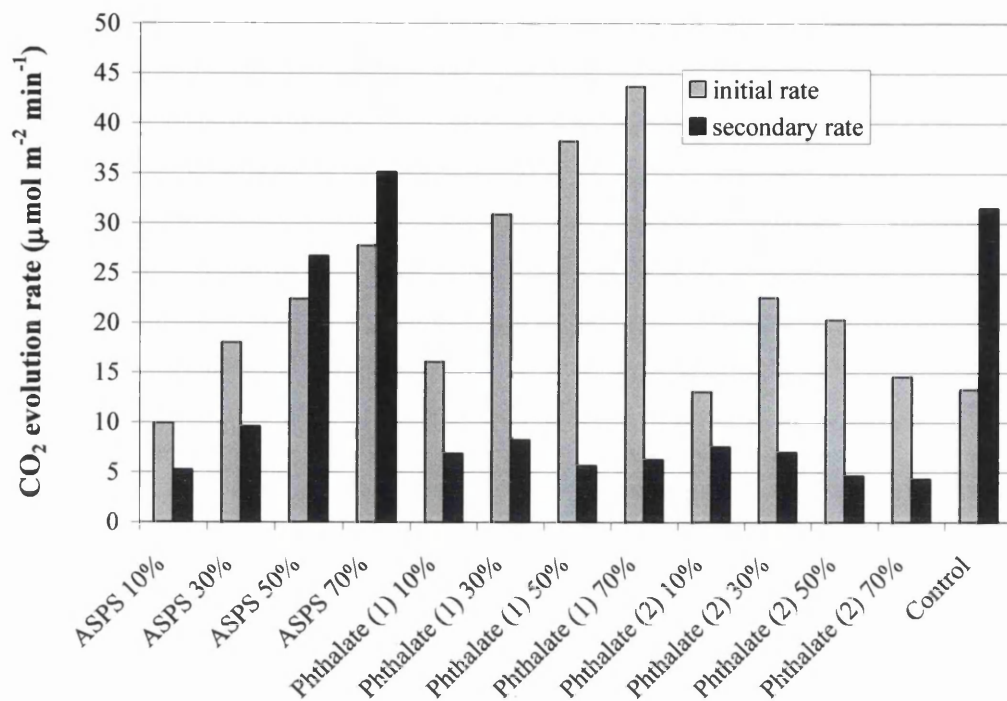


Figure 4.5: The initial (0-50 minutes) and secondary rates (800-1000) of CO₂ evolution for ASPS and Phthalate (1) and (2) at the loadings of 0, 10, 30, 50 and 70%.

Another way of considering the effect of additions on degradation is to plot the instantaneous rates of CO₂ evolution as a function of irradiation time. The effects of plasticiser additions on the instantaneous rates of CO₂ production are shown in Figures 4.6-4.9. The transition from an initial rate to higher secondary rate is clearly shown for the un-plasticised case in Figures 4.6-4.9 (blue points). As discussed previously this is likely to be an acid catalysis as a result of the production of HCl since it is removed by removing hydrochloric acid. All of the plasticisers show a decreasing instantaneous rate from the initial which is high. The high initial rate has been discussed [10], and is related to the rapid oxidation of pre-absorbed plasticiser molecules and this reduces the attack on the PVC matrix itself. The failure to produce HCl prevents catalysis of the TiO₂ and any HCl produced will attack the ester linkage on the plasticiser and create weaker carboxylic acids that will not catalyse the TiO₂ photoactivity.

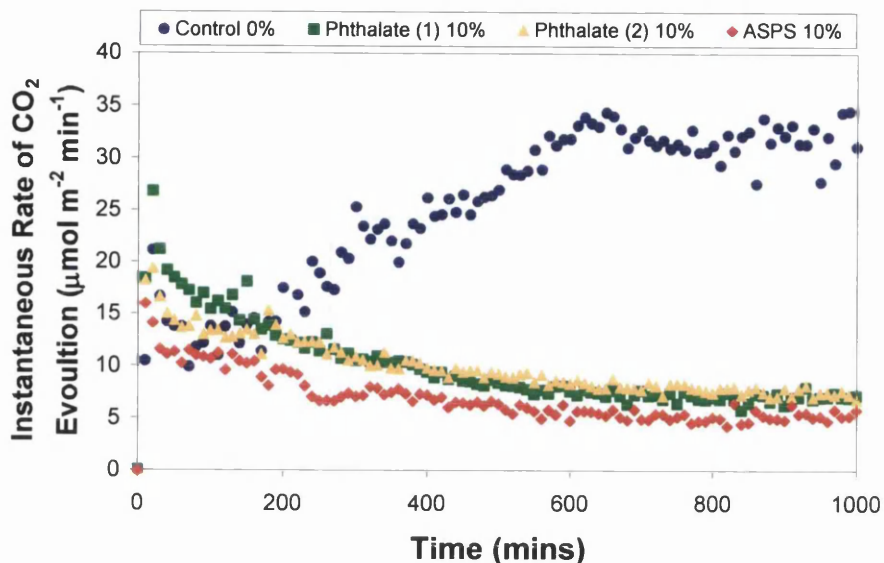


Figure 4.6: Instantaneous rate of CO₂ evolution for 10% plasticised model PVC systems.

A similar trend in the instantaneous rate is shown in Figure 4.7 for the 30% loading of plasticiser. Once more there is an initial rapid evolution of CO₂ which levels off to a lower continuous rate over time. In both the 10% and 30% cases all the plasticisers have a rather similar performance with the ASPS generally displaying lower overall rates of degradation. The difference becomes noticeable in the case of the 50% and 70% loaded films as shown in Figure 4.8 and Figure 4.9. Again there is an increase in the initial rate of degradation with plasticiser addition and both the phthalate films show levelling off to lower rates as they did in the 10% and 30% loadings. The ASPS plasticiser does not following the same trend as the phthalate films as it actually shows rate acceleration similar to the un-plasticised film. This is very interesting and signifies that the breakdown products from the ASPS plasticiser are likely to catalyse TiO₂ photodegradation. In this case the sulphonic acid products [13] of the breakdown of the ASPS plasticiser will be stronger acids than the carboxylic acids produced from the phthalate plasticisers. The difference in performance is most evident in the highest loadings of plasticiser (70%). The phthalate (1) has clearly degraded more rapidly (to CO₂ at least) than the phthalate (2), but still shows levelling off to a lower rate. The

ASPS plasticiser shows a rapid initial rate and then a steady state rate similar to the un-plasticised film which is consistent with some acid catalysis.

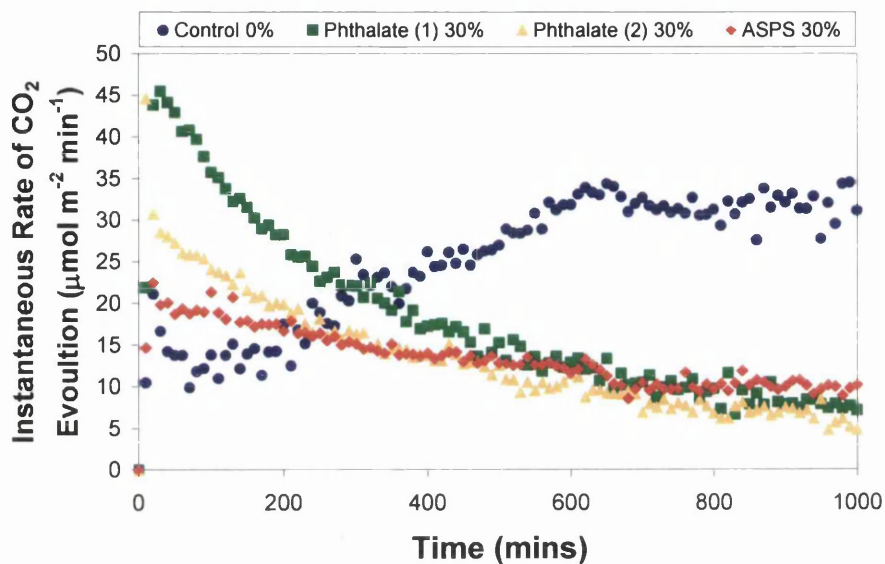


Figure 4.7: Instantaneous rate of CO₂ evolution for 30% plasticised model PVC systems.

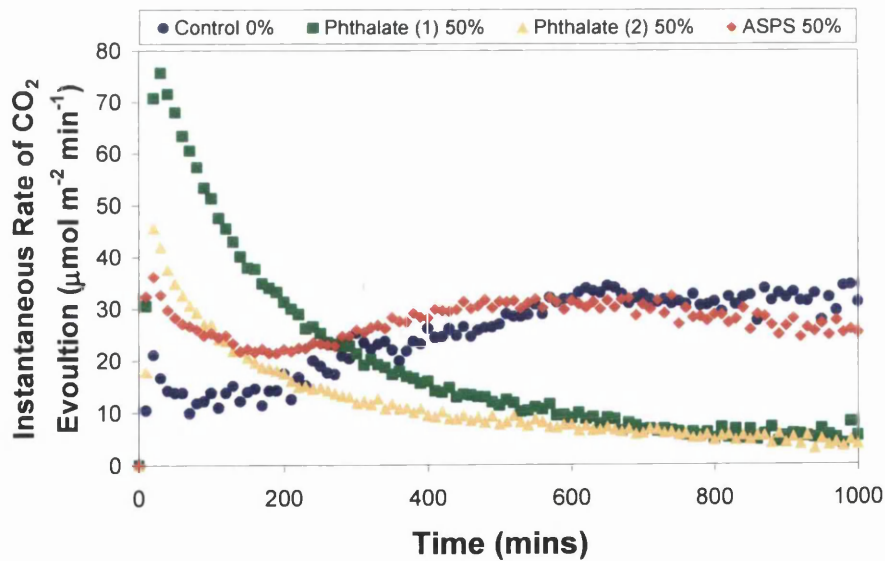


Figure 4.8: Instantaneous rate of CO₂ evolution for 50% plasticised model PVC systems.

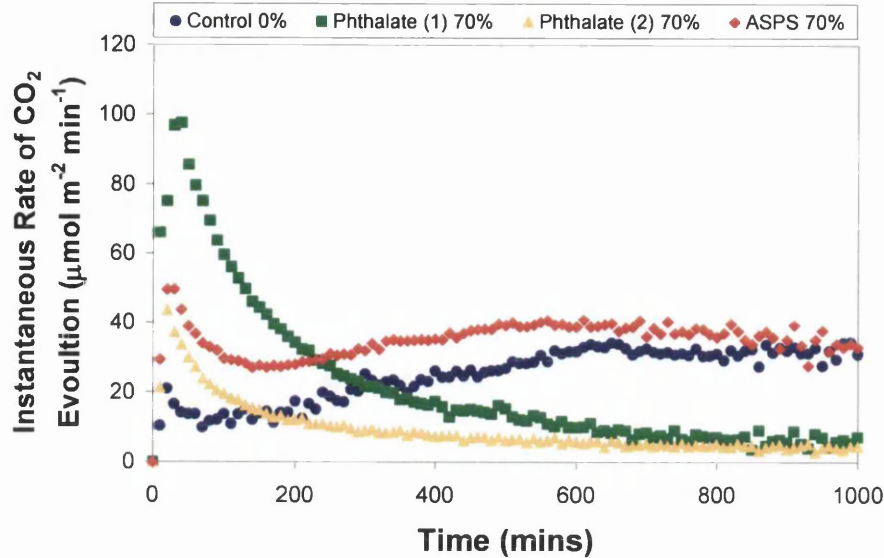


Figure 4.9: Instantaneous rate of CO₂ evolution for 70% plasticised model PVC systems.

4.3.4 Weight loss

In order to gain an appreciation of longer term irradiations samples were exposed to identical UVA environment for up to 6500 minutes (i.e. over six times longer than for CO₂ evolution tests). The effects of weight loss of plasticiser type and loading are shown in Figure 4.10-4.12. In Figure 4.10 the phthalate (1) sample shows the same trend as the CO₂ in the early stages of UVA exposure. The un-plasticised control sample has shown a significantly larger weight loss than the plasticised samples in line with the CO₂ evolution (Figure 4.1). The 30%, 50% and 70% loadings show very similar trends to CO₂ evolution in the initial stages before 1080 minutes and then the weight loss tails off. The 10% loading follows a similar trend until 4320 minutes, when it seems HCl acid formation begins to occur by the degradation of the PVC matrix the consumption of the plasticiser around the TiO₂. This causes the film to be heavily degraded and increases weight loss.

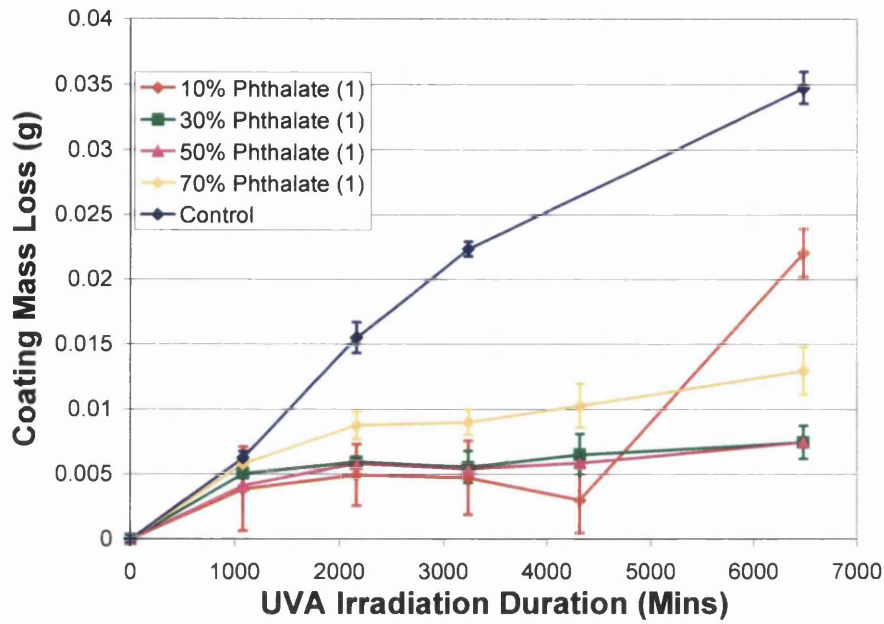


Figure 4.10: Weight loss of coating (g) for 0-70% loadings of Phthalate 1 plasticiser.

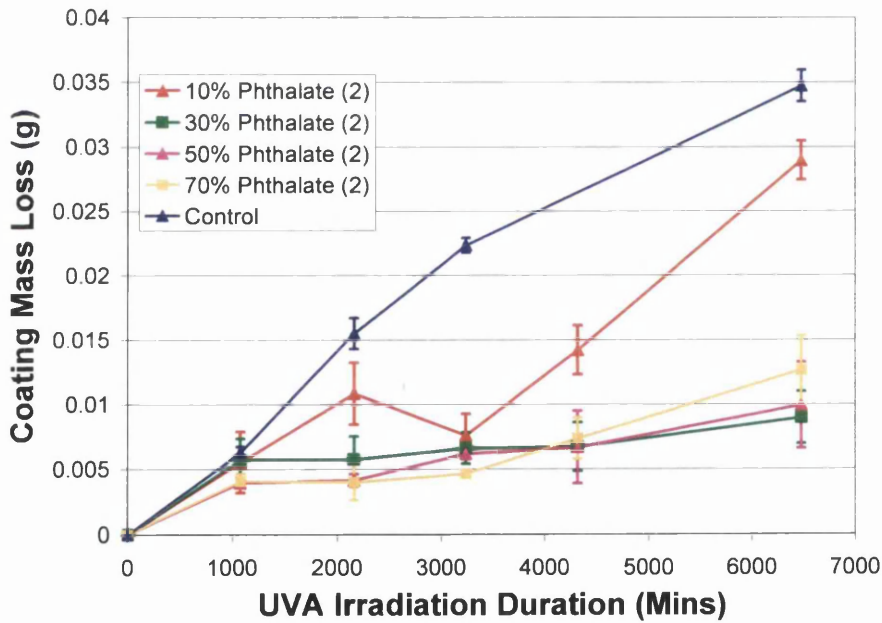


Figure 4.11: Weight loss of coating (g) for 0-70% loadings of Phthalate 2 plasticiser.

In Figure 4.11, the 30%, 50% and 70% loadings of the phthalate (2) films, follow the same trends with similar weight losses to the phthalate (1) films. The 10% loading shows the increase in weight loss as in the 10% phthalate (1) film. Although this does occur slightly earlier than the phthalate 1 film and the final weight loss from the film is greater for the phthalate (2) film. It should be noted that for both phthalates there is a weight gain after the initial weight loss. This is reproducible and suggests oxidation products held in the film. The phthalate (2) plasticiser (10%) is producing HCl after 3240 minutes in the same way as the phthalate (1) (10%) film. It can still be seen that the weight loss from all the phthalate (2) films is less than the un-plasticised control film.

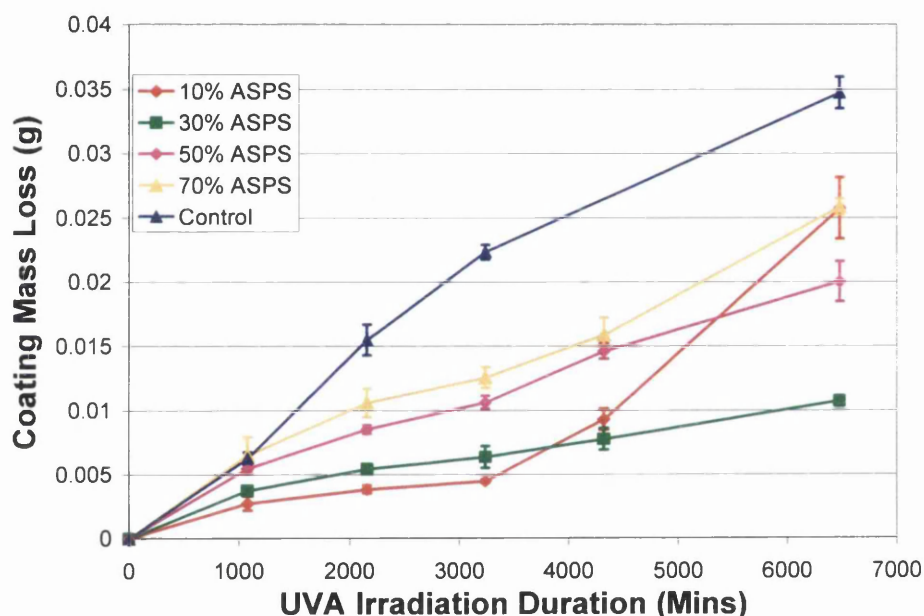


Figure 4.12: Weight loss of coating (g) for 0-70% loadings of ASPS plasticiser.

In Figure 4.12, there is clear indication that as the plasticiser loading is increased the weight loss of the films increases in the first half of the experiment. The un-plasticised sample is showing the highest weight loss hence the plasticiser is protecting the PVC to a great extent. Within the first 1080 minutes of the experiment the weight loss results follow the same trend as the CO₂ evolution, but with further UVA exposure the un-plasticised sample is heavily chalked as the PVC matrix is readily degraded. The 10%

loading shows a dramatic increase in weight loss after 3240 minutes due to the consumption of the plasticiser and formation of sulphonic acids.

The un-plasticised control sample shows the highest % organic mass loss which is above 40% and all additions of plasticiser help protect the PVC matrix in Figure 4.13. Without this protection PVC matrix is degraded and the formation of HCl acid accelerates photodegradation. In Figure 4.13 the total % organic mass loss after 6480 minutes, shows approximately 10% mass loss for phthalate 1 and 2 for the loadings of 30, 50 and 70%. It can clearly be seen that both ASPS and phthalate films have an organic mass loss around 35% for a 10% loading of plasticiser. This is down to the formation of HCl acid fragments accelerating the photodegradation within the film after the consumption of the plasticiser. As the plasticiser level in ASPS is increased from 30% to 70% an increase in mass loss percentage is seen. Although a small addition (10%) of plasticiser does offer the best CO₂ evolution it increases the weight loss with longer UVA exposure due to these acid fragments being formed. It is clear from Figure 4.13 that the phthalates provide an effective stabilisation against weight loss but ASPS does not hence in moving to a phthalate free product the use of stabilisers (particularly to remove acidic compounds) is vital.

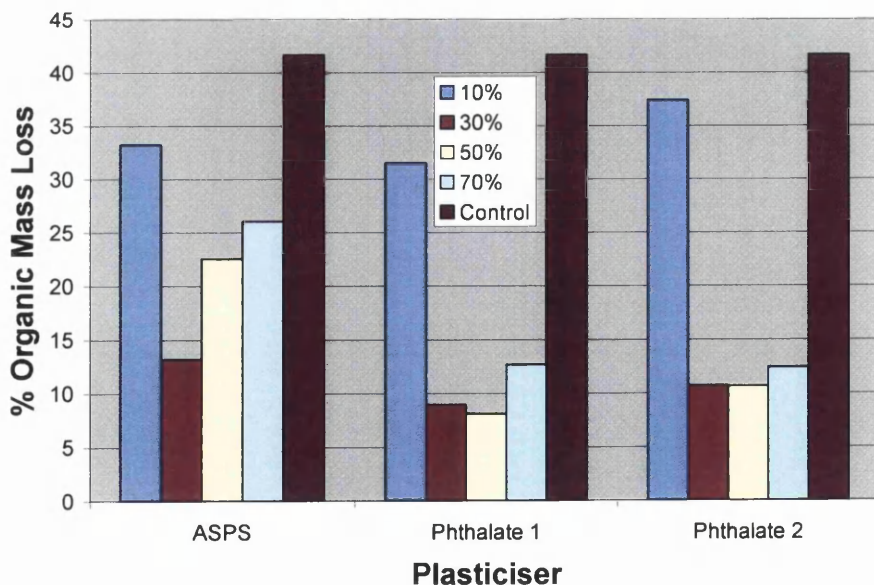


Figure 4.13: Total percentage organic mass loss after 6480 minutes.

4.4 Conclusions

With the exception of Phthalate 2 increasing the levels of plasticiser will lead to an increase in the initial rate of CO₂ evolved during UVA irradiation of a plasticised PVC system. The phthalate 2 plasticiser has been the best performing with very little change in CO₂ evolution even when the plasticiser loadings are increased. The inclusion of phthalate plasticisers into films disrupts the HCl catalysis mechanism thus preventing the rapid acceleration of CO₂ evolution. During the extended irradiations the phthalate plasticisers CO₂ evolution level to a low level with no further production. This must mean that the phthalate ester is more easily degraded and is also able to remove HCl leading to a stabilising effect and reduction in acid catalysis. The HCl evolution test of the phthalate films confirms this as a very small amount of HCl is observed. The phthalate compound also leads to very low levels of weight loss in more prolonged irradiations.

In the phthalate (1) systems the CO₂ evolution profiles are slightly higher than the phthalate (2), reflecting the greater stability of the branched phthalate. In all cases, plasticiser addition results in the rapid initial production of CO₂ as plasticiser molecules adsorbed on and close to the titania surface are preferentially oxidised. This preferential attack on the plasticiser and consequent failure to produce significant amounts of strongly acid breakdown fragments means that for the phthalates tested there is no subsequent acid catalysis of the TiO₂ which is observed in the absence of plasticiser.

ASPS is a sulphonic ester and has a very different photomineralisation mechanism compared to the phthalate plasticised systems. At low concentrations this leads to low rates of degradation and CO₂ evolution. At levels above 30% the rate degradation and CO₂ evolution is very high when compared with the phthalate plasticisers. The ASPS plasticiser, can be degraded to produce strongly acidic fragments and HCl results from attack on the PVC since the ASPS is not as readily degraded as the phthalate. These acid species are capable of catalysing the titanium dioxide leading to increasing CO₂ production and weight loss. Hence the best solution to a phthalate free coating system would appear to be one which contains the ASPS and a suitable stabilising agent to remove any acidic fragments capable of catalysing the TiO₂. This will be the subject of the next body of work.

4.5 References

1. Sears, J.K., Darby, J.R., *The Technology of Plasticisers*. 1982, New York: Wiley and Sons.
2. Wilson, A.S., *Plasticisers: Principles and Practice*, ed. T.I.O. Materials. 1995, London.
3. Howick, C., *Plastics, Rubber and Composites Processing and Applications*. 1995. **23**: p. P53.
4. Braun, D., *Pure & Appl. Chem.* 1981. **53**: p. 549.
5. Murase, A., Suguiura, M., Araga, T., *Polymer Degradation and Stability*, 1994. **43**: p. 415.
6. Chemistry, S.I.o.C., *Chemistry in Britian*. 1990. **November**.
7. Crank, J., Park, G.S., *Diffusion in Polymers*. London Academic Press, 1968.
8. Horsley, R.A., *Progress in Plastics*. 1957(wd. Morgan, P., Liffé and Sons): p. 77.
9. Jian, L., Dafei, Z., *Polymer Degradation and Stability*, 1991. **31**: p. P1.
10. Searle, J.R., *Titanium Dioxide Pigment Photocatalysed Degradation of PVC and Plasticised PVC Coatings*. EngD University of Wales Swansea, 2002.
11. Robinson, A.J., Searle, J.R., and Worsley, D.A., *Materials Science and Technology*, 2004. **20**: p. 1041.
12. Searle, J.R., Worsley, D.A., *Materials Science and Technology*, 2002. **31**: p. P329.
13. Robinson, A.J., *The Development of Organic Coatings for Strip Steels with Improved Resistance to Photodegradation*. EngD Thesis, University Of Wales Swansea, 2005.

Chapter 5

Stabilisation of Near Commercial Plastisol Systems

5.1 Introduction and Aims

From previous work described in chapter 3, the use of Hydrotalcite (HT) as a stabiliser looks very promising in model paints [1] with the benefits of being non toxic and a readily available natural raw material. The model system is a very basic system and is a good initial way of testing additives in very short and quick experiments. The next stage is to test the Hydrotalcite in a near commercial system using different pigment grades which are more stable than the highly photoactive grade of Degussa P25 used in the model systems. The last chapter also indicated the importance of appropriate acid stabilisation in the transition to a phthalate free system.

The aim of this work is to evaluate the HT stabilised system with the current commercial stabilisers (BaZn and Sn1/Sn2) described in chapter 3 using different pigment grades A, B, C and U in a series of near commercial white plastisols, also looking at the effect of adding HT to various coloured [2] commercial plastisol systems.

5.2 Experimental

A full investigation was carried out that looked at the near commercial coating using the current phthalate free grade and two historic grades of plastisol (using the plasticisers from Chapter 4) made from a standard commercial base. A matrix of samples was created covering a range of different stabiliser concentrations (described in Tables 5.1, 5.2 and 5.3) using the novel Hydrotalcite stabiliser, Sn1/Sn2 and the current BaZn stabiliser. The samples were subject to conventional accelerated weathering in QUVA cabinets. The weathering process was completed and the resultant samples subject to a variety of tests to assess levels of degradation. At each stage of the weathering process the samples were also subject to individual colour and gloss measurements.

5.2.1 Sample Preparation

The samples were prepared in a similar way to that outlined in Section 2.1.5. Plastisol bases were supplied by Akzo Nobel and the required amount of plasticiser, pigment and stabiliser were added to this base and dispersed using an industrial high

shear mixer. The stabiliser concentration, pigment type and base are outlined in Table 5.1 for the white formulations. The colour formulations (shown in Figure 5.1) with 14% K1001 TiO₂ pigment for HPS200 and HP200 are outlined in Tables 5.2 and 5.3. After formulating the paint and ensuring a uniform viscosity samples were cast onto ready primed Galvalloy (4.2% Aluminium, 95.8% Zinc) coated steel samples 16cm x 18cm in size using a standard 200µm draw down bar. Each sample was cured in a paint curing oven for 50 seconds reaching a peak metal temperature of ca 220°C then water quenched to room temperature. To ensure continuity across different samples gloss measurements were made of each cured sample. Finally each panel was guillotined to the required sample size. A total of 96 formulations were tested in total, 2 of each formulation (192 panels) as shown below in Table 5.1, 5.2, 5.3 and 5.4.

Table 5.1: The base, pigment type and stabiliser for white formulations.

Base	14% TiO ₂ Pigment (Grade)	Stabiliser	Identification No.
HPS200	K2220 (A)	1% BaZn	1
Phthalate free	K2220 (A)	1% Sn1/Sn2	2
ASPS plasticised	K2220 (A)	5% HT	3
	K2220 (A)	No Stab	4
	K2300 (B)	1% BaZn	37
	K2300 (B)	1% Sn1/Sn2	38
	K2300 (B)	5% HT	39
	K2300 (B)	No Stab	40
	K2063 (C)	1% BaZn	41
	K2063 (C)	1% Sn1/Sn2	42
	K2063 (C)	5% HT	43
	K2063 (C)	No Stab	44
	K1001 (U)	1% BaZn	13
	K1001 (U)	1% Sn1/Sn2	14
	K1001 (U)	5% HT	15
	K1001 (U)	No Stab	16
	No Pigment	1% BaZn	25
	No Pigment	1% Sn1/Sn2	26
	No Pigment	5% HT	27
	No Pigment	No Stab	28
MK II	K2220 (A)	1% BaZn	5
Phthalate 1	K2220 (A)	1% Sn1/Sn2	6
plasticised	K2220 (A)	5% HT	7
	K2220 (A)	No Stab	8

	K1001 (U)	1% BaZn	17
	K1001 (U)	1% Sn1/Sn2	18
	K1001 (U)	5% HT	19
	K1001 (U)	No Stab	20
	No Pigment	1% BaZn	29
	No Pigment	1% Sn1/Sn2	30
	No Pigment	5% HT	31
	No Pigment	No Stab	32
HP200	K2220 (A)	1% BaZn	9
Phthalate 2	K2220 (A)	1% Sn1/Sn2	10
plasticised	K2220 (A)	5% HT	11
	K2220 (A)	No Stab	12
	K1001 (U)	1% BaZn	21
	K1001 (U)	1% Sn1/Sn2	22
	K1001 (U)	5% HT	23
	K1001 (U)	No Stab	24
	No Pigment	1% BaZn	33
	No Pigment	1% Sn1/Sn2	34
	No Pigment	5% HT	35
	No Pigment	No Stab	36

Table 5.2: The stabiliser and colour pigment for the HPS200 colour formulations.

Base	Stabiliser	Colour Pigment	Identification No.
HPS200	1% BaZn	0.5% C	45
ASPS	1% BaZn	1% C	46
plasticised	1% BaZn	1.5% C	47
	1% BaZn	1% BLP (Blue)	48
	1% BaZn	1% GLSM (Blue)	49
	1% BaZn	1% DPP (Red)	50
	1% BaZn	1% GLN (Green)	51
	1% Sn1/Sn2	0.5% C	52
	1% Sn1/Sn2	1% C	53
	1% Sn1/Sn2	1.5% C	54
	1% Sn1/Sn2	1% BLP (Blue)	55
	1% Sn1/Sn2	1% GLSM (Blue)	56
	1% Sn1/Sn2	1% DPP (Red)	57
	1% Sn1/Sn2	1% GLN (Green)	58
	5% HT	0.5% C	59
	5% HT	1% C	60

	5% HT	1.5% C	61
	5% HT	1% BLP (Blue)	62
	5% HT	1% GLSM (Blue)	63
	5% HT	1% DPP (Red)	64
	5% HT	1% GLN (Green)	65
	1% BaZn	1% Yellow	93
	1% Sn1/Sn2	1% Yellow	94
	5% HT	1% Yellow	95

Table 5.3: The stabiliser and colour pigment for the HP200 colour formulations.

Base	Stabiliser	Colour Pigment	Identification No.
HP200	1% BaZn	0.5% C	66
Phthalate 2	1% BaZn	1% C	67
plasticised	1% BaZn	1.5% C	68
	1% BaZn	1% BLP (Blue)	69
	1% BaZn	1% GLSM (Blue)	70
	1% BaZn	1% DPP (Red)	71
	1% BaZn	1% GLN (Green)	72
	1% Sn1/Sn2	0.5% C	73
	1% Sn1/Sn2	1% C	74
	1% Sn1/Sn2	1.5% C	75
	1% Sn1/Sn2	1% BLP (Blue)	76
	1% Sn1/Sn2	1% GLSM (Blue)	77
	1% Sn1/Sn2	1% DPP (Red)	78
	1% Sn1/Sn2	1% GLN (Green)	79
	5% HT	0.5% C	80
	5% HT	1% C	81
	5% HT	1.5% C	82
	5% HT	1% BLP (Blue)	83
	5% HT	1% GLSM (Blue)	84
	5% HT	1% DPP (Red)	85
	5% HT	1% GLN (Green)	86

Table 5.4: Details of the coloured pigments used in Tables 5.2 and 5.3.

Prefix	Composition	Colour
C	Carbon	Printex Black
DPP	Diketo-pyrrolo-pyrrole	Irgazin Red
BLP	Phthalocyanines	Irgazin Blue
GSLM	Phthalocyanines	Blue 15B
GLN	Phthalocyanines	Irgalite Green
Yellow	Chromo-Tin—Titanium-oxide	Sicotan Yellow

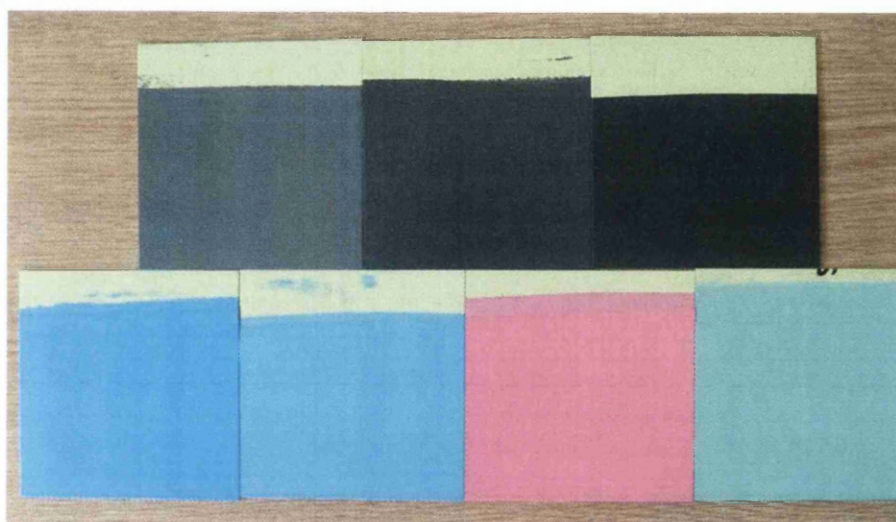


Figure 5.1: A photo of the coloured pigmented panels with 14% K1001 TiO₂. Top row from left 0.5% C, 1% C and 1.5% C. Bottom row from the left 1% BLP, 1% GLSM. 1% DPP and 1% GLN

5.2.2 Accelerated Weathering (QUVA)

The sample panels were irradiated using a QUV Accelerated Weathering Tester (Q-Panel Company) fitted with UVA lamps. The setup of this QUV cabinet is covered in more detail in Section 2.7.1. Each panel was subject to 750 hours of weathering cycles consisting of 8 hours UVA radiation and 4 hours condensation. In every 24 hour period this allows two complete cycles. The panel temperature for both cycles (UV and condensation) were set at 40°C and a light intensity of 0.68 W/m²/nm at 340nm. The light intensity was calibrated every 2 weeks. The samples were placed in a different random position and none of the four end positions were used as UV strength can be slightly

lower. This was performed so as to minimise any intensity variation effects within the weathering cabinet. The panels with K1001 pigment and all the colours were weathered for a total of 2000h weathering cycles at which point they had failed completely. All the white formulations with K2220, K2300, K2063 and no pigment were weathered for a total of 3000 hours.

5.2.3 Gloss Loss Measurements

All the panels were measured for gloss loss with a Minolta Multi-Gloss 268 using the 60° angle setting as described in Section 2.7.2. Each panel was measured at ten separate points and the average value recorded. The gloss loss measurements are given as a gloss retention as the initial un-weathered 60° gloss values can vary substantially from panel to panel. This is mainly due to the small differences in the curing process so the gloss value of a weathered panel needs to be related to the initial gloss before weathering of that specific panel to be relevant. The gloss retention is calculated with a simple formula:

$$\text{Gloss Retention (\%)} = (100 * \text{Gloss Weathered}) / \text{Gloss un-weathered}$$

5.2.4 Colour Change Measurements

Colour was measured in the form of a reflectance spectrum and the difference in reflectance spectrum after total weathering was calculated. The colour reflectance was completed by using a Gretag-Macbeth measuring reflectance over the range 370nm-730nm. The spectrum was recorded excluding the effect of the gloss components. The reflectance measurements for each panel were calculated by taking the average value from ten separate measurements [3]. Each panel was measured after 750h, 1500h, 2000h and 3000h (only the whites apart from K1001).

5.3 Results and Discussion

5.3.1 HPS200, Mk II and HP200 base with No Pigment

To clarify the HPS200 formulation is plasticised with ASPS, Mk II with Phthalate (1) and HP200 with Phthalate (2).

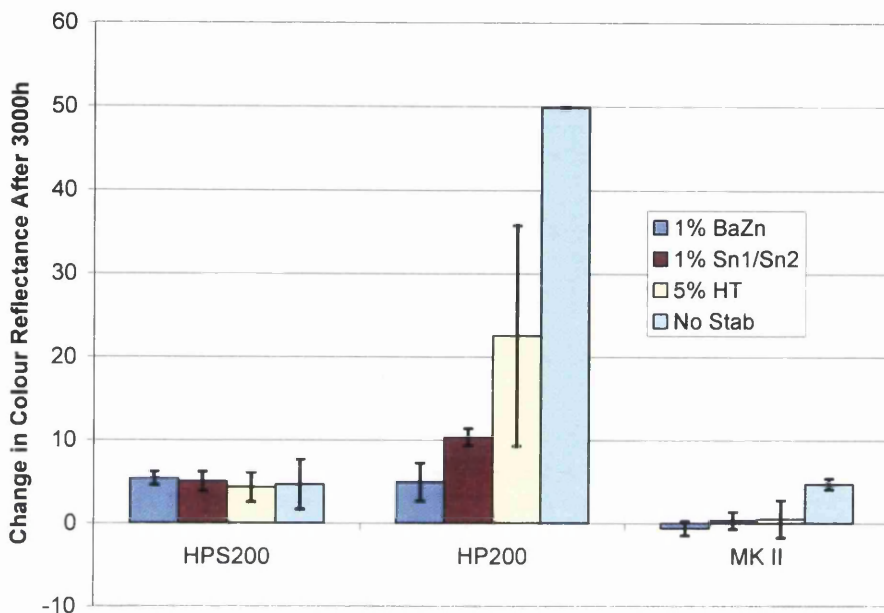


Figure 5.2: Colour reflectance after 3000h for stabiliser systems with no pigment in HPS200, HP200 and MK II bases.

Figure 5.2 shows the performance of the stabilisers in the latest formulation HPS200 and historic bases of HP200 and MKII. In the HP200 system it can be seen that the unstabilised system shows the most darkening (+ve change in colour) and the addition of Hydrotalcite (HT) improves the performance. Although the BaZn and Sn1/Sn2 show significant benefit from darkening (dehydrochlorination) for this base primary since they can remove HCl gas as well as hydrochloric acid. The oldest base formulation (MK II) shows the greatest resistance to dehydrochlorination. The un-stabilised coating shows a small amount of darkening and this is significantly improved as BaZn, Sn1/Sn2 and HT are added to the base. The performance for these are very similar with very little to choose between them. In the phthalate free base formulation (HPS200) all the systems

perform similarly although there is a slight darkening effect. HT does seem to show a slightly better darkening resistance in this instance than the BaZn, Sn1/Sn2 and the un-stabilised system.

5.3.2 HPS200, Mk II and HP200 base with K2220 TiO₂

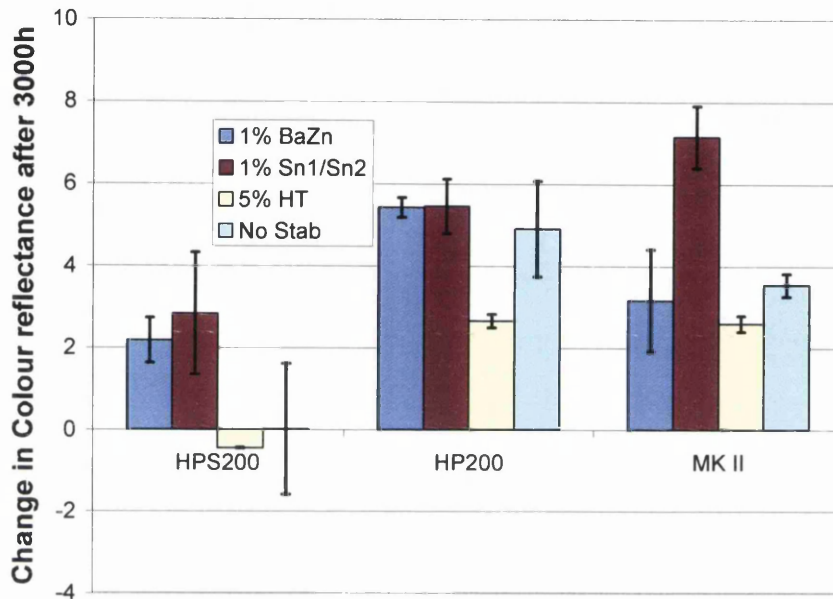


Figure 5.3: The effect of pigmentation systems after 3000h QUVA.

Figure 5.3 shows the effect of adding an A grade pigment (K2220) to the three commercial systems. The HPS200 system is the best overall system when TiO₂ is added to the paint system. The two commercial stabilisers (BaZn or Sn1/Sn2) show the most darkening in all three commercial systems. The Sn1/Sn2 in the MK II system is noticeably different to the other stabilisers showing that this stabiliser is potentially allowing HCl formation and causing dehydrochlorination. The addition of HT prevents the extent of the darkening and in the HPS200 system it even causes a slight whitening effect (-ve change in colour). The un-stabilised system for HPS200 shows no change though the error bars show a lot of variation indicating that the colour reflectance is very patchy across the panel which is undesirable.

5.3.3 The Effect of Different Pigments Using HPS200 Base.

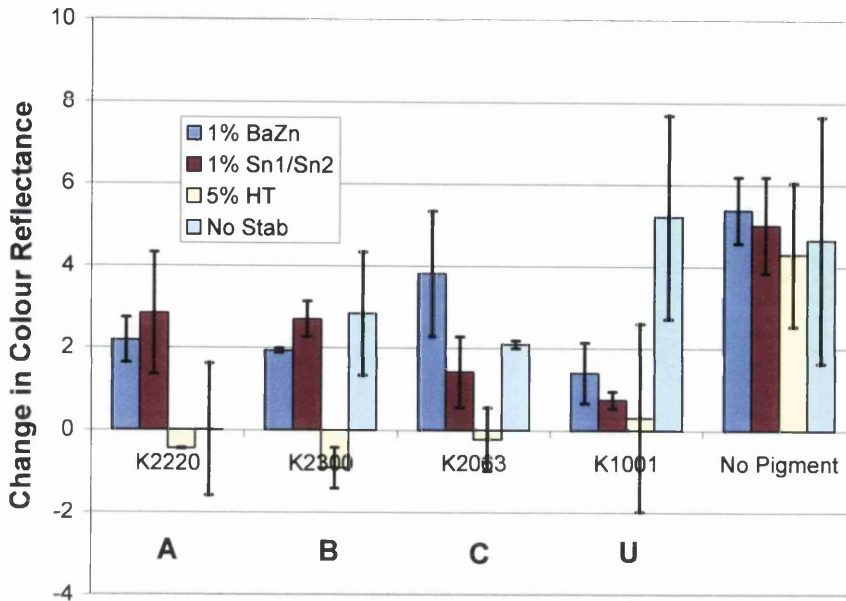


Figure 5.4: The colour reflectance for HPS200 on various pigmented systems.

Figure 5.4 shows the performance of the stabilisers with various pigment grades within the phthalate free HPS200 system. The A grade (K2220), B grade (K2300), C grade (K2063) after 3000 hours QUVA and U grade (K1001) after 2000 hours QUVA after which the paint was completely degraded. The general trend as the pigment grade goes from A to C the darkening (dehydrochlorination) effect is greater. The lower the grade of pigment the more photoactive it is due to the poor Al/Si coating on TiO₂ as discussed in 1.8.1.3. The addition of HT in all grades (A, B and C) shows a slight whitening effect and a significant improvement to the organic stabilisers (BaZn and Sn1/Sn2). The HT in these white panels appears to be the most consistent and best stabiliser in terms of colour reflectance. This is clearer when considering the data from section 5.3.4. The K1001 pigment is a U graded pigment and is a highly photoactive grade of TiO₂ being 25 times more reactive than the K2220 which is an A graded pigment [4]. The colour reflectance after 2000h of these panels doesn't show as much darkening as the better grade pigments. This is due to heavy photodegradation of the highly photo active pigment K1001, causing chalking on the surface. As the TiO₂ is left

on the surface of the coating, colour reflectance shows little change as it is the measurement of the colour of the TiO₂. As such this data for K1001 is less representative of dehydrochlorination.

5.3.4 Gloss Retention of Whites.

For samples with grade A-C pigments regardless of stabiliser the gloss retention was reasonably consistent and >95% in the 3000h irradiation period as shown in appendix 1.

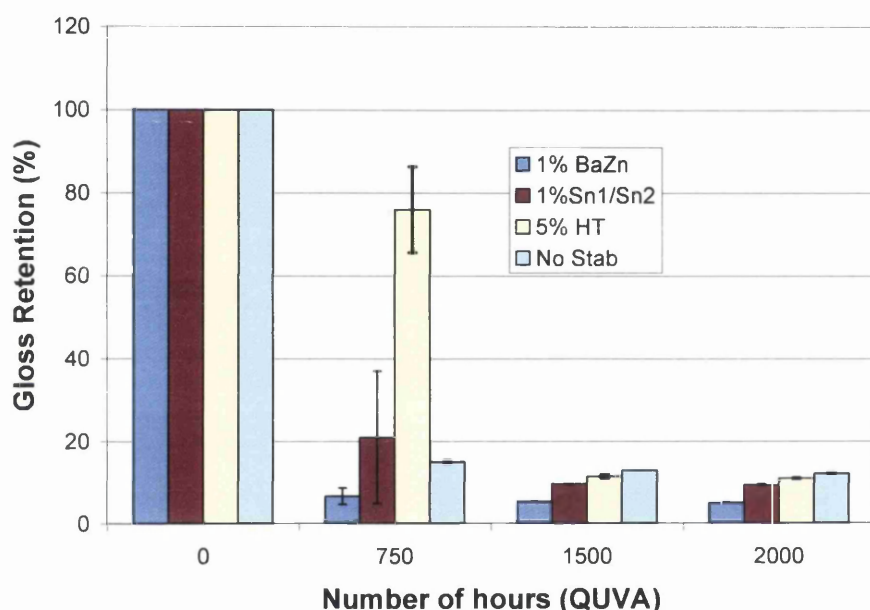


Figure 5.5: shows the gloss retention for K1001 pigmented HPS200 system.

Figure 5.5 shows the gloss retention for the HPS200 whites with the K1001 which was the only white paint showing a major gloss change. After 750 hours of QUVA the HT stabilised system shows the best performance of 75% gloss retention and indicates the start of chalking. The three other systems (BaZn, Sn1/Sn2 and No Stab) give gloss retentions below 20% and show heavy chalking after only 750 hours. After 1500 hours QUVA all systems show heavy chalking and the gloss retentions are around 12%.

5.3.5 Gloss Retentions of HPS200 and HP200 Coloured Pigments.

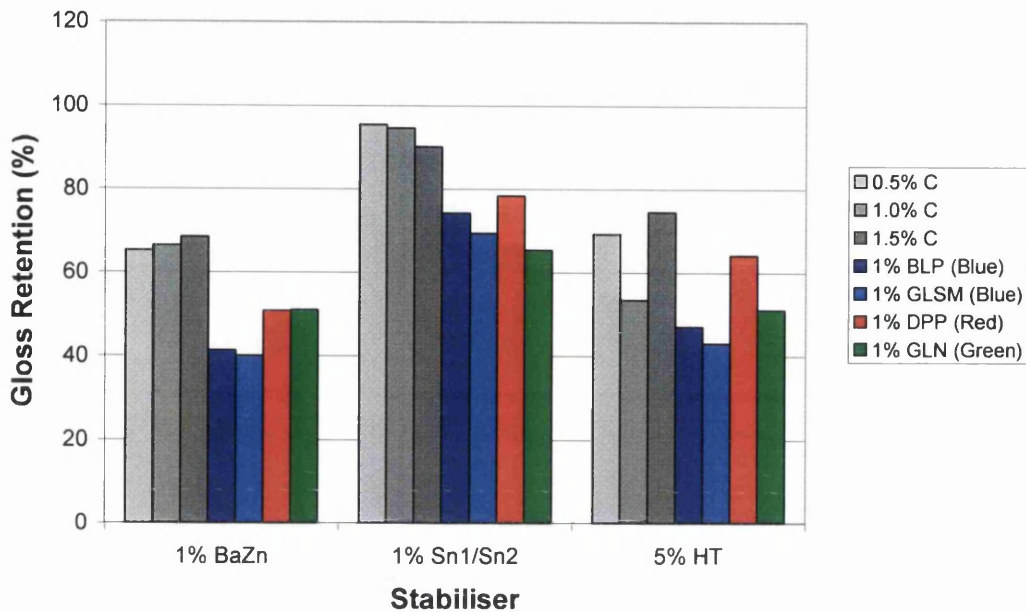


Figure 5.6: Gloss Retention of HP200 (Phthalate (1)) colours after 750h.

Figure 5.6 shows the gloss retentions of HP200 base with 14% K1001 pigment and the addition of some coloured pigments. After 750 hours the carbon black samples show the best gloss retentions for all stabiliser systems. In general the BaZn stabilised systems show the worst gloss retentions ranging from 40-60%. The Sn1/Sn2 systems are in general the best performing systems in the HP200 base with gloss retentions ranging from 65-95%. The HT stabiliser performs significantly better than the BaZn currently used with gloss retentions between 43-75% after 750h expose to UVA. The gloss retentions all show significant loss due to the use of the photoactive K1001 TiO₂ pigment.

After 1500 hours (for full data see appendix 1) gloss retentions are less than 6% for the BaZn stabilised systems. For the Sn1/Sn2 systems only GLSM (Blue) and GLN (Green) have gloss retentions below 10% after 1500h. The gloss retentions are 28%, 35%, 58%, 65% and 68% for the DPP (Red), BLP (Blue), 0.5% C, 1% C and 1.5% C respectively. After 2000 hours all the gloss retentions are below 7% apart from the C

(black) pigmented samples (0.5%, 1% and 1.5% C). The gloss retentions after 2000 hours are 28% for 0.5% C, 55% for 1% C and 42% for 1.5% C. After 1500h and 2000h the HT stabilised systems all have gloss retentions less than 10% apart from 1% C (22%) and 1.5% C (28%).

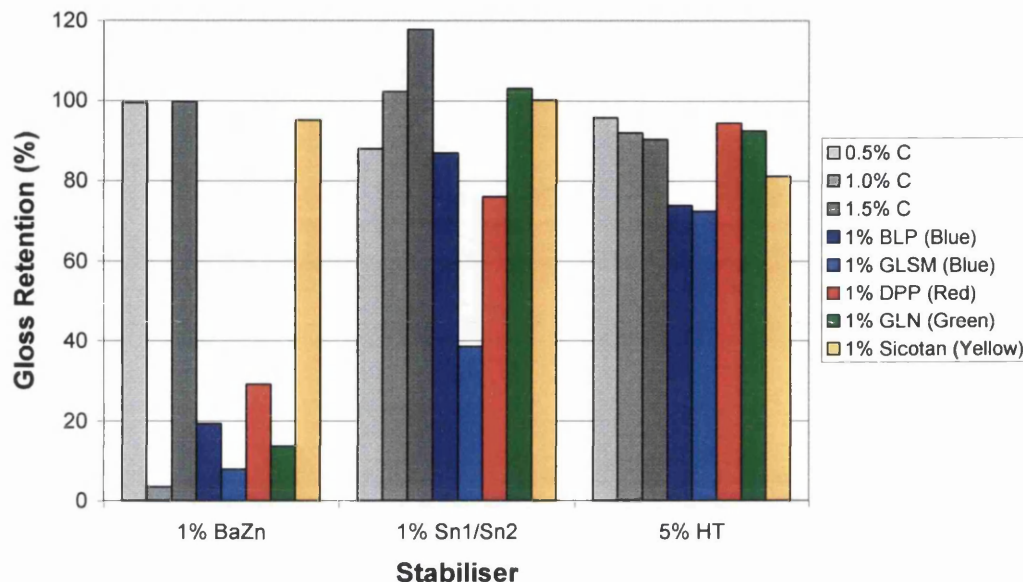


Figure 5.7: Gloss Retention of HPS200 (ASPS) colours after 750h.

Figure 5.7 shows the gloss retentions for the coloured pigments in the HPS200 formulation. After 750 hours the BaZn systems show the worst gloss retentions with the two blue, red, 1% C and green pigments with less than 30% gloss retentions, although the other two C and yellow pigments have performed significantly better. The Sn1/Sn1 performs better than BaZn and the gloss retentions in general are above 75% apart from GLSM blue pigment which is below 40%. The HT system is the best performing stabiliser in general for the HPS200 systems as all of the colour systems showed a gloss retention above 75%. The HPS200 system gloss retentions are better than the HP200 system with the HT stabiliser. This reflects the problems of acid catalysis shown in previous model systems which HT removes.

After 1500 hours the gloss retentions (Appendix 1) for all stabilised systems are below 12%, due to the heavy chalking of the samples including the highly active TiO₂ grade of K1001.

5.3.6 Colour Reflectance of HPS200 and HP200 Coloured Pigments.

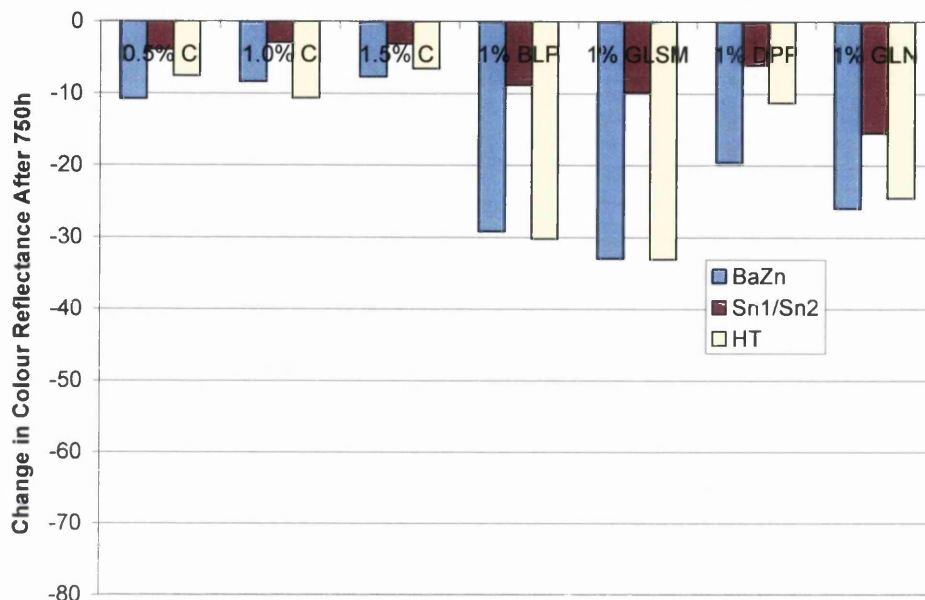


Figure 5.8: Colour Reflectance of HP200 colours.

Figures 5.8 and 5.9 show the change in colour reflectance after 750 hours for the HP200 and HPS200 bases pigmented with different colours and stabilisers. Due to the highly photoactive TiO₂ (K1001) both formulations (HP200 and HPS200) show significant whitening (-ve colour change) due to chalking. As the coating is being heavily degraded leaving the TiO₂ on the surface of the coating making it appear whiter. After 750 hours the HP200 formulation shows less colour change in general compared with the HPS200 formulation. The two blue colours (BLP and GLSM) show the worst colour change for both formulations. For the HP200 formulation the best performing stabiliser is the Sn1/Sn2 whereas HT is the best stabiliser in the HPS200 formulation. The BaZn stabiliser is the worst performing and shows the most change in colour reflectance. The addition of carbon black significantly improves the performance especially with the

stabilisers Sn1/Sn2 and HT. The effectiveness of HT in the ASPS (HPS200) matrix is clear as it gives the best performance without phthalates and tin.

In appendix 1 the results after 1500h and 2000h are shown although due to the highly photoactive K1001 pigment used all samples are heavily chalked and the colour change is very high. The panels all show signs of serious attack by photodegradation and the integrity of the coating is seriously affected.

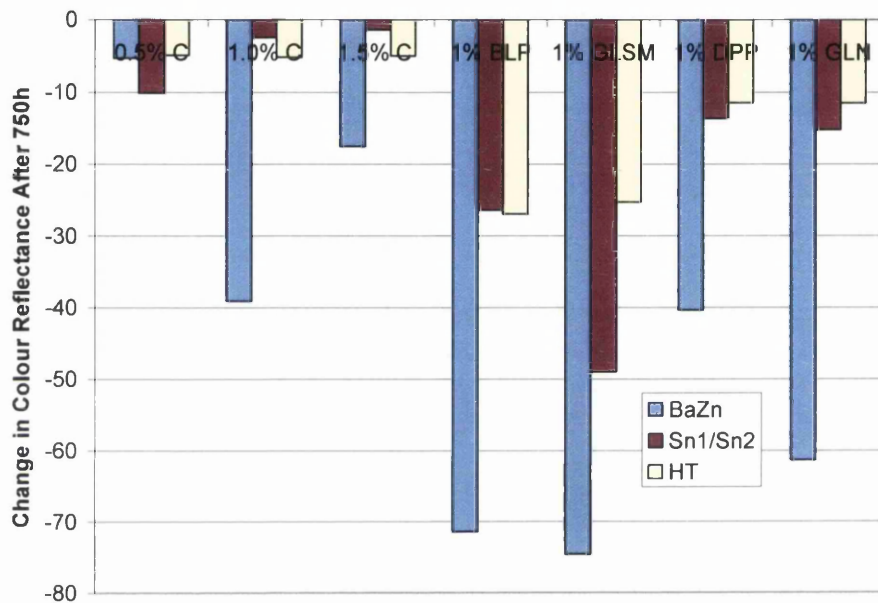


Figure 5.9: Colour Reflectance of HPS200 colours.

5.4 Conclusions

The addition of HT in commercial systems particularly those which are phthalate free looks very promising as it prevents dehydrochlorination (darkening) and even seems to have a whitening effect on white formulations up to 3000 hours of accelerated weathering. For the HPS200 formulation, HT out performs the more expensive organic stabilisers and has the added benefit of being non toxic. The performance reflects the ability of HT to remove sulphonic acid fragments and hydrochloric acid demonstrated in chapter 3.

5.5 References

1. Martin, G.P., Robinson, A.J., and Worsley, D.A., , *Hydrotalcite mineral stabilisation of titanium dioxide photocatalysed degradation of unplasticised polyvinylchloride*. *Materials Science and Technology*, 2006. **22**(No. 3): p. 375-378.
2. Robinson, A.J., Wray, J., and Worsley, D.A.,, *Effect of coloured pigmentation on titanium dioxide photo catalysed PVC degradation*. *Materials Science and Technology*, 2006. **22**(12): p. 1503-1508.
3. Wijdekop, M., *The weathering of organic coated steel and application of mathematical modeling*. 2004.
4. Robinson, A.J., *The Development of Organic Coatings for Strip Steels with Improved Resistance to Photodegradation*. EngD Thesis, University Of Wales Swansea, 2005.

Chapter 6

Stabilisation of Fully Formulated Commercial Plastisol Systems

6.1 Introduction and Aims

The benefit of Hydrotalcite (HT) as a stabiliser has been shown in model paint [1] systems (Chapter 3) and in near commercial systems (Chapter 5). This section of work investigates the durability of a fully commercial phthalate free plastisol (White, Grey and Brown) in longer QUV accelerated weathering. The aim was to evaluate HT against other stabilisers in a coating system mirroring a line material.

6.2 Experimental

A full investigation was carried out looking at the fully formulated coating using the current grade of plastisol made from a standard commercial base. A matrix of samples was created covering a range of different stabiliser concentrations (Table 6.1) using Hydrotalcite stabiliser and the current BaZn stabiliser and a new CaZn system. The samples were subjected to conventional accelerated weathering in QUVA cabinets. The weathering process was completed and the resultant samples subjected to a variety of tests to assess levels of degradation. At each stage (every 1000h) of the weathering process the samples were also subjected to individual colour and gloss measurements.

6.2.1 Sample Preparation

The samples were prepared in a similar way to that outlined in Section 2.1.6. A plastisol base was supplied by Akzo Nobel and the required amounts of plasticiser, pigment and stabiliser were added to this base and dispersed using an industrial high shear mixer. The stabiliser concentration, pigment (K2220) and colour are outlined in Table 6.1. After formulating the paint and ensuring a uniform viscosity, samples were cast onto ready primed Galvalloy (4.2% Aluminium, 95.8%) coated steel samples 16cm x 18cm using a standard 200µm draw down bar. Each sample was cured in a paint curing oven for 50 seconds reaching a peak metal temperature of ca 220°C then water quenched to room temperature. To ensure continuity across different samples gloss measurements were made of each cured sample. Finally each panel was guillotined to the required

sample size. A total of 44 panels were tested, 2 of each formulation as shown below in Table 6.1.

Table 6.1: Pigment loading, colour and stabiliser addition under test.

Stabiliser	White (20% TiO₂)	Goosewing Grey (14% TiO₂)	Van Dyke Brown (0% TiO₂)
3% BaZn	○	●	●
3% BaZn 1% HT	○	●	●
2% BaZn 2% HT	○		
1% BaZn 1% HT	○	●	●
1% HT	○	●	●
4% HT	○	●	●
3% CaZn	○		
3% CaZn 1% HT	○		
2% CaZn 2% HT	○		

6.2.2 Accelerated Weathering in QUVA

The sample panels were irradiated using a QUV Accelerated Weathering Tester (Q-Panel Company) fitted with UVA lamps. The setup of this QUV cabinet is covered in more detail in Section 2.7.1. Each panel was subjected to 6000 hours of weathering cycles consisting of 8 hours UVA radiation and 4 hours condensation. In every 24 hour period this allowed two complete cycles. The panel temperatures for both cycles (UV and condensation) were set at 40°C with a light intensity of 0.68 W/m²/nm at 340nm. The light intensity was calibrated every 2 weeks. The samples were placed in a different random position and none of the four end positions were used as UV strength can be slightly lower. This was performed so as to minimise any intensity variation effects within the weathering cabinet. The panels were weathered for periods of 1000 hours at a time which consisted of a total 667 hours of UV irradiation and 333 hours of condensation. Panels were subjected to a total of 6000 hours weathering cycles.

6.2.3 Accelerating Weathering in QUVB

The sample panels (white formulations only) were irradiated using a QUV Accelerated Weathering Tester (Q-Panel Company) fitted with UVB lamps. Each panel was subjected to 1715 hours weathering cycles consisting of 4 hours UVB radiation and 4 hours condensation. The panel temperatures were set at 60°C for UVB light cycle and 50°C for condensation cycle. The light intensity of 0.67 W/m²/nm at 313nm was set and calibrated every 2 weeks. The panels were weathered for a total period of 1715 hours, 857.5 hours of UV irradiation and 857.5 hours of condensation.

6.2.4 Gloss Loss Measurements

All of the panels were measured for gloss loss with a Minolta Multi-Gloss 268 using the 60° angle setting as described in Section 2.7.2. Each panel was measured at ten separate points and the average value recorded. The gloss loss measurements are given as gloss retention as the initial un-weathered 60° gloss values can vary substantially from panel to panel. This is mainly due to the small differences in the curing process so the gloss value of a weathered panel needs to be related to the initial gloss before weathering of that specific panel to be relevant. The gloss retention is calculated with a simple formula:

$$\text{Gloss Retention (\%)} = (100 * \text{Gloss Weathered}) / \text{Gloss un-weathered}$$

6.2.5 Colour Change Measurements

Colour was measured in the form of a reflectance spectrum and the difference in reflectance spectrum after 6000h was calculated. The colour reflectance was performed using a Gretag-Macbeth measuring reflectance over the range 370nm-730nm which measures the reflectance spectrum ignoring the gloss components. The reflectance measurements for each panel were calculated by taking the average value from ten separate measurements [2]. Each panel was measured after every 1000 hour interval and these results are shown in appendix 2.

6.3 Results and Discussion

6.3.1 White Formulations (QUVA).

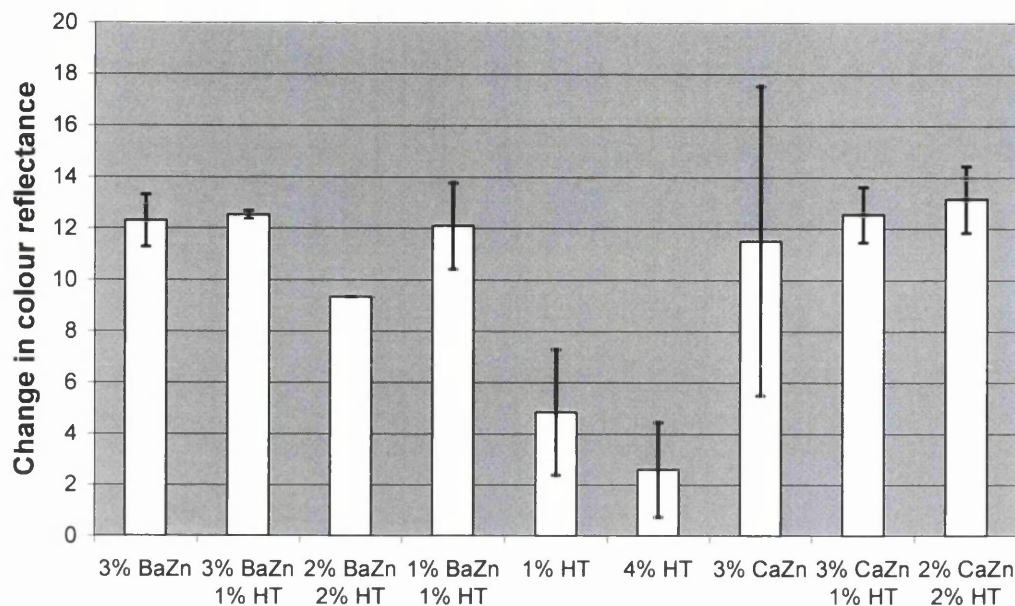


Figure 6.1: Change in colour reflectance for white formulations after 6000h QUVA.

The more positive the colour change the darker the paint has become after being exposed to UVA. The BaZn stabilised systems show a significant darkening effect compared with the HT only systems. The CaZn stabilised formulations show slightly more darkening when compared with the BaZn formulations. As the concentration of HT is increased to 2% in the BaZn/HT system the performance improves significantly. HT additions at 4% appear to be most effective in preventing colour change, however commercially the BaZn also offers a heat stabilisation which ensures a colour consistency in oven curing. As such the combination of BaZn and HT looks quite promising.

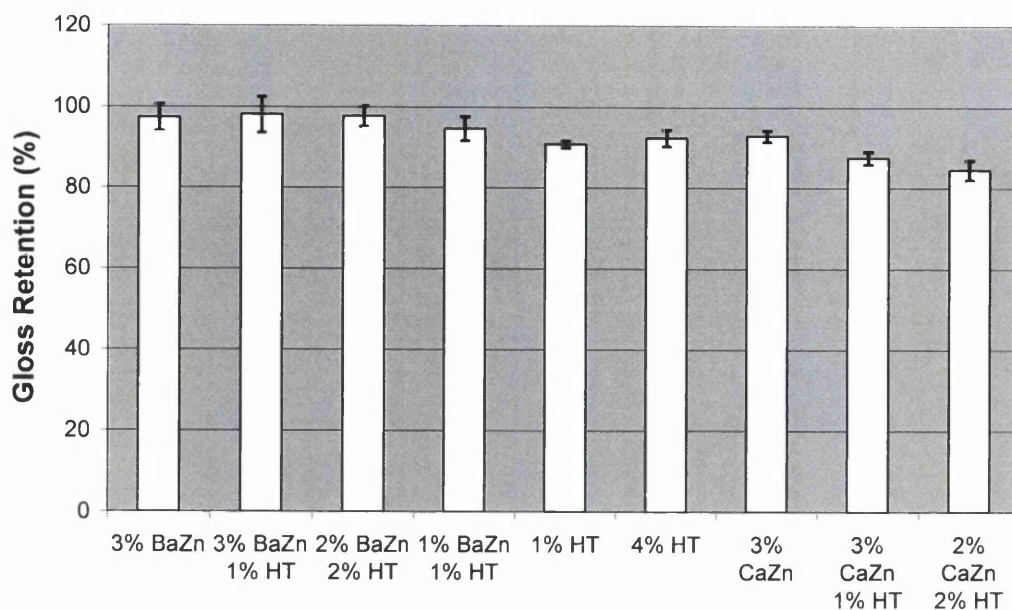


Figure 6.2: Gloss Retention of White Formulations after 6000 QUVA.

All of the gloss retention values were acceptable but there are some minor differences shown in Figure 6.2. The CaZn systems show the worst gloss retentions (85-92%) especially when the concentration of CaZn is reduced and combined with HT and this combined with poor colour retention is not promising. The BaZn systems show good gloss retentions >95% with very little change when the concentration of BaZn is reduced and HT added. The HT formulation gloss retentions are above 90% and actually only show an initial drop in gloss and very little drop in gloss retention afterwards (see appendix 2). The gloss values for the HT start off slightly higher and after the initial drop at the first measurement (899h) they are comparable with the 3% BaZn.

6.3.2 White Formulations (QUVB).

Data for 1715 hours QUVB is shown in Figure 6.3. Under the harsher conditions of irradiation of UVB the CaZn stabilised system shows significant darkening at the 3% concentration and 3% CaZn / 1% HT, although the 2% concentration of CaZn shows a significant improvement with more HT addition as the colour change is 3 compared with

12.5 and 15.8 respectively. The BaZn only formulation shows a colour change of 6 and with the addition of HT the colour change improves and in some cases becomes slightly whiter (lighter). The addition of HT only shows an improvement on the colour change compared with Ba/Zn system but the best performance appears to be a combination of BaZn and HT.

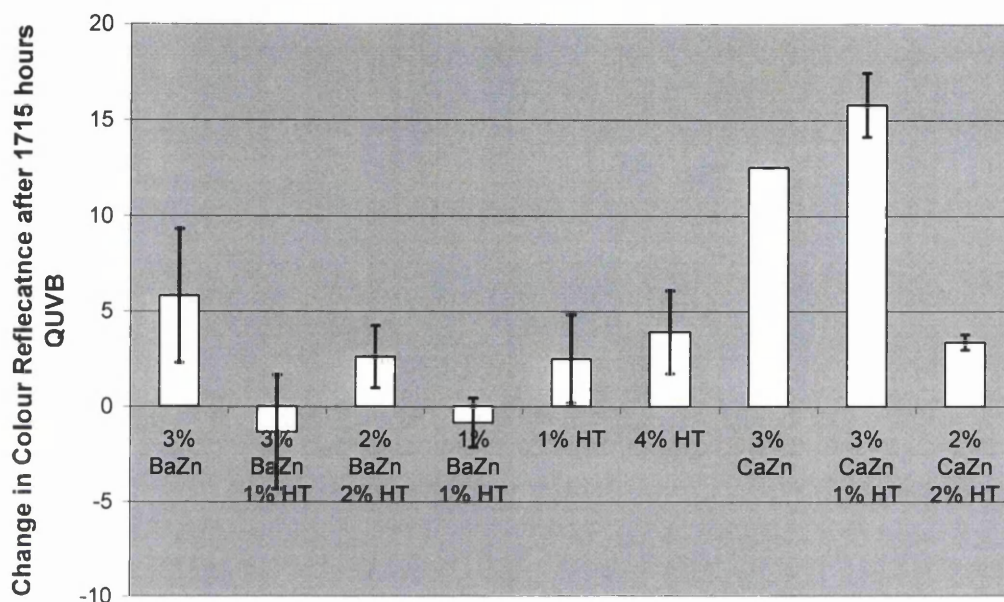


Figure 6.3: Change in colour reflectance for white formulations after 1715h QUVB.

The gloss retention of the BaZn system is significantly improved as the BaZn concentration is reduced with the addition of HT. The CaZn stabilised system shows slightly better gloss retention than the BaZn and HT does appear to improve this in the same way as in the BaZn. The HT only stabilised systems perform the best in these gloss tests reflecting the greater production of hydrochloric acid in UVB exposure.

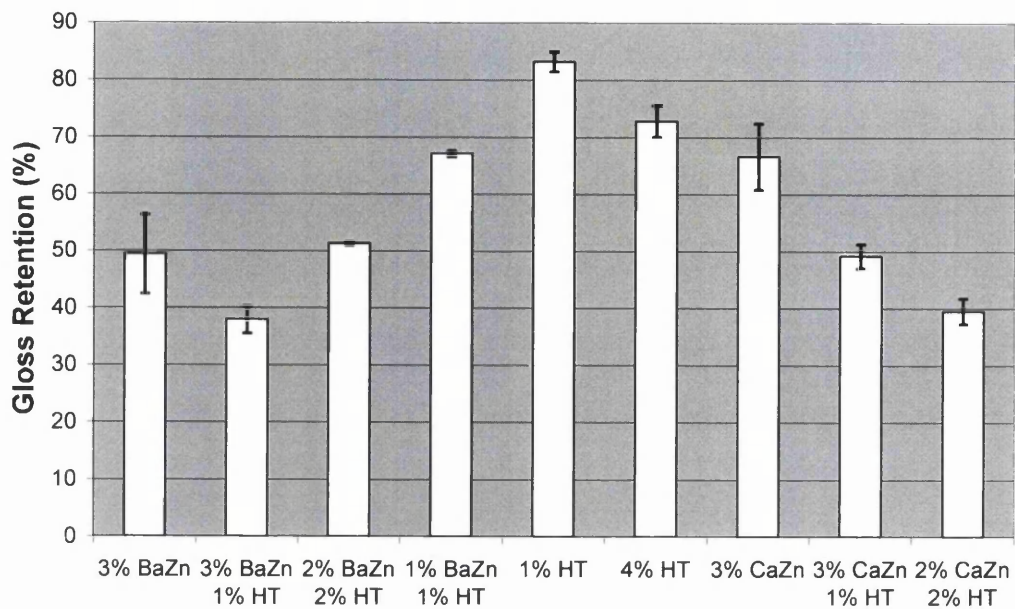


Figure 6.4: Gloss Retention of white formulations after 1715h QUVB.

6.3.3 Goosewing Grey Formulations (UVA).

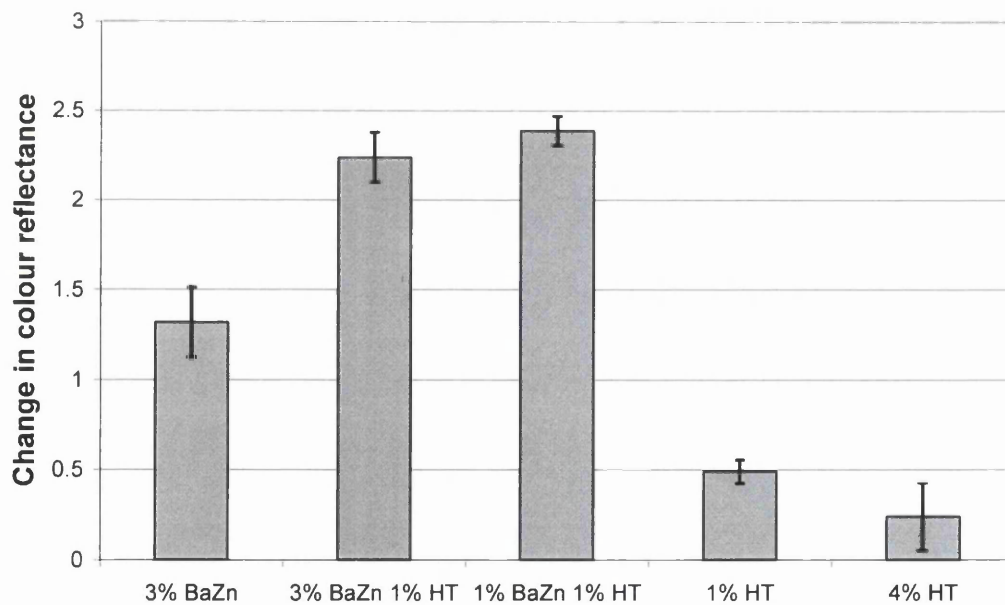


Figure 6.5: Change in colour reflectance for Goosewing Grey formulations after 6000h QUVA.

The goosewing grey has carbon addition and as shown in chapter 5 this reduces degradation significantly in all cases. The BaZn only system performs slightly better than the lower concentrations and HT combinations in this instance. The HT only system significantly improves the colour performance and as the level of HT is increased the coating shows very little change in colour through 6000h exposure.

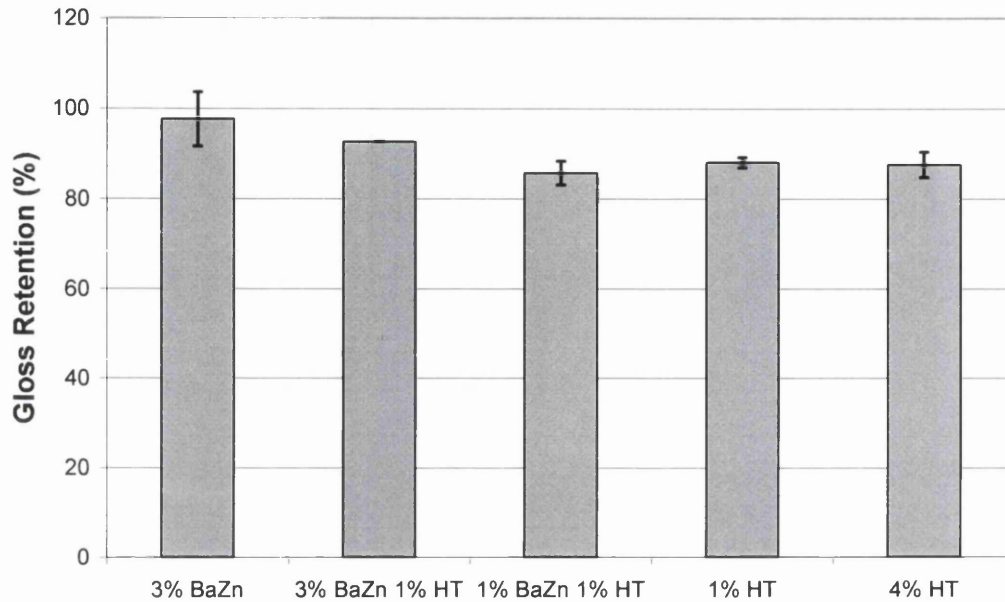


Figure 6.6: Gloss Retention of Goosewing Grey Formulations after 6000 QUVA.

In Figure 6.6 all the gloss retentions are acceptable and above 85%. The 1% BaZn 1% HT is showing the worst performance and the 3% BaZn is showing the best gloss retention of 97%. The HT additions gloss retentions are around 90% after 6000 hours QUVA. The HT samples again show an initial drop with the gloss values then similar to BaZn as in the whites (full data in appendix 2).

6.3.4 Van Dyke Brown Formulations (UVA).

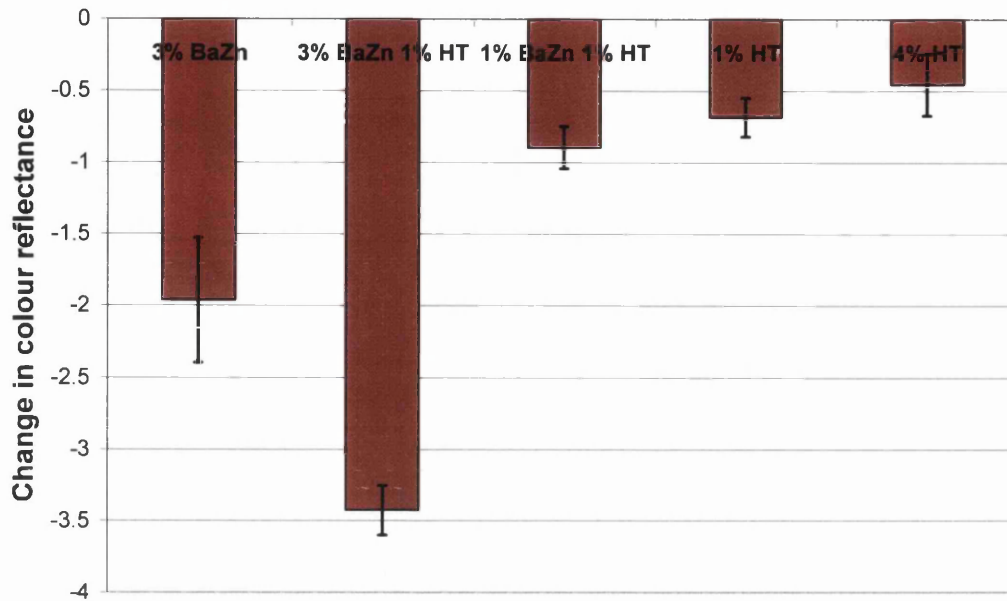


Figure 6.7: Change in colour reflectance for Van Dyke Brown formulations after 6000h QUVA.

The addition of BaZn destabilises the paint system and shows the most colour change (Figure 6.7). In this case all systems show a negative colour change meaning that the coating is becoming whiter (lightening). This reflects a real colour change. There is not any TiO₂ and so no chalking is observed. As the concentration of BaZn is reduced the lightening effect is less. The addition of HT improves performance and as the concentration is increased to 4% this significantly reduces colour change.

The gloss retentions (Figure 6.8) are all acceptable and above 83%. 3% BaZn is the highest at 92%. The gloss retentions for the HT additions are comparable with BaZn/HT combinations. The HT only system shows the same initial drop as the white and goosewing grey formulations (see appendix 2).

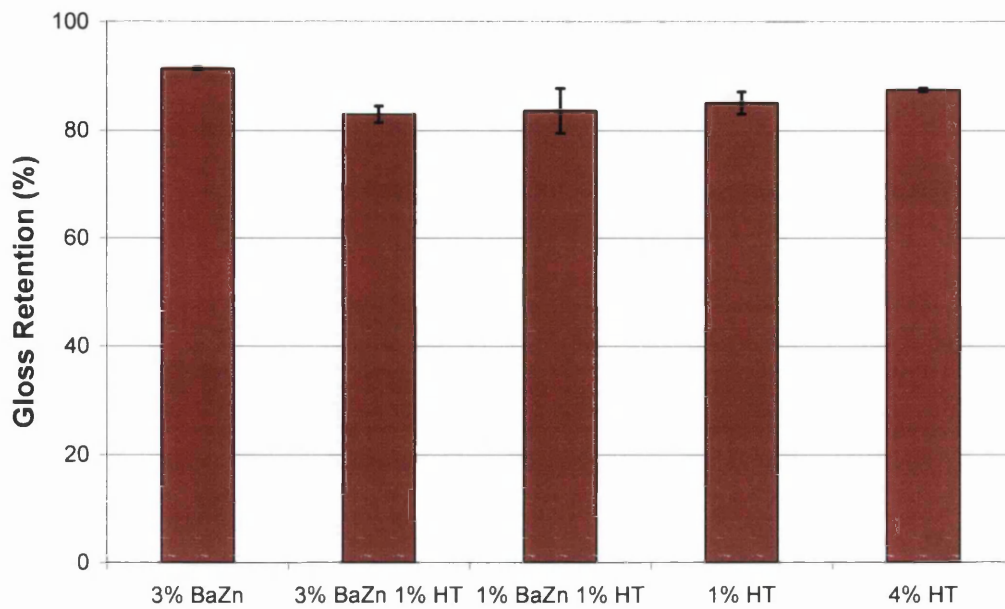


Figure 6.8: Gloss Retention of Van Dyke Brown Formulations after 6000 QUVA.

6.4 Conclusion

In order to provide an illustration of the effectiveness of CaZn, BaZn and HT the data for all the tests has been summarised into a single plot. Performance is ranked 1 (best) to 3 (worst). This is illustrated in Figure 6.9.

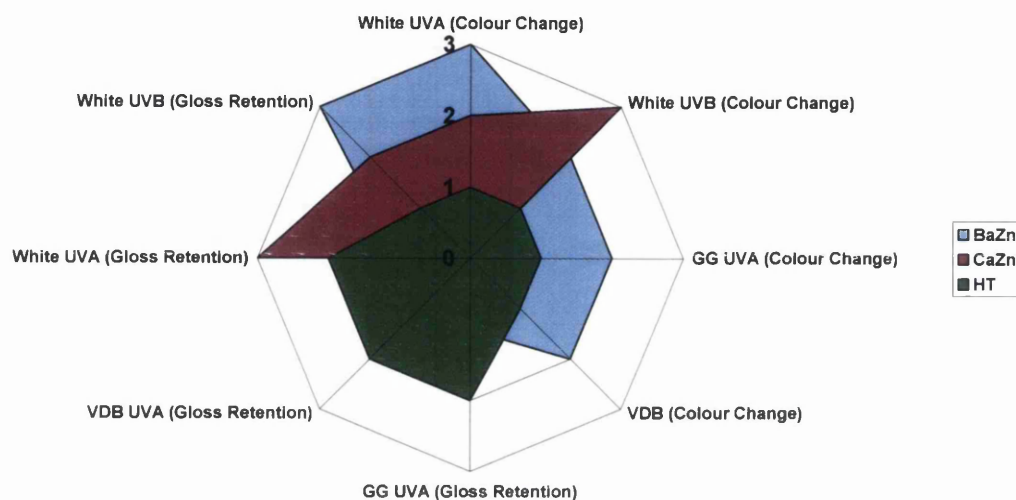


Figure 6.9: Ranking of 3% BaZn, 3% CaZn and 4% HT in different shades measurements after 6000.

Figure 6.9 shows the addition of HT is more effective than the two stabilisers (BaZn and CaZn used alone) in UVA and UVB conditions at preventing darkening (dehydrochlorination) of the white formulations. The gloss retention for the HT samples is comparable to the others after their initial drop. The ranking of HT is slightly poorer in the gloss retention tests for all shades due to this initial drop in gloss. The gloss values for the HT samples start off slightly higher and after this initial drop are comparable to the BaZn and CaZn stabilised systems. This initial drop is probably down to the relaxing of the coating after the initial irradiation following the oven curing.

HT is the most effective in preventing darkening in Goosewing Grey and the gloss values are comparable with BaZn stabilised system after the initial drop. In Van

Dyke Brown the addition of HT prevents the coating from lightening. The gloss retentions for HT are comparable with BaZn for Van Dyke Bown.

The addition of HT into a fully commercial product seems to work effectively in the coating to prevent the dehydrochlorination (darkening) and making the coating whiter for longer. It also has the benefit of being readily available, non toxic and only £1.69 a kilo while BaZn and CaZn are £3.50 and £3.80 respectively. It shows potential as an additive or filler material that is able to give the coating better resistance to weathering and degradation.

6.5 References

1. Martin, G.P., Robinson, A.J., and Worsley, D.A., , *Hydrotalcite mineral stabilisation of titanium dioxide photocatalysed degradation of unplasticised polyvinylchloride*. *Materials Science and Technology*, 2006. **22**(No. 3): p. 375-378.
2. Wijdekop, M., *The weathering of organic coated steel and application of mathematical modeling*. 2004.

Chapter 7

Conclusions and Future Work

7.1 Conclusions and Future Work

In order to provide an illustration of the effectiveness of CaZn, BaZn and HT in white model and fully commercial systems the data for all tests has been summarised into a single plot. Performance is ranked 1 (best) to 3 (worst) and is illustrated in Figure 7.1.

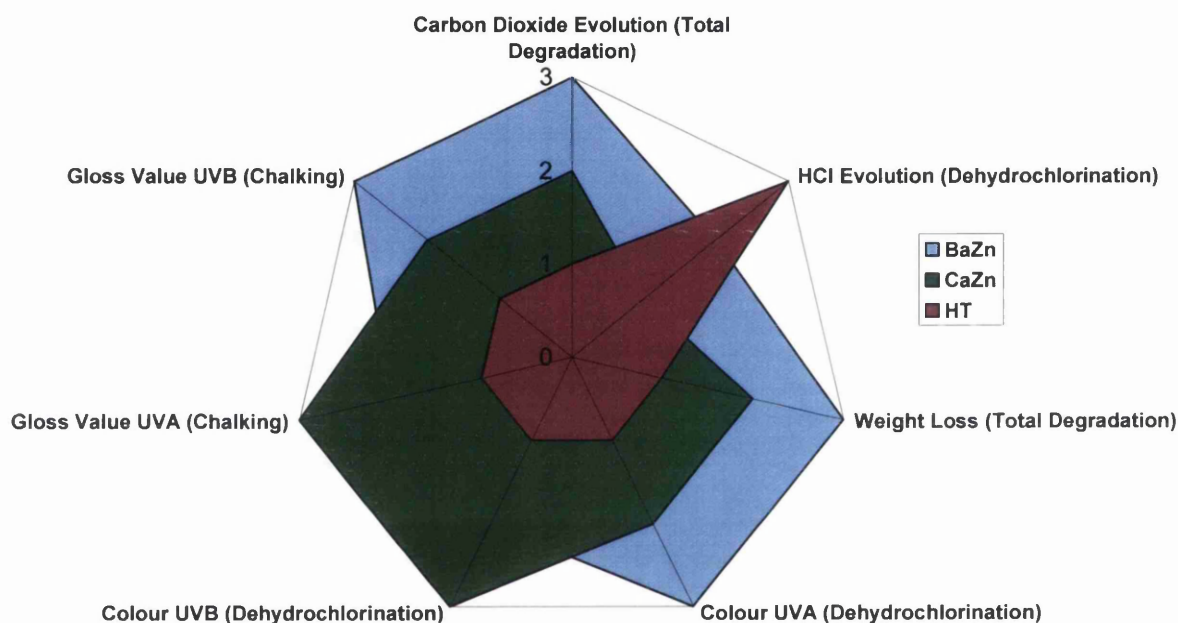


Figure 7.1: Ranking of 3% BaZn, 3% CaZn and 4% HT in model system tests and fully commercial system tests.

Figure 7.1 is a visual summary of the effects of HT compared to BaZn, CaZn and shows HT is more effective in preventing darkening than the two stabilisers (BaZn and CaZn) when used alone in UVA and UVB conditions. It also performs the best in model system tests (Weight Loss and CO₂ evolution) showing correlation to the results in fully commercial system tests of QUVA and QUVB.

Hydrotalcite is not the best performing stabiliser in the model system test of HCl evolution as it is unable to stop the formation of or absorb HCl gas in an analogous fashion to BaZn and CaZn stabilisers. As HT addition is increased, it decreases the HCl evolution slightly, however not to the same extent as the organic (BaZn and CaZn) stabilisers. Although a small addition of HT in a model system removes the hydrochloric acid and prevents the occurrence of a faster secondary rate and it is the best stabilising compound in all the other tests.

Hydrotalcite performance in a fully commercial PVC plastisol (Chapter 6) after long term QUVA and QUVB exposure is very encouraging in terms of preventing dehydrochlorination (darkening) of the coating. The stabiliser is a cheaper alternative to a traditional stabilising compound and has no toxicity as well as being extremely easy to incorporate into a coating system. Further work is needed after prolonged external natural weathering and possible line trials using HT in an industrial coating process to ensure that HT additions do not introduce undesirable viscosity effects at high sheer rates used in coil coating.

The addition of plasticisers to a model system can dramatically alter the rates of degradation. All plasticisers seem to be preferentially attacked over the PVC matrix and yield faster initial rates of degradation. The phthalate systems produce no strong acid fragments and do not subsequently catalyse degradation. The sulphonic acid ester (phthalate free) plasticiser when irradiated degrade to produce strongly acid fragments and HCl which can cause acid catalysis of the titanium dioxide to occur. As such, the best solution for a phthalate free coating system would appear to be one which contains the ASPS and a suitable stabilising agent to remove acidic fragments capable of catalysing TiO₂. The work undertaken in this thesis suggests that HT is such a compound.

Future work should be undertaken in the investigation of CO₂ evolution in a model system exposed to different laboratory controlled environmental conditions (temperature and moisture). Figure 7.2 shows the initial results of removing moisture from the environment using magnesium perchlorate drying in two Dreschel bottles

connected in series within the flat panel reactor. The complete removal of moisture from within the system indicates changes in the CO₂ evolution profile with no acid catalysis (since HCl production will not yield hydrochloric acid and HCl will remain as a gas). During experiments carried out for this thesis the change in relative humidity (40-60%) within the lab had no affect on the repeatability of the results between coatings. A total removal of moisture has a similar affect to that seen with a high concentration (10%) of BaZn or CaZn. Hence it is clear that the moisture content is critical in determining degradation rate and a series of experiments at defined humidity should be undertaken to define this effect absolutely. In addition, such experimentation should also be undertaken on other polymer films, which are used for structural plastic and paint systems to determine the influence of moisture on their photodegradation rates.

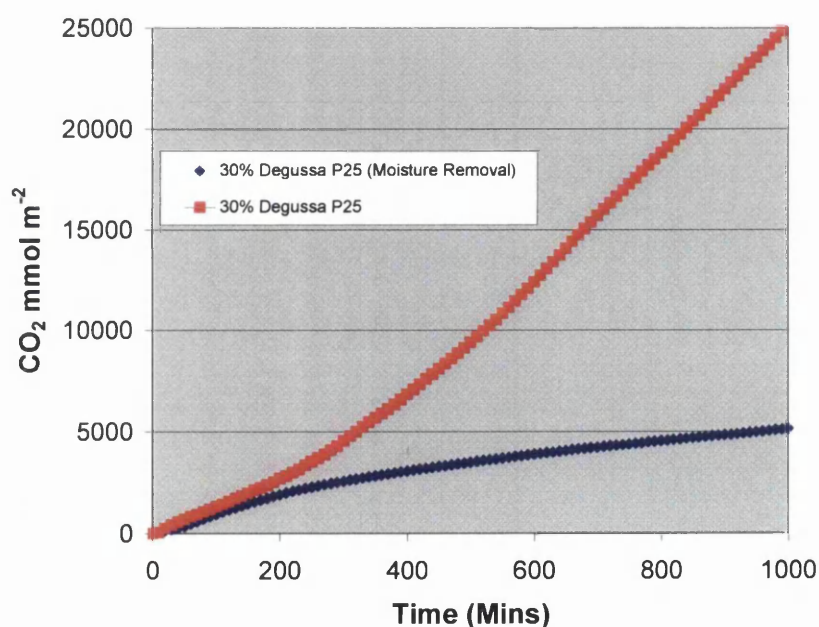


Figure 7.2: The effect of removing moisture from flat panel reactor on a standard 30% P25 TiO₂.

Appendix 1

White Formulations				Gloss Values						Gloss Retention					
Ident. No.	Base	Pigment	Stab	0h	750h	1500h	2000h	3000h	0h	750h	1500h	2000h	3000h		
1	HPS200	14% K2220 (A)	1% BaZn	29.40	36.98	32.31	32.09	33.47	100	125.81	109.90	109.16	113.86		
2	HPS200	14% K2220 (A)	1% Sn1/Sn2	19.05	20.76	20.56	21.53	18.65	100	108.99	107.91	112.99	97.90		
3	HPS200	14% K2220 (A)	5% Hydrotalcite	21.82	16.77	20.69	23.98	20.00	100	76.87	94.83	109.90	91.68		
4	HPS200	14% K2220 (A)	No Stab	22.48	23.94	23.23	16.31	20.31	100	106.51	103.36	72.58	90.35		
5	Mk II	14% K2220 (A)	1% BaZn	29.36	27.43	27.71	26.98	27.23	100	93.41	94.37	91.89	92.75		
6	Mk II	14% K2220 (A)	1% Sn1/Sn2	25.79	25.72	23.23	23.45	23.40	100	99.72	90.08	90.93	90.73		
7	Mk II	14% K2220 (A)	5% Hydrotalcite	30.51	15.91	18.53	17.89	17.70	100	52.16	60.73	58.65	58.02		
8	Mk II	14% K2220 (A)	No Stab	37.53	30.00	31.48	33.60	32.90	100	79.95	83.88	89.54	87.67		
9	HP200	14% K2220 (A)	1% BaZn	27.31	24.62	26.63	22.09	19.11	100	90.15	97.49	80.88	69.96		
10	HP200	14% K2220 (A)	1% Sn1/Sn2	25.55	22.49	23.29	23.44	22.89	100	88.06	91.16	91.75	89.60		
11	HP200	14% K2220 (A)	5% Hydrotalcite	24.25	19.86	18.94	15.99	18.88	100	81.91	78.12	65.93	77.84		
12	HP200	14% K2220 (A)	No Stab	25.93	23.83	22.54	22.29	19.95	100	91.91	86.94	85.95	76.94		
37	HPS200	14% 2300 (B)	1% BaZn	15.26	18.68	16.46	19.40	15.64	100	122.46	107.92	127.17	102.51		
38	HPS200	14% 2300 (B)	1% Sn1/Sn2	14.56	16.18	15.93	15.09	15.85	100	111.13	109.41	103.66	108.88		
39	HPS200	14% 2300 (B)	5% Hydrotalcite	16.06	15.04	14.72	15.75	13.89	100	93.70	91.68	98.10	86.50		
40	HPS200	14% 2300 (B)	No Stab	15.00	16.07	15.71	16.29	14.29	100	107.16	104.78	108.62	95.28		
41	HPS200	14% K2063 (C)	1% BaZn	14.01	17.58	17.42	17.16	16.45	100	125.49	124.33	122.50	117.42		
42	HPS200	14% K2063 (C)	1% Sn1/Sn2	18.69	19.38	19.03	22.34	18.11	100	103.69	101.85	119.55	96.90		
43	HPS200	14% K2063 (C)	5% Hydrotalcite	14.18	14.88	15.02	14.74	14.08	100	104.94	105.95	103.97	99.34		
44	HPS200	14% K2063 (C)	No Stab	15.74	18.16	17.56	15.25	17.71	100	115.39	111.58	96.89	112.49		

White Formulations				Gloss Values						Gloss Retention					
Ident. No.	Base	Pigment	Stab	0h	750h	1500h	2000h	3000h	0h	750h	1500h	2000h	3000h		
13	HPS200	14% K1001 (U)	1% BaZn	34.75	2.30	1.81	1.83	-	100	6.62	5.22	5.25	-		
14	HPS200	14% K1001 (U)	1% Sn1/Sn2	19.22	4.01	1.83	1.85	-	100	20.88	9.50	9.63	-		
15	HPS200	14% K1001 (U)	5% Hydrotalcite	17.80	13.51	2.03	1.98	-	100	75.93	11.41	11.10	-		
16	HPS200	14% K1001 (U)	No Stab	14.03	2.10	1.80	1.70	-	100	14.97	12.83	12.12	-		
17	Mk II	14% K1001 (U)	1% BaZn	34.36	12.61	2.00	1.90	-	100	36.69	5.82	5.53	-		
18	Mk II	14% K1001 (U)	1% Sn1/Sn2	24.85	24.24	24.03	23.42	-	100	97.54	96.69	94.25	-		
19	Mk II	14% K1001 (U)	5% Hydrotalcite	26.16	17.28	6.42	3.50	-	100	66.06	24.54	13.38	-		
20	Mk II	14% K1001 (U)	No Stab	23.99	17.41	1.96	1.80	-	100	72.60	8.16	7.50	-		
21	HP200	14% K1001 (U)	1% BaZn	30.38	17.27	1.99	1.89	-	100	56.85	6.56	6.21	-		
22	HP200	14% K1001 (U)	1% Sn1/Sn2	26.17	20.53	11.03	2.06	-	100	78.47	42.16	7.88	-		
23	HP200	14% K1001 (U)	5% Hydrotalcite	23.50	15.79	2.99	1.90	-	100	67.20	12.72	8.09	-		
24	HP200	14% K1001 (U)	No Stab	23.93	12.67	2.04	1.90	-	100	52.95	8.52	7.94	-		

No Pigment (Clear Base)

Ident. No.	Base	Pigment	Stab	Gloss Values						Gloss Retention					
				0h	750h	1500h	2000h	3000h	0h	750h	1500h	2000h	3000h		
25	HPSS200	No Pigment	1% Bazn	11.68	12.10	11.23	11.29	11.34	100	103.60	96.16	96.64	97.12		
26	HPSS200	No Pigment	1% Sn1/Sn2	12.57	13.82	12.01	11.28	11.73	100	109.98	95.60	89.73	93.31		
27	HPSS200	No Pigment	5% Hydrotalcite	13.78	13.10	12.44	11.36	13.06	100	95.10	90.34	82.49	94.78		
28	HPSS200	No Pigment	No Stab	11.12	11.25	10.98	10.75	10.34	100	101.21	98.74	96.72	93.06		
29	Mik II	No Pigment	1% Bazn	26.12	24.05	24.23	24.57	25.67	100	92.08	92.75	94.05	98.28		
30	Mik II	No Pigment	1% Sn1/Sn2	27.23	25.23	25.56	25.26	24.98	100	92.66	93.88	92.75	91.74		
31	Mik II	No Pigment	5% Hydrotalcite	29.67	23.50	21.40	23.10	22.80	100	79.20	72.13	77.86	76.85		
32	Mik II	No Pigment	No Stab	33.06	28.06	25.89	26.79	25.87	100	84.88	78.34	81.05	78.26		
33	HP200	No Pigment	1% Bazn	21.90	21.15	20.83	19.64	18.83	100	96.58	95.12	89.67	85.99		
34	HP200	No Pigment	1% Sn1/Sn2	19.65	19.54	19.19	17.19	17.71	100	99.45	97.67	87.49	90.13		
35	HP200	No Pigment	5% Hydrotalcite	25.26	21.19	21.28	17.69	18.77	100	83.89	84.27	70.04	74.32		
36	HP200	No Pigment	No Stab	23.15	22.18	19.73	21.88	17.11	100	95.81	85.25	94.51	73.91		

White Formulations Colour Reflectance Area and Colour Change After 3000h

Ident. No.	Base	Pigment	Stab	0h	750h	1500h	2000h	3000h	Change
1	HPSS200	14% K2220 (A)	1% BaZn	282.67	280.49	285.60	279.96	280.49	2.18
2	HPSS200	14% K2220 (A)	1% Sn1/Sn2	277.75	274.83	280.20	275.21	274.91	2.83
3	HPSS200	14% K2220 (A)	5% Hydrotalcite	283.09	283.82	286.30	283.57	283.54	-0.45
4	HPSS200	14% K2220 (A)	No Stab	281.00	280.78	285.70	279.50	280.99	0.01
5	Mk II	14% K2220 (A)	1% BaZn	280.03	278.17	271.76	270.44	276.87	3.16
6	Mk II	14% K2220 (A)	1% Sn1/Sn2	283.24	281.39	274.05	271.08	276.09	7.15
7	Mk II	14% K2220 (A)	5% Hydrotalcite	280.94	280.55	274.43	276.05	278.34	2.60
8	Mk II	14% K2220 (A)	No Stab	281.78	280.40	273.41	274.59	278.24	3.54
9	HP200	14% K2220 (A)	1% BaZn	278.90	274.22	277.97	272.75	273.49	5.42
10	HP200	14% K2220 (A)	1% Sn1/Sn2	281.30	279.38	281.10	276.82	275.85	5.45
11	HP200	14% K2220 (A)	5% Hydrotalcite	279.10	277.04	281.63	276.37	276.43	2.66
12	HP200	14% K2220 (A)	No Stab	290.31	286.64	289.88	285.29	285.40	4.90
37	HPSS200	14% 2300 (B)	1% BaZn	272.87	270.62	274.27	270.66	270.90	1.97
38	HPSS200	14% 2300 (B)	1% Sn1/Sn2	280.43	279.14	283.35	278.31	277.43	3.00
39	HPSS200	14% 2300 (B)	5% Hydrotalcite	284.35	286.20	288.07	285.95	285.62	-1.27
40	HPSS200	14% 2300 (B)	No Stab	277.23	276.90	281.57	274.84	275.46	1.77
41	HPSS200	14% K2063 (C)	1% BaZn	285.32	281.42	285.91	280.41	280.43	4.89
42	HPSS200	14% K2063 (C)	1% Sn1/Sn2	279.57	277.95	281.84	277.56	277.54	2.02
43	HPSS200	14% K2063 (C)	5% Hydrotalcite	281.16	283.60	286.11	282.49	281.92	-0.76
44	HPSS200	14% K2063 (C)	No Stab	279.45	279.30	282.81	277.40	277.43	2.02

White Formulations Colour Reflectance Area and Colour Change After 2000h

Ident. No.	Base	Pigment	Stab	0h	750h	1500h	2000h	3000h	Change
13	HPSS200	14% K1001 (U)	1% BaZn	284.46	289.67	290.90	283.59	-	0.87
14	HPSS200	14% K1001 (U)	1% Sn1/Sn2	284.03	285.86	289.48	283.14	-	0.89
15	HPSS200	14% K1001 (U)	5% Hydrotalcite	285.94	286.02	292.99	287.26	-	-1.32
16	HPSS200	14% K1001 (U)	No Stab	286.96	283.64	283.15	279.99	-	6.96
17	Mk II	14% K1001 (U)	1% BaZn	281.81	296.19	277.81	281.30	-	4.00
18	Mk II	14% K1001 (U)	1% Sn1/Sn2	280.00	277.12	272.98	278.10	-	7.02
19	Mk II	14% K1001 (U)	5% Hydrotalcite	286.86	300.36	292.53	290.32	-	-5.67
20	Mk II	14% K1001 (U)	No Stab	283.26	292.02	281.27	285.77	-	1.98
21	HP200	14% K1001 (U)	1% BaZn	291.94	291.03	291.63	286.25	-	0.31
22	HP200	14% K1001 (U)	1% Sn1/Sn2	297.33	286.55	291.34	289.52	-	5.99
23	HP200	14% K1001 (U)	5% Hydrotalcite	293.84	291.97	299.10	289.68	-	-5.26
24	HP200	14% K1001 (U)	No Stab	298.29	285.56	293.42	286.50	-	4.87

No Pigment (Clear Base) Colour Reflectance Area and Colour Change After 3000h

Ident. No.	Base	Pigment	Stab	0h	750h	1500h	2000h	3000h	Change
25	HPSS200	No Pigment	1% BaZn	165.23	162.42	163.76	161.87	160.42	4.80
26	HPSS200	No Pigment	1% Sn1/Sn2	168.70	167.35	167.70	165.50	162.87	5.84
27	HPSS200	No Pigment	5% Hydrotalcite	171.94	171.67	173.44	170.35	168.89	3.05
28	HPSS200	No Pigment	No Stab	175.08	173.46	174.29	171.54	168.30	6.78
29	Mk II	No Pigment	1% BaZn	156.39	157.97	154.67	155.27	157.60	-1.20
30	Mk II	No Pigment	1% Sn1/Sn2	157.10	157.48	153.66	155.67	156.03	1.07
31	Mk II	No Pigment	5% Hydrotalcite	159.10	163.37	158.32	159.35	160.18	-1.09
32	Mk II	No Pigment	No Stab	157.72	159.48	156.30	158.05	152.55	5.17
33	HP200	No Pigment	1% BaZn	172.10	170.45	171.59	169.75	168.78	3.32
34	HP200	No Pigment	1% Sn1/Sn2	168.07	165.95	167.17	162.58	158.47	9.60
35	HP200	No Pigment	5% Hydrotalcite	170.29	169.38	167.96	164.75	157.15	13.14
36	HP200	No Pigment	No Stab	168.42	165.73	155.87	139.63	118.42	50.01

HPSS200 Colour Formulations - Colour Reflectance Areas

Ident. No.	Base	Pigment	Stab	Colour Pig.	0h	750h	1500h	2000h
45	HPSS200	14% K1001 (U)	1% BaZn	0.5% C	41.91	47.26	87.45	82.39
46	HPSS200	14% K1001 (U)	1% BaZn	1.0% C	25.18	64.31	53.69	51.72
47	HPSS200	14% K1001 (U)	1% BaZn	1.5% C	21.40	38.94	41.60	42.32
48	HPSS200	14% K1001 (U)	1% BaZn	1% BLP (Blue)	85.12	156.54	161.93	149.16
49	HPSS200	14% K1001 (U)	1% BaZn	1% GLSM (Blue)	94.56	169.17	166.16	156.23
50	HPSS200	14% K1001 (U)	1% BaZn	1% DPP (Red)	158.91	199.35	210.06	202.28
51	HPSS200	14% K1001 (U)	1% BaZn	1% GLN (Green)	116.55	177.88	188.94	174.15
52	HPSS200	14% K1001 (U)	1% Sn1/Sn2	0.5% C	40.92	51.10	81.98	74.27
53	HPSS200	14% K1001 (U)	1% Sn1/Sn2	1.0% C	25.64	28.12	53.15	50.42
54	HPSS200	14% K1001 (U)	1% Sn1/Sn2	1.5% C	20.16	21.59	46.89	42.28
55	HPSS200	14% K1001 (U)	1% Sn1/Sn2	1% BLP (Blue)	86.28	112.73	163.44	156.57
56	HPSS200	14% K1001 (U)	1% Sn1/Sn2	1% GLSM (Blue)	91.97	141.00	163.52	152.35
57	HPSS200	14% K1001 (U)	1% Sn1/Sn2	1% DPP (Red)	152.21	165.90	198.55	190.56
58	HPSS200	14% K1001 (U)	1% Sn1/Sn2	1% GLN (Green)	108.38	123.64	174.15	164.11
59	HPSS200	14% K1001 (U)	5% HT	0.5% C	47.13	52.11	80.43	74.72
60	HPSS200	14% K1001 (U)	5% HT	1.0% C	27.70	32.89	48.85	46.14
61	HPSS200	14% K1001 (U)	5% HT	1.5% C	21.84	26.87	46.51	39.59
62	HPSS200	14% K1001 (U)	5% HT	1% BLP (Blue)	83.97	110.99	167.43	155.24
63	HPSS200	14% K1001 (U)	5% HT	1% GLSM (Blue)	94.47	119.83	172.04	163.65
64	HPSS200	14% K1001 (U)	5% HT	1% DPP (Red)	156.68	168.16	201.82	199.63
65	HPSS200	14% K1001 (U)	5% HT	1% GLN (Green)	113.39	124.92	183.08	171.38
87	HPSS200	No pigment	1% BaZn	1.5% C	5.91	5.81	6.27	7.05
88	HPSS200	No pigment	1% Sn1/Sn2	1.5% C	5.09	4.90	5.71	6.27
89	HPSS200	No pigment	5% HT	1.5% C	5.80	7.39	7.18	7.44
93	HPSS200	14% K1001 (U)	1% BaZn	1% Yellow	238.83	240.92	244.65	213.02
94	HPSS200	14% K1001 (U)	1% Sn1/Sn2	1% Yellow	236.89	235.97	246.16	210.71
95	HPSS200	14% K1001 (U)	5% HT	1% Yellow	238.57	241.49	245.60	211.93

HPSS200 Colour Formulations - Gloss Values and Gloss Retentions

Ident. No.	Base	Pigment	Stab	Colour	Gloss Values					Gloss Retentions				
					0h	750h	1500h	2000h	Before	750h	1500h	2000h		
45	HPSS200	14% K1001 (U)	1% Bazn	0.5% C	15.10	14.99	0.64	0.51	100	99.33	4.26	3.40		
46	HPSS200	14% K1001 (U)	1% Bazn	1.0% C	20.16	0.70	0.46	0.44	100	3.47	2.29	2.17		
47	HPSS200	14% K1001 (U)	1% Bazn	1.5% C	9.75	9.72	0.32	0.35	100	99.68	3.27	3.59		
48	HPSS200	14% K1001 (U)	1% Bazn	1% BLP (Blue)	12.05	2.33	0.95	0.89	100	19.29	7.88	7.37		
49	HPSS200	14% K1001 (U)	1% Bazn	1% GLSM (Blue)	13.46	1.05	0.88	0.82	100	7.80	6.50	6.08		
50	HPSS200	14% K1001 (U)	1% Bazn	1% DPP (Red)	9.38	2.73	1.28	1.27	100	29.13	13.60	13.53		
51	HPSS200	14% K1001 (U)	1% Bazn	1% GLN (Green)	12.04	1.64	1.16	1.10	100	13.60	9.60	9.13		
52	HPSS200	14% K1001 (U)	1% Sn1/Sn2	0.5% C	20.61	18.13	0.61	0.50	100	87.93	2.97	2.43		
53	HPSS200	14% K1001 (U)	1% Sn1/Sn2	1.0% C	12.01	12.28	0.45	0.45	100	102.19	3.75	3.75		
54	HPSS200	14% K1001 (U)	1% Sn1/Sn2	1.5% C	10.03	11.81	0.52	0.41	100	117.76	5.17	4.11		
55	HPSS200	14% K1001 (U)	1% Sn1/Sn2	1% BLP (Blue)	8.96	7.79	1.00	0.93	100	86.89	11.16	10.39		
56	HPSS200	14% K1001 (U)	1% Sn1/Sn2	1% GLSM (Blue)	18.33	7.07	0.95	0.90	100	38.56	5.18	4.91		
57	HPSS200	14% K1001 (U)	1% Sn1/Sn2	1% DPP (Red)	20.01	15.21	1.28	1.30	100	76.01	6.37	6.50		
58	HPSS200	14% K1001 (U)	1% Sn1/Sn2	1% GLN (Green)	10.77	11.09	1.22	1.14	100	103.02	11.32	10.56		
59	HPSS200	14% K1001 (U)	5% HT	0.5% C	10.23	9.79	0.59	0.50	100	95.66	5.78	4.89		
60	HPSS200	14% K1001 (U)	5% HT	1.0% C	13.46	12.38	0.40	0.30	100	91.92	2.97	2.23		
61	HPSS200	14% K1001 (U)	5% HT	1.5% C	12.78	11.54	0.41	0.30	100	90.27	3.23	2.35		
62	HPSS200	14% K1001 (U)	5% HT	1% BLP (Blue)	13.72	10.13	1.00	0.99	100	73.85	7.29	7.24		
63	HPSS200	14% K1001 (U)	5% HT	1% GLSM (Blue)	10.96	7.93	1.00	0.98	100	72.35	9.12	8.89		
64	HPSS200	14% K1001 (U)	5% HT	1% DPP (Red)	12.75	12.03	1.34	1.32	100	94.36	10.54	10.34		
65	HPSS200	14% K1001 (U)	5% HT	1% GLN (Green)	9.68	8.94	1.20	1.11	100.00	92.38	12.40	11.49		
87	HPSS200	No pigment	1% Bazn	1.5% C	13.01	14.50	15.58	14.25	100.00	111.48	107.46	91.46		
88	HPSS200	No pigment	1% Sn1/Sn2	1.5% C	14.58	15.38	15.78	14.99	100.00	105.53	108.28	102.83		
89	HPSS200	No pigment	5% HT	1.5% C	35.91	26.96	33.77	32.60	100.00	75.08	94.03	90.78		
93	HPSS200	14% K1001 (U)	1% Bazn	1% Yellow	22.16	21.06	1.75	1.66	100.00	95.06	7.90	7.48		
94	HPSS200	14% K1001 (U)	1% Sn1/Sn2	1% Yellow	15.73	15.74	1.79	1.70	100.00	100.12	11.37	10.81		
95	HPSS200	14% K1001 (U)	5% HT	1% Yellow	21.75	17.64	1.80	1.69	100.00	81.12	8.30	7.76		
96	HPSS200	14% K1001 (U)	No Stab	1% Yellow	17.09	3.00	1.70	-	100.00	17.56	56.67	-		

HP200 Colour Formulations - Colour Reflectance Areas

Ident. No.	Base	Pigment	Stab	Colour Pig.	0h	750h	1500h	2000h
66	HP200	14% K1001 (U)	1% Bazn	0.5% C	34.48	45.31	79.30	73.66
67	HP200	14% K1001 (U)	1% Bazn	1.0% C	19.72	28.12	52.77	49.24
68	HP200	14% K1001 (U)	1% Bazn	1.5% C	14.50	22.21	45.35	40.88
69	HP200	14% K1001 (U)	1% Bazn	1% BLP (Blue)	83.11	112.31	156.33	160.39
70	HP200	14% K1001 (U)	1% Bazn	1% GLSM (Blue)	90.16	123.14	155.88	150.76
71	HP200	14% K1001 (U)	1% Bazn	1% DPP (Red)	152.44	172.00	210.11	206.70
72	HP200	14% K1001 (U)	1% Bazn	1% GLN (Green)	108.78	134.74	188.23	192.46
73	HP200	14% K1001 (U)	1% Sn1/Sn2	0.5% C	35.26	39.18	48.82	61.19
74	HP200	14% K1001 (U)	1% Sn1/Sn2	1.0% C	21.13	24.06	30.62	33.61
75	HP200	14% K1001 (U)	1% Sn1/Sn2	1.5% C	14.89	18.00	23.39	28.03
76	HP200	14% K1001 (U)	1% Sn1/Sn2	1% BLP (Blue)	82.16	90.99	118.13	141.63
77	HP200	14% K1001 (U)	1% Sn1/Sn2	1% GLSM (Blue)	90.91	100.75	137.61	148.85
78	HP200	14% K1001 (U)	1% Sn1/Sn2	1% DPP (Red)	153.08	159.12	183.82	182.36
79	HP200	14% K1001 (U)	1% Sn1/Sn2	1% GLN (Green)	108.10	123.62	166.90	175.03
80	HP200	14% K1001 (U)	5% HT	0.5% C	35.02	42.61	78.82	68.90
81	HP200	14% K1001 (U)	5% HT	1.0% C	22.11	32.78	59.67	49.09
82	HP200	14% K1001 (U)	5% HT	1.5% C	17.27	23.85	43.69	41.02
83	HP200	14% K1001 (U)	5% HT	1% BLP (Blue)	84.17	114.40	152.15	159.57
84	HP200	14% K1001 (U)	5% HT	1% GLSM (Blue)	93.05	126.12	162.62	160.44
85	HP200	14% K1001 (U)	5% HT	1% DPP (Red)	156.34	167.65	208.19	200.28
86	HP200	14% K1001 (U)	5% HT	1% GLN (Green)	114.04	138.58	187.17	201.36
90	HP200	No pigment	1% Bazn	1.5% C	2.83	3.01	3.32	3.78
91	HP200	No pigment	1% Sn1/Sn2	1.5% C	2.86	3.21	3.51	4.18
92	HP200	No pigment	5% HT	1.5% C	3.37	4.73	5.08	5.56

HP200 Colour Formulations - Gloss Values and Gloss Retentions

Ident. No.	Base	Pigment	Stab	Colour	Gloss Values				Gloss Retentions			
					0h	750h	1500h	2000h	Before	750h	1500h	2000h
66	HP200	14% K1001 (U)	1% BaZn	0.5% C	32.74	21.33	0.67	0.57	100	65.16	2.04	1.74
67	HP200	14% K1001 (U)	1% BaZn	1.0% C	39.18	26.00	0.51	0.36	100	66.37	1.29	0.93
68	HP200	14% K1001 (U)	1% BaZn	1.5% C	35.19	24.07	0.63	0.39	100	68.39	1.78	1.12
69	HP200	14% K1001 (U)	1% BaZn	1% BLP (Blue)	22.36	9.23	1.20	1.14	100	41.29	5.37	5.09
70	HP200	14% K1001 (U)	1% BaZn	1% GLSM (Blue)	31.87	12.73	1.12	1.16	100	39.93	3.51	3.63
71	HP200	14% K1001 (U)	1% BaZn	1% DPP (Red)	45.13	22.90	1.45	1.40	100	50.74	3.21	3.10
72	HP200	14% K1001 (U)	1% BaZn	1% GLN (Green)	49.98	25.48	1.35	1.25	100	50.98	2.70	2.50
73	HP200	14% K1001 (U)	1% Sn1/Sn2	0.5% C	36.72	35.04	21.59	10.59	100	95.42	58.81	28.85
74	HP200	14% K1001 (U)	1% Sn1/Sn2	1.0% C	29.59	27.98	19.40	16.37	100	94.57	65.57	55.32
75	HP200	14% K1001 (U)	1% Sn1/Sn2	1.5% C	31.39	28.29	21.41	13.31	100	90.11	68.21	42.39
76	HP200	14% K1001 (U)	1% Sn1/Sn2	1% BLP (Blue)	25.58	18.96	9.14	0.97	100	74.14	35.73	3.79
77	HP200	14% K1001 (U)	1% Sn1/Sn2	1% GLSM (Blue)	26.63	18.47	1.34	1.03	100	69.37	5.02	3.85
78	HP200	14% K1001 (U)	1% Sn1/Sn2	1% DPP (Red)	29.79	23.34	8.59	1.40	100	78.35	28.83	4.70
79	HP200	14% K1001 (U)	1% Sn1/Sn2	1% GLN (Green)	16.93	11.06	1.36	1.30	100	65.30	8.01	7.68
80	HP200	14% K1001 (U)	5% HT	0.5% C	29.59	20.47	3.11	3.11	100	69.17	10.50	10.50
81	HP200	14% K1001 (U)	5% HT	1.0% C	23.53	12.58	5.19	5.19	100	53.44	22.05	22.05
82	HP200	14% K1001 (U)	5% HT	1.5% C	21.41	15.96	6.12	6.12	100	74.52	28.58	28.58
83	HP200	14% K1001 (U)	5% HT	1% BLP (Blue)	21.91	10.29	1.04	1.04	100	46.99	4.76	4.76
84	HP200	14% K1001 (U)	5% HT	1% GLSM (Blue)	21.88	9.41	1.10	1.10	100	43.00	5.03	5.03
85	HP200	14% K1001 (U)	5% HT	1% DPP (Red)	32.94	21.12	1.49	1.49	100	64.12	4.52	4.52
86	HP200	14% K1001 (U)	5% HT	1% GLN (Green)	24.35	12.42	1.35	1.35	100	51.00	5.54	5.54
90	HP200	No pigment	1% BaZn	1.5% C	36.14	36.15	33.79	-	100	100.02	93.48	-
91	HP200	No pigment	1% Sn1/Sn2	1.5% C	27.68	24.87	23.74	-	100	89.86	85.77	-
92	HP200	No pigment	5% HT	1.5% C	26.05	20.61	19.22	-	100	79.13	73.78	-

Appendix 2

Appendix 2

White HPS200 Formulation (20% TiO₂)

Gloss Values	Before	899h	2000h	3000h	4000h	5000h	6000h
3% Bazn	50.13	50.18	48.62	50.08	47.01	48.46	48.76
3% Bazn 1% HT	44.91	43.64	42.30	43.26	41.61	43.84	43.98
2% Bazn 2% HT	47.05	45.88	44.58	45.54	43.58	45.97	45.92
1% Bazn 1% HT	50.80	48.94	46.88	48.84	46.34	49.52	48.06
1% HT	54.80	50.06	47.36	49.37	47.53	48.67	49.76
4% HT	45.17	38.16	39.22	40.11	38.21	40.52	41.74
No Adds	49.44	48.79	48.50	50.14	47.83	48.78	48.81
3% CaZn	60.53	56.86	55.75	57.68	53.83	56.21	56.18
3% CaZn 1% HT	58.56	50.26	48.44	49.36	46.59	50.32	51.20
2% CaZn 2% HT	60.68	53.44	49.96	50.79	47.12	51.89	51.26

Gloss Retentions	Before	899h	2000h	3000h	4000h	5000h	6000h
3% Bazn	100.00	100.14	97.02	99.91	93.79	96.71	97.28
3% Bazn 1% HT	100.00	97.23	94.26	96.41	92.73	97.62	98.04
2% Bazn 2% HT	100.00	97.58	94.80	96.90	92.74	97.77	97.66
1% Bazn 1% HT	100.00	96.31	92.28	96.13	91.22	97.47	94.60
1% HT	100.00	91.38	86.42	90.08	86.76	88.80	90.80
4% HT	100.00	84.51	86.84	88.78	84.56	89.71	92.37
No Adds	100.00	98.80	98.20	101.56	96.85	98.79	98.86
3% CaZn	100.00	93.96	92.11	95.29	88.93	92.87	92.82
3% CaZn 1% HT	100.00	85.89	82.72	84.29	79.60	85.95	87.45
2% CaZn 2% HT	100.00	88.10	82.36	83.71	77.69	85.55	84.51

Goosewing Grey HPS200 Formulation (14% TiO₂)

Gloss Values	Before	899h	2000h	3000h	4000h	5000h	6000h
3% Bazn	48.52	50.83	50.36	50.18	49.45	47.76	47.29
3% Bazn 1% HT	45.15	45.25	46.06	44.83	44.20	44.94	41.83
1% Bazn 1% HT	54.20	50.42	51.63	49.29	48.63	48.95	46.47
1% HT	55.93	50.27	51.89	51.45	50.71	50.51	49.26
4% HT	49.76	44.88	45.98	44.64	44.13	44.41	43.58

Gloss Retentions	Before	899h	2000h	3000h	4000h	5000h	6000h
3% Bazn	100.00	104.84	103.86	103.48	102.04	98.55	97.60
3% Bazn 1% HT	100.00	100.26	102.05	99.37	97.98	99.65	92.64
1% Bazn 1% HT	100.00	93.03	95.27	90.95	89.72	90.30	85.76
1% HT	100.00	89.88	92.78	92.00	90.67	90.32	88.07
4% HT	100.00	90.18	92.41	89.71	88.67	89.22	87.59

Van Dyke Brown HPS200 Formulation (0% TiO₂)

Gloss Values	Before	899h	2000h	3000h	4000h	5000h	6000h
3% Bazn	43.39	44.76	43.18	43.29	41.23	41.69	39.63
3% Bazn 1% HT	42.92	36.55	37.34	37.76	35.33	38.49	35.62
1% Bazn 1% HT	46.62	40.20	41.34	41.48	38.54	40.38	38.95
1% HT	46.04	37.46	41.11	41.31	39.91	42.27	39.19
4% HT	44.48	36.40	39.63	39.21	38.44	41.61	38.93

Gloss Retentions	Before	899h	2000h	3000h	4000h	5000h	6000h
3% Bazn	100.00	103.15	99.51	99.77	95.01	96.09	91.33
3% Bazn 1% HT	100.00	85.17	87.00	87.97	82.31	89.69	82.99
1% Bazn 1% HT	100.00	86.30	88.72	89.04	82.68	86.76	83.64
1% HT	100.00	81.37	89.30	89.72	86.70	91.83	85.13
4% HT	100.00	81.85	89.11	88.16	86.42	93.55	87.52

White HPS200 Formulation (20% TiO₂)

Colour Reflectance Area	before	899h	2000h	3000h	4000h	5000h	6000h
3% BaZn	293.86	294.58	286.37	286.30	282.08	283.31	281.57
3% BaZn 1% HT	293.20	295.23	286.93	285.33	285.57	284.48	280.67
2% BaZn 2% HT	289.53	291.66	285.08	282.89	279.23	282.62	280.19
1% BaZn 1% HT	296.65	300.41	292.44	291.40	287.20	289.77	284.56
1% HT	286.54	295.80	288.40	285.70	285.42	282.35	281.70
4% HT	290.46	301.01	294.04	290.53	290.74	288.79	287.87
No Adds	290.24	298.88	291.69	290.36	288.42	286.91	284.91
3% CaZn	291.33	291.66	284.61	280.49	282.40	281.83	279.81
3% CaZn 1% HT	292.91	294.14	286.77	284.46	283.79	281.14	280.37
2% CaZn 2% HT	291.63	294.51	286.83	282.31	282.97	283.65	278.48

Goosewing Grey HPS200 Formulation (14% TiO₂)

Colour Reflectance Area	Before	899h	2000h	3000h	4000h	5000h	6000h
3% BaZn	150.26	150.43	149.96	150.09	149.77	149.81	148.94
3% BaZn 1% HT	152.77	151.95	152.00	151.90	152.00	151.61	150.53
1% BaZn 1% HT	154.78	153.85	153.77	153.67	153.42	152.99	152.40
1% HT	155.36	157.05	156.71	156.90	156.18	155.77	154.87
4% HT	157.30	159.62	159.13	160.22	158.66	157.95	157.06

Van Dyke Brown HPS200 Formulation (0% TiO₂)

Colour Reflectance Area	Before	899h	2000h	3000h	4000h	5000h	6000h
3% BaZn	13.18	15.44	15.41	15.10	15.39	15.50	15.14
3% BaZn 1% HT	13.33	17.26	17.35	16.41	16.85	17.06	16.76
1% BaZn 1% HT	13.43	14.76	14.63	14.19	14.34	14.49	14.33
1% HT	13.67	14.78	14.76	14.22	14.39	14.60	14.36
4% HT	14.36	15.96	15.70	15.12	15.32	15.16	14.82

Change in Reflectance (Before - After)	899h	2000h	3000h	4000h	5000h	6000h
3% BaZn	-0.72	7.49	7.56	11.78	10.55	12.29
3% BaZn 1% HT	-2.03	6.26	7.87	7.62	8.72	12.52
2% BaZn 2% HT	-2.13	4.45	6.65	10.30	6.91	9.34
1% BaZn 1% HT	-3.76	4.21	5.25	9.45	6.88	12.09
1% HT	-9.26	-1.86	0.84	1.12	4.19	4.84
4% HT	-10.55	-3.57	-0.06	-0.28	1.67	2.60
No Adds	-8.64	-1.44	-0.12	1.82	3.33	5.33
3% CaZn	-0.33	6.72	10.84	8.93	9.50	11.51
3% CaZn 1% HT	-1.22	6.14	8.45	9.12	11.77	12.54
2% CaZn 2% HT	-2.88	4.79	9.31	8.66	7.98	13.14

Change in Reflectance (Before - After)	899h	2000h	3000h	4000h	5000h	6000h
3% BaZn	-0.17	0.30	0.17	0.48	0.45	1.32
3% BaZn 1% HT	0.81	0.76	0.86	0.77	1.16	2.24
1% BaZn 1% HT	0.93	1.01	1.11	1.36	1.80	2.39
1% HT	-1.69	-1.35	-1.55	-0.82	-0.41	0.49
4% HT	-2.32	-1.83	-2.92	-1.37	-0.65	0.24

Change in Reflectance (Before - After)	899h	2000h	3000h	4000h	5000h	6000h
3% BaZn	-2.26	-2.23	-1.92	-2.22	-2.32	-1.96
3% BaZn 1% HT	-3.93	-4.02	-3.08	-3.52	-3.73	-3.43
1% BaZn 1% HT	-1.33	-1.20	-0.76	-0.91	-1.06	-0.90
1% HT	-1.10	-1.09	-0.54	-0.71	-0.92	-0.68
4% HT	-1.60	-1.34	-0.76	-0.95	-0.79	-0.45